The Role of Occult Amyloid in the Elderly with Aortic Stenosis

PhD Thesis

UCL

Cardiology

2020

Student: Dr Paul Richard Scully

Student Number: 16141603

Primary Supervisor: Prof James C Moon

Secondary Supervisor: Prof Philip N Hawkins

This work was supported by a British Heart Foundation Clinical Research Training Fellowship for Dr Paul Richard Scully (FS/16/31/32185).

Declaration

I, Paul Richard Scully confirm that the work presented in this thesis is my own. Where information has been derived from other sources, I confirm that this has been indicated in the thesis.

Signature: 

Name: Dr Paul Richard Scully **Date:** 26/10/2019

For Amy and Joshua

Abstract

Aortic stenosis (AS) is common in the elderly. Transcatheter aortic valve implantation (TAVI) is increasingly being used to treat patients with symptomatic, severe AS. Another disease that is common in the elderly is cardiac amyloidosis, which can now be diagnosed non-invasively using bone scintigraphy. Cardiac computed tomography (CT) can also detect elevations in myocardial extracellular volume (ECV) associated with amyloid deposition. The prevalence and clinical impact of dual AS-amyloid pathology in the elderly TAVI population is not yet known.

I aimed to confirm the prevalence of occult cardiac amyloidosis in patients referred for TAVI and the clinical impact it may have (procedural complications, symptom response and mortality). I also sought to explore the role of ECV quantification by CT (ECV_{CT}), as well as quantification techniques for ^{99m}Tc-labelled-3,3-diphosphono-1,2-propanodicarboxylic acid (DPD) scintigraphy.

AS-amyloid was present in 1 in 8 elderly patients referred for TAVI. It was not associated with a higher periprocedural complication rate or mortality, although further larger studies are needed to verify these findings. Patients with AS-amyloid derived significant mortality benefit from TAVI compared to medical therapy, so patients should not be declined TAVI on the basis of dual pathology alone. AS-amyloid is different from lone AS, however may also be distinct from isolated cardiac amyloidosis. Furthermore, there may be an interaction between the AS-primed myocardium and amyloid, which needs further exploration.

ECV_{CT} can be used to detect AS-amyloid and may offer a simple screening tool for co-existent cardiac amyloidosis in patients already undergoing CT. Importantly, this parameter also tracks mortality in patients with lone AS, which is the first time this has been demonstrated.

Finally, I validated single photon emission tomography (SPECT)/CT quantification of bone scintigraphy as a means of quantifying amyloid burden and of improving diagnostic accuracy. For centres not performing SPECT/CT, heart/contralateral lung planar quantification is a viable alternative. These techniques may provide a means of monitoring response to novel amyloid-specific therapies.

Impact Statement

My work over the last three years at Barts Heart Centre and the John Radcliffe Hospital has identified a 13% prevalence of AS-amyloid in elderly patients referred for TAVI with severe AS. Such a high prevalence is quite remarkable and the implications are potentially far reaching. Clinically, these findings will alert clinicians who are managing similar patients to the risk of this dual pathology and encourage them to have a low threshold for further investigation when suspected. This will ultimately benefit patients – allowing the appropriate diagnosis to be made and the necessary management strategies pursued. From an academic perspective, there is now a great deal of interest in this area – in part driven by access to non-invasive means of diagnosing cardiac amyloidosis, as well as the success of novel amyloid-specific therapies, but also by research such as this, which has begun to highlight just how common this condition is. Our interim results were published in the Journal of the American College of Cardiology (JACC) in 2018 in an effort to highlight to the wider medical community this high prevalence of dual pathology. We also published an article in the British Heart Foundation Heart Matters magazine to help inform the patients themselves. The final results have since been published in the European Heart Journal and in JACC: Cardiovascular Imaging. I have presented these findings at both national and international conferences for which I won one young investigator award, been a finalist for another and short-listed for a third.

Another insight from this work is that dual AS-amyloid pathology does not seem to be associated with a worse outcome compared to lone AS and that patients with AS-amyloid derive significant mortality benefit from TAVI compared to medical therapy (similar to their lone AS counterparts). This is both a surprising and exciting finding, which has significant implications for patient care – suggesting that these patients should not be declined TAVI simply on the basis of this dual pathology. This also generates a wealth of associated questions, which are likely to form the basis for further, multi-centre, international research collaborations – some of which are already ongoing and with which I am involved.

ECV_{CT} could play a key role in the diagnostic work-up of patients undergoing CT, helping clinicians identify those patients who would benefit from further testing.

Perhaps, more importantly, it could avoid often elderly patients having unnecessary testing, by effectively ruling out the spectre of cardiac amyloidosis. Not only is this important for patient care, but also has financial and research implications as well. For example, what better way to enrich one's recruitment for patients with AS-amyloid, in order to investigate the condition? The scope of this technique goes beyond the AS population and I am involved with ongoing research to validate the technique in patients with known myocardial infarction, dilated cardiomyopathy and renal failure.

Finally, I validated a novel imaging biomarker with excellent diagnostic performance that could be relevant for all centres performing bone scintigraphy and for future studies validating novel amyloid-specific therapies. It is likely to have important implications for patient care and may also help the research community by offering a technique that could be easily validated using multiple radiotracers and imaging timepoints.

Acknowledgements

Thank you to all of the patients for kindly agreeing to be involved with this research, without whose kindness this would not have been possible.

Thank you to the British Heart Foundation (BHF) for funding this research through a Clinical Research Training Fellowship (FS/16/31/32185).

Finally, thank you to all those individuals below, without whose help and support this thesis would never have been written.

My wife Amy, my son Joshua and my parents.

My supervisors:
Prof James Moon and Prof Philip Hawkins.

My colleagues at Barts Heart Centre and University College London:
Dr Thomas Treibel, Dr Kush Patel, Dr Bunny Saberwal, Dr Rebecca Hughes, Dr George Thornton, Dr João Augusto, Dr Leon Menezes, Dr Francesca Pugliese, Dr Guy Lloyd, Dr Michael Mullen, Dr Simon Kennon, Dr Muhiddin Ozkor, Dr Neil Hartman, Prof Christopher McGregor, Dr Charlotte Manisty, Dr Anna Herrey, Dr Mark Westwood, Dr Ceri Davies, Dr Sveeta Badiani, Dr Kris Knott, Dr Anish Bhuva, Dr Katia Menacho, Dr Gaby Captur, Dr Sam Mohiddin, Dr Sucharitha Chadalavada, Dr Michail Katsoulis, Dr Petros Syris and Dr Saadullah Ahmed-Villiers.

My collaborators at the John Radcliffe Hospital:
Dr Andrew Kelion, Dr Nikant Sabharwal, Dr Jim Newton, Ellie Corps, Stephanie Lloyd, Sergei Pavlitchouk, Simon Overy and all the team.

My collaborators at the National Amyloidosis Centre:
Dr Marianna Fontana and Prof Julian Gillmore.

My collaborators at Siemens Healthineers:
Ernst Klotz and Ulrike Haberland

The TAVI Nurses:
Rhian Richards, Melanie Jerrum, Helen Queenan and Kerry Bedford.

Joanna Yap-Sanderson, Jennifer Maxwell, Emily Castle, Joanne Dowling and all the cardiac CT team at BHC.

Salma Mohammed, Joanne Vickers, Susan Thornton and all the team in the Cardiac Imaging Department at BHC.

Elizabeth Morris, Maria Burniston and all the Medical Physics team at BHC.

Salma Subhani, Giorgio Testanera, Arifa Khan, Maryam Modu and Shanaaz Billimoria in the Nuclear Medicine Department at BHC.

Saniyah Khan and all the team in the Echocardiography Department at BHC.

Abbreviations

6-MWT	6-minute walk test
AHA	American Heart Association
AL amyloidosis	Primary light chain amyloidosis
ANOVA	Analysis of variance
ApoA1	Apolipoprotein-A1
AS	Aortic stenosis
ATTR	Transthyretin amyloidosis
ATTRact-AS	A Study Investigating the Role of Occult Cardiac Amyloid in Aortic Stenosis
AU	Agatston units
AUC	Area under the curve
AV	Aortic valve
AVA	Aortic valve area
AVR	Aortic valve replacement
BHC	Barts Heart Centre
BHF	British Heart Foundation
BSCMR	British Society of Cardiovascular Magnetic Resonance
CMR	Cardiovascular magnetic resonance
CT	Computed tomography
DPD	^{99m}Tc-labelled-3,3-diphosphono-1,2-propanodicarboxylic acid
DPH	Disproportionate hypertrophy
DSE	Dobutamine stress echocardiography
FDA	Food and Drug Administration
EAMS	Early Access to Medicines Scheme
ECG	Electrocardiogram
ECV	Extracellular volume
ECV_{CMR}	Extracellular volume quantification by cardiovascular magnetic resonance
ECV_{CT}	Extracellular volume quantification by computed tomography
eGFR	Estimated glomerular filtration rate

EQ-5D-5L	EuroQol-5-dimension-5-level
EQ-VAS	EuroQol visual analogue scale
EVINCI	Evaluation of Integrated Cardiac Imaging
Exp (B)	Exponentiation of the B coefficient
FAP	Familial amyloid polyneuropathy
FDA	Food and Drug Administration
GBCAs	Gadolinium-based contrast agents
GLS	Global longitudinal strain
H/CL ratio	Heart/contralateral lung ratio
HCT	Haematocrit
Hereditary ATTR	Hereditary transthyretin amyloidosis
HFpEF	Heart failure with preserved ejection fraction
HMDP	^{99m}Tc-labelled-hydroxymethylene diphosphonate
hsTnT	High-sensitivity troponin T
HU	Hounsfield units
IVSd	Interventricular septal diameter
LBBB	Left bundle branch block
LGE	Late gadolinium enhancement
LV	Left ventricle
LVEDV	Left ventricular end-diastolic volume
LVEF	Left ventricular ejection fraction
LVESV	Left ventricular end-systolic volume
LVH	Left ventricular hypertrophy
LVIDd	Left ventricular internal diameter at end-diastole
LVOT	Left ventricular outflow tract
MACE	Major adverse cardiovascular events
MCF	Myocardial contraction fraction
MGUS	Monoclonal gammopathy of undetermined significance
MI	Myocardial infarction
MR	Mitral regurgitation
MVDT	Mitral valve deceleration time
NAC	National Amyloidosis Centre
NHLBI	National Heart, Lung and Blood Institute
NIHR	National Institute for Health Research

NT-proBNP	N-terminal pro-brain natriuretic peptide
NYHA	New York Heart Association Functional Classification
PET	Positron emission tomography
PIB	^{11}C-Pittsburgh compound B
PPM	Permanent pacemaker
PWd	Posterior wall diameter
PYP	^{99m}Tc-labelled-pyrophosphate
RBBB	Right bundle branch block
REC	Research Ethics Committee
ROC	Receiver operating characteristic
ROI	Region of interest
RV	Right ventricle
RWT	Relative wall thickness
S-L criteria	Sokolow-Lyon criteria
SAP	Serum amyloid P component
SAVR	Surgical aortic valve replacement
siRNA	Small interfering RNA
SPECT	Single photon emission computed tomography
SUV	Standardised uptake value
SUV_{peak}	Peak standardised uptake value
SVi	Indexed stroke volume
TAVI	Transcatheter aortic valve implantation
TGF	Transforming growth factor
TTR	Transthyretin
V/M ratio	Voltage/mass ratio
VARC-2 criteria	Valve Academic Research Consortium-2 criteria
VOI	Volume of interest
VTI	Velocity time integral
wtATTR	Wild-type transthyretin amyloidosis (formerly senile systemic amyloidosis)

Contents

List of Figures

List of Tables

Chapter 1: Background

1.1 Aortic Stenosis

The normal aortic valve (AV) has three leaflets (tricuspid), which separate fully along the commissures in systole, creating an opening of 3-4cm^2 [1,2]. Valvular aortic stenosis (AS) is characterised by the failure of the AV leaflets to open fully, which worsens over time. Sub-valvular and supra-valvular AS can also occur, however for the purposes of this thesis, we will be focusing on valvular AS.

Congenital abnormalities of the AV exist – an example of which is when there are only two leaflets (known as a bicuspid aortic valve). This represents the most common congenital cardiac abnormality seen in adults and is present in 1-2% of the population [3,4]. It is also the commonest cause of AS requiring surgical AV replacement in those aged under 70 [5]. Rheumatic heart disease can also cause AS in the younger population, but rarely in isolation (often in association with mitral valve disease) [6].

The commonest cause of AS in developed countries (where rheumatic heart disease has fortunately become much less common) is progressive degeneration and calcification of the aortic valve [1,7,8], known as degenerative calcific AS. This accounts for the aetiology of AS in over 80% of patients in Europe [7]. The valve leaflets (normally <1mm in thickness) over time become thicker, more fibrosed and calcified [9]. Initially, leaflet mobility may be maintained (so called aortic sclerosis), however as this progresses the leaflets become stiffer, with reduced excursion – resulting in AS (figure 1) [9].

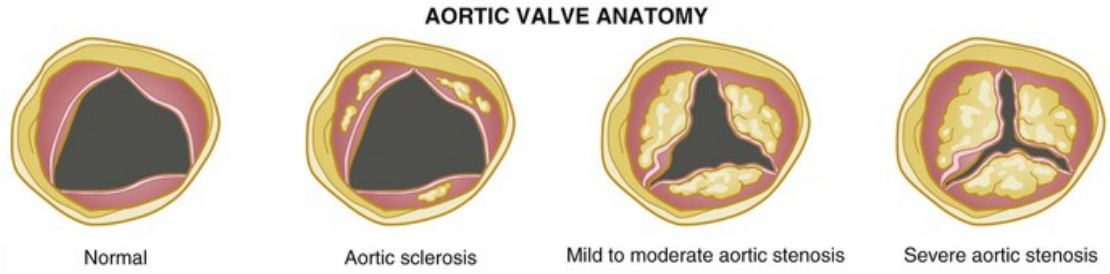

Figure 1: *The progression of calcific aortic stenosis from sclerosis to severe aortic stenosis [10].*

This progression of calcific AS appears to be an active process, akin to atherosclerosis [9]. Initial endothelial damage from mechanical stress, combined with subsequent lipid deposition results in inflammation and eventual fibrosis and calcification of the valve [9].

The severity of AS is graded as mild, moderate or severe, which is based on parameters derived from the echocardiogram (table 1).

	Aortic sclerosis	Mild	Moderate	Severe
Peak velocity (m/s)	≤2.5 m/s	2.6–2.9	3.0–4.0	≥4.0
Mean gradient (mmHg)	–	<20	20–40	≥40
AVA (cm^2)	–	> 1.5	1.0–1.5	<1.0
Indexed AVA (cm^2/m^2)	–	>0.85	0.60–0.85	<0.6
Velocity ratio	–	> 0.50	0.25–0.50	<0.25

Table 1: *Grading of aortic stenosis severity from the European Association of Cardiovascular Imaging and the American Society of Echocardiography [11]. AS = aortic stenosis, AVA = aortic valve area, indexed AVA = aortic valve area indexed for body surface area.*

Subgroups exist within those patients with AS and an aortic valve area (AVA) of <1.0cm^2 [11–13]:

1. 'High gradient AS' – mean gradient ≥40mmHg or peak velocity ≥4m/s.
2. 'Classical low-flow, low-gradient AS with reduced left ventricular ejection fraction (LVEF)' – mean gradient <40mmHg or peak velocity <4m/s, with LVEF <50% and an indexed stroke volume (SVi) <35ml/m^2.
3. 'Low-flow, low-gradient AS with normal LVEF' or 'paradoxical low-flow AS' – mean gradient <40mmHg or peak velocity <4m/s with LVEF >50% and an SVi of <35ml/m^2.

Dobutamine stress echocardiography can be helpful in the 'classical low-flow, low gradient AS' (where the LVEF is impaired) to ascertain whether there is truly severe AS that is causing the left ventricular (LV) systolic dysfunction or conversely that the AS is not actually severe (so called pseudosevere AS) and there is another underlying cause for the LV dysfunction, such as a previous myocardial infarction (MI) [11]. In truly severe AS the AVA never exceeds 1cm^2, while the peak velocity increases to ≥4m/s or the mean gradient to >30-40mmHg [11,13,14]. If the AVA

increases to >1cm^2 this suggests that the AS is not severe [11,13]. Finally, if there is no LV contractile reserve (failure to augment stroke volume by 20% in response to the dobutamine) this is associated with worse outcomes following surgical aortic valve replacement (SAVR), although still better than with medical therapy alone (figure 2) [15,16].

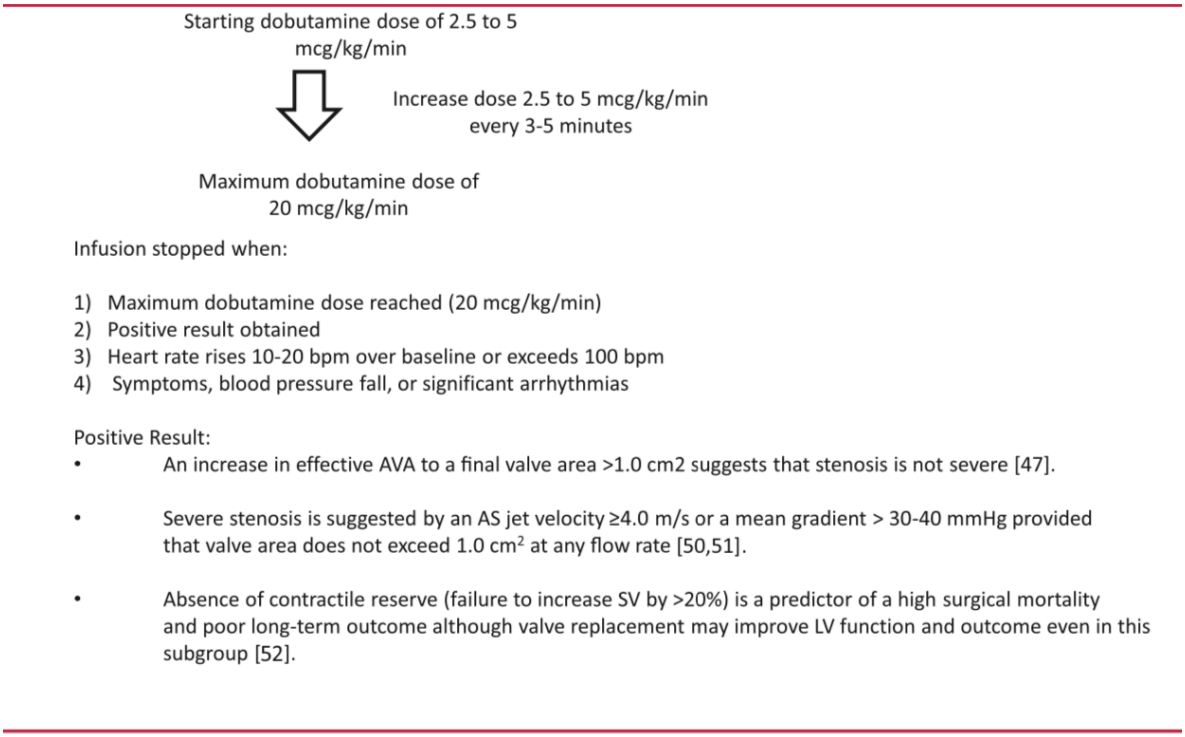

Figure 2: *Low-dose dobutamine stress echocardiography protocol for the assessment of classical 'low flow, low gradient' aortic stenosis [11].*

The final subgroup of patients with paradoxical low-flow AS can be the most difficult to adequately assess and are often characterised by small, hypertrophied ventricles with low flow (SVi <35ml/m^2), despite an apparently normal LVEF. One small study has suggested that DSE may also be helpful in these patients, where values for the AVA and mean AV gradient at rest and peak stress can be used to calculate a 'projected AVA,' which may better reflect AS severity [17]. It is also important to ensure the AVA estimation on echocardiography is accurate – particularly the LV outflow tract (LVOT) diameter, which can introduce large errors in the calculated AVA with only small (mm) changes in measurement (as it is squared in the calculation of the LVOT cross-sectional area, as part of the continuity equation used to calculate the AVA) [11].

In equivocal cases (particularly in those with paradoxical low-flow AS), cardiac computed tomography (CT) can be useful to calcium score the AV [11,13]. There is a good correlation between the degree of aortic valve calcification and AS severity on echocardiography - in terms of the AVA, the indexed AVA, the mean gradient and the peak velocity [18] (figure 3).

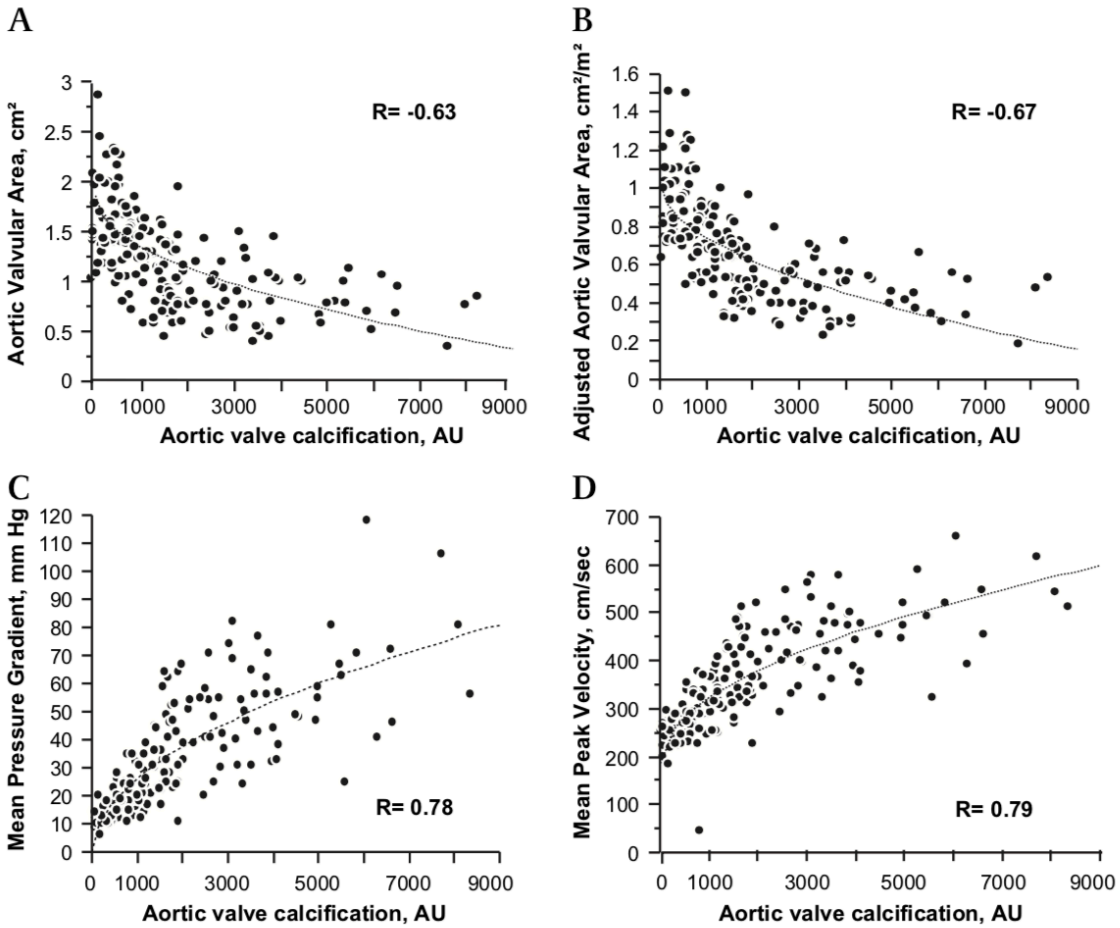

Figure 3: *Correlation between aortic valve calcification as assessed by CT and aortic valve area (**A**), indexed aortic valve area (**B**), mean pressure gradient (**C**) and peak velocity (**D**) as assessed by echocardiography [18].*

Subsequent larger studies revealed that there is a significant gender difference in the degree of AV calcification seen in severe AS, with men having a higher burden of AV calcification for a similar degree of AS [19,20]. Thresholds for the AV calcium score have been proposed which reflect this, with severe AS being *very likely* with an AV calcium score of ≥3,000 Agatston Units (AU) in men and ≥1,600 AU in women, *likely* when ≥2,000 AU in men and ≥1,200 AU in women and *unlikely* when <1600 AU in men and <800 AU in women [11,20]. A higher initial AV calcium score is predictive of a more rapid progression in existing calcification burden [21], while subsequent

international, multicentre studies have found that it is also independently associated with survival in patients with AS [22,23]. Given the differences in underlying pathophysiology, these calcium score thresholds are unlikely to prove useful in rheumatic AV disease and need further validation in the bicuspid AV population [24].

Prevalence

As mentioned earlier, the early calcification and thickening of the AV leaflets, in the presence of preserved mobility, is termed aortic sclerosis [10]. This can act as a precursor to AS (in 16% of cases it will progress to at least mild AS) and is present in approximately one quarter of those aged over 65 and more than a third of patients aged 75 and over [25]. Degenerative AV disease is associated with traditional cardiovascular risk factors including increasing age (two-fold increased risk per 10 years), male gender (two-fold increased risk), current smoking (35% increased risk), a history of hypertension (20% increased risk), and increasing low-density lipoprotein levels [25]. It is perhaps no surprise then that just the presence of aortic sclerosis is associated with a significantly increased risk of cardiovascular events (including mortality) compared to those patients with a normal AV [22–24].

AS is the most common valve disease in the developed world [7]. The prevalence of moderate or severe AS increases with age from as low as 0.02% in those aged 18-44 years, up to 2.8% in those aged 75 and over (figure 4) [1].

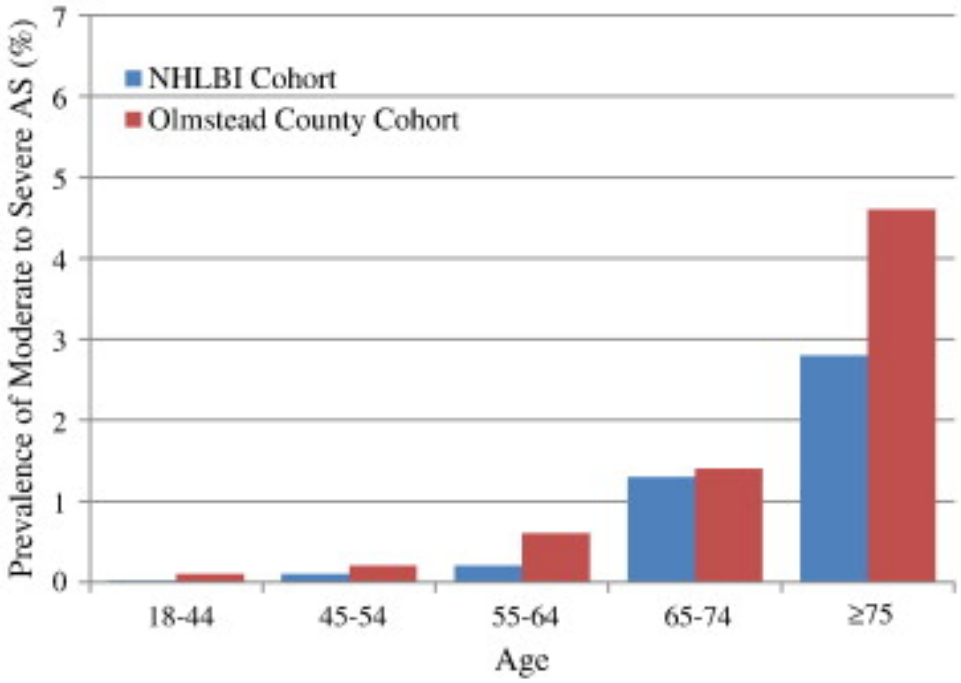

Figure 4: *The increasing prevalence of moderate to severe aortic stenosis (AS) with age in two large cohorts of patients who underwent echocardiography: one from the National Heart, Lung and Blood Institute (NHLBI) and the other from Olmstead County [1,29]. Note the higher prevalence in the Olmstead County cohort, who were referred for echocardiography, as compared to the randomly selected NHLBI cohort who received screening echocardiography.*

Lindroos et al found a similar prevalence in 501 randomly selected patients aged 75 and over from the Helsinki Ageing Study [30]. They found that 4.8% of patients had at least 'moderate' aortic stenosis (defined as an AVA of $\leq 1.2cm^2$ and a velocity ratio of ≤ 0.35) and that 2.9% had 'critical' aortic stenosis (defined as an AVA of $\leq 0.8cm^2$ and a velocity ratio of ≤ 0.35) [30].

Myocardial Response

AS increases myocardial afterload and in order to maintain cardiac output, the LV responds with compensatory hypertrophy (LVH). This myocardial response eventually becomes maladaptive, giving way to varying degrees of myocardial fibrosis and subsequent LV impairment (figure 5) [9,31]. It is at this tipping point that patients tend to develop symptoms: classically of shortness of breath, chest pain and/or syncope.

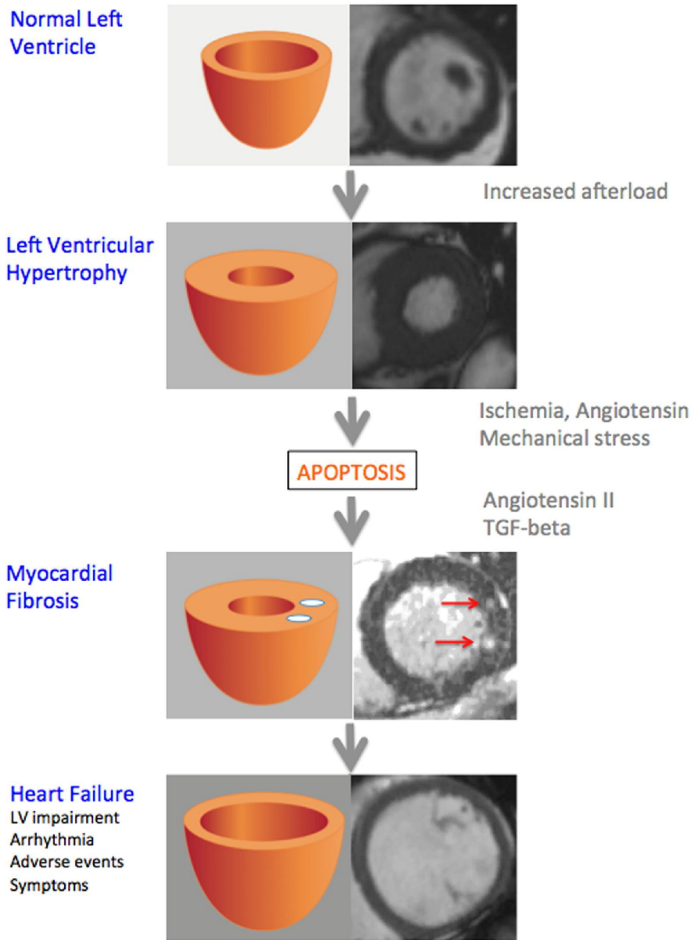

Figure 5: *The myocardial response to the increased afterload of aortic stenosis, with cardiovascular magnetic resonance images. Red arrows demonstrate late gadolinium enhancement seen on cardiovascular magnetic resonance corresponding to areas of myocardial fibrosis [9]. TGF = transforming growth factor.*

Interestingly, in those patients with AS, the degree of LVH seems to be only weakly (if at all) associated with the valve severity [32,33]. Instead in AS it seems to be more related to age [32] and gender [34,35]. Older patients (aged >65 years) tend to have a higher LV mass on echocardiography (independent of AS severity) [32]. Male patients tend to have more concentric and eccentric hypertrophy compared to women, as well as more myocardial fibrosis in response to the AS (figure 6) [35].

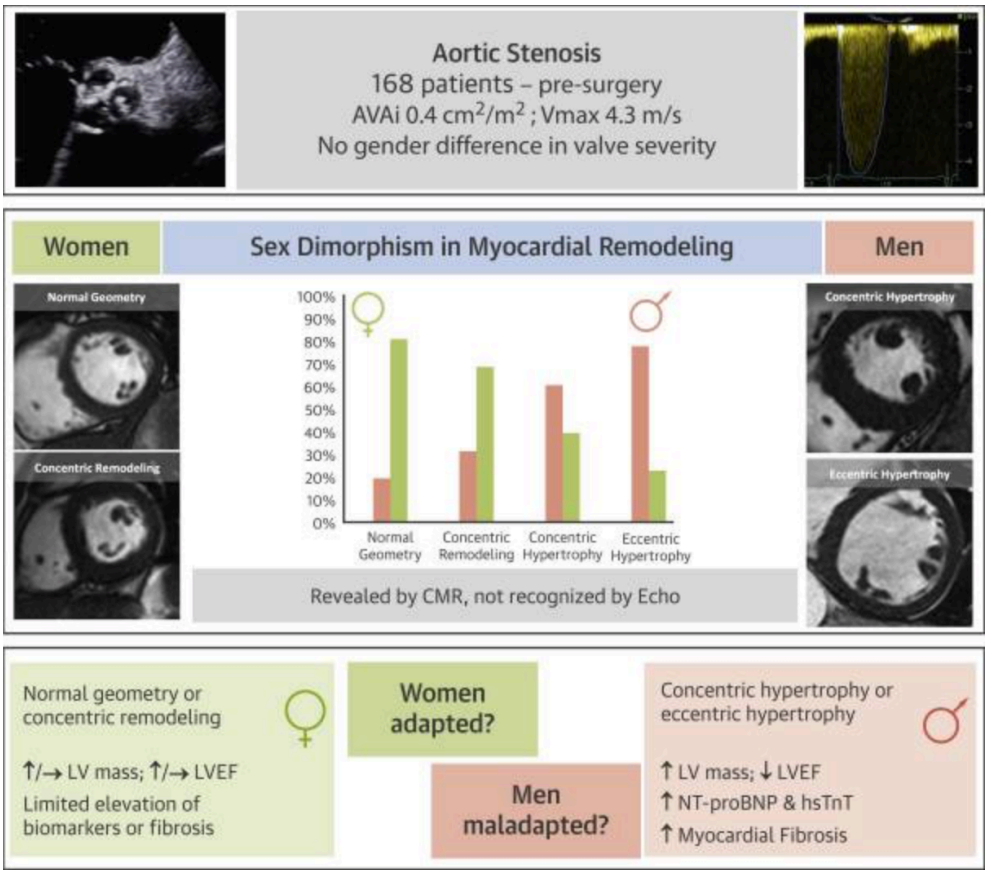

Figure 6: *Gender differences in myocardial remodelling in response to severe AS [35].*

Although we will touch on this more in due course, in order to highlight how important this maladaptive fibrotic response is, a recent study from the British Society of Cardiovascular Magnetic Resonance (BSCMR) Valve Consortium involving 674 patients undergoing valve replacement for severe AS, demonstrated scar on cardiovascular magnetic resonance (CMR) in 51% of patients (non-infarct pattern in a third of the overall population), which was associated with a two-fold higher late mortality [36].

Treatment

In the absence of symptoms, there is an approximately 1% per year incidence of sudden cardiac death associated with severe AS [37]. Unfortunately, most patients with significant AS will develop symptoms within 5 years [37] and once symptomatic outcomes are poor (figure 7), unless the valve is replaced either surgically (SAVR) or via transcatheter aortic valve implantation (TAVI). Average survival is only 2-3 years after symptom onset without intervention [32–35]. SAVR is known to improve this

survival dramatically [39] and, more recently, TAVI has been shown to do the same - reducing 1-year mortality by up to 20% compared to medical management [42,43].

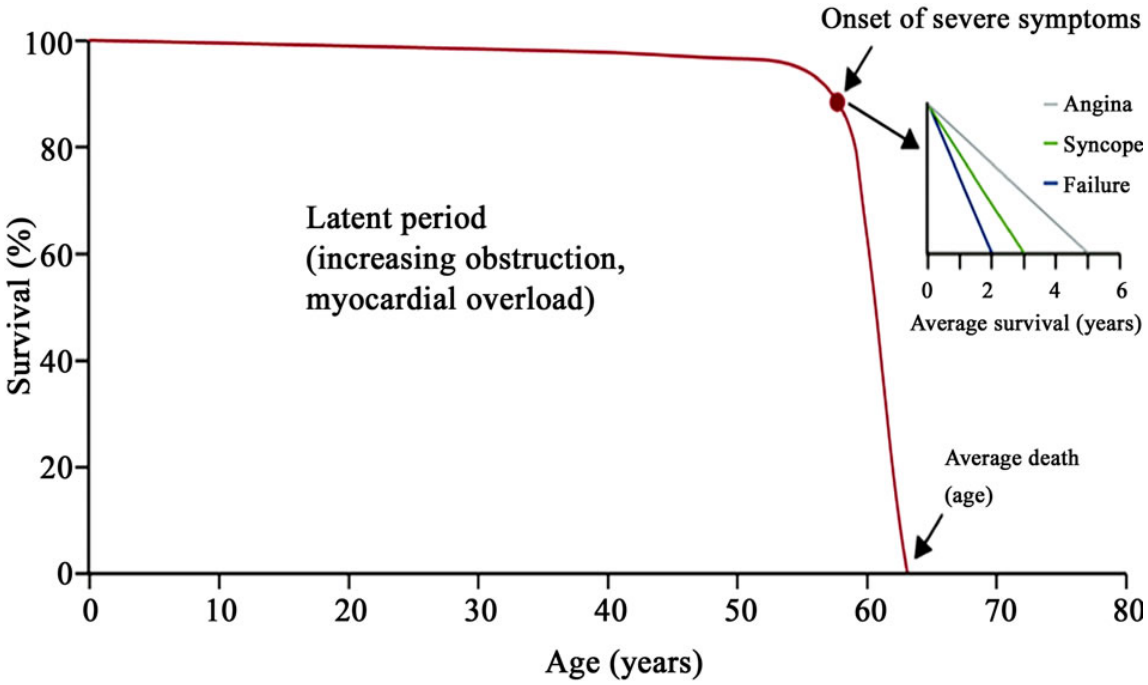

Figure 7: *Survival in aortic stenosis. Adapted from Ross and Braunwald [38].*

It is also known that mortality in high-risk patients following TAVI is equivalent to, or indeed better than, SAVR [38–40]. Reflecting this, its use has been reserved (until recently) for more elderly patients or those with significant co-morbidities, deemed too high risk for conventional SAVR – indeed current guidelines from the European Society of Cardiology and European Association for Cardiothoracic Surgery support this (figure 8) [13]. The most recent committee comments from the National Institute for Health and Care Excellence in their interventional procedures guidance for TAVI also advocate its role in patients with aortic stenosis deemed not suitable for SAVR [47].

B) Choice of intervention in symptomatic aortic stenosis		
Aortic valve interventions should only be performed in centres with both departments of cardiology and cardiac surgery on site and with structured collaboration between the two, including a Heart Team (heart valve centres).	I	C
The choice for intervention must be based on careful individual evaluation of technical suitability and weighing of risks and benefits of each modality (aspects to be considered are listed in *Table 7*). In addition, the local expertise and outcomes data for the given intervention must be taken into account.	I	C
SAVR is recommended in patients at low surgical risk (STS or EuroSCORE II < 4% or logistic EuroSCORE I < 10%[d] and no other risk factors not included in these scores, such as frailty, porcelain aorta, sequelae of chest radiation).[93]	I	B
TAVI is recommended in patients who are not suitable for SAVR as assessed by the Heart Team.[91,94]	I	B
In patients who are at increased surgical risk (STS or EuroSCORE II ≥ 4% or logistic EuroSCORE I ≥ 10%[d] or other risk factors not included in these scores such as frailty, porcelain aorta, sequelae of chest radiation), the decision between SAVR and TAVI should be made by the Heart Team according to the individual patient characteristics (see *Table 7*), with TAVI being favoured in elderly patients suitable for transfemoral access.[91,94–102]	I	B
Balloon aortic valvotomy may be considered as a bridge to SAVR or TAVI in haemodynamically unstable patients or in patients with symptomatic severe aortic stenosis who require urgent major non-cardiac surgery.	IIb	C
Balloon aortic valvotomy may be considered as a diagnostic means in patients with severe aortic stenosis or other potential causes for symptoms (i.e. lung disease) and in patients with severe myocardial dysfunction, pre-renal insufficiency or other organ dysfunction that may be reversible with balloon aortic valvotomy when performed in centres that can escalate to TAVI.	IIb	C

Figure 8: *European Society of Cardiology and the European Association for Cardio-Thoracic Surgery 2017 Guidelines for the Management of Valvular Heart Disease. Current indications for transcatheter aortic valve implantation (TAVI), as opposed to surgical aortic valve replacement (SAVR) [13].*

In the US however, following the results of the PARTNER 2, SAPIEN 3 and SURTAVI trials, the Food and Drug Administration (FDA) initially approved Medtronic's Corevalve Evolut TAVI valve and Edwards' Sapien XT and Sapien 3 TAVI valves for use in intermediate surgical risk patients [42–44]. In August this year, FDA approval was expanded further for the Edwards' Sapien 3 and Sapien 3 Ultra TAVI valves, as well as Medtronic's CoreValve Evolut R and CoreValve Evolut PRO TAVI valves to include those patients with a low surgical risk. This followed the results of both the PARTNER 3 [51] and Evolut Low-Risk trials [52], which were published in May this year. The PARTNER 3 trial demonstrated that TAVI for severe AS in low surgical risk patients was associated with a lower rate of the composite endpoint of death, stroke or rehospitalisation at one year than SAVR [51]. Important limitations of this study included: follow-up was limited to only one year, patients with biscuspid aortic valves and poor transfemoral access were excluded and adjudication of trial endpoints was not blinded, which in turn could have resulted in bias [51]. Despite this, the results of PARTNER 3 were supported by both the Evolut Low-Risk trial, which showed non-inferiority of TAVI to SAVR in terms of a composite endpoint of death or disabling stroke at 2 years [52] and the earlier all-comer NOTION trial, which found no significant difference in the composite rate of death from any cause, stroke or MI at 1 year between TAVI and SAVR [53]. Five year data from the same trial support this further, with no difference in major clinical outcomes

between TAVI and SAVR [54]. Further trials are ongoing in the intermediate (UK TAVI trial) and low surgical risk populations (NOTION 2 and Corevalve LR trials), however with this growing body of evidence TAVI practice worldwide is likely to change.

TAVI numbers have increased dramatically since the first TAVI was performed in France in 2002 [55] and this is particularly true in the UK (figure 9). According to data from the British Cardiovascular Intervention Society, a total of 66 TAVI procedures were performed in the UK in 2007, compared to 4,019 in 2017. In view of the expanding role of TAVI and our ageing population, these numbers are only likely to increase.

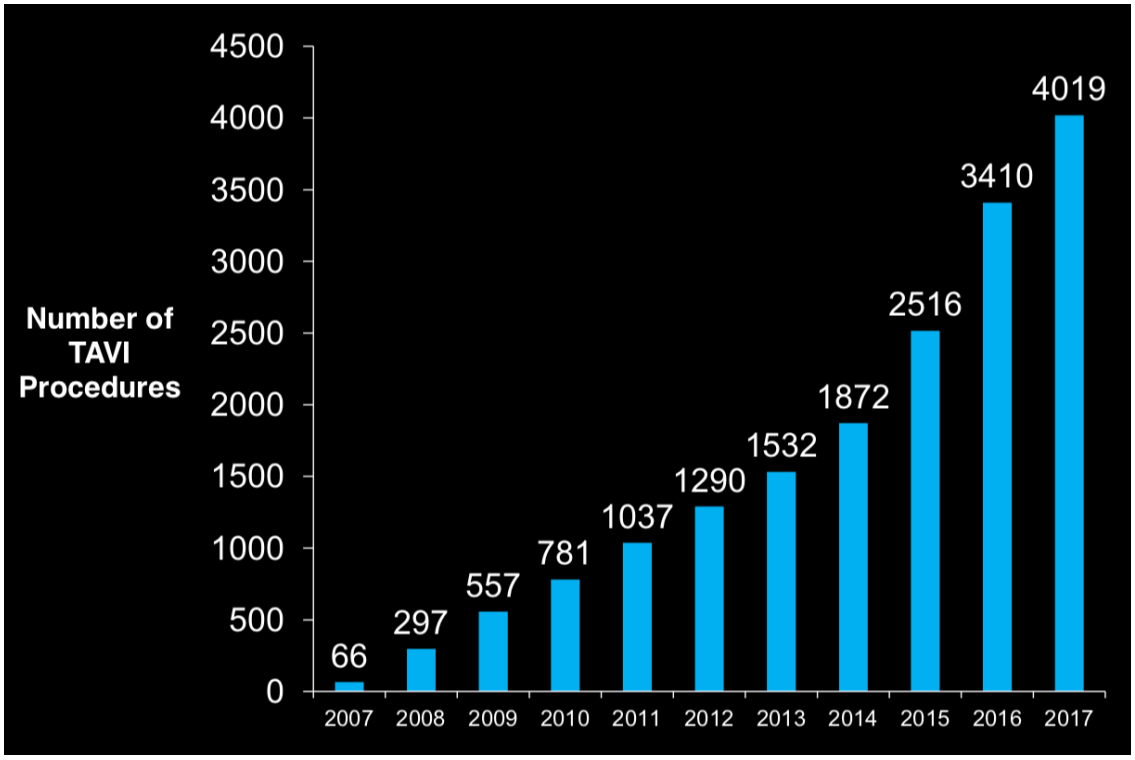

Figure 9: *Numbers of transcatheter aortic valve implantations (TAVIs) performed in the UK from 2007 to 2017. Data from the British Cardiovascular Intervention Society UK TAVI Audit (available on their website).*

Despite the very promising results of TAVI, there remain a significant proportion of patients who do not gain such benefit from the procedure [56]. Indeed, nearly one third of patients in the all-comer NOTION trial were still symptomatic – New York Heart Association Functional Classification (NYHA) Class II or more – at 1 year post-TAVI (figure 10) [53], while ~20% of patients in the Partner 1 trial (cohort A) felt only

slightly better, no better or worse [57]. This is perhaps not wholly surprising, given the prevalence of comorbidities in these elderly patients. Those with severe chronic lung or kidney disease [58] tend to do worse, as well as those with diabetes [58] and increased frailty [59]. From a cardiac point of view, those with known coronary artery disease [58], pre-procedural atrial fibrillation [58] and a low-flow AS phenotype tend to have worse outcomes (irrespective of LVEF) [60]. Moderate-severe concomitant mitral regurgitation (MR) is also associated with worse outcome, however the degree of MR improves significantly in half of these patients following TAVI [61].

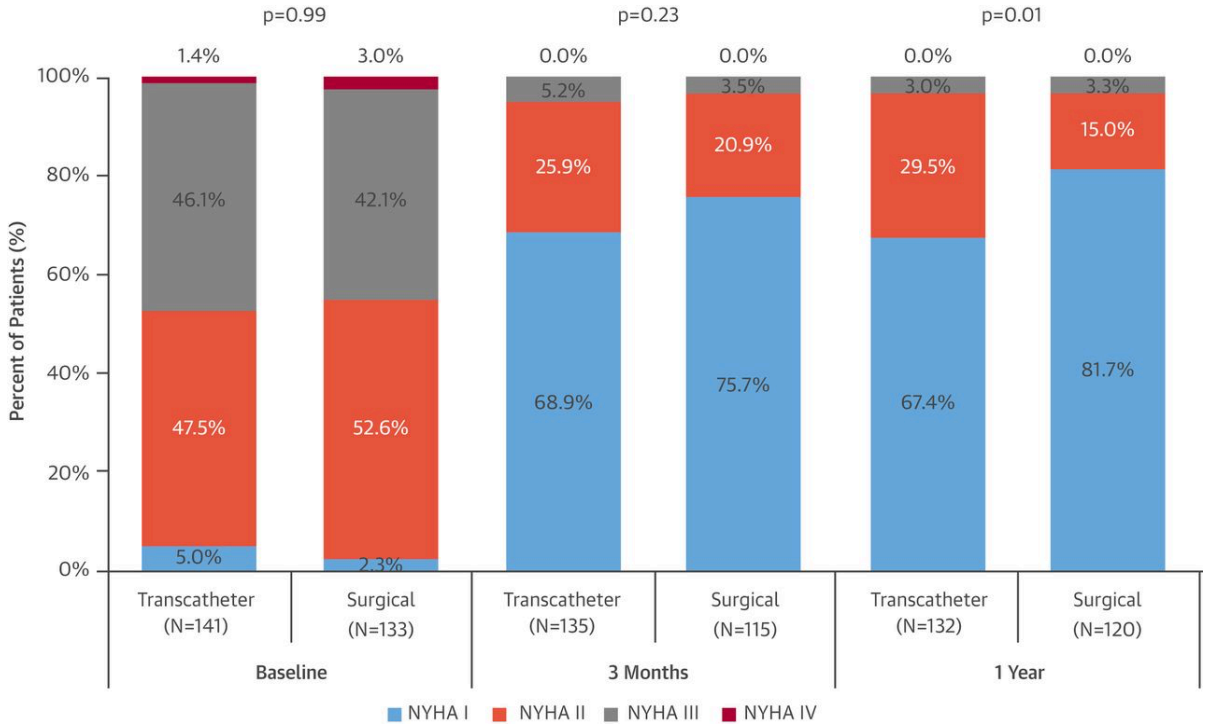

Figure 10: *Data from the NOTION trial demonstrating the symptomatic benefit seen post-TAVI and SAVR at 3 months and 1 year. Note, there is still a significant proportion of patients (32.5%) who remain symptomatic (NYHA II or more) at 1 year post-TAVI [53]. NYHA = New York Heart Association functional classification.*

1.2 Amyloidosis

Amyloidosis is characterised by the extracellular deposition of abnormally folded protein [62], which can deposit in a variety of organs, resulting in progressive organ dysfunction. 27 different types of protein are known to form such amyloid fibrils in humans [63]. Cardiac involvement is a leading cause of mortality and morbidity in these patients [62].

There are three main types of amyloidosis that involve the heart: primary light chain (AL) amyloidosis, wild-type transthyretin (wtATTR) and hereditary transthyretin amyloidosis (hereditary ATTR). The very rare hereditary apolipoprotein A-1 (ApoA1) can also sometimes affect the heart, resulting in a similar phenotype [64]. AA amyloidosis can complicate any condition associated with a prolonged increase in serum amyloid A protein production (such as chronic inflammatory conditions) and cardiac involvement is very rare, with renal involvement usually dominant [64].

Cardiac amyloidosis results in a progressive restrictive cardiomyopathy, often with small QRS complexes on electrocardiogram (ECG) despite sometimes marked LVH on echocardiography (a combination reported to have a sensitivity of 72% and a specificity of 91% for cardiac amyloidosis) [65]. The associated clinical presentation is usually one of heart failure, although syncope is not uncommon (due to amyloid deposition within the myocardial conduction system, ventricular arrhythmia or intravascular fluid depletion in conjunction with autonomic neuropathy) [62]. Atrial arrhythmias are common, as is atrial thrombus particularly in AL amyloidosis (even before atrial fibrillation is evident) [66]. Myocardial ischaemia from microvascular dysfunction and LV outflow tract obstruction from marked septal hypertrophy have also been reported [67].

Primary Light Chain (AL) Amyloidosis

AL amyloidosis is caused by the deposition of immunoglobulin light chain fragments, which are secreted by a monoclonal proliferation of plasma cells [68]. The light chain fragments are deposited most commonly in the kidneys, heart, liver and peripheral nerves, resulting in progressive organ failure [69].

AL amyloidosis carries a particularly poor prognosis, with an approximately 70% mortality within two years of diagnosis, increasing to 84% within five years [70]. It can be associated with multiple myeloma, B-cell malignancies (such as Waldenstrom's macroglobulinaemia) or indolent lymphomas (such as marginal zone lymphoma), however most commonly the underlying plasma cell dyscrasia would be considered a monoclonal gammopathy of undetermined significance (MGUS) if it were not for the related amyloid deposition [71].

According to results from the National Amyloidosis Centre (NAC) database, the majority of patients (62%) affected by AL amyloidosis tend to be aged between 50 and 70 years at diagnosis, with a smaller proportion (28%) aged over 70 years at diagnosis [71].

The most common clinical features include: nephrotic syndrome (with or without renal failure), congestive heart failure, sensorimotor and or peripheral neuropathy and hepatomegaly [71]. Macroglossia is pathognomonic of AL amyloidosis, however is not always present [71]. A quarter of patients have dominant symptomatic cardiac involvement at diagnosis, resulting in a poorer prognosis [71].

Transthyretin Amyloidosis (ATTR)

Transthyretin (TTR) is a protein that is produced in the liver and choroid plexus. It normally functions as a thyroxine transporter and retinol-binding protein (involved in vitamin A transport) [68]. The associated gene is located on chromosome 18 and has over 130 pathogenic variants [68].

Wild-type Transthyretin Amyloidosis

WtATTR, formerly known as senile systemic amyloidosis, is *not* associated with any known TTR gene mutation. It is characterised by cardiac deposition in almost all cases, often with a preceding history (by 5-10 years) of carpal tunnel involvement, otherwise extracardiac involvement is rare (although can occur, for example in the spine or bladder) [62,68].

A Finnish study (n=256 patients) found some cardiac deposits of wtATTR at autopsy in 25% of patients aged 85 and over, however only 5.5% of the overall population had moderate or severe deposits [72]. The mean age of presentation is usually in the mid-70s, with, traditionally, the majority being male (reportedly over 80%, but many studies reporting closer to 94-98%) [68,73,74]. This male predominance is, interestingly, not reflected in the heart failure with preserved ejection fraction (HFpEF) population [75]. Median survival from diagnosis ranges from 24-69 months [39–43].

Hereditary Transthyretin Amyloidosis

Of the known 130 pathogenic variants in the TTR gene, most are inherited in an autosomal dominant fashion, with variable penetrance [68]. The clinical phenotype is closely related to the particular inherited mutation. The commonest TTR gene mutations to involve the heart are Val122Ile, Val30Met and Thr60Ala [68]. These patients tend to have varying degrees of cardiac involvement with peripheral neuropathy and/or autonomic dysfunction (table 2).

Genetic variant	Presenting age (mean)	Common ethnicity	Cardiac involvement	Other systemic involvement
Primary (AL)	60–70 years	Any	40%–50%	Kidney, liver, soft tissue, nerves, spleen
ATTR (wild type)	70–80 years	Caucasian	Almost 100%	Carpal tunnel, spine, bladder
ATTR (Val122Ile)	≥60 years	African/Caribbean	Almost 100%	Carpal tunnel, rarely nerves
ATTR (Thr60Ala)	≥60 years	Caucasian (Irish)	90%	Nerves common
ATTR (Val30Met)	30–40 or 50–60 years	Any (Portuguese, Swedish, Japanese)	Uncommon in early onset, 40% of late onset	Nerves common

Table 2: *Summary of the commonest types of amyloidosis to involve the heart, including hereditary transthyretin genetic variants [68].*

Val122Ile

The Val122Ile mutation is most commonly seen in patients of African descent, being present in up to 4% of all African-Americans and 23% of African-Americans with cardiac amyloidosis [62]. It is the commonest variant in the United States [76]. In the UK, it is the underlying aetiology in nearly 12% of Afro-Caribbean patients aged over 60 years with heart failure and is associated with the worst prognosis (median survival from diagnosis is 2.6 years) [77]. Cardiac involvement is almost universal, while peripheral neuropathy is relatively rare (although reported) [68]. Similar to wtATTR, carpal tunnel involvement can be seen, although less commonly [68]. The cardiac phenotype is similar to wtATTR, although patients by comparison are generally younger, with a higher proportion of women and African-Americans [76,78].

Val30Met

Commonly seen in areas of Portugal, Japan and Sweden, Val30Met is the commonest TTR gene mutation worldwide [68,79]. There tends to be a bimodal distribution in the disease presentation: earlier onset disease occurring in 3rd and 4th decades rarely involving the heart, compared to later onset disease occurring in the 6th and 8th decades frequently resulting in cardiac involvement [68,80]. Neuropathy, particularly affecting the lower limbs (familial amyloid polyneuropathy or FAP), tends to occur in all forms of the disease [68]. Penetrance is variable and may be related

to regional variation, as well as the source parent (maternal inheritance being associated with an earlier presentation) [81]. Survival can vary widely and tends to be better than for other TTR gene mutations, which is likely due to the variability in cardiac involvement (the main cause of mortality) – with a mean survival of 4.3 years from diagnosis (or 7.3 years from symptom onset) in those with late onset disease [82,83].

Thr60Ala

Thr60Ala is the most common TTR gene mutation resulting in cardiac involvement seen in the UK [84]. It is particularly prevalent in patients of Irish descent. Median age of onset is 63 years and over 90% have evidence of cardiac involvement on echocardiography at presentation [84]. Most affected patients also have some degree of autonomic or peripheral neuropathy. Median survival is 3.4 years from diagnosis (or 6.6 years from symptom onset), with cardiac involvement responsible for much of this mortality [84].

Imaging in Cardiac Amyloidosis

While, there will always be a role for endomyocardial biopsy for the detection of cardiac amyloidosis (and indeed this has been considered the 'gold standard' for its detection for many years), imaging now plays an increasingly important role in its diagnosis and in many cases now precludes the need for biopsy.

Bone Scintigraphy

The use of bone scintigraphy in diagnosing amyloidosis is not a new concept, with case reports dating as far back as 1977 showing localisation of ^{99m}Tc-diphosphonate to the heart in possible cardiac amyloidosis [85]. Despite this, it was not until Perugini and colleagues published their paper in 2005 on the use of ^{99m}Tc-labelled-3,3-diphosphon-1,2-propanodicarboxylic acid (DPD) scintigraphy in the diagnosis of cardiac amyloidosis [86], that the potential of bone scintigraphy begun to be realised. They showed in 25 patients with cardiac amyloidosis (15 ATTR, 10 AL) that DPD scintigraphy was highly sensitive in detecting ATTR cardiac amyloidosis (100%), bearing in mind that their evidence for cardiac amyloidosis was based on echocardiography [86].

They developed the visual grading system based on the 3-hour planar DPD image (figure 11) [86]:

Grade 0 = absent cardiac uptake and normal bone uptake.

Grade 1 = mild cardiac uptake, inferior to bone uptake.

Grade 2 = moderate cardiac uptake, with attenuated bone uptake.

Grade 3 = strong cardiac uptake, with mild/absent bone uptake.

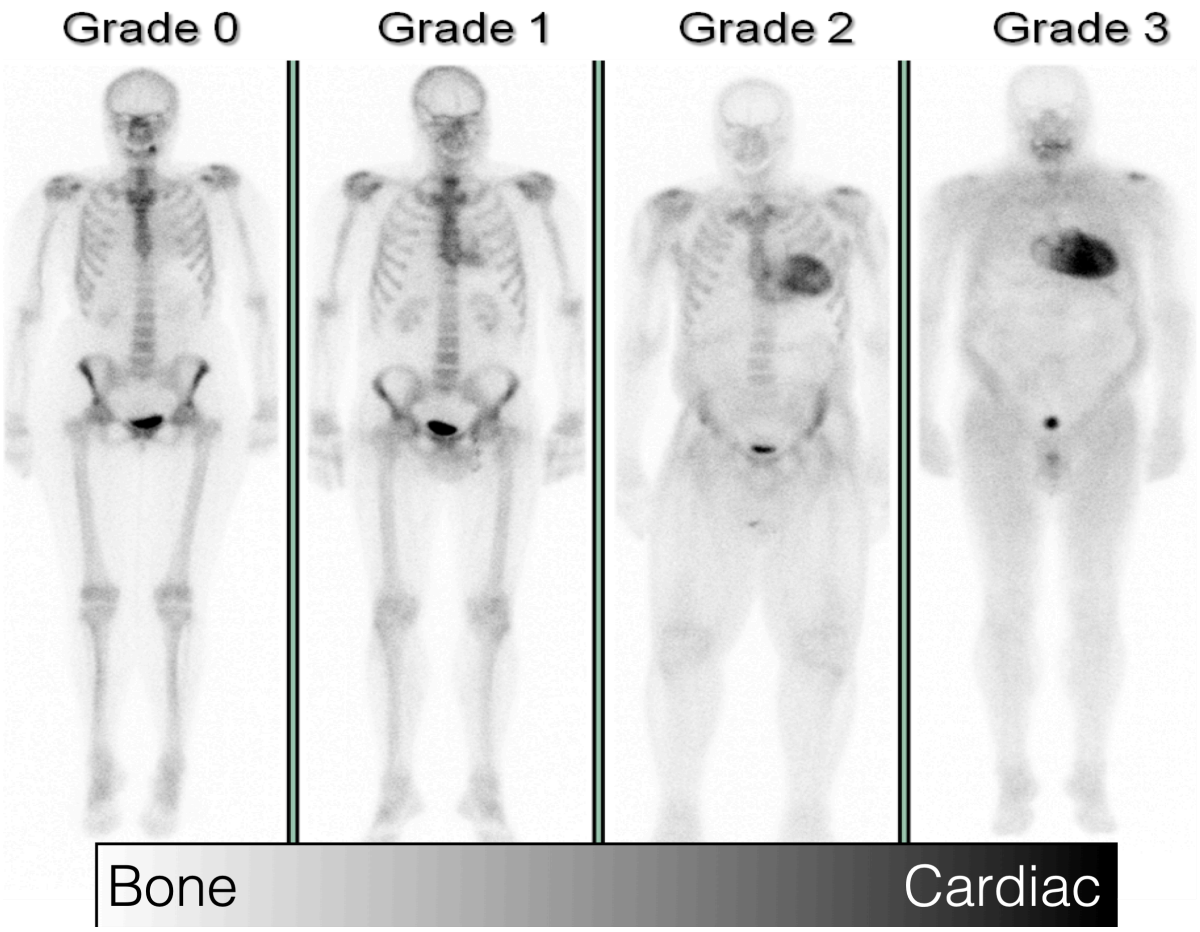

Figure 11: *3-hour DPD whole-body planar images demonstrating the Perugini grading system [86]. Grade 0 is 'negative' with no cardiac retention of tracer. Grades 1-3 are 'positive' and demonstrate increasing cardiac retention of tracer (plateauing at grades 2 and 3) combined with progressive soft tissue uptake (red arrows over deltoid, gluteal and abdominal wall area – characteristic of ATTR amyloidosis) masking underlying bone uptake.*

^{99m}Tc-labelled pyrophosphate (PYP) and ^{99m}Tc-labelled hydroxymethylene diphosphonate (HMDP) are alternative bone seeking tracers commonly used in the United States (US) and France respectively. A subsequent multi-centre study involving over 1200 patients (374 with histologically proven cardiac amyloid on endomyocardial biopsy) investigating the diagnostic potential of bone scintigraphy –

DPD, as well PYP and HMDP – revealed a sensitivity of >99% and a specificity of 68% for ATTR cardiac amyloid [88]. False positives were almost exclusively due to cardiac uptake seen in patients with AL cardiac amyloidosis (51% of patients with AL cardiac amyloidosis on endomyocardial biopsy had a positive DPD scan – nearly 60% of which were grade 1) [88]. The authors took their work further and devised a diagnostic algorithm for ATTR cardiac amyloid, precluding the need for endomyocardial biopsy in some patients (figure 12) [88]. This pathway has been included in recent expert consensus recommendations for multimodality imaging in cardiac amyloidosis [89,90].

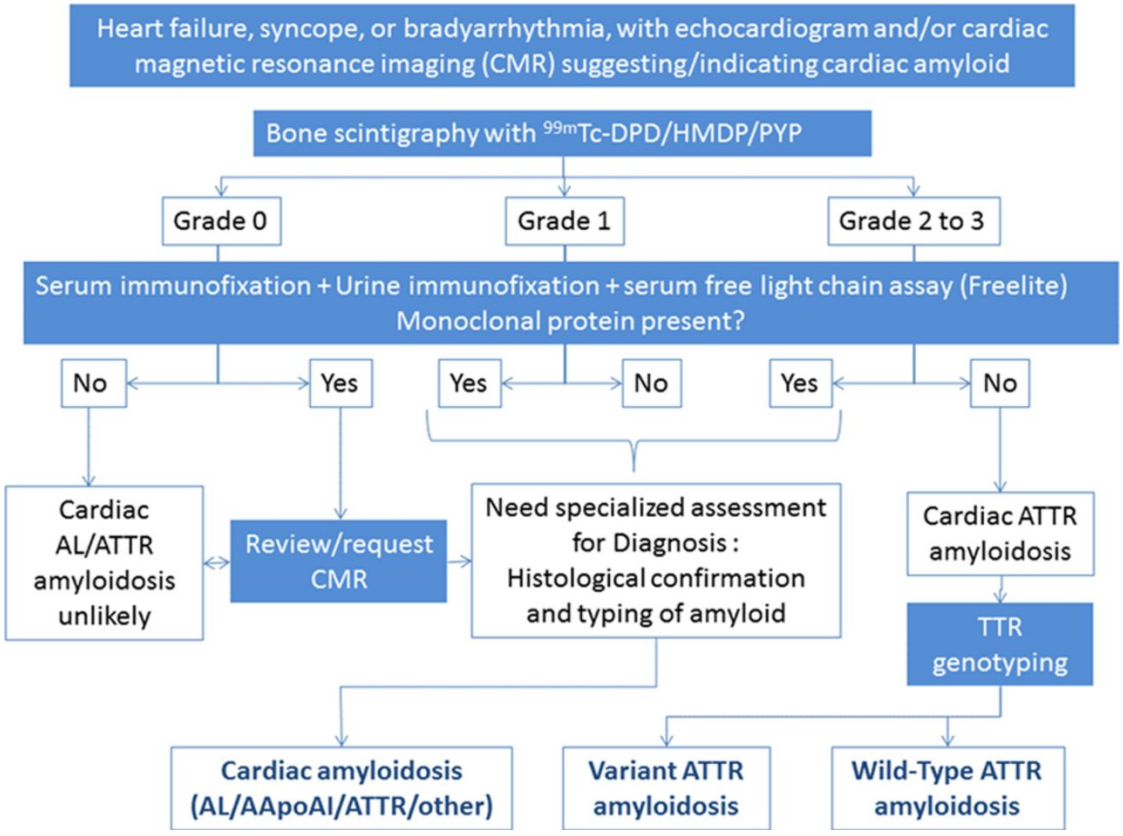

Figure 12: *Diagnostic algorithm for patients with suspected cardiac amyloidosis. AApoA1 = apolipoprotein A-1; DPD = ^{99m}Tc-labelled 3,3-diphosphono-1,2-propanodicarboyxlic acid; HMDP = ^{99m}Tc-labelled hydroxymethylene disphosphonate; PYP = ^{99m}Tc-labelled pyrophosphate [88].*

Quite why bone scintigraphy is so sensitive for the detection of ATTR cardiac amyloid is unclear and the topic of some debate. One hypothesis is that microcalcifications present within the amyloid and which are more prevalent in ATTR compared to AL cardiac amyloidosis are responsible [91].

It is known from recent published work from the NAC that, although highly sensitive for detecting ATTR cardiac amyloidosis, the Perugini visual grading system alone unfortunately offers little prognostic significance in DPD scintigraphy (figure 13) [92].

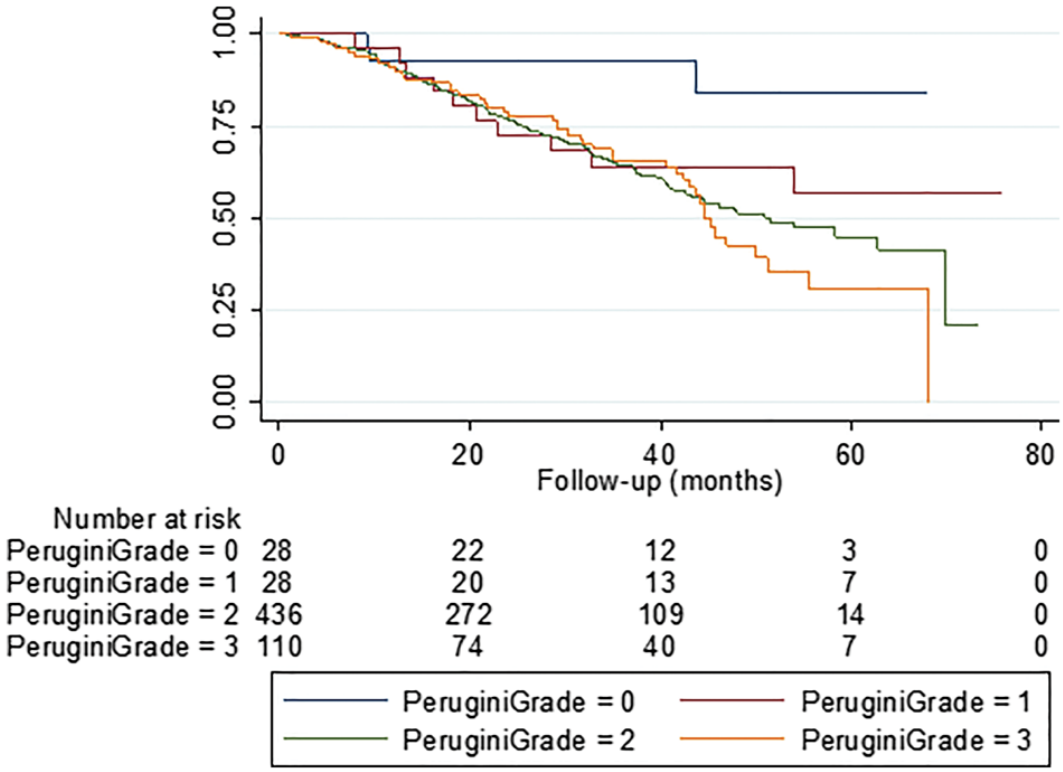

Figure 13: *Survival of all patients with ATTR amyloidosis (n=602) by DPD Perugini grade [92]. Patients with a negative DPD scan (Perugini grade 0) survived significantly longer than those with a positive scan (Perugini grade 1-3), however there was no difference in survival between grades 1-3. Note the small number of patients with a Perugini grade 1 DPD.*

Despite the apparent divergence by Perugini grade seen on the Kaplan-Meier plot above, there was no significant difference in survival in patients with a Perugini grade 1, 2 or 3 DPD in 602 patients with ATTR amyloidosis (95% of whom had abnormal cardiac uptake on DPD) [92]. Patients with no abnormal cardiac uptake on their DPD scan (Perugini grade 0) had lower mortality than those with any cardiac uptake ($p<0.04$), however there was no significant difference in survival between the other DPD grades [92].

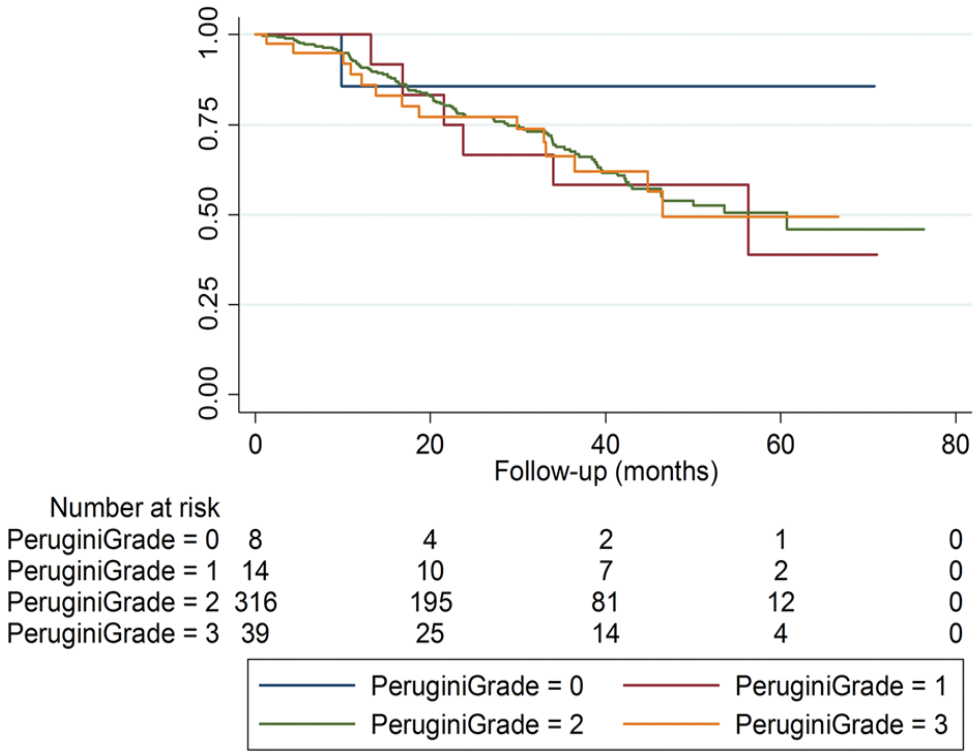

Figure 14: *Survival of patients with wtATTR amyloidosis (n=377) by DPD Perugini grade [92]. Patients with a negative DPD scan (Perugini grade 0) survived significantly longer than those with a positive scan (Perugini grade 1-3), however there was no difference in survival between grades 1-3. Note the small number of patients with a Perugini grade 1 DPD.*

This lack of prognostic significance of a positive DPD scan (Perugini grades 1-3) is even more apparent in the subset of patients with wtATTR amyloidosis (n=377) (figure 14), however note the small numbers of patients with a grade 1 DPD scan – limiting the conclusions that can be drawn regarding this subset of patients.

It can also be challenging to differentiate very subtle cardiac uptake (i.e. a 'mild' Perugini grade 1) from a negative scan with some residual blood pool activity – despite the additional use of SPECT. The clinical importance of this is not fully understood, however indications are that this is significant, given the worse prognosis associated with any degree of positive DPD (figures 13 and 14) [92] and in light of the new armamentarium of amyloid-specific therapies in development [93–95].

A semi-quantitative analysis was also described by Perugini et al in their original publication regarding the visual planar grading system, which involved the calculation of heart and whole-body retention, as well as a heart/whole-body ratio

from the planar images [86]. They found that the heart tracer retention and heart/whole-body retention ratio were higher in those with ATTR cardiac amyloidosis as compared to AL – bearing in mind that none of the patients with AL (n=10) had a positive visual DPD score in the first place [86]. They also found that the whole-body retention was significantly higher in those with ATTR or AL cardiac amyloidosis compared to controls [86]. Further work was done 6 years later by the same group in Italy in 63 patients with variant ATTR amyloidosis (44 with cardiac involvement evident on DPD), they found that the heart/whole-body ratio was positively correlated with LV mean wall thickness (Pearson's r = 0.695, *p<0.001*) and negatively with LV ejection fraction (r = -0.368, *p=0.004*) (figure 15) [96].

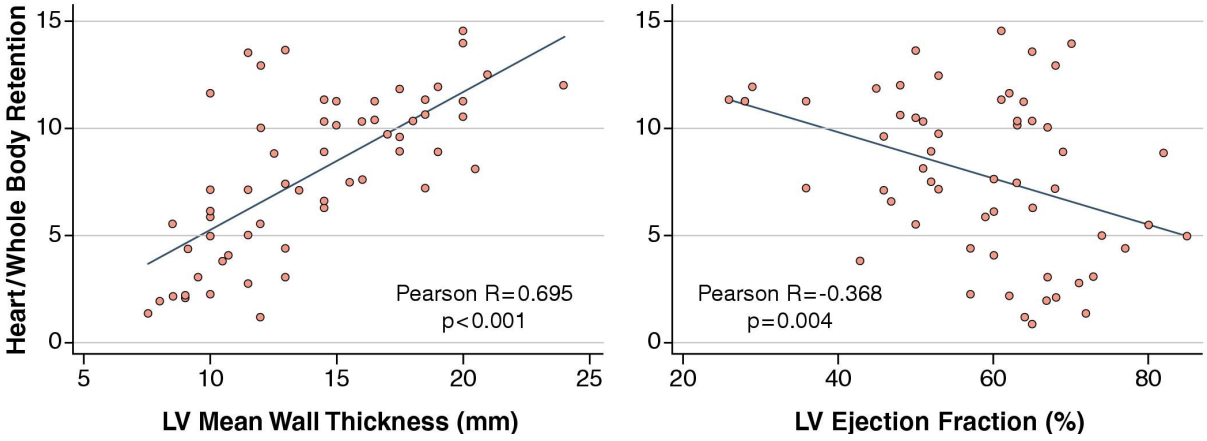

Figure 15: *Heart/whole-body ratio and it's positive correlation with LV wall thickness on the left and it's negative correlation with LV ejection fraction on the right [96]. LV = left ventricle.*

They also found that a heart/whole body ratio >7.5 was an unfavourable predictor of major adverse cardiac event-free survival [96]. Although interesting, these results regarding survival are likely heavily influenced by the 23 patients (38%) without obvious cardiac involvement – meaning that these findings more support the notion that cardiac involvement is the main driver of poor outcome in these patients, rather than that heart/whole-body ratio offers a means of quantifying cardiac amyloid burden that tracks prognosis. Furthermore, little subsequent research has been done using this semi-quantitative technique since 2011 to validate these findings in a more robust setting. In fact, anecdotally some UK centres performing DPD scans have moved away from this semi-quantitative technique in favour of the simpler visual grading system.

The most commonly used protocol for DPD scintigraphy involves the administration of 700MBq of DPD followed by an 'early' whole body planar image taken immediately after tracer injection. Three hours later a 'late' whole body planar image is performed to assess cardiac retention of tracer, followed by a single photon emission computed tomography (SPECT) with low-dose CT of the heart to confirm/refute cardiac involvement.

Regarding the other bone seeking tracers, HMDP scintigraphy, which is commonly used in France, generally uses a similar imaging protocol and reporting methodology to that used for DPD, although work has been done involving the calculation of skull retention in addition to heart and whole-body retention [97]. By comparison, imaging in PYP scintigraphy in the US is currently performed at 1-hour post-injection with both SPECT and planar acquisitions, combined with an optional 3-hour SPECT or planar acquisition [98]. While the 3-hour images are usually reported with a visual grading system that is similar to that previously proposed by Perugini et al, the earlier 1-hour acquisitions are generally reported using a more quantitative heart to contralateral lung (H/CL) ratio from the planar images, with ratios ≥1.5 at 1-hour classified as ATTR-positive [98,99]. Despite the name, it is emphasized in both the American Society of Nuclear Cardiology practice points for PYP imaging and the recent expert consensus recommendations that AL cardiac amyloidosis should always be excluded regardless of how positive the PYP scan is [89,98].

Importantly, a multi-centre study of PYP imaging in 171 patients (121 with ATTR cardiac amyloidosis) demonstrated that a H/CL ratio of ≥1.6 in patients with ATTR cardiac amyloidosis seems to predict worse survival (hazard ratio 3.91, 95% confidence interval 1.16-13.25) over five years (figure 16) [100].

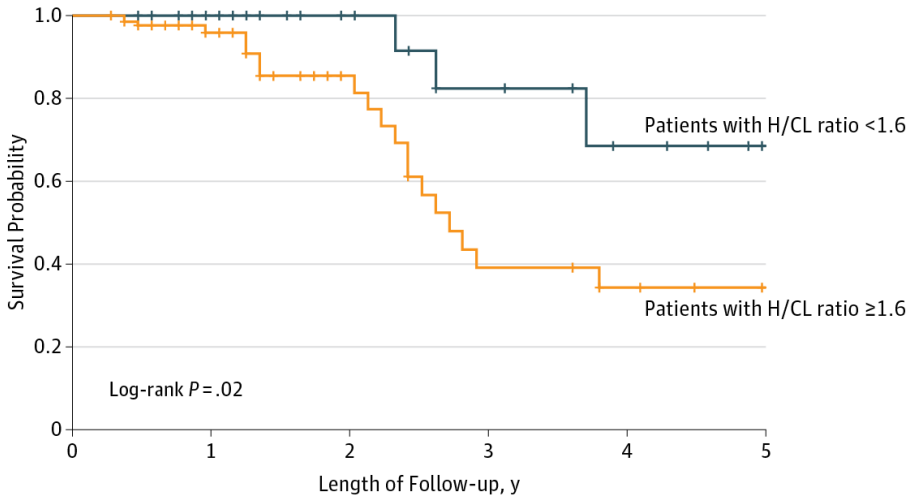

No. at risk

Patients with H/CL ratio <1.6	38	18	12	7	4	0
Patients with H/CL ratio ≥1.6	83	39	19	9	3	0

Figure 16: *Kaplan-Meier curves over five year period in patients with ATTR cardiac amyloidosis (n=121) based on H/CL ratio, showing a worse outcome with a ratio ≥ 1.6 (log-rank p=0.02) [100].*

Serum Amyloid P Component Scintigraphy

Serum amyloid P component (SAP) is a plasma glycoprotein of the pentraxin family that binds avidly to all amyloid fibril types resulting in high concentrations within amyloid deposits [101]. Hawkins et al in 1988 took advantage of this and developed a new non-invasive imaging technique for systemic amyloidosis involving the injection of ^{123}I-labelled purified human SAP [101]. Early work by the same group established that it could be used to assess the extent of organ involvement in systemic amyloidosis [102]. Later work showed a diagnostic sensitivity for systemic AA and AL amyloidosis of 90% (but a lower sensitivity for ATTR amyloidosis of 48%), with a specificity of 93% [103].

Patients are scanned 24 hours after the injection of 200MBq radiolabelled SAP (effective dose 4.5mSv), which binds with high affinity, through a likely calcium-dependent process, the amyloid fibrils [104,105]. Amyloid deposits within the liver, kidneys, spleen, adrenal glands and bone marrow can be identified [105]. In fact amyloid deposition within the liver can be detected by SAP scintigraphy even prior to the development of abnormal liver function tests or hepatomegaly [106]. Bone marrow uptake is relatively specific for AL amyloidosis, however differentiating the type of amyloid using SAP scintigraphy alone can be challenging, with substantial overlap in organ involvement between types [103,105]. Serial SAP scintigraphy can

be useful in all types of systemic amyloidosis to monitor response to therapy or disease progression [105].

Unfortunately, one of the major limitations of this technique is that cardiac amyloid deposits *cannot* be detected, likely due to the inability of the large 127kDa SAP molecule to pass into the myocardium within the half-life of the ^{123}I isotope (13 hours) due to the absence of a fenestrated endothelium [103]. Myocardial movement artefact and the proximity of the ventricular blood pool may also play a role [103]. SAP scintigraphy is also unable to visualise uptake within the gastrointestinal tract, skin or nervous system [105].

Echocardiography

There are a wide range of echocardiographic findings in cardiac amyloidosis and many of the more classical findings are not present until late in the disease [64,107]. Rather than any single parameter, it is usually a constellation of echocardiographic findings interpreted in the clinical context that raises the suspicion of cardiac amyloidosis. Appearances are usually those of a restrictive cardiomyopathy with a restrictive filling pattern, often marked concentric or eccentric LVH (with perhaps right ventricular involvement), biatrial dilatation, valve thickening and a small pericardial effusion [108,109]. Differentiating some of these changes from ventricular remodelling in response to AS can be challenging. The increased echogenicity of the myocardium, sometimes seen in advanced cardiac amyloidosis, can result in a 'speckled' appearance on echocardiography, unfortunately since the advent of tissue harmonic imaging this is can commonly be seen in even patients without cardiac amyloidosis, making it no longer a particularly useful parameter [105,110].

Impaired longitudinal LV systolic function is often an early finding, generally occurring before any evidence of LV radial systolic dysfunction [111]. The classical longitudinal strain pattern associated with all types of cardiac amyloidosis is one of apical sparing [111]. This pattern likely reflects regional changes in total amyloid mass, combined with differences in LV structure (such as greater variation in the myocyte/matrix orientation at the apex) and a greater tendency to remodelling seen in the basal segments (relating to LVOT turbulence and higher stress forces)

[112,113]. combined with Progressive diastolic dysfunction and impaired longitudinal systolic function eventually give way to overt radial systolic dysfunction in end-stage disease.

As LV wall thickness increases, LVEF and longitudinal strain tend to worsen (although the apical sparing pattern often remains throughout disease progression) [111]. WtATTR tends have greater wall thickness and often lower ejection fraction compared to hereditary ATTR and AL cardiac amyloidosis [111], however reliably differentiating them is often challenging on echocardiography alone.

Cardiovascular Magnetic Resonance

Similar to echocardiography, almost any pattern of LVH has been associated with cardiac amyloidosis on CMR, although there is evidence that asymmetrical septal LVH is the most common distribution seen in ATTR cardiac amyloidosis [114]. The degree of LVH can be quite marked (usually greater in ATTR than AL) and often disproportionate to that usually seen in hypertension or aortic stenosis [115]. LV outflow tract obstruction, normal geometry or even a DCM phenotype have also been reported (figure 17) [115]. Right ventricular (RV) hypertrophy is common [115].

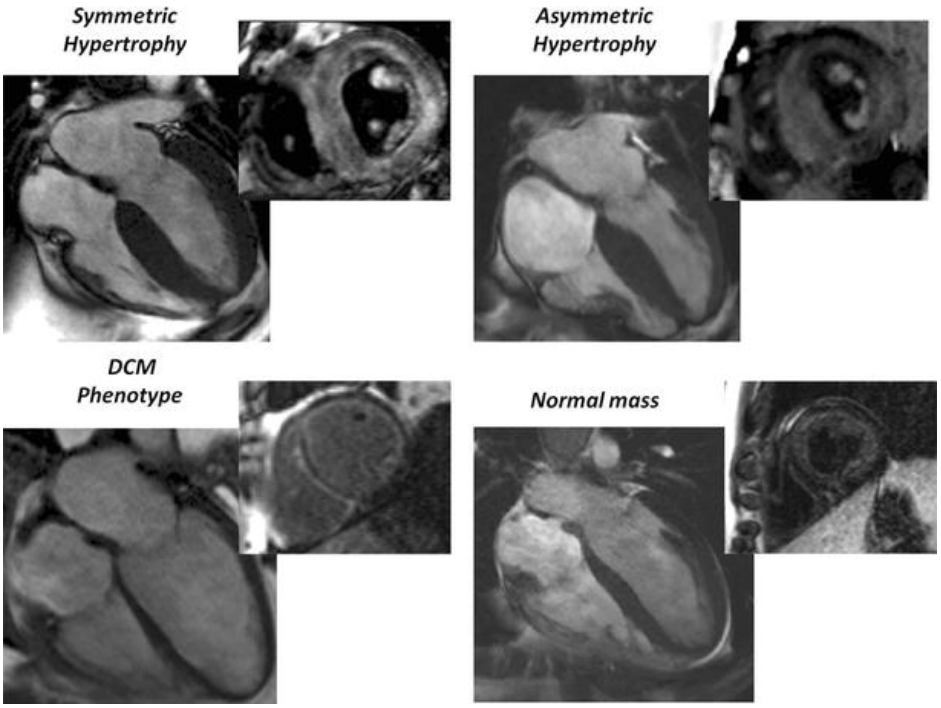

Figure 17: *Four chamber cine cardiovascular magnetic resonance images demonstrating the range of left ventricular phenotypes seen in cardiac amyloidosis, with associated short-axis late gadolinium enhancement image [115].*

One the great strengths of CMR is the non-invasive myocardial tissue characterisation it offers. The cornerstone of this is the late gadolinium enhancement (LGE) technique, which exploits the propensity for gadolinium-based contrast agents (GBCAs) to accumulate in areas of fibrosis [116]. GBCAs profoundly shorten T1, giving an increased signal on T1 weighted images and appearing bright on a T1 inversion recovery image. As a result, areas of focal fibrosis (appearing bright) are easily visualised by their relative difference in T1 compared to the adjacent normal myocardium (appearing dark) [117].

The classical LGE pattern seen in cardiac amyloidosis is global transmural or subendocardial enhancement, not conforming to a single coronary territory, however localised, diffuse or patchy LGE patterns have also been reported [118]. It has been suggested that LGE is more substantial, more often transmural and more frequently involves the right ventricle in ATTR cardiac amyloidosis compared to AL [119]. When classical, the LGE appearance in cardiac amyloidosis can be virtually pathognomonic [115].

LGE (being a relative difference test) is excellent at detecting areas of focal fibrosis, however can struggle when diffuse fibrosis is present (i.e. where there is little or no normal myocardium to help delineate the abnormal myocardium). In this situation it can become difficult to identify the normal myocardium to null and therefore the operator may erroneously null the abnormal myocardium [115]. LGE is also not easily quantified, making it less reliable at assessing change on serial imaging (for example in response to treatment) [115].

Native (pre-contrast) T1 and extracellular volume (ECV) mapping are newer techniques, which can provide quantitative information regarding the signal from the myocardium [120]. They enable the non-invasive detection of diffuse fibrosis, something which has previously been limited to the domain of the pathologist [116]. The absolute value of myocardial T1 or ECV respectively is represented in colour on the map (see figure below).

Native T1 is a composite signal of the cardiac myocytes as well as the extracellular (interstitial) space and increases with fibrosis, oedema and amyloid deposition, but

decreases with increased cellularity (athleticism), iron (thalassaemia) or fat (Anderson Fabry Disease) [116].

Conversely, ECV quantification by CMR (ECV_{CMR}) takes advantage of the extracellular nature of GBCAs and using the formula below offers a measure of the extracellular space only [121].

$$\mathbf{ECV_{CMR} = (1\text{-}haematocrit) \times (\Delta(1/T1_{myo}) / \Delta(1/T1_{blood}))}$$

Normal myocardial ECV_{CMR} is in the region of 20-26%, however varies with field strength, T1 mapping sequence and scanner manufacturer [116]. Importantly, increases in ECV_{CMR} are associated with a worse outcome and may be as important for mortality as LV ejection fraction [122]. Cardiac amyloidosis (because of the extracellular nature of the amyloid deposition) results in some of the highest ECVs of any non-ischaemic cardiomyopathy (figure 18) [123].

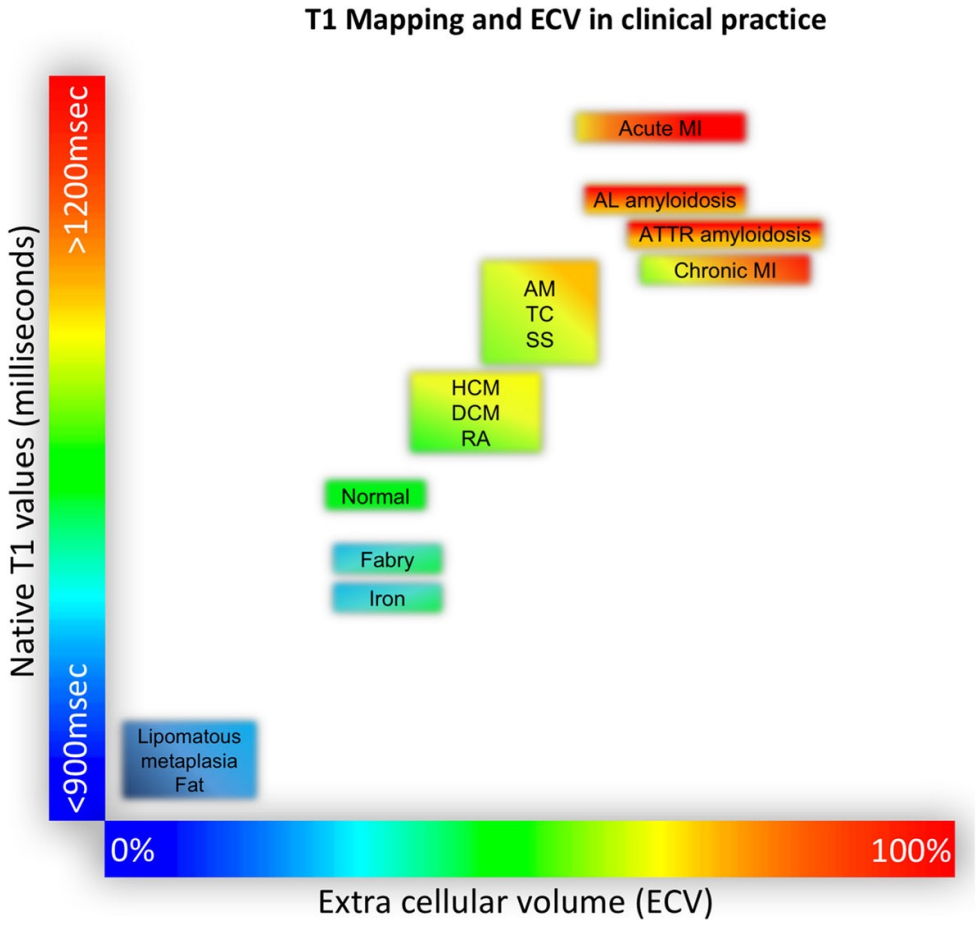

Figure 18: *Native T1 and ECV mapping in health and disease [120,124]. AM = acute myocarditis, DCM = dilated cardiomyopathy, HCM = hypertrophic cardiomyopathy, RA = rheumatoid arthritis, SS = systemic sclerosis, TC = Takotsubo cardiomyopathy.*

Native T1 and ECV_{CMR} predict mortality in both cardiac AL and ATTR [125,126], with only ECV_{CMR} remaining a significant predictor in ATTR on multivariate analysis (hazard ratio for every 3% increase in ECV_{CMR} is 1.23) [126]. ECV_{CMR} also tracks increases in DPD Perugini grade in cardiac ATTR, with some plateauing between grades 2 and 3 (figure 19) [126]. Furthermore, last year the NAC published work demonstrating in 31 patients with AL cardiac amyloidosis, that ECV_{CMR} could be used to track cardiac amyloid regression in response to chemotherapy, potentially making it an imaging biomarker capable of quantifying response to therapy [127].

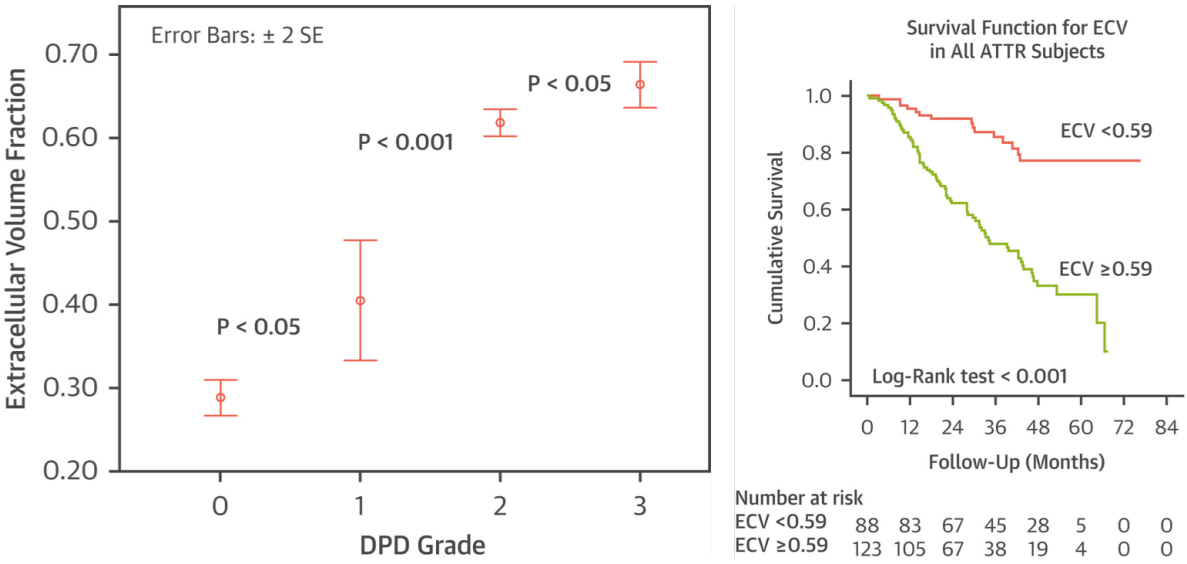

Figure 19: *On the left, a graph demonstrating change in myocardial* ECV_{CMR} *by DPD Perugini grade [126]. On the right, a Kaplan-Meier plot showing survival in patients with ATTR cardiac amyloidosis by myocardial* ECV_{CMR} *[126].*

Cardiac Computed Tomography

ECV_{CMR} is a technique commonly used clinically in many centres [120] and, as we have already discussed, offers a non-invasive means of quantifying any process which results in an increase in the myocardial extracellular space – namely amyloidosis, oedema or fibrosis [123,128]. By comparison, extracellular volume quantification by CT (ECV_{CT}), is not yet in routine clinical use, but is an attractive concept, particularly in the elderly population who may be unable to tolerate the longer scanning times of CMR or in those with implanted devices (common in patients with cardiac amyloidosis) where CMR is not yet available in all centres. CT is also less expensive and more widely available – such availability is only likely to increase with the expanded role of cardiac CT in the updated National Institute for

Health and Care Excellence clinical guideline (CG95) on the assessment of chest pain of recent onset [129]. It is particularly attractive as a simple addition to an already clinically-indicated cardiac CT scan – for example in the TAVI population, who routinely undergo cardiac CT as part of their work-up pre-procedure.

ECV_{CT} relies on a similar formula to the one used in ECV_{CMR} and again utilises the extracellular nature of the iodine-based contrast agents commonly used in CT (figure 20), however has the distinct advantage of measuring the direct effect of the iodine-based contrast agent on the measured signal (where as ECV_{CMR} measures the effect of GBCAs on protons) [116].

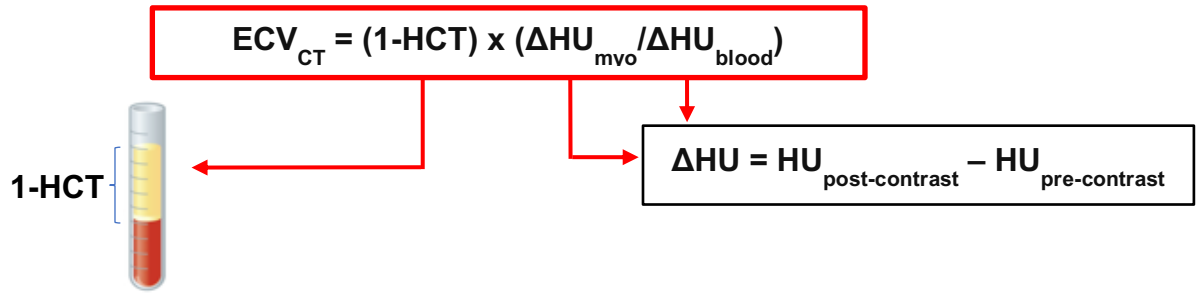

Figure 20: *Calculating ECV_{CT}. HU = Hounsfield units, HCT = haematocrit, myo = myocardium.*

The evidence base behind ECV_{CT} is growing, having been first validated in humans by Nacif et al in 2012, where it compared favourably with ECV_{CMR} in 24 healthy volunteers and patients with heart failure (r = 0.82, $p<0.001$) [130]. They used a 10-minute post-contrast image [130]. Soon after this Bandula and colleagues validated the technique against the gold standard – invasive endomyocardial biopsy (as well as ECV_{CMR}) in 23 patients with severe AS [131]. They used a bolus of contrast agent followed by an infusion to achieve equilibrium and found a good correlation with both histological markers of fibrosis (r = 0.71, $p<0.001$) and ECV_{CMR} (r = 0.73) (figure 21) [131].

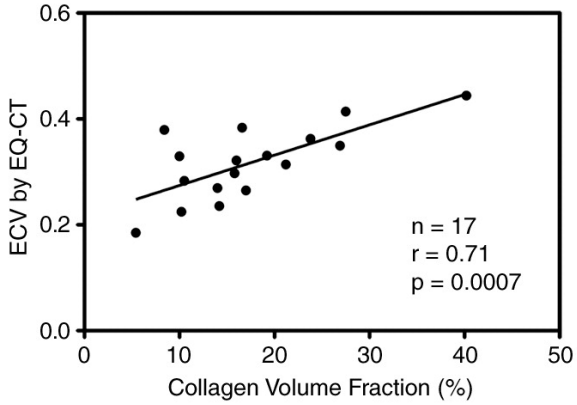

Figure 21: *The correlation between ECV_{CT} (using a contrast bolus followed by infusion) and collagen volume fraction from histology [131].*

Subsequent work by our group compared ECV_{CT} calculated using 5-minute and 15-minute post-contrast acquisitions in 26 patients with cardiac amyloidosis (18 with ATTR, 8 with AL) and 27 with AS [132]. ECV_{CT} calculated using the earlier, 5-minute post-contrast acquisition showed better correlation with ECV_{CMR} (r^2 = 0.85 vs 0.74) (figure 22) [132].

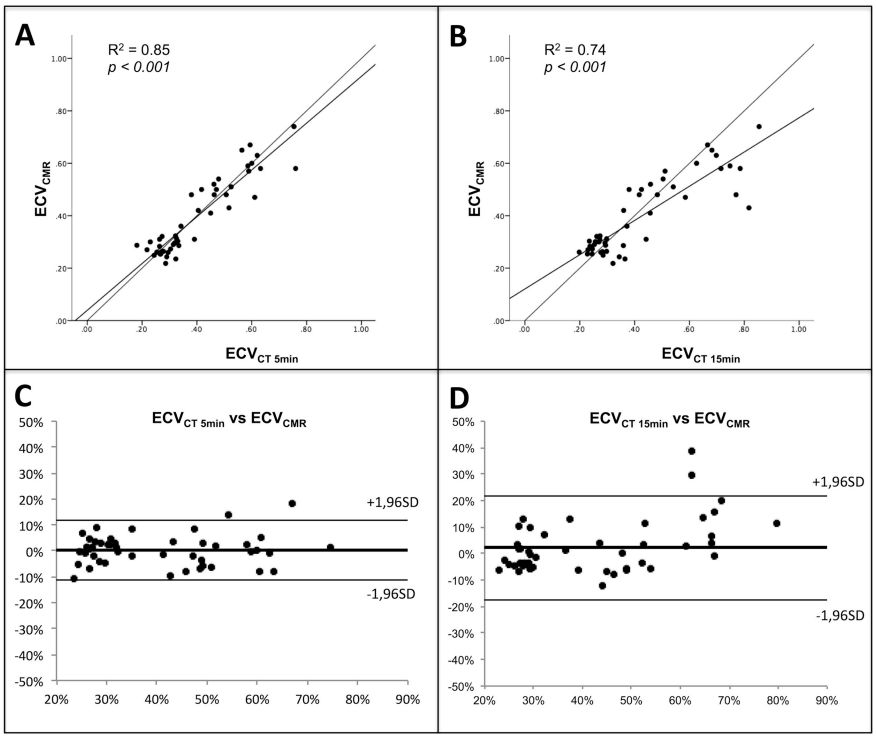

Figure 22: *The correlation and agreement between ECV_{CMR} and ECV_{CT} calculated using 5 and 15-minute post-contrast protocols. The top row demonstrates the better correlation with ECV_{CMR} seen with the earlier 5-minute (**A**, R^2 = 0.85) compared to the later 15-minute (**B**, R^2 = 0.74) post-contrast ECV_{CT} protocol. The bottom row shows the Bland-Altman plots comparing ECV_{CMR} with ECV_{CT} calculated using the 5 (**C**) and 15-minute (**D**) post-contrast protocols. ECV differences are expressed as a percentage and are calculated by subtracting ECV_{CT} from ECV_{CMR}. The thick black line represents the mean, with the lower (bottom thin line) and upper (top thin line) 95% limits of agreement [132].*

Of note, ECV_{CT} was significantly higher in those patients with definite cardiac amyloidosis than those with AS (54±11% vs 28±4%, *p<0.001*) (figure 23) and seemed to track amyloid burden in patients with ATTR as measured by DPD Perugini grade (figure 24) [132].

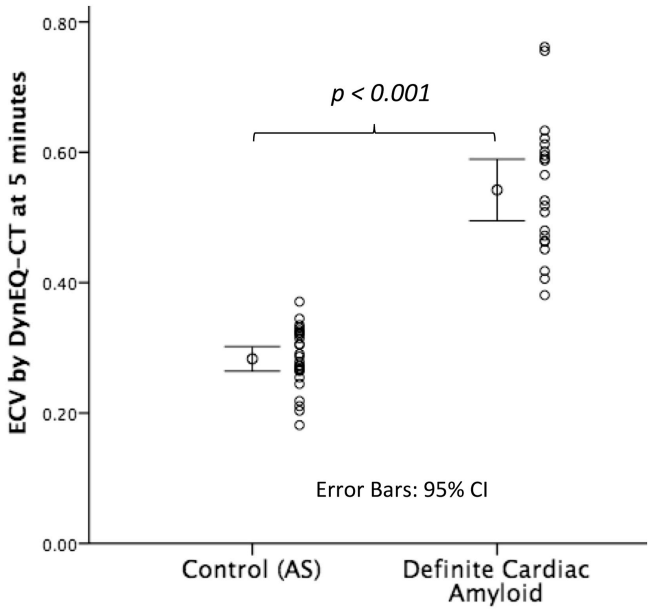

Figure 23: *ECV_{CT} was significantly higher in those patients (n=21) with definite cardiac amyloid (defined as DPD Perugini grade 2 or 3) compared to those with lone AS (54±11% vs 28±4%, p<0.001) [132].*

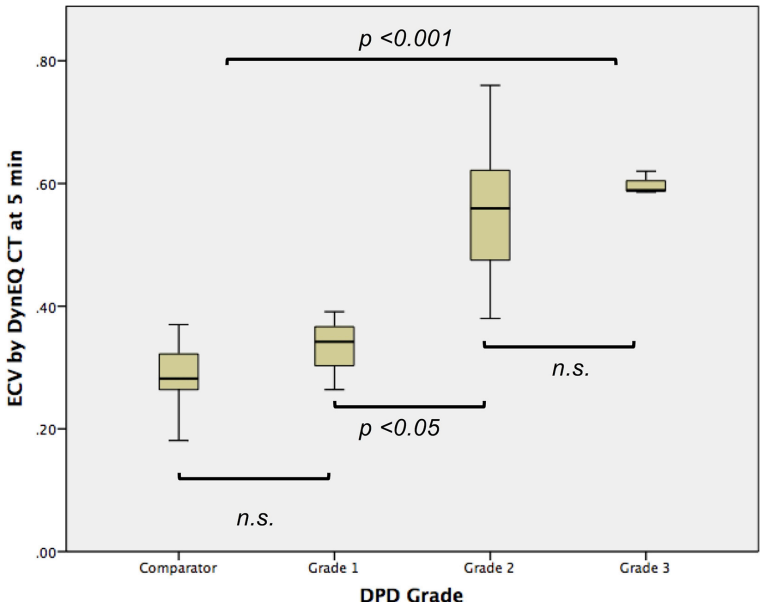

Figure 24: *ECV_{CT} tracked amyloid burden in patients with ATTR cardiac amyloidosis, as measured by DPD Perugini grade [132].*

Positron Emission Tomography

There is a great deal of interest in the validation of positron emission tomography (PET) amyloid-binding radiotracers, commonly used for cerebral amyloid imaging in Alzheimer's disease, for the diagnosis of AL and ATTR cardiac amyloidosis, but studies are small.

^{11}C-Pittsburgh compound B (PIB) is one such example, which has shown promise in the detection of both AL and ATTR cardiac amyloidosis [133,134]. Early work in 2012 showed that cardiac uptake of ^{11}C-PIB was present in 10 patients with cardiac amyloid (3 ATTR, 7 AL), but not in healthy controls (n=5) [133]. This was confirmed three years later by Lee et al, who showed that 13/15 patients with biopsy proven cardiac AL showing cardiac uptake of ^{11}C-PIB [134]. Unfortunately, one major limitation is that an onsite cyclotron is required for carbon-11 production (the half-life is only 20 minutes).

A small pilot study using ^{18}F-florbetapir (n=14) showed both LV and RV uptake in all patients with cardiac amyloid (5 AL and 4 ATTR) compared to controls (n=5), with a trend towards a higher myocardial retention index in those with cardiac AL compared to the cardiac ATTR cohort (*p=0.057*) (figure 25) [135].

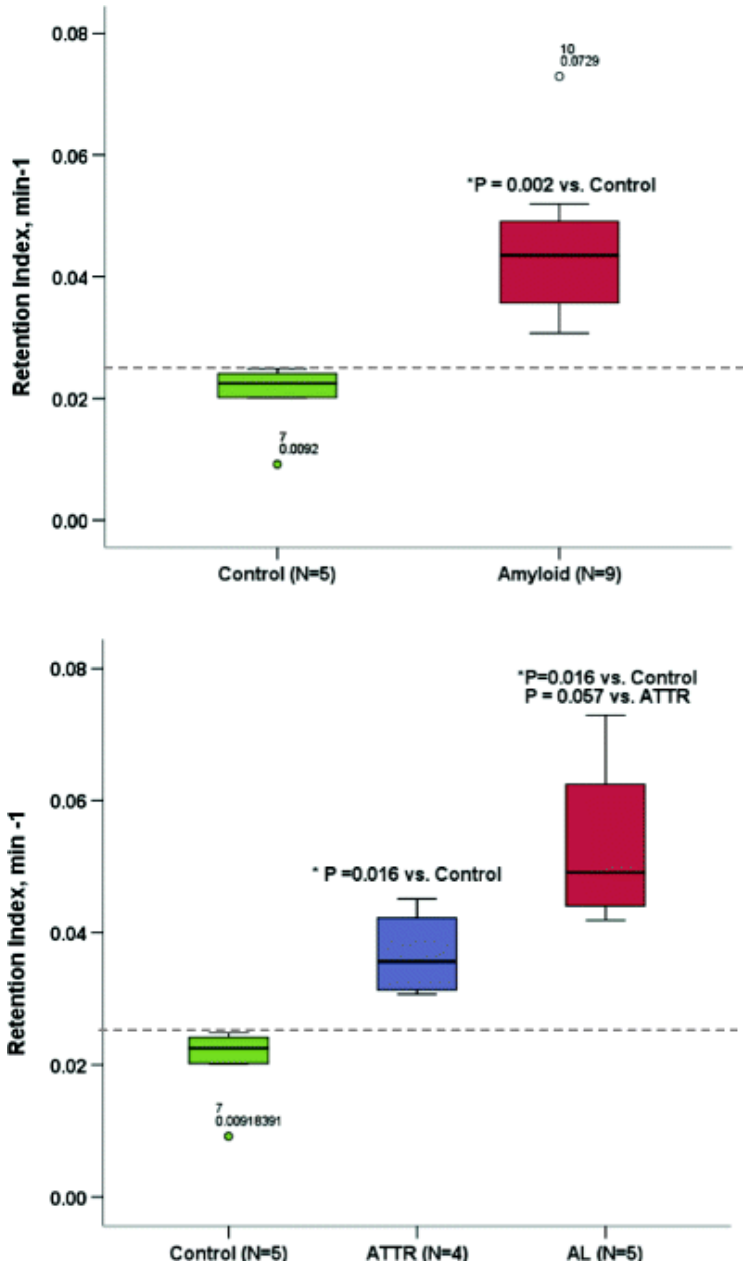

Figure 25: *Box and whisker plots showing the results of a pilot study using ^{18}F-florbetapir, showing a significantly higher retention index in patients with cardiac amyloid (n=9) compared to controls (top) and a trend towards higher values in ATTR cardiac amyloid compared to AL (bottom) [135].*

This work was supported more recently in 11 patients (3 controls, 4 cardiac AL, 4 cardiac ATTR), where there was noticeably higher cardiac uptake of ^{18}F-florbetapir in those with cardiac amyloid (both AL and ATTR) compared to controls within as little as 10 minutes after injection [136]. The longer half-life of fluorine-18 (110 minutes) means that it's distribution to sites without a cyclotron is feasible.

Another fluorine-based agent, ^{18}F-florbetaben has also been evaluated in patients with both cardiac AL (n=5) and ATTR (n=5) amyloidosis, as well as controls with hypertensive heart disease (n=4) [137]. Percentage myocardial retention of ^{18}F-

florbetaben was higher in patients with AL and ATTR cardiac amyloid, compared to controls (76.2% vs 71.2% vs 28.8%, *p=0.018*) [137] and also seemed to inversely correlate with both LV global and RV free wall longitudinal strain [137]. Further work has been carried out only this year in 22 patients with proven (n=5) or a clinical suspicion (n=17) of cardiac amyloidosis using ^{18}F-florbetaben in addition to CMR, echocardiography and bone scintigraphy in diagnostic work-up of these patients [138]. They found moderate or intense myocardial tracer retention in 14 patients (8 AL, 5 ATTR and 1 AA), while the diagnosis of cardiac amyloidosis was considered unlikely in the remainder (from follow-up imaging or biopsy) [138]. Myocardial tracer retention was significantly higher in AL compared to ATTR cardiac amyloidosis (*p<0.01*) and in cardiac amyloidosis generally compared to those without (<0.001) (figure 26).

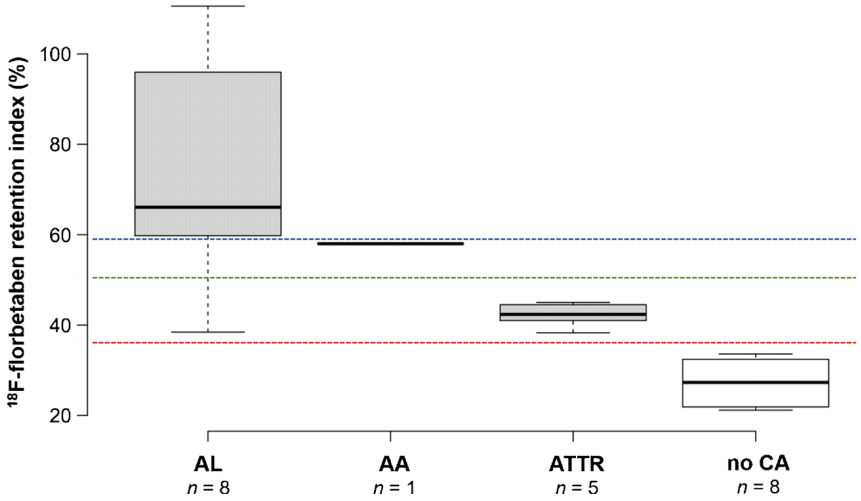

Figure 26: *Box and whisker plots showing the results of a pilot study using ^{18}F-florbetaben, showing a higher myocardial retention index in those patients with cardiac amyloidosis and in AL compared to ATTR cardiac amyloidosis [138].*

They also performed follow-up imaging with ^{18}F-florbetaben in four patients (three with AL and one with ATTR) and showed reasonable correlation with disease progression, regression or stabilisation associated with treatment strategy for these patients [138]. This is exciting data, as it may suggest that ^{18}F-florbetaben could have a role in differentiating AL from ATTR cardiac amyloidosis, as well as monitoring disease response, however numbers remain small. It is also too early for any conclusions regarding myocardial retention in AA cardiac amyloidosis, as this seems to be the only reported case in the literature [138].

Finally, results of a pilot study in 12 patients using ^{18}F-flutemetamol showed cardiac uptake in 7/8 patients with cardiac amyloidosis and none in the control patients [139]. Similar to the results with ^{18}F-florbetaben [138], the single patient in their study with AL showed a higher target-to-background ratio than those patients with ATTR cardiac amyloidosis [139].

Cardiac Biomarkers in Cardiac Amyloidosis

In a large study involving over 600 patients with wtATTR and hereditary ATTR elevations in troponin T and N-terminal pro-brain natriuretic peptide (NT-proBNP) concentration were found to be significantly associated with patient survival on univariate analysis [92].

In a separate study, an NT-proBNP of over 3000ng/L, was shown to be significantly associated with death in patients with wtATTR or hereditary ATTR related heart failure (although patients with a Val30Met mutation were excluded) [74]. As a result, it was included in a simple staging system proposed by the NAC, which also included estimated glomerular filtration rate (eGFR) [74]:

Stage I: NT-proBNP ≤3000ng/L and eGFR ≥45ml/min.

Stage II: those not included in stage I or III.

Stage III: NT-proBNP >3000ng/L and eGFR <45ml/min.

Median survival was significantly associated with disease stage (69 months for stage I vs 47 months for stage II vs 24 months for stage III) [74].

The original Mayo staging system for AL amyloidosis risk stratification was developed 15 years ago and incorporated both NT-proBNP and troponin T – where both are elevated the median survival was only 4.1 months compared to if both were normal when it was 26.4 months [140]. The more recent, updated prognostic staging system now involves serum free light chain measurements as well [141].

Treatment of ATTR Cardiac Amyloidosis

While the treatment of AL cardiac amyloidosis revolves around intensive chemotherapy and possible autologous stem cell transplantation to treat the underlying clonal proliferation of plasma cells, the management of patients with ATTR cardiac amyloidosis is very different. Currently the main focus of management

in these patients is the control of symptoms, generally through the maintenance of euvolaemia (using loop diuretics or aldosterone antagonists as needed), coupled with careful monitoring for the development of conduction disease requiring pacemaker insertion [142]. Conventional heart failure treatment (including angiotensin-converting enzyme inhibitors and beta blockers) is often poorly tolerated and as a result has a limited role. Patients with cardiac amyloidosis are particularly sensitive to calcium channel blockers, which are therefore best avoided in this population (particularly non-dihydropyridine calcium channel blockers). The mechanism for this sensitivity is unclear, although there is speculation it may be related to the affinity of ATTR cardiac amyloidosis for bone tracers such as DPD [142]. A similar (although generally less severe) sensitivity is also seen to digoxin, which has been shown in vitro to bind directly to the amyloid fibrils [143], so digoxin should only be used with caution if needed in these patients.

Liver transplantation has a role in the treatment of patients with hereditary ATTR and dominant neuropathic involvement (particularly due to the Val30Met mutation) [142,144]. Unfortunately, cardiac amyloid deposition in these patients can progress despite transplantation (perhaps more so in mutations other than Val30Met) [145,146], nor does it prevent related arrhythmias requiring permanent pacemaker (PPM) insertion [147]. Heart or combined heart and liver transplantation have been performed, however patients undergoing heart transplantation for cardiac amyloidosis seem to have a lower survival compared to those with other forms of cardiomyopathy [142]. Data from 2005 from the United Network of Organ Sharing showed a 49% mortality within a mean follow-up of 40 months post orthotopic heart transplant in patients with a diagnosis of amyloidosis (however the type was not stipulated) [142]. However, there are now small case series showing improved outcomes post cardiac transplant in selected patients, particularly those with AL cardiac amyloidosis, where adjunctive autologous stem cell transplantation seems to offer improved survival post cardiac transplantation [149,150]. Furthermore, these patients (particularly those with wtATTR) are often elderly with multiple comorbidities, which may make cardiac transplantation both unfeasible and unethical (given the shortage of donor organs) in many cases [142].

Fortunately, novel, potentially disease modifying therapies have been and are being developed for ATTR cardiac amyloidosis.

Tetramer Stabilising Agents

The results of the phase 3 ATTR-ACT trial have recently been published looking at the role of the tetramer stabilising agent Tafamidis in the management of patients with ATTR cardiac amyloidosis [93]. They demonstrated a significant reduction in all-cause mortality, cardiovascular-related hospitalisations and a reduction in the decline in functional capacity and quality of life as compared to placebo (figure 27) [93].

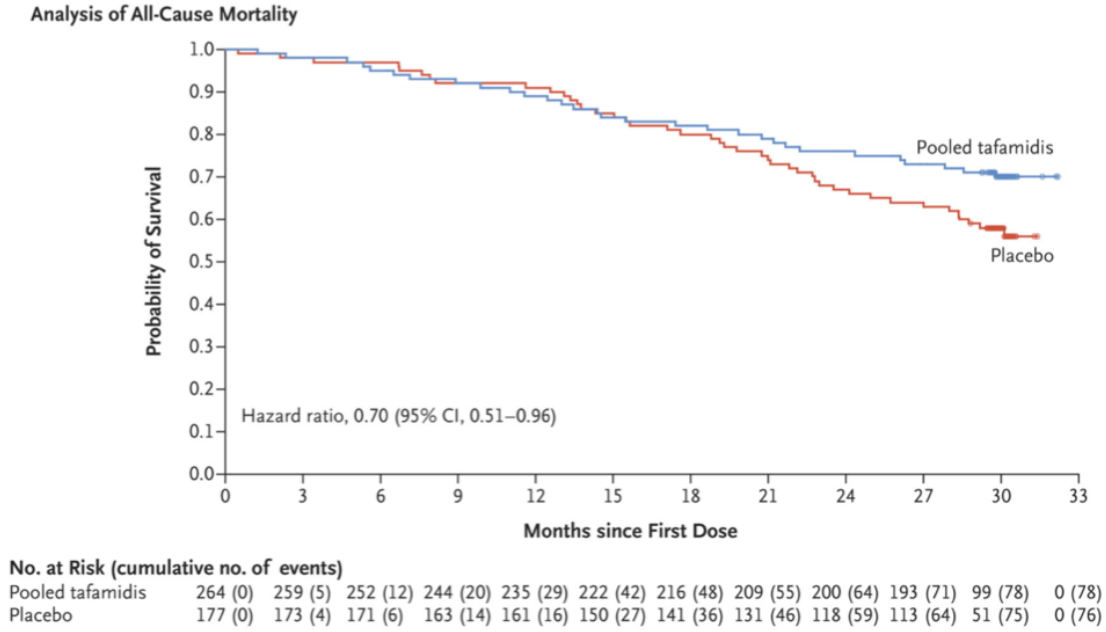

Figure 27: *Results from the ATTR-ACT study – analysis of all-cause mortality. Kaplan-Meier plot showing survival in patients with ATTR cardiac amyloidosis treated with Tafamidis or placebo over a 30 month follow-up period [93].*

It is important to note that patients with NYHA class IV symptoms were excluded from this study and in the subgroup analysis patients with NYHA class III had no improvement in mortality or cardiovascular-related hospitalisation with Tafamidis [93].

As a result of these study findings, Tafamidis was initially approved for use in the UK in patients with wild-type or hereditary ATTR cardiomyopathy under the Early Access to Medicines Scheme (EAMS). Subsequently, in October this year, the National Institute for Health and Care Excellence released its final appraisal of Tafamidis and

the outcome was that it is not recommended for use in the treatment of patients with wild-type of hereditary ATTR cardiomyopathy (the appeals process is still ongoing).

AG10 mimics the protective effect of the T119M mutation, which reduces TTR tetramer dissociation compared to wild-type, acting therefore as a selective TTR stabiliser [151,152]. AG10 restored serum TTR to the normal range in both mutant and wild-type patients in a placebo controlled trial of 49 patients with ATTR cardiomyopathy over a period of 28 days [151]. A phase 3 trial is now ongoing (Study of AG10 in Amyloid Cardiomyopathy, NCT03458130).

Another tetramer stabilising agent, Diflusinal, is a non-steroidal anti-inflammatory drug, which has a role in the treatment of FAP – slowing the progression of neurological impairment and maintaining quality of life [153]. It's use in the treatment of ATTR cardiac amyloidosis however is controversial – primarily due to the risks associated with the inhibition of cyclooxygenase enzymes (gastrointestinal bleeding, fluid retention, renal dysfunction and hypertension) [142].

Doxycycline and Tauroursodeoxycholic Acid

Doxycycline and Tauroursodeoxycholic acid in combination have been shown to have a synergistic action at removing amyloid fibrils from the gastrointestinal tract of TTR Val30Met transgenic mice [154]. A subsequent phase 2 study in 20 patients showed no serious adverse events and no progression in cardiac or neurological involvement over one year [154]. A phase 3 study is now ongoing in patients with ATTR cardiac amyloidosis (NCT03481972).

Anti-SAP Antibodies

As previously discussed, all amyloid deposits (regardless of protein precursor) contain large amounts of SAP, a plasma glycoprotein. A phase 1 trial using (R)-1-[6-[(R)-2-carboxy-pyrrolidin-1-yl]-6-oxo-hexanoyl]pyrrolidine-2-carboxylic acid (CPHPC or Miredesap) to remove SAP from the plasma, followed by administration of a fully humanised monoclonal IgG1 anti-SAP antibody (Dezamizumab) to target remaining SAP in amyloid deposits proved safe and effective in 15 patients at initiating clearance of established amyloid deposits from the liver, kidney and a lymph node [155]. Part B of the phase 1 trial was published early last year and demonstrated, in

small numbers of patients (most with AL amyloidosis), a dose-related clearance of liver, kidney and spleen amyloid deposits on SAP scintigraphy [156]. In the six patients with cardiac amyloidosis (3 AL, 3 ATTR) who were included in the study – four developed a transient (up to fivefold) rise in NT-proBNP and one with AL exhibited a significant (17%) reduction in LV mass following treatment, however no change was seen in the LV mass or DPD Perugini grade in those three patients with cardiac ATTR [156].

Small Interfering RNA Therapy

Alnylam Pharmaceuticals have developed small interfering RNA (siRNA) therapies, which target a sequence in the 3' untranslated region of mRNA in TTR (both mutant and non-mutant) [157]. Phase 1 trials of ALN-TTR01 and the second generation ALN-TTR02 showed great promise resulting in reductions in transthyretin levels of up to 94% [157]. Unfortunately, the phase 3 clinical trial ENDEAVOUR, looking at Resuviran (ALN-TTRSC) in the treatment of patients with hereditary ATTR and cardiac involvement had to be stopped early due to deaths in the study population. The phase 3 APOLLO trial investigating the role of Patisiran (ALN-TTR02) in the treatment of patients with hereditary TTR polyneuropathy showed improvement in multiple clinical manifestations of the disease (including quality of life scores and gait speed) [158]. Subsequent analysis of the cardiac sub-population of the study (n = 126 patients) showed a reduction in NT-proBNP levels, LV wall thickness, increased end-diastolic volume, GLS and an improved stroke volume relative to placebo [94]. There were also lower rates of all-cause hospitalisation and mortality at a median follow-up of 18.7 months in those patients treated with Patisiran (figure 24) [94].

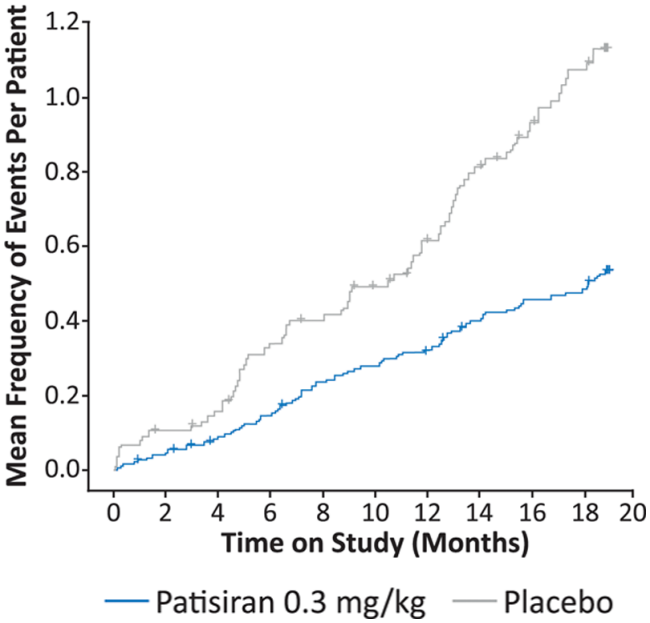

Figure 24: *Results from the APOLLO study. Graph of the average number of events per patient over the 18 months of follow-up on Patisiran compared to placebo. Event = composite rate of all-cause hospitalisation and mortality [94].*

Antisense Oligonucleotides

Inotersen (previously known as IONIS-TTR$_{Rx}$ or ISIS-TTR$_{Rx}$) is a chimeric antisense inhibitor of TTR [159]. It prevents production of both wild-type and mutant TTR protein by binding to the TTR mRNA resulting in degradation of TTR mRNA by RNase H [159]. Initial results in monkeys showed an 80% reduction in liver TTR mRNA and plasma wild-type TTR [159]. Early findings in humans showed an approximately 50% reduction in plasma TTR by Day 29 of treatment [159]. The NEURO-TTR trial assessing the role of Inotersen in the treatment of TTR-related FAP, improved patient quality of life and neuropathy impairment scores over 66 weeks compared to placebo [160]. The 108 (63%) patients in the study with 'cardiomyopathy' (defined as either a diagnosis of hereditary ATTR cardiomyopathy, or an interventricular wall thickness ≥13mm) showed similar improvements in health scores [161]. A separate investigator sponsored trial of Inotersen was started in 2014 for patients with hereditary ATTR and wtATTR cardiac amyloidosis [95]. So far they have enrolled 33 patients, all of whom have biopsy proven TTR and an interventricular septal diameter of ≥13mm [95]. At 3 years they have seen a ~14% reduction in LV mass, a 14m improvement in 6-minute walk test distance and stabilisation of LVEF, LV strain and BNP [95]. They have also suggested that

Inotersen may improve survival given that 93% of patients with 3 years of follow-up are alive [95].

Biopsy

Amyloid fibrils show a pathognomonic apple-green birefringence under cross-polarised light microscopy, when stained with Congo Red (figure 25) [62]. Electron microscopy can also be used to identify amyloid deposits in cases where Congo Red results are inconclusive [62]. Once the presence of amyloid fibrils is confirmed, immunohistochemistry can be used to identify fibril type in around 60-70% of cases (figure 29) [62]. If this fails, proteomic typing of the amyloid can be performed using mass spectrometry [162].

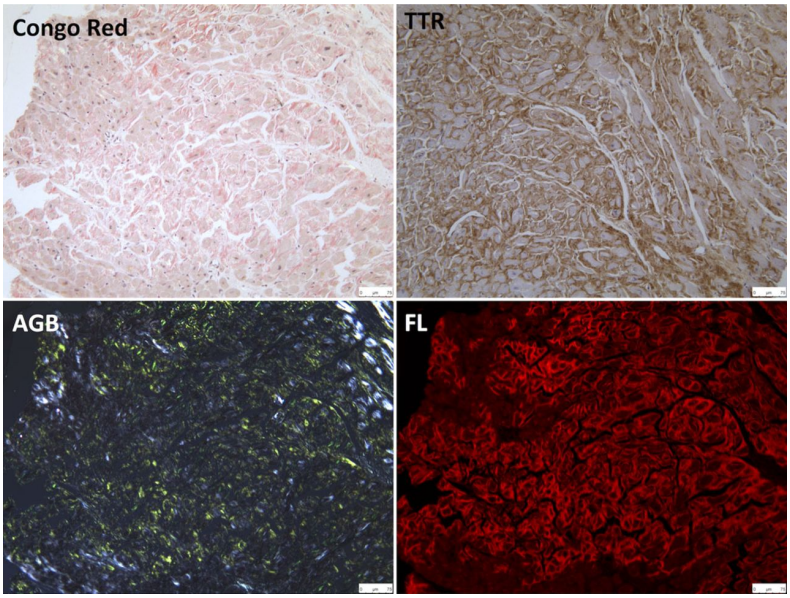

Figure 29: *Endomyocardial biopsy results for a patient with severe AS and ATTR cardiac amyloidosis [163]. Congo red staining under brightfield light (Congo Red), under cross-polarised light with typical apple green birefringence (AGB) and under fluorescent microscopy (FL). Top right panel (TTR) shows transthyretin-specific immunohistochemistry demonstrating widespread ATTR cardiac amyloid deposition (brown).*

Non-cardiac Biopsy

Abdominal fat pad, salivary gland, bone marrow or rectal biopsy can be useful in the work-up of patients with suspected cardiac amyloidosis – particularly if imaging and blood tests have proven unhelpful in typing the amyloidosis to hopefully obviate the need for a more invasive endomyocardial biopsy. The sensitivity however of these invasive techniques very much depends on the type of underlying amyloid. Congo red staining of fat aspirates can detect amyloid deposits in 84% of patients with

cardiac AL amyloidosis (allowing typing as AL by immunohistochemistry in 47%), compared to only 45% of hereditary ATTR and 15% of wtATTR [164]. In short, a negative fat aspirate does not exclude ATTR (particularly wtATTR).
By comparison salivary gland biopsy has a ~60% sensitivity in AA and AL amyloidosis [165] and importantly has similar sensitivity in those with AL amyloidosis who had a negative fat aspirate [166]. Rectal biopsy is frequently positive in hereditary ATTR (~80%), compared to 50% of wtATTR [167], however bear in mind this study only performed a rectal biopsy on four patients with wtATTR. Bone marrow biopsy is positive in ~40% of patients with hereditary ATTR and 30% of those with wtATTR [167].

Endomyocardial Biopsy

Until recently, the gold standard for diagnosing cardiac amyloidosis has been endomyocardial biopsy, however the development of a non-invasive diagnostic pathway for ATTR, means that it is no longer necessary in all patients with suspected cardiac amyloidosis. It is perhaps now most commonly performed where there remains a suspicion of AL cardiac amyloidosis (in the event of a plasma cell dyscrasia) – to exclude or confirm the diagnosis, before starting life-changing chemotherapy in an often elderly person for what could prove to be an unrelated, incidental MGUS (present in 7.5% of those aged 85 and over) [168].

Endomyocardial biopsy is an invasive procedure, which carries some associated risk – with overall complication rates of up to 6% [169,170], however this is likely to have improved over time, such that major complications (eg RV perforation) occur much less frequently (<1%) [170,171]. Complication rates will also vary depending on whether the left or right ventricle is sampled.

Another significant risk of this procedure is sampling error, with only one quarter of endomyocardial biopsies providing a diagnosis when done for unexplained heart failure [171]. Specifically, in those patients with an unexplained restrictive cardiomyopathy (into which category patients with cardiac amyloidosis are likely to fall), the pick-up rates are somewhat better at nearly 30% [171]. This will of course depend on the number of samples taken (average was 5.6 in this particular study [171]), the nature of the disease and the site of sampling.

1.3 Early Evidence for Dual Pathology

Given the high prevalence of both AS and ATTR cardiac amyloid in the elderly, it was highly likely that the two would co-exist, however when this project was beginning in 2016, there was only limited evidence for this in the literature. Nietlispach and colleagues had found that in patients with AS, who had undergone TAVI and subsequent valve explantation at autopsy (n=17) or surgery (n=3), cardiac amyloidosis was present in a third of patients and contributed to patient death in the majority [172]. There was also an abstract, which had just been published at that time using PYP scintigraphy to screen 40 patients undergoing TAVI, which had found a 10% prevalence of cardiac amyloidosis [173].

Indeed, our previous work also supported this – we had found that 6% of patients (aged over 65 years) undergoing SAVR for severe AS had evidence of wtATTR cardiac amyloidosis on endomyocardial biopsy, which in turn was associated with a higher mortality (50% compared to 9%, figure 30) [163].

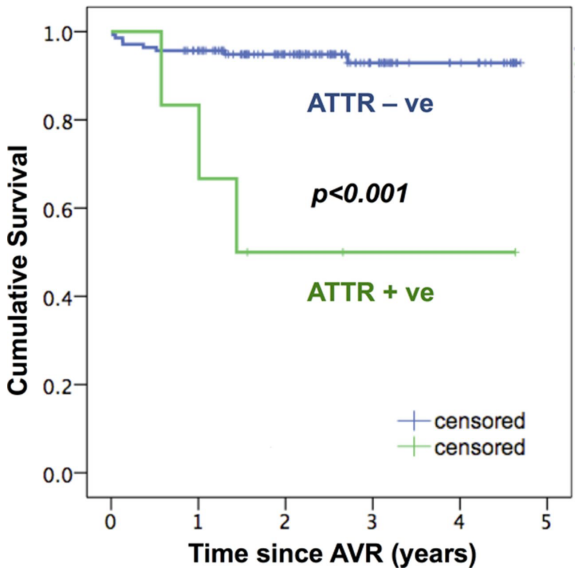

Figure 30: *Results from the RELIEF-AS study. Kaplan-Meier plot comparing cumulative survival in AS patients post SAVR with and without biopsy proven wtATTR cardiac amyloidosis. Median follow-up was 2.3 (0.02-4.7) years [163].*

This study was therefore the natural progression of this previous work, particularly as the TAVI population is often older and therefore likely to have a higher prevalence of cardiac amyloidosis.

Chapter 2: Study Design and Methodology

2.1 ATTRact-AS

ATTRact-AS (A sTudy invesTigating the Role of occult cArdiaC amyloid in The elderly with Aortic Stenosis) is registered on ClinicalTrials.gov under the identifier NCT03029026. This study forms the bulk of my PhD, for which I was awarded a British Heart Foundation Clinical Research Training Fellowship (FS/16/31/32185) on 9th May 2016.

It was clear when planning this study that endomyocardial biopsy would not be possible, nor appropriate, as a means of diagnosing cardiac amyloidosis in our study patients. In view of the recently publish non-invasive diagnostic guidelines for cardiac amyloidosis involving the use of DPD scintigraphy and its reported sensitivity of 99% for ATTR cardiac amyloidosis [88], it was felt that this would be the most appropriate, ethical and practical means of detecting cardiac amyloidosis in our patients.

Initial Research Ethics Committee (REC) approval was obtained on 8th August 2016, followed by Health Research Authority approval on 23rd August 2016 - as the heart muscle sub-study of the Evaluation of Integrated Cardiac Imaging (EVINCI), REC Reference: 10/H0721/79, IRAS ID: 63298. This study conformed to the principles of the Helsinki Declaration and all participants provided written consent for their involvement. Site approval to begin recruitment at Barts Heart Centre (BHC) was obtained on 30th September 2016.

To support recruitment and improve the generalisability of our results the decision was made to include the John Radcliffe Hospital in Oxford as a second centre for study patient recruitment and DPD scanning. REC approval of a substantial amendment to this effect was obtained on 9th January 2018.

2.2 Aims

We know that AS and cardiac amyloid can coexist in the younger SAVR population, however to what extent this is the case in the elderly TAVI population is not known, nor are the clinical implications of this dual pathology in this cohort of patients.

ECV_{CT} is an appealing means of potentially identifying patients with suspected cardiac amyloidosis, particularly in the TAVI population, as it can be done in the same sitting as their TAVI work-up CT, however its use as a screening tool in these patients has never been explored.

Finally, DPD scintigraphy now plays a central role in the non-invasive diagnostic work-up of patients with suspected cardiac amyloid, but a means of quantifying tracer uptake reliably (outside of the Perugini grading system) is currently lacking [86].

The aims of this thesis were therefore threefold:

1. To confirm the prevalence of occult cardiac amyloidosis in patients referred for TAVI and the clinical impact it may have (procedural complications, symptom response, mortality).
2. To investigate the potential role of ECV_{CT} in the detection of occult cardiac amyloidosis, in patients referred for TAVI.
3. To explore DPD quantification techniques and potentially develop a novel DPD imaging biomarker for therapeutic monitoring.

The results pertaining to each of these aims will be presented in chapters three, four and five.

2.3 Methodology

ATTRact-AS was a prospective observational cohort study with a minimum of 1-year follow-up. Patients aged 75 or older referred to either the BHC in London or the John Radcliffe Hospital in Oxford for consideration of TAVI for severe AS were eligible for inclusion in the study. The only exclusion criteria were previous AV replacement or an inability to provide informed consent. The proposed total sample size was 200 patients recruited from both sites.

Patients were recruited *prior* to TAVI, so in order to capture the best representation of the elderly AS population, both those patients undergoing intervention and those decided for medical therapy (or surveillance) were recruited.

Recruitment took place at the BHC site predominantly from TAVI clinics, whereas recruitment at the John Radcliffe Hospital was from telephone contact with patients on their TAVI waiting list and I would then travel to the John Radcliff Hospital for ~1 day/month to supervise scanning the patients (figure 31). Recruitment at the John Radcliffe Hospital site generally yielded fewer patients as overall there were fewer TAVI procedures performed there (therefore smaller recruitment pool, figure 31), but also importantly patients were contacted by telephone and asked to attend for an additional hospital visit solely for research purposes, which was often challenging for these patients (who may not live particularly locally) and therefore meant that many, understandably, declined. This compares to those patients at the BHC site, who were met in person and the hospital visit was usually timed with another clinical appointment (therefore avoiding an additional journey to hospital for many patients).

Measures of Exposure:

The prevalence of cardiac amyloidosis was assessed in those patients referred for TAVI with severe AS using DPD scintigraphy. In addition to this, those undergoing TAVI work-up CT at the BHC site underwent ECV_{CT}.

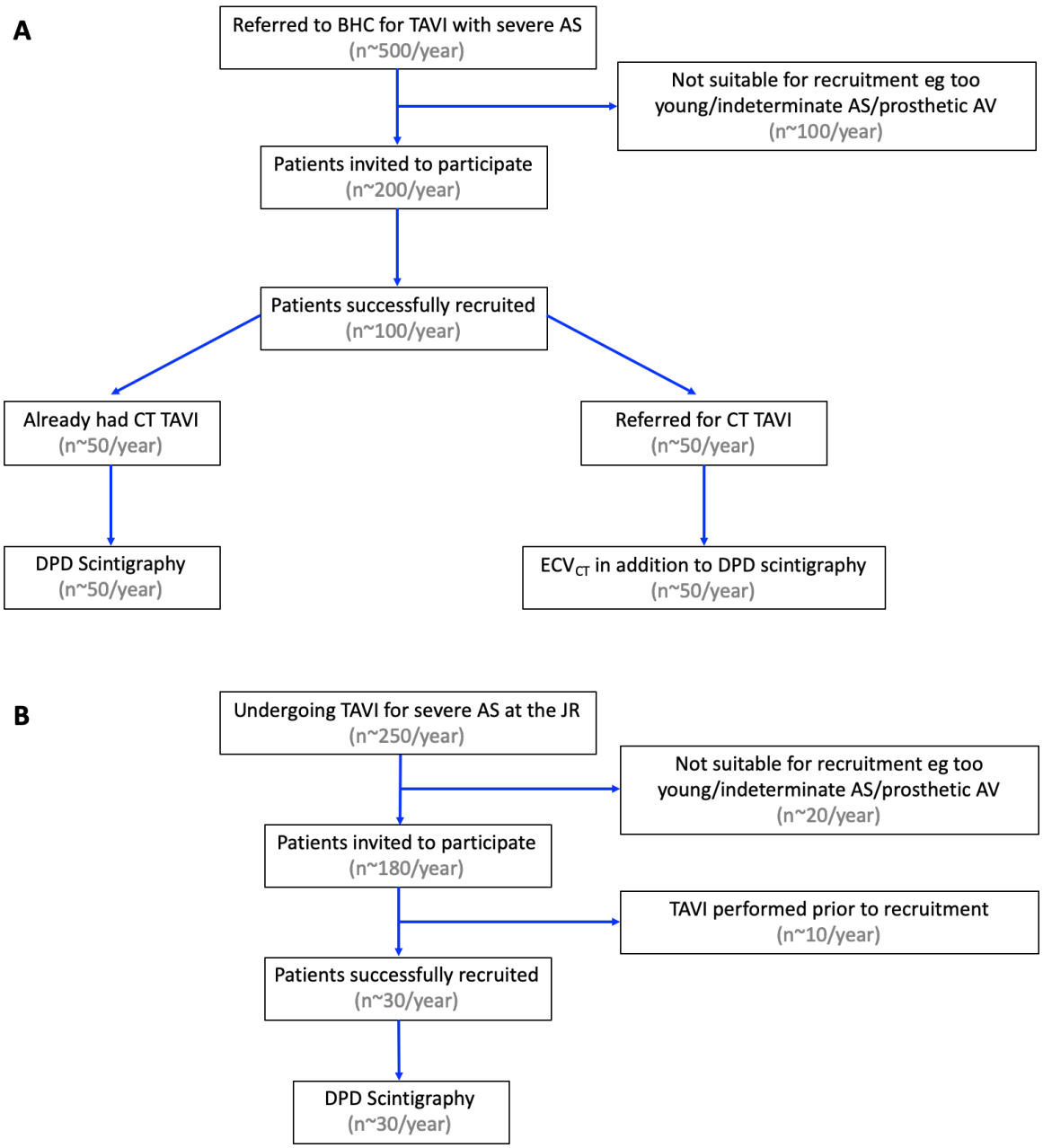

Figure 31: *Flow chart demonstrating the recruitment pathway for ATTRact-AS and estimated numbers at both BHC (**A**) and the John Radcliffe Hospital (**B**). BHC = Barts Heart Centre, JR = the John Radcliffe Hospital.*

Outcome Measures:

The primary outcome measure was patient mortality. Secondary outcome measures were peri-procedural complications and symptomatic benefit post-TAVI.

Power Calculations:

The sample size calculation was based on a TAVI patient 1-year mortality of 21.4% [174] and a wtATTR prevalence in the population of 20% [72,172]. Our early data in

patients undergoing SAVR for severe AS suggested a significantly increased mortality in those found to have concomitant cardiac amyloid compared to those who did not (50% vs 6.9% mortality at a median of 2.3 years follow-up) [163]. Using this preliminary data and knowing that the TAVI cohort are generally older and frailer than SAVR cohorts, we estimated that a 40% mortality at 1-year was likely in those patients with dual AS and cardiac amyloid pathology. In order to detect this mortality rate with adequate power, with a p-value of 0.05, a total sample size of 188 was required. This was felt to be a realistic recruitment target (approximately 500 TAVI procedures per year at BHC site alone).

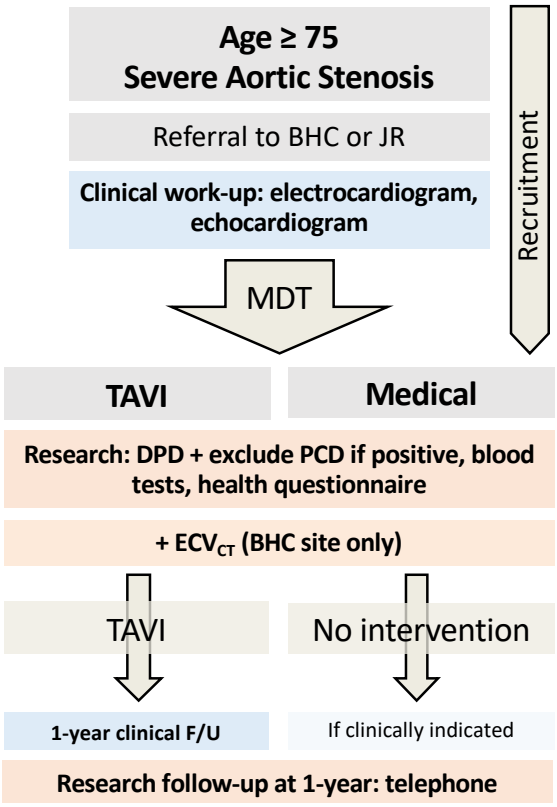

Figure 28: *Overview of ATTRact-AS protocol and investigations performed. BHC = Barts Heart Centre, DPD = ^{99m}Tc-3,3-diphosphono-1,2-propanodicarboxylic, ECV_{CT} = extracellular volume quantification by CT, JR = John Radcliffe Hospital, PCD = plasma cell dyscrasia, TAVI = transcatheter aortic valve intervention.*

Baseline Investigations:

The baseline assessment included: clinical history, quality of life questionnaire (EuroQol-5-dimension-5-level, EQ-5D-5L) [175], a 6-minute-walk test [56,176], blood sampling for haematocrit, biomarkers (NT-proBNP and high sensitivity troponin T, hsTnT) and biobanking (also for AL exclusion if DPD scintigraphy is positive, as we

know that 51% of patients with cardiac AL will have a positive DPD scan), as well as tests performed as part of the routine pre-TAVI work-up (including clinical ECG).

Health Questionnaire

The EQ-5D-5L health questionnaire was recorded at baseline (recruitment) and at 1-year post-TAVI in those who underwent the procedure. The questionnaire is broken down into two parts: the first consists of multiple-choice questions on five key domains: mobility, self-care, usual activities, pain/discomfort and anxiety/depression (figure 33).

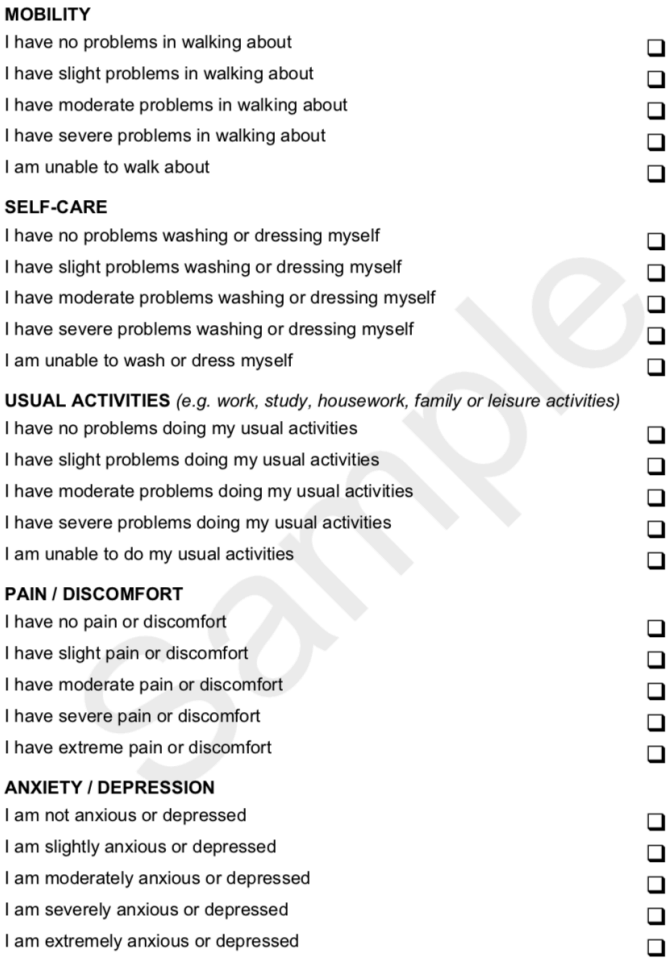

MOBILITY
I have no problems in walking about ❑
I have slight problems in walking about ❑
I have moderate problems in walking about ❑
I have severe problems in walking about ❑
I am unable to walk about ❑

SELF-CARE
I have no problems washing or dressing myself ❑
I have slight problems washing or dressing myself ❑
I have moderate problems washing or dressing myself ❑
I have severe problems washing or dressing myself ❑
I am unable to wash or dress myself ❑

USUAL ACTIVITIES *(e.g. work, study, housework, family or leisure activities)*
I have no problems doing my usual activities ❑
I have slight problems doing my usual activities ❑
I have moderate problems doing my usual activities ❑
I have severe problems doing my usual activities ❑
I am unable to do my usual activities ❑

PAIN / DISCOMFORT
I have no pain or discomfort ❑
I have slight pain or discomfort ❑
I have moderate pain or discomfort ❑
I have severe pain or discomfort ❑
I have extreme pain or discomfort ❑

ANXIETY / DEPRESSION
I am not anxious or depressed ❑
I am slightly anxious or depressed ❑
I am moderately anxious or depressed ❑
I am severely anxious or depressed ❑
I am extremely anxious or depressed ❑

Figure 33: *The first part of the EQ-5D-5L health questionnaire (sample example taken from the EuroQol website).*

Those patients rating themselves as having moderate or more problems were considered as having 'significant' difficulty in that particular domain. The second part of the health questionnaire is the EuroQol visual analogue scale (EQ-VAS), which is a self-reported score from 0 (worst health imaginable) to 100 (best health

imaginable). The use of the EQ-5D-5L as part of ATTRact-AS has been registered online with the EuroQol Research Foundation.

Electrocardiogram

The was performed as part of routine clinical care prior to consideration of TAVI. Sokolow-Lyon (S-L) criteria was calculated as the sum of the voltage of the S-wave in lead V1 and the R-wave in lead V5 or V6 (whichever was greater) [177]. The voltage/mass (V/M) ratio was defined as the S-L total divided by the indexed LV mass by echocardiography [178]. The V/M ratio or S-L criteria were not calculated in patients with bundle-branch block or a ventricular paced rhythm [179]. Low limb lead voltages were defined as all limb leads with an amplitude $\leq$ 0.5mV. Unfortunately, ECGs were not available from the medical records in 23 patients (12%, 4 with AS-amyloid, 19 with lone AS) and were not collected routinely for research purposes, as this was not included in our original research protocol.

Echocardiography

All study patients underwent clinical transthoracic echocardiogram (TTE), primarily for assessment of AS severity (including aortic valve peak velocity, mean gradient, and valve area quantification), any concomitant valve pathology, left and right ventricular systolic and left ventricular diastolic function, according to the local protocol, which is based on the American Society of Echocardiography, the British Society of Echocardiography, as well as the European Association of Cardiovascular Imaging guidelines [11,180,181].

LVEF was calculated using Simpson's biplane where possible, or otherwise was quantified visually. Indexed stroke volume (SVi) was quantified using the left ventricular outflow tract (LVOT) velocity time integral (VTI) and the LVOT diameter, which was then indexed to body surface area. Relative wall thickness (RWT) was defined as: (2 x posterior wall diameter) / (LV internal diameter at end-diastole) [182]. Disproportionate hypertrophy (DPH) was defined as an IVSd >1.9cm in males or >1.6cm in females. LV mass was calculated using the formula from Devereux et al [183]:

$$\textbf{LV mass} = 0.8 \times 1.04 \times [(IVSd + LVIDd + PWd)^3 - LVIDd^3] + 0.6$$

Where IVSd is the interventricular septal diameter, LVIDd is the left ventricular internal diameter at end-diastole and PWd is the posterior wall diameter, all measured in 2D. Global longitudinal strain (GLS) analysis was performed offline using Tomtec 2D Cardiac Performance analysis software.

For quantifying myocardial contraction fraction (MCF), left ventricular end-diastolic volume (LVEDV) was calculated as 4.5 x $LVIDd^2$, left ventricular end-systolic volume (LVESV) was calculated as 3.72 x $LVIDs^2$ and stroke volume was LVEDV – LVESV [184]. LV mass for MCF was calculated using a slightly different formula (in keeping with the wider literature) [184]:

$$\textbf{LV mass} = 1.04 \times [(IVSd + LVIDd + PWd)^3 - LVIDd^3]$$

Myocardial volume was calculated by dividing this LV mass by the mean density of myocardium (1.04g/ml). The MCF was calculated by dividing the stroke volume by the myocardial volume [184].

Severe AS was defined as an aortic valve area (AVA) of <1.0cm^2 (or AVA indexed for body surface area <0.6cm^2/m^2), a peak aortic velocity of >4m/s and a mean pressure gradient of >40mmHg. Where equivocal, AS severity was adjudicated using low-dose dobutamine stress echocardiography, the CT-derived aortic valve calcium score or by clinical assessment (often with multidisciplinary team input) [11,20]. 'Classical' low-flow, low gradient was defined as an aortic valve area ≤1.0cm^2, with an LVEF <50%, an indexed SV <35mls/m^2, a peak aortic valve velocity <4m/s and a mean gradient <40mmHg, conversely 'paradoxical' low-flow, low-gradient was defined as an LVEF ≥50%, but an indexed SV <35mls/m^2, peak velocity <4m/s and mean gradient <40mmHg [11,12].

DPD Scintigraphy

Scanning at the BHC site was performed using a hybrid Philips Brightview SPECT/CT or a Siemens Symbia SPECT gamma camera after intravenous injection of 700MBq of DPD (effective dose ~4mSv). The set-up was reviewed by the NAC who also quality controlled analyses. The acquisition technique consisted of an early (immediately following radiotracer injection) and late (3 hours) whole-body planar acqusition, followed by SPECT/CT of the chest.

Scanning at the John Radcliffe Hospital used an IS2 Pulse CDC gamma camera. The same dose of DPD was used. Only a 3-hour (late) planar image was taken of the chest, followed by SPECT of the chest.

DPD scintigraphy is very safe, but there were considerations given that this is a radioactive tracer. UK practice is to have no specific restrictions on patients following tracer injections, however blood testing was always performed pre-injection, as was the echocardiography to avoid unnecessary exposure, with pragmatic practices to minimise staff exposure.

Qualitative visual (Perugini) scoring of the cardiac uptake (0 being negative and grades 1-3 increasingly positive) was performed from the 3-hour planar images by two experienced clinicians. The SPECT or SPECT/CT of the chest was reviewed in each patient to confirm uptake was confined to within the myocardium (rather than blood pool or adjacent rib/sternum) [86]. DPD scan findings were independently reviewed by the NAC.

Managing clinicians were blinded to the results of the DPD scintigraphy until after the patient's TAVI procedure (or decision for medical management was made), unless it was requested clinically (n=16, of which 7 were positive), or one of two criteria were met:

1. **Cardiac uptake on DPD scintigrahy** – we know that 51% of patients with AL cardiac amyloid will have some cardiac uptake and therefore in the event of any cardiac uptake on DPD, blood and urine samples were sent for serum free light-chains, serum and urine immunofixation. These results were discussed with the NAC contemporaneously and if AL amyloidosis was felt possible, patients and clinicians were unblinded *pre*-intervention for full work-up (n=6, although 50% were requested clinically, so clinicians were already unblinded as above). The usual work-up for these patients at the NAC included: a detailed clinical history, SAP scintigraphy, echocardiography, CMR, genotyping and abdominal fat pad biopsy (as well as consideration of endomyocardial biopsy as needed).
2. **Significant incidental findings** (e.g. unexpected bone metastases) – disclosure to patients and clinicians *pre*-intervention (not necessary in any study patient).

All patients with a positive DPD scan were discussed with the managing clinicians and, where appropriate, referred to the NAC for further review (if not pre-TAVI following unblinding, then post-TAVI).

DPD Quantification Techniques

These techniques were performed on those DPD scans acquired at the BHC site only, primarily because the scanning protocol at the John Radcliffe site involved a planar scan and SPECT of the chest only at 3-hours post DPD injection (meaning that conventional planar and SPECT/CT quantification were generally not possible). On the Bart's site, planar whole-body scans were performed at a scan speed of 20cm/min – the matrix size was 256x1024 on the Siemens Symbia and 512x1024 on the Phillips Brightview. SPECT acquisitions used a contoured orbit with 120 views in a 360° orbit, with 20 seconds per view and a matrix size of 128x128. CT acquisitions of the chest (performed as part of the SPECT/CT) were ungated, free-breathing and non-contrast.

Conventional Planar Quantification

The heart retention, whole-body retention and heart/whole-body ratio were calculated as described by Perugini et al [86], albeit using an irregular ROI rather than a rectangular ROI (to minimise bone content within the ROI, which would be above background and could artificially increase retention). It involved the drawing of regions of interest (ROIs) over the heart, kidneys and bladder on the anterior and posterior late (3-hour) planar images (figure 34) [86]. All ROIs were mirrored between anterior and posterior planar images and were corrected for background counts (by subtracting the background counts from the values obtained from each ROI, corrected for area). All ROIs were reported as the geometric mean of background-subtracted counts in anterior and posterior views. Whole-body retention was calculated by taking the ratio of the counts in the late planar images (corrected for decay and subtracting the activity in the kidneys and bladder) and the background-corrected total counts from the early planar images (representing injected activity) [86].

Whole-body retention = [whole-body$_L$ – (bladder$_L$ + kidneys$_L$)] / whole-body$_E$

L represents the late planar images and E represents the early planar images. Decay correction was performed by applying an appropriate decay factor, which was calculated as $e^{-\lambda t}$, where λ is the decay constant (calculated as ln(2) / $t_{1/2}$, where $t_{1/2}$ is the half-life of technetium or 6.01 hours) and t is the time elapsed between the start of the early and late planar scans [185]. The total counts from the early planar images were available in the DICOM header (which could be viewed using the Hermes Medical software), but were also available as part of the metadata on the gamma camera itself. Heart retention was calculated using the background- and decay-corrected counts of the heart in the late planar images, divided by background-corrected total counts in the early planar image [86].

$$\textbf{Heart retention} = \textbf{heart}_L / \textbf{whole-body}_E$$

Finally, the heart/whole-body ratio was calculated by dividing the background- and decay-corrected counts in the heart, by those in the whole-body on the late planar images [86].

$$\textbf{Heart/whole-body ratio} = \textbf{heart}_L / [\textbf{whole-body}_L - (\textbf{bladder}_L + \textbf{kidneys}_L)]$$

All ROIs were drawn and results reported using the HybridViewer package from Hermes Medical.

Figure 34: *An example of the conventional planar quantification technique with regions of interest over the heart (pink) on the early anterior and posterior images (left hand side) and over the heart (pink), kidneys (blue and orange) and bladder (green) on the late anterior and posterior planar images (right hand side). The regions of interest for background counts are shown across the top of the respective images (yellow).*

Heart/Contralateral Lung Ratio Quantification

A 2D region of interest (ROI) was placed over the heart and then mirrored onto the contralateral lung on the late anterior whole-body planar images (acquired 3 hours post DPD tracer injection) (figure 35). Mean counts per pixel were recorded for each ROI. As per the ASNC practice points for PYP scintigraphy [98], the H/CL ratio was calculated as the mean counts per pixel in the cardiac ROI divided by the same in the contralateral lung ROI.

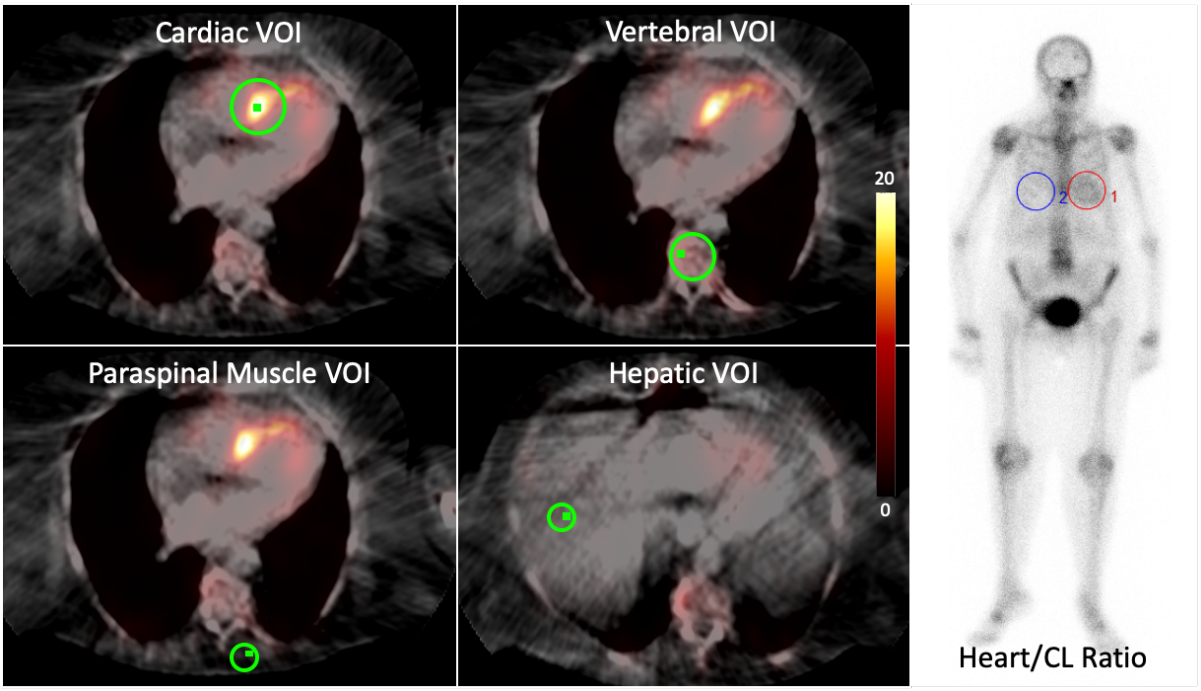

Figure 35: *Fused axial SPECT/CT DPD images demonstrating example VOI (green) positioning for SUV quantification on the left. The small green square within each VOI represents the SUV_{peak}, which enables the reporter to ensure that the recorded SUV_{peak} lies within the desired organ/tissue. On the right is a 3-hour planar, whole-body DPD image of a different patient with regions of interest over the heart (red, 1) and contralateral lung (blue, 2) demonstrating the H/CL ratio quantification. H/CL = heart/contralateral lung, VOI = volume of interest.*

SPECT/CT (SUV) Quantification

SPECT/CT acquisitions of the chest were reconstructed using Hybrid Recon (Hermes Medical). Injected dose, residual dose, height, weight and timing were inputted and recorded counts per voxel were converted into activity per unit volume and then displayed as a standardised uptake value or SUV (a parameter representing the concentration of the radiopharmaceutical in the respective tissues). 3D volumes of interest (VOI) were placed over the heart, adjacent vertebra, paraspinal muscle and liver, and peak SUV (SUV_{peak}) recorded (figure 35). SUV_{peak}

is the highest average SUV within a 1cm^3 volume. Care was taken to avoid severe degenerative tracer uptake in the vertebra when placing the relevant VOI. The vertebra was chosen, as this was an easily identifiable bony landmark visible within the field of view adjacent to the heart. The paraspinal muscle was chosen as this is a relatively conserved muscle (even in those with relatively less muscle bulk, such as the particularly frail or elderly), it is easily identifiable and within the field of view adjacent to the heart. The liver was used (in addition to being easily identifiable and within the field of view), to provide an idea of DPD uptake within another organ other than the heart, as an expected control.

In an effort to account for the competition for the DPD tracer from the vertebra and paraspinal muscle, the exploratory composite parameter of SUV retention index was devised, which was calculated as:

(cardiac SUV_{peak} / vertebral SUV_{peak}) x paraspinal muscle SUV_{peak}

ECV Quantification by Cardiac Computed Tomography

ECV_{CT} was only performed on patients scanned at the BHC site (primarily for logistical reasons, as well as the fact that many of the patients at the John Radcliffe site had already undergone their clinical TAVI work-up CT at the time of recruitment). All CT scans at BHC were performed using a Somatom FORCE scanner (Siemens Healthineers, Erlangen, Germany).

Computed Tomography Protocol

The TAVI work-up CT protocol at BHC involves: a topogram (used to plan CT volumes), calcium score, timing bolus, gated CT coronary angiogram (CTCA) acquired retrospectively and a FLASH whole body (lung apices down to the lesser trochanters). Beta blockers and glyceryl trinitrate are not routinely given in these patients, as per the TAVI protocol. The total volume of Omnipaque (iohexol) 300 contrast was fixed at 90mls (including the 10mls timing bolus) for the clinical scan, with no additional contrast used for research purposes.

The additional acquisitions for research were: a baseline, pre-contrast axial shuttle mode dataset (performed after the calcium score) and further ‘pseudo-equilibrium’ axial shuttle mode datasets at 3- and 5-minutes post-contrast (performed following

the FLASH whole body scan). All axial shuttle mode datasets (usually four repetitions every other heartbeat, single breath hold) were acquired prospectively with ECG-gating, which was triggered at a fixed 250ms after the R wave. A fixed timepoint in the R-R interval was chosen, as there is little dependence of contraction time on heart rate, it is robust and generally less affected by ectopics. 250ms was chosen as the trigger, as this is generally end-systole and therefore provides optimal wall thickness for ECV_{CT} quantification, but is neither too early (giving the CT scanner sufficient time to react to the R trigger) and nor too late in the R-R interval (such the scan is performed in diastole). This axial shuttle mode protocol was optimised for the accurate measurement of image Hounsfield units (HU), by virtually combining two scan types: one optimised for coronary imaging (180^o scan with higher temporal resolution), the other a 360^o scan (lower temporal resolution, but better HU stability across the field-of-view) [186,187]. These two virtual scans are separately reconstructed and then combined using multiband frequency filtration, resulting in a temporally sharp image with good HU stability. Images were reconstructed with a 2 mm slice thickness and 1 mm increment. A fixed tube voltage of 80kV and a tube current-time product of 370mAs were used, with a gantry rotation time of 250ms. Care was taken to ensure the same field of view was used for the baseline and post-contrast acquisitions. An additional dataset was reconstructed from the retrospectively acquired CTCA at 250ms of the R-R interval, with a field of view matching that of the axial shuttle mode datasets (figure 36).

There were 20 control patients who underwent ECV_{CT} and were included in the analysis to provide a comparison to lone AS and an estimate of normal myocardial ECV_{CT} (as there is little published data available on this topic). These patients were recruited by Dr Bunny Saberwal for a separate study (HEART-QIT: Evaluation of the Heart using Quantitative Imaging Techniques) evaluating the role of CT perfusion (including ECV_{CT}) in patients with suspected coronary artery disease. All had contemporary CMR demonstrating normal biventricular size and function, with no late gadolinium enhancement. Dr Kush Patel and I performed the ECV_{CT} analyses for these control patients. REC approval for this study was under EVINCI (REC Reference: 10/H0721/79, IRAS ID: 63298).

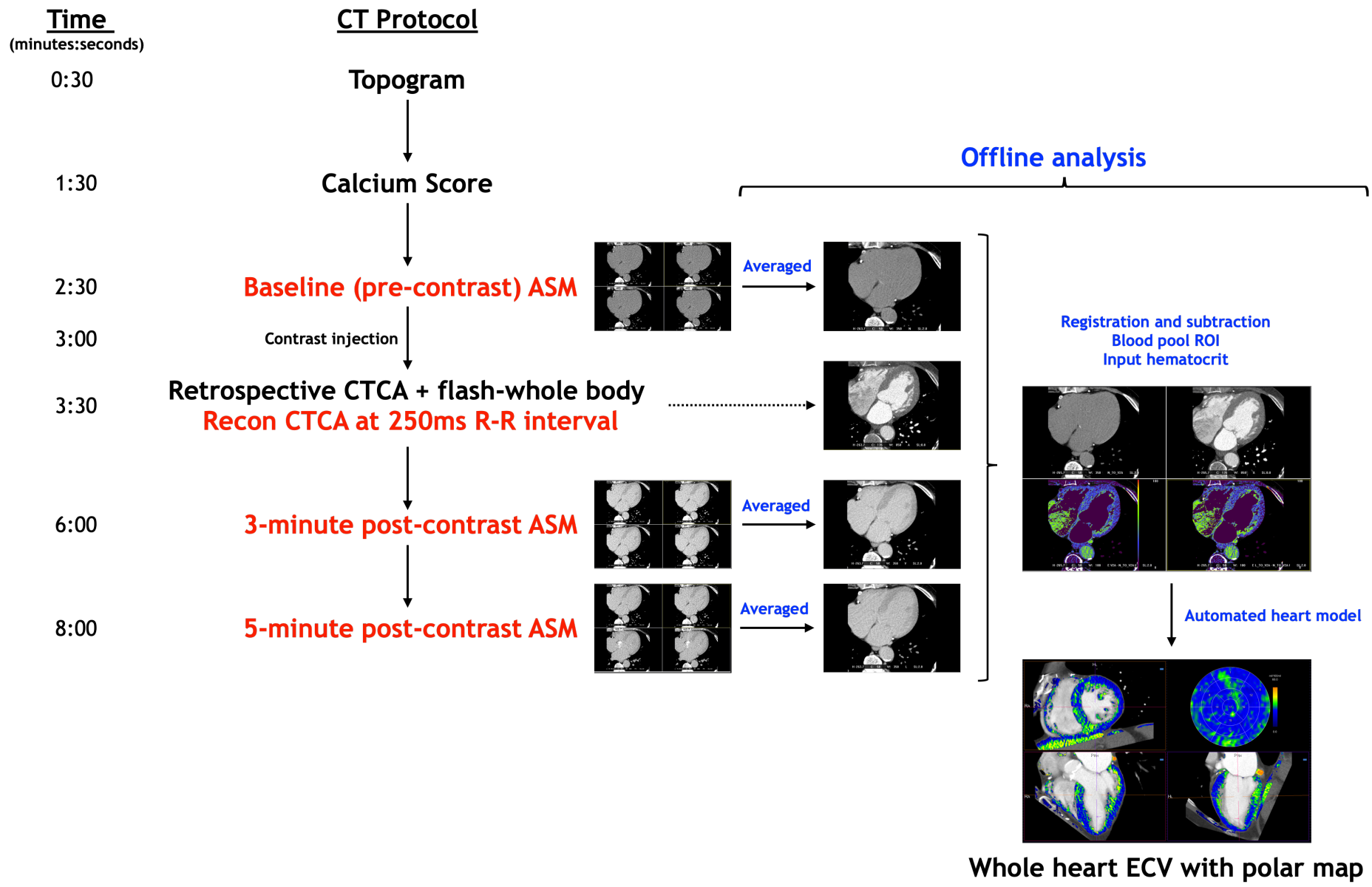

Figure 36: *ECV_{CT} protocol and offline analysis outline. Text in red represents additional image acquisition/reconstruction in scanning protocol for ECV quantification. Text in blue represents steps in offline analysis. ASM = axial shuttle mode, ECV = extracellular volume, recon = reconstruct and ROI = region of interest.*

Myocardial Extracellular Volume Analysis

Non-rigid registration software (Hepacare, Siemens Healthineers, Erlangen, Germany) allowed averaging and aligning of the axial shuttle mode datasets to improve image quality and reduce noise (figure 36). The averaged baseline image was then subtracted from the averaged 3- and 5-minute post-contrast images (providing a partition coefficient) and then registered with the CTCA image. A region of interest was placed in the LV blood pool on the CTCA image and the haematocrit (usually taken on the same day) inputted, generating a myocardial ECV map using the formula:

$$\mathbf{ECV_{CT} = (1 - haematocrit) \times (\Delta HU_{myo} / \Delta HU_{blood})}$$

ΔHU is the change in Hounsfield unit attenuation pre- and post-contrast (i.e. $HU_{post\text{-}contrast} - HU_{pre\text{-}contrast}$) [130,132,188], as described in chapter one. These results were loaded into prototype software (Cardiac Function, Siemens Healthineers, Erlangen, Germany), which allowed the ECV map to be superimposed on the CTCA image, the myocardial contours to be edited and the results to be displayed as an American Heart Association (AHA) 17-segment polar map (figures 36 and 37). The colour look-up table for myocardial ECV_{CT} was constructed as follows:

ECV_{CT} 0 – 25%:	black to bright blue
ECV_{CT} 25 – 35%:	bright blue to bright green
ECV_{CT} 35 – 45%:	bright green to bright yellow
ECV_{CT} 45 – 60%:	yellow to orange

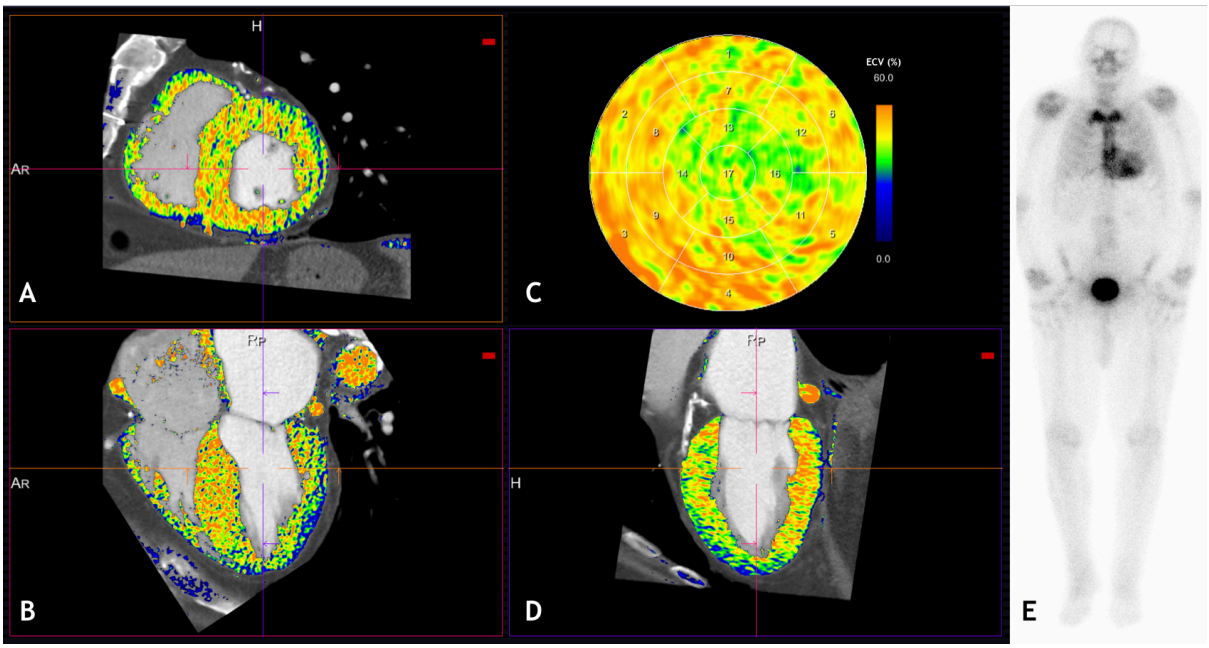

Figure 37: *Automated heart model output with the ECV_{CT} map superimposed upon the CTCA images (**A,B,D**) and corresponding 3-hour planar DPD image demonstrating Perugini grade 2 cardiac uptake (**E**). The endo- and epicardial contours can be edited in the short axis (**A**), four-chamber (**B**) and two-chamber views (**D**) to produce an ECV_{CT} AHA 17-segment polar map (**C**). The global myocardial ECV_{CT} was elevated at 47% in this patient (note the yellow-orange appearance of ECV_{CT} map in keeping with this elevation). ECV = extracellular volume, CTCA = computed tomography coronary angiography, AHA = American Heart Association, AS = aortic stenosis, DPD = ^{99m}Tc-3,3-diphosphono-1,2-propanodicarboxylic acid scintigraphy.*

Global ECV_{CT} was calculated as the mean of all AHA segments from the polar map. When calculating this, focally elevated areas of ECV (eg due to an MI) were not excluded, but AHA segments with significant beam hardening artefact from adjacent pacing wires (n=4) were excluded (figure 38).

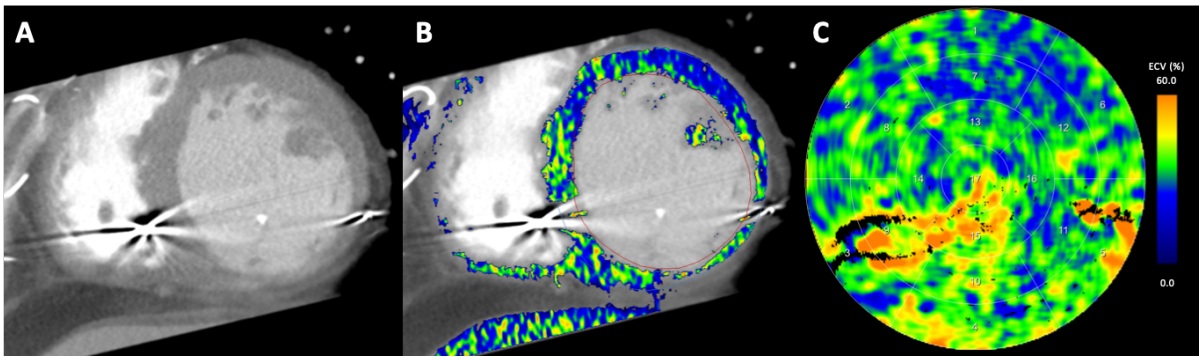

Figure 38: *A patient with a cardiac resynchronisation therapy defibrillator (CRT-D), with beam hardening clearly evident on the contrast-enhanced CTCA short-axis image (**A**), causing artefact on both the co-registered ECV_{CT}/CTCA image (**B**) and the ECV_{CT} polar map (**C**). Note the focal areas of ECV_{CT} elevation in yellow/orange on the polar map (arrows on panel **C**) corresponding to the segments of beam hardening artefact seen on the CTCA (**A**). The relevant AHA segments in this patient without cardiac amyloid were excluded (the mean ECV_{CT} of the remaining segments was slightly elevated at 34%).*

Septal ECV_{CT} was defined as the average ECV_{CT} of the basal inferior and basal anterior segments (AHA segments two and three). The indexed matrix volume was calculated as [189]:

(ECV_{CT} x CT-derived indexed LV mass) / 100

Given the superior spatial resolution of CT, it was possible to divide the myocardial ECV_{CT} even further into endocardial, mid-myocardial and epicardial compartments. Allowing for a 10% offset for the blood-myocardial and myocardial-pericardial interface (to avoid contamination), we defined endocardium as the inner 10% to 50% of the myocardium, mid-myocardium as the middle 25-75% and the epicardium as the outer 50-90%. The ECV_{CT} results for the endocardium have been presented throughout this thesis (unless otherwise stipulated), as early analysis indicated that this had the highest diagnostic accuracy for AS-amyloid.

Follow-up Assessment:

Mortality was recorded from the National Health Service (NHS) Spine and was 100% complete. Follow-up otherwise consisted of a telephone interview with completion of another quality of life questionnaire (EQ-5D-5L) at 1-year following intervention (or decision for medical therapy if the patient did not undergo intervention), as well as a simple subjective assessment of the effect of the intervention on symptoms (not applicable for those patients who did not have intervention). A minority of patients were still attending BHC at the time their follow-up was due – in these cases the health questionnaire was performed in person.

Loss to follow-up was unlikely to affect the primary outcome (as mortality was recorded remotely), however a proportion of patients were likely to prove uncontactable for the 1-year telephone interview.

Periprocedural Complications

Periprocedural complications were defined using the Valve Academic Research Consortium-2 (VARC-2) criteria and occurred *prior to* discharge, except one occurring within 2 months of the procedure [190]. The degree of post-TAVI aortic regurgitation (AR) or AS was based on departmental echocardiography when available (rather than 'on table' imaging), which was performed clinically in the majority of patients prior to discharge. Mild TAVI AV stenosis was defined using the

VARC-2 criteria as a peak velocity ≥3m/s or a mean gradient ≥20mmHg and moderate/severe AS was defined as a peak velocity >4m/s or a mean gradient >40mmHg [190]. In those patients with impaired LVEF, the degree of TAVI AV stenosis was assessed using the flow independent doppler velocity index (LVOT VTI divided by the AV VTI) and as per the VARC-2 criteria mild stenosis was defined as 0.35-0.25 and moderate/severe stenosis was defined as <0.25 [190].

Statistical Analysis

Statistical analysis used IBM SPSS Statistics (Version 25) software. Where appropriate, results are described as mean ± standard deviation or median ± interquartile range. Box and whisker plots show the median as the central bold line, with the first and third quartiles as the bottom and top of the box respectively. The range (excluding outliers and extreme values) is represented by the lines (or whiskers). An outlier is defined as a value 1.5-3 times larger than the third quartile or smaller than the first quartile and are represented as dots. Extreme values are more than 3 times higher than the third quartile or lower than the first quartile and are also represented as dots. Normality was initially assessed using the Kolmogorov-Smirnov test or the Shapiro-Wilk test depending on sample size and then (when indicated) plotted on a histogram. Kruskal-Wallis analysis of variance (ANOVA) was used when comparing more than two groups as the omnibus test, with the Dunn-Bonferroni test for pairwise comparison. The Student's t-test or Mann-Whitney U test was used to compare continuous variables depending on normality and either Chi-Squared or Fisher's Exact test was used for comparing categorical data. McNemar's test was used for comparing binary paired data. Univariate and multivariate analysis was performed using binary logistic regression with the presence of AS-amyloid as the dependent variable. Variables for the multivariate analysis were selected based on statistical significance on univariate analysis and clinical relevance, while avoid multicollinearity (eg only one parameter reflecting LV mass was included). Bland Altman analysis and Pearson correlation was performed to compare 3- and 5-minute post-contrast ECV_{CT} timepoints, as well as the impact of dose reduction. A two-sided *p*-value <0.05 was considered significant.

Chapter 3: Prevalence and Outcome of AS-amyloid in the TAVI Population

For this section of work, I was responsible for obtaining all relevant study approvals, for the recruitment of all patients, for coordinating the scans, for interpreting the DPD images (in conjunction with Dr Leon Menezes and Prof Philip Hawkins for quality control) and for all the subsequent patient follow-up. The echocardiograms were reported clinically, however I quality-controlled analyses and re-analysed these as needed. Dr Kush Patel performed the longitudinal strain analysis on echocardiography and also helped with quality-control of the echocardiogram reports, as well as coordinating the scans. Dr Michail Katsoulis provided statistical support for the final publication. Dr Saadullah Ahmed-Villiers helped with coordinating some of the scans. I also coordinated the ECG analysis, which was performed by Dr George Thornton and Dr Rebecca Hughes. Dr Sucharitha Chadalavada helped with assessing patient mortality.

3.1 Introduction

As discussed earlier in chapter one, AS is common in the elderly, with nearly 5% of patients aged 75 and over having at least moderate AS [1,30]. Symptomatic severe AS requires treatment, either in the form of SAVR or TAVI, without which average survival is only 2-3 years [38–41,191].

Another disease that is common in the elderly is cardiac amyloidosis, with wtATTR deposits seen in the heart at autopsy in 25% of patients aged 85 and over [72]. So, it follows that cardiac amyloidosis is likely to co-exist in a significant proportion of elderly patients with AS (AS-amyloid). Bone scintigraphy (DPD, PYP or HMDP), coupled with a negative search for a plasma cell dyscrasia, now offers a non-invasive diagnostic strategy for ATTR cardiac amyloidosis, supported by recent expert consensus recommendations [88,89].

The aim of this chapter was to ascertain how common AS-amyloid is in the elderly AS population who have been referred for TAVI using DPD scintigraphy and what clinical impact this dual pathology may have (in terms of mortality and potential symptom benefit following intervention).

3.2 Results

200 patients (mean age 85±5 years, 50% male) were recruited – 30 from the John Radcliffe site and the remaining 170 from the BHC site. Co-morbidities (hypertension, hypercholesterolemia, diabetes, pre-intervention atrial fibrillation and permanent pacemakers) were common, as would be expected in this population (table 3). Baseline LVEF was 54±11% and aortic valve measurements were: peak velocity 4.13±0.65m/s, mean gradient 41±14mmHg, area 0.73±0.22cm^2. As of September 2019, 149 (75%) patients had undergone TAVI, 2 (1%) surgical aortic valve replacement and 49 (24%) were being managed medically (15 were for conservative management; the remainder for ongoing surveillance).

AS-amyloid Prevalence and Type

AS-amyloid was found in 26 patients, a prevalence of 13%. The amyloid burden was skewed with no patients with a Perugini grade 3 DPD, but more with grade 2 than grade 1 (grade 1 in 8, grade 2 in 18, grade 3 in 0). A plasma cell dyscrasia was detected in 6 patients (23%), necessitating unblinding (although 50% were clinically requested, so already unblinded) and a referral to the NAC, but following detailed review (which has been described in more detail in chapter two), AL amyloid was felt unlikely in all cases. All genotyped patients to date (n=12) were wild-type ATTR.

	AS-amyloid (n=26)	Lone AS (n=174)	*p*-value
Demographics			
Male	16 (62%)	83 (48%)	0.19
Age	88±5	85±5	**0.001**
Clinical Parameters			
Hypertension	19 (73%)	135 (78%)	0.61
Hypercholesterolemia	9 (35%)	75 (43%)	0.41
Diabetes Mellitus	3 (12%)	45 (26%)	0.11
Atrial Fibrillation	11 (42%)	63 (36%)	0.55
Permanent Pacemaker	4 (15%)	19 (11%)	0.51
6-MWT (m)	94 (48-239)	138 (66-260)	0.36
ECG Parameters			
Heart rate (bpm)	70±13	73±16	0.32
Low voltage limb leads	0	5 (3%)	1.00
S-L Criteria (mV)	1.9±0.7	2.5±0.9	**0.03**
1st Degree AV Block*	1 (5%)	34 (22%)	0.08
QRS duration (ms)	118±27	109±28	0.16
LBBB*	1 (5%)	19 (12%)	0.48
RBBB*	8 (36%)	20 (13%)	**0.01**
Echo Parameters			
Left Ventricle			
LVEF (%)	54±14	54±11	0.99
Indexed SV (ml/m^2)	34±10	38±11	0.12
IVSd (cm)	1.4±0.3	1.3±0.2	**0.02**
PWd (cm)	1.3±0.4	1.1±0.2	**0.001**
DPH	2 (8%)	7 (4%)	0.33
RWT (cm)	0.61±0.28	0.50±0.16	0.07
Indexed LV mass (g/m^2)	136±36	118±38	**0.03**
MCF (%)	20.3±8.8	23.8±8.8	0.08
Mitral annular S' (m/s)	0.05±0.01	0.06±0.02	**0.04**
GLS (%)	-15±6	-14±6	0.29
Diastolic Function			
E/A ratio	1.28 (0.75-2.15)	0.78 (0.68-1.22)	0.09
Lateral E/E'	20±13	16±8	0.16
MVDT (ms)	241±88	237±86	0.84
LA diameter (cm)	4.4±0.6	4.1±0.7	0.06
Right Ventricle			
TAPSE (cm)	1.8±0.5	1.9±0.5	0.56
TR peak velocity (m/s)	2.96±0.46	2.87±0.56	0.54
PASP (mmHg)	43±12	40±15	0.42

Table Continued	AS-amyloid (n=26)	Lone AS (n=174)	*p*-value
Echo Parameters Continued			
Aortic Valve			
Peak velocity (m/s)	3.95±0.73	4.15±0.62	0.15
Mean gradient (mmHg)	37±14	42±14	0.12
AVA (cm^2)	0.74±0.23	0.73±0.22	0.69
Classical LFLG AS	3 (12%)	16 (9%)	0.72
Paradoxical LFLG AS	5 (19%)	26 (15%)	0.57
Composite Parameters			
V/M Ratio ($mV/g/m^2$)	0.017±0.007	0.025±0.012	**0.03**
CT Parameters			
AV Calcium Score (HU)	3149±1916	2619±1600	0.17
Blood Results			
Creatinine (mmol/L)	118±38	105±46	0.20
eGFR ($ml/min/1.73m^2$)	50±14	56±17	0.08
hsTnT (ng/L)	41 (25-84)	21 (14-34)	**<0.001**
NT-proBNP (ng/L)	3702 (1286-5626)	1254 (598-2769)	**0.001**

Table 3: *Basic demographics, baseline echo parameters, aortic valve calcium score and clinical parameters for patients with lone AS and those with dual pathology (AS-amyloid) prior to TAVI. 6-MWT = 6-minute walk test, AVA = aortic valve area, DPH = disproportionate hypertrophy, eGFR = estimated glomerular filtration rate, GLS = global longitudinal strain, hsTnT = high-sensitivity troponin T, IVSd = interventricular septum diameter, LBBB = left bundle branch block, MCF = myocardial contraction fraction, MVDT = mitral valve deceleration time, NT-proBNP = N-terminal pro-brain natriuretic peptide, PASP = pulmonary artery systolic pressure, PWd = posterior wall diameter, RBBB = right bundle branch block, RWT = relative wall thickness, S-L = Sokolow-Lyon criteria, TAPSE = tricuspid annular plane systolic excursion, TR = tricuspid regurgitation, V/M ratio = voltage/mass ratio. Values represent mean±standard deviation or median (interquartile range) where appropriate. *Missing ECG data in 4 AS-amyloid and 19 lone AS patients – percentages and statistics quoted reflect this.*

AS-amyloid vs Lone AS at Baseline

AS-amyloid patients were on average three years older (88±5 vs 85±5 years, *p=0.001*) and slightly more were male, although this did not reach statistical significance (62% vs 48% male, *p=0.19*) (table 3).

Those patients with AS-amyloid had a lower S-L criteria (1.9±0.7 vs 2.5±0.9mV, *p=0.03*) and a higher prevalence of right bundle branch block, RBBB (36% vs 13%, *p=0.01*), however low limb lead voltages hardly occurred in our cohort (n=5 total, all lone AS) (table 3).

LV mass and wall thickness were slightly greater in the AS-amyloid cohort, however there was no difference in the prevalence of DPH (*p=0.33*). There was no difference

in the prevalence of either 'classical' (impaired LVEF) low-flow, low-gradient AS (12% vs 9%, *p=0.72*) or 'paradoxical' (normal LVEF) low-flow, low-gradient AS (19% vs 15%, *p=0.57*) or any other parameters of AS severity. The degree of AV calcification was not significantly different between the two groups (3149±1916 vs 2619±1600 HU, *p=0.17*). Mitral annular S' was slightly lower in the AS-amyloid patients (0.05±0.01 vs 0.06±0.02m/s, *p=0.04*), but LVEF, stroke volume, GLS, myocardial contraction fraction, LA size, RV function and all other diastolic measures were similar. Combining ECG and echocardiography, the V/M ratio was lower (0.017±0.007 vs 0.025±0.012, *p=0.03*) (table 3).

NT-proBNP and hsTnT were approximately double: hsTnT 41(25-84) ng/L vs 21(14-34) ng/L, *p<0.001* and NT-proBNP 3702 (1286-5626) ng/L vs 1254(598-2769) ng/L, *p=0.001*, differences that were independent of renal function (table 3). Both hsTnT and NT-proBNP tracked increasing amyloid burden by DPD Perugini grade (*p<0.001* and *0.002* respectively for trends, figure 39). Pairwise analysis revealed that within the trend, the significant difference was between patients with a grade 0 and a grade 2 DPD (*p<0.001* for hsTnT and *0.003* for NT-proBNP).

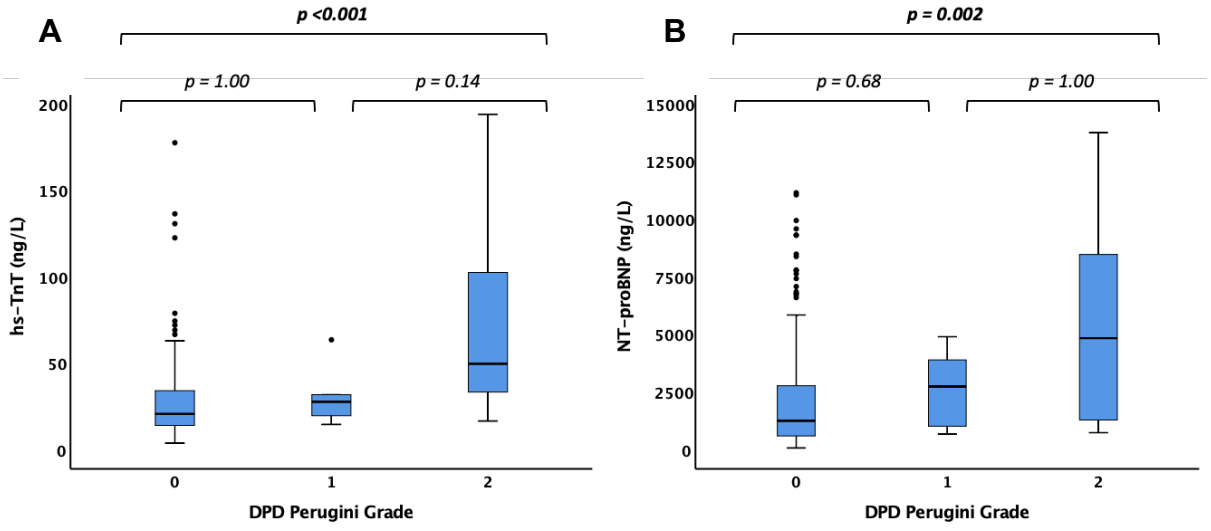

Figure 39: *Box and whisker plots demonstrating elevated hsTnT (**A**) and NT-proBNP (**B**) in AS-amyloid compared to lone AS and with amyloid burden measured by DPD Perugini grade: 0 = negative (lone AS), 1-2 = increasingly positive (AS-amyloid). Outliers with an hsTnT greater than 200ng/L and an NT-proBNP greater than 150000 have been excluded from this figure, but included in the statistical analysis (n=2 and n=4 respectively). DPD = ^{99m}Tc-3,3-diphosphono-1,2-propanodicarboxylic acid scintigraphy, HsTnT = high-sensitivity troponin T, NT-proBNP = N-terminal pro-brain natriuretic peptide.*

HsTnT had an area under the curve (AUC) of 0.76 (95% confidence interval 0.67 – 0.85), with a cut off of 24ng/L giving an 81% sensitivity and 57% specificity for the detection of AS-amyloid. For the detection of only DPD Perugini grade 2 AS-amyloid, this AUC was 0.83 (95% confidence interval 0.74 – 0.93) and a similar hsTnT threshold of 24ng/L offered a sensitivity of 89% and a specificity of 56%

NT-proBNP had an AUC of 0.70 (95% confidence interval 0.61 – 0.80), with a threshold of 1180ng/L giving a sensitivity of 81% and a specificity of 47%. For the detection of only DPD Perugini grade 2 AS-amyloid, the AUC was 0.73 (95% confidence interval 0.62 – 0.85) and an NT-proBNP cut off of 1277ng/L offered a sensitivity of 83% and a specificity of 50%.

Quality of Life

Patients with AS-amyloid had a significantly lower EQ-VAS score at baseline (EQ-VAS 50 vs 65, *p=0.04*), suggesting a lower quality of life – despite no difference in baseline comorbidities (table 3) and a similar 6-minute walk distance (94 vs 138m, *p=0.36*). More patients with AS-amyloid reported significant (moderate or more) difficulties with anxiety/depression at baseline (46% vs 21%, *p=0.04)*, but other domains were similar between the two cohorts (see table 4 and figure 40).

Baseline Reported Difficulty	Overall (n=200)	AS-amyloid (n=26)	Lone AS (n=174)	*p*-value
Mobility	67%	65%	67%	0.87
Self-care	17%	23%	16%	0.40
Usual Activities	57%	62%	57%	0.64
Pain/discomfort	47%	38%	49%	0.34
Anxiety/depression	24%	46%	21%	**0.005**
EQ-VAS	60 (50-75)	50 (40-69)	65 (50-75)	**0.04**

Table 4: *Breakdown of the results of the EQ-5D-5L health questionnaire in the overall study population at baseline.*

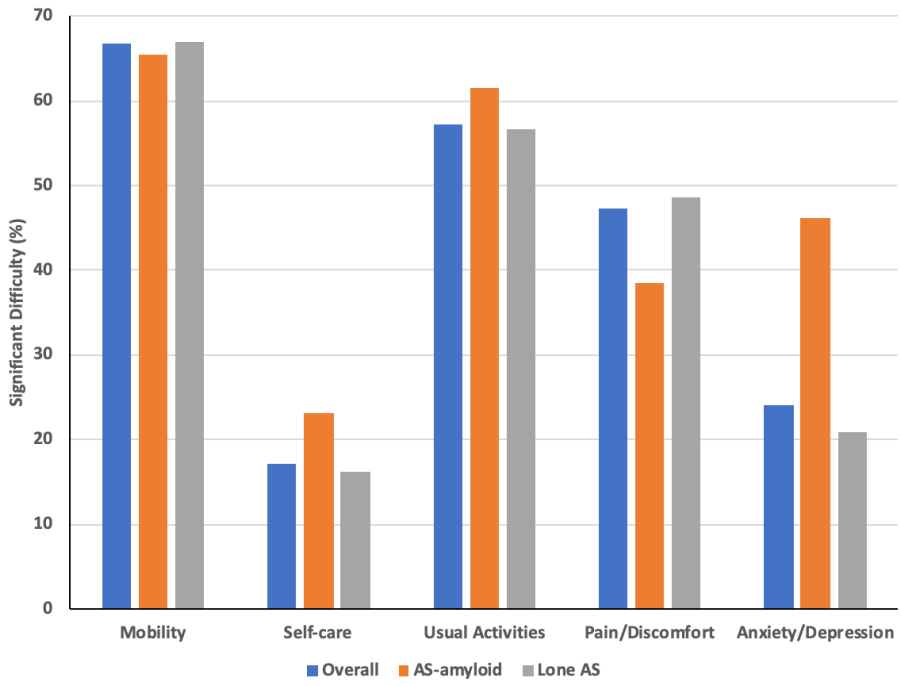

Figure 40: *Baseline responses to part one of the EQ-5D-5L health questionnaire. Each domain of the questionnaire is shown on the x-axis, with the percentage of patients reporting significant (moderate or more) difficulty with the respective domain on the y-axis. The overall cohort is in blue (n=200), the AS-amyloid cohort (n=26) in orange and the lone AS cohort in grey (n=174).*

Multivariate Analysis

Increasing age, troponin and the presence of RBBB were associated with AS-amyloid on multivariate analysis (table 5). V/M ratio was also associated (*p=0.045*), however the analysis was performed separately (table 6) to avoid underpowering the main model, as the voltage component of the V/M ratio cannot be reliably assessed in bundle-branch block or ventricular paced rhythm, present in 30% of patients [179].

Univariate Analysis			Multivariate Analysis		
Variable	***p*-value**	**Exp (B)**	***p*-value**	**Exp (B)**	**CI for Exp (B)**
Demographics					
Age (per year increase)	**0.002**	1.15	**0.04**	1.13	1.00-1.27
Gender (male)	0.19	1.75			
Clinical Parameters					
6-MWT (per m decrease)	0.48	1.00			
Pre-TAVI EQ-VAS (per unit decrease)	0.08	0.98			
Post-TAVI EQ-VAS (per unit decrease)	0.71	1.00			
ECG Parameters					
S-L Criteria (per mV decrease)	**0.03**	0.39			
LBBB	0.29	0.33			
RBBB	**0.01**	3.42	**0.005**	6.88	1.81-26.21

Univariate Analysis Continued			Multivariate Analysis Continued		
Variable	***p*-value**	**Exp (B)**	***p*-value**	**Exp (B)**	**CI for Exp (B)**
Echo Parameters					
Left Ventricle					
LVEF (per % decrease)	0.99	1.00			
Indexed SV (per ml/m^2 decrease)	0.12	0.97			
IVSd (per cm increase)	**0.02**	6.66			
PWd (per cm increase)	**0.003**	8.72	0.14	3.95	0.65-23.91
RWT (per cm increase)	**0.01**	12.1			
Indexed LV Mass (per g/m^2 increase)	**0.03**	1.01			
MCF (per % decrease)	0.08	0.95			
Mitral Annulus S' (per m/s decrease)	**0.046**	0.00	0.13	0.00	0.00-43640.00
GLS (%)	0.29	0.96			
Diastolic Function					
E/A Ratio (per unit increase)	**0.03**	1.67			
Lateral E/E' (per unit increase)	**0.04**	1.05	0.56	1.02	0.96-1.08
MVDT (per ms increase)	0.84	1.00			
LA Diameter (per cm increase)	0.07	1.90			
Right Ventricle					
TAPSE (per cm decrease)	0.56	0.76			
TR peak velocity (per m/s increase)	0.53	1.36			
PASP (per mmHg increase)	0.42	1.02			
Aortic valve					
Peak velocity (per m/s decrease)	0.15	0.61			
Mean gradient (per mmHg decrease)	0.12	0.97			
AVA (per cm^2 increase)	0.69	2.06			
Composite Parameters					
V/M Ratio (per mV/g/m^2 decrease)	**0.03**	0.00			
CT Parameters					
AV Calcium Score (per HU increase)	0.18	1.00			
Blood Results					
hsTnT (per ng/L increase)	**0.001**	1.02	**0.03**	1.02	1.00-1.03
NT-proBNP (per ng/L increase)	0.06	1.00	0.41	1.00	1.00-1.00

Table 5: *Univariate and multivariate binary logistic regression analysis showing that age, hsTnT and the presence of RBBB were all associated with the presence of AS-amyloid. Only one parameter reflecting LV mass was used in the multivariate analysis to avoid multicollinearity. 6-MWT = 6-minute walk test, AVA = aortic valve area, CI = 95% confidence interval, Exp (B) = exponentiation of the B coefficient, GLS = global longitudinal strain, EQ-VAS = EuroQol visual analogue scale, hsTnT = high-sensitivity troponin T, HU = Hounsfield units, IVSd = interventricular septum diameter, LV = left ventricle, LBBB = left bundle branch block, MCF = myocardial contraction fraction, MVDT = mitral valve deceleration time, NT-proBNP = N-terminal pro-brain natriuretic peptide, PASP = pulmonary artery systolic pressure, PWd = posterior wall diameter, RBBB = right bundle branch block, RWT = relative wall thickness, S-L = Sokolow-Lyon, TAPSE = tricuspid annular plane systolic excursion, TR = tricuspid valve, V/M ratio = voltage/mass ratio.*

Multivariate Analysis			
Variable	***p*-value**	**Exp (B)**	**CI for Exp (B)**
Age (per year increase)	0.16	1.11	0.96-1.29
Gender (male)	0.12	3.18	0.74-13.75
V/M Ratio (per mV/g/m^2 decrease)	**0.045**	0.00	0.00-0.13

Table 6: *Multivariate binary logistic regression analysis for voltage/mass ratio with gender and age. Performed separately to avoid underpowering the main model by excluding the 30% of patients with bundle branch block or a ventricular paced rhythm. CI = 95% confidence interval, Exp (B) = exponentiation of the B coefficient, V/M ratio = voltage/mass ratio.*

Exploratory Subgroup Analysis

In terms of echocardiographic parameters, only IVSd, PWd, RWT and E/A ratio tracked DPD grade (*p<0.05* for trend for all, table 7 and figure 41), pairwise analysis revealed that the significant difference for all of these was between patients with a grade 0 DPD and a grade 2. Of note, there was no significant trend seen between grades in any of the other echocardiographic parameters assessed in table 3.

	Lone AS (n=200)	**Grade 1 AS-amyloid (n=8)**	**Grade 2 AS-amyloid (n=18)**	***p*-value**
IVSd	1.3±0.2	1.2±0.2	1.5±0.3	**0.03**
PWd	1.1±0.2	1.2±0.2	1.4±0.5	**0.03**
RWT	0.50±0.16	0.48±0.15	0.67±0.30	**0.02**
E/A Ratio	0.78 (0.68-1.22)	0.68 (0.63-1.02)	1.4 (0.93-2.64)	**0.02**

Table 7: *A breakdown of the results for those echocardiographic parameters, which showed a significant trend across DPD Perugini grades. IVSd = interventricular septum diameter, PWd = posterior wall diameter, RWT = relative wall thickness.*

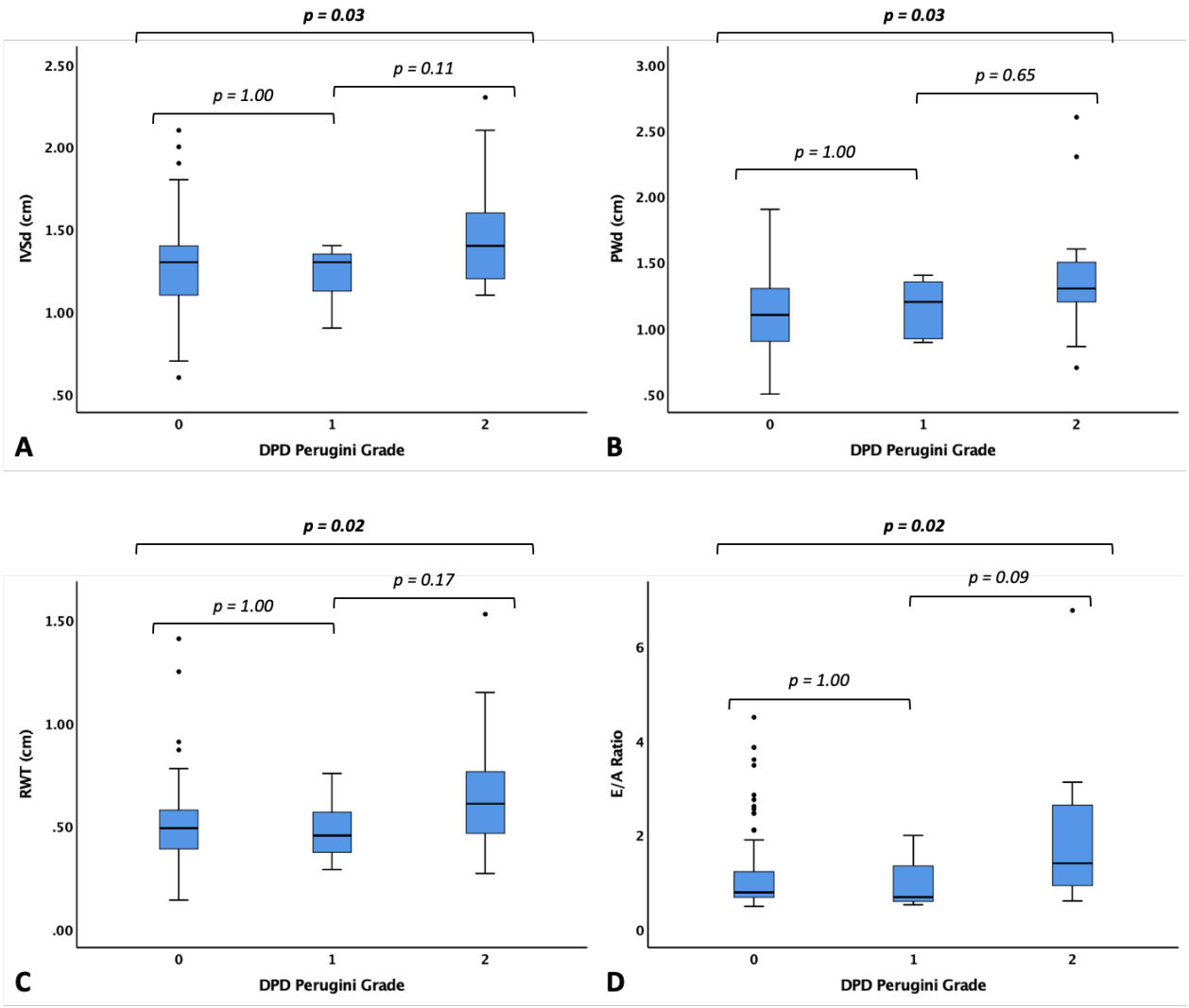

Figure 41: *Box and whisker plots illustrating the increase in IVSd (**A**), PWd (**B**), RWT (**C**) and E/A ratio (**D**) with increasing DPD Perugini grade: 0 = lone AS, 1-2 = increasingly positive (AS-amyloid). DPD = ^{99m}Tc-3,3-diphosphono-1,2-propanodicarboxylic acid scintigraphy, IVSd = interventricular septum diameter, PWd = posterior wall diameter, RWT = relative wall thickness.*

Periprocedural Complications

In the 149 (75%) patients who underwent TAVI (16 AS-amyloid, 133 lone AS), complication rates were equivalent to those published in international trials [42,48]. The overall rate of major complication (composite of major bleeding, major vascular injury or stroke/TIA) was low: 1 (6%) vs 10 (8%), *p=1.00*. Specifically, the rates of permanent pacemaker insertion were no different between the two groups: 3 (19%) vs 7 (5%), *p*=0.08. Using strict criteria and capturing all major and minor events via VARC-2, complications occurred at the same rate in AS amyloid: 6 (38%, total 8 complications) vs 46 (35%, total 59 complications), *p=0.82* by patient (table 8). No patient died within the first 30 days post-TAVI.

Complication	AS-amyloid (n=16)	Lone AS (n=133)
AKI	1	8
Arrhythmia/conduction disturbance	3	16
Bleeding		
Minor	1	8
Major	0	1
Life-threatening	0	1
More than mild valve regurgitation	1	9
Valve stenosis		
Mild	1	0
Moderate/severe	0	1
Valve-in-valve	0	2
Vascular		
Minor	0	4
Major	1	3
Stroke/TIA	0	6
TOTAL	**8**	**59**

Table 8: *A breakdown of post-TAVI complications in the lone AS and AS-amyloid cohorts, using the Valve Academic Research Consortium-2 (VARC-2) criteria [190]. AKI = acute kidney injury, AR = aortic regurgitation, TIA = transient ischemic attack. Note: percentages not quoted as values represent number of complications rather than patients affected.*

Mortality

At a median follow-up post-DPD scan of 19 (10–27) months, 42 (21%) patients had died. 6 (23%) patients with AS-amyloid died, compared to 36 (21%) with lone AS, (*p=0.71*), with no difference in mortality by DPD Perugini grade, *p=0.93* (figure 42).

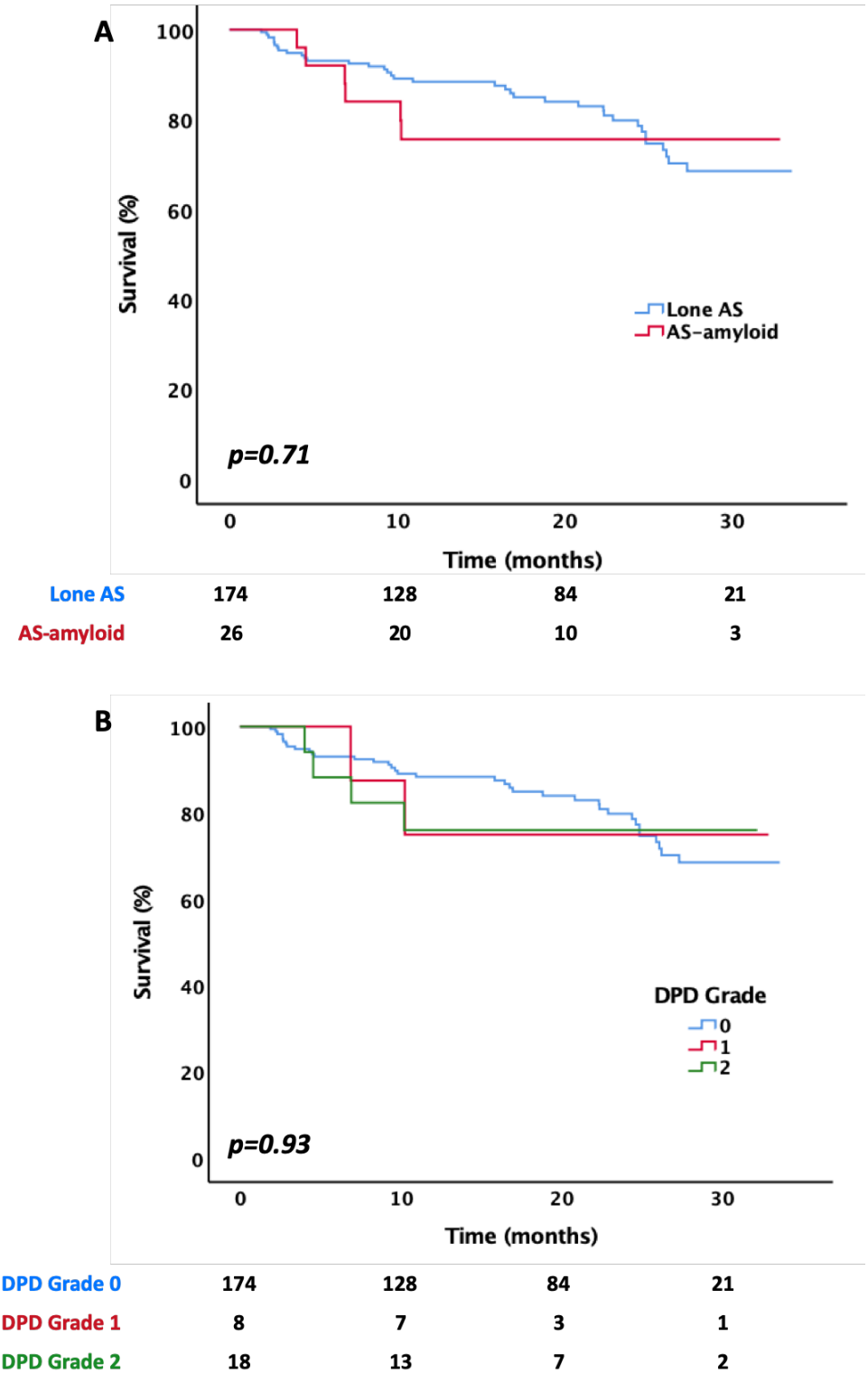

Figure 42: *Kaplan-Meier survival curves over a median follow up of 19 months (IQR 10 – 27 months) by lone AS vs AS-amyloid (**A**) and by DPD Perugini grade (**B**). DPD grade 0 = negative (lone AS), DPD grades 1 and 2 = increasingly positive (AS-amyloid).*

There remained no significant difference in survival between those with AS-amyloid and those with lone AS when the follow-up was limited to 1-year (p=0.10).

There was also no significant difference in mortality when only those patients who underwent TAVI (n=149) were included in the survival analysis and the index time point was changed from time of recruitment to time of intervention (AS-amyloid vs lone AS, *p=0.47*).

Looking at survival by management strategy, patients with lone AS who underwent TAVI had significantly lower mortality compared to those undergoing medical management (*p*<0.001). Importantly, this was also the case for those with AS-amyloid (*p*=0.03) (figure 43).

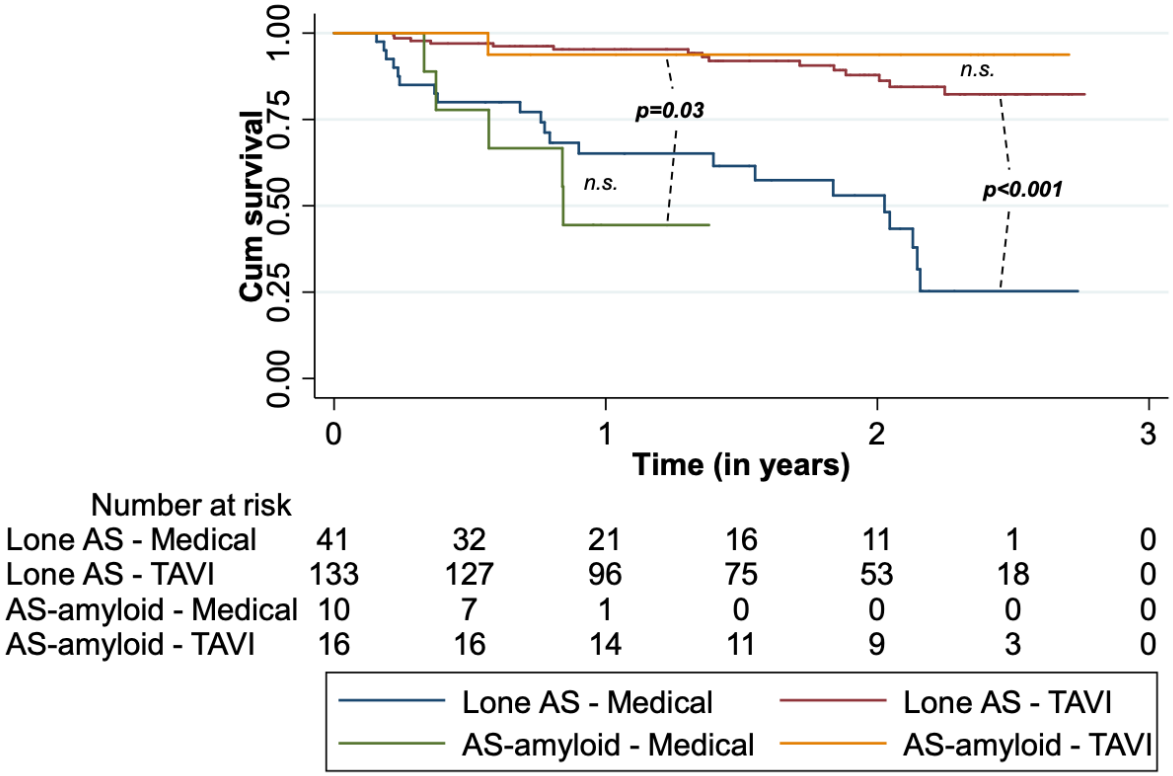

Figure 43: *Kaplan-Meier survival curves over a median follow up of 19 months (IQR 10 – 27 months) by management strategy (p=0.03 for TAVI vs medical management in AS-amyloid, p<0.001 for TAVI vs medical management in lone AS, p=0.48 in the post TAVI arm for AS-amyloid vs lone AS and p=0.39 in the medical management arm for AS-amyloid vs lone AS). NS = not significant, TAVI = transcatheter aortic valve implantation.*

One Year Follow-up

103 post-TAVI patients (67%) had completed their 1-year follow-up at the time of writing this thesis, of whom 100 completed the full EQ-5D-5L health questionnaire, which included 14 patients with AS-amyloid. 8 patients in the AS-amyloid cohort (57%) reported feeling the same or worse at 1-year post-TAVI, compared to 28 in the

lone AS cohort (31%) (*p=0.08*). There was no difference in the EQ-VAS result between the two groups post-TAVI: 65 (50-75) in the AS-amyloid cohort vs 70 (50-75) in the lone AS cohort (*p=0.69)*. There was also no difference in the improvement in quality of life (as measured by the EQ-VAS) post-TAVI between the groups: 3.0±20.0 in the AS-amyloid cohort vs 1.1±20.1 in the lone AS cohort (*p=0.74)*. There was no difference in the proportion of patients in each cohort experiencing at least moderate difficulty post-TAVI with mobility, self-care, usual activities, pain/discomfort or anxiety/depression (table 9).

Post-TAVI Reported Difficulty	Overall (n=100)	AS-amyloid (n=14)	Lone AS (n=86)	*p*-value
Mobility	63%	64%	63%	0.91
Self-care	23%	21%	23%	1.00
Usual Activities	50%	50%	51%	0.97
Pain/Discomfort	51%	36%	54%	0.20
Anxiety/depression	26%	36%	24%	0.51
EQ-VAS	70 (50-75)	65 (50-75)	70 (50-75)	0.69
Difference in EQ-VAS	1.3±20.0	3.0±20.0	1.1±20.1	0.74

Table 9: *Breakdown of the results of the EQ-5D-5L health questionnaire in the post-TAVI patients who completed it (n=100). Note the difference in EQ-VAS was calculated as the result post-TAVI minus the result pre-TAVI for each patient to reflect any improvement.*

There was a 14% reduction in the proportion of patients with AS-amyloid reporting at least moderate anxiety/depression and a similar reduction in those reporting at least moderate difficulty with usual activities post TAVI, however this did not reach statistical significance (*p*=0.63 for both) (figure 44 and table 10). There was no significant change in any of the other domains following intervention (figure 44 and table 10).

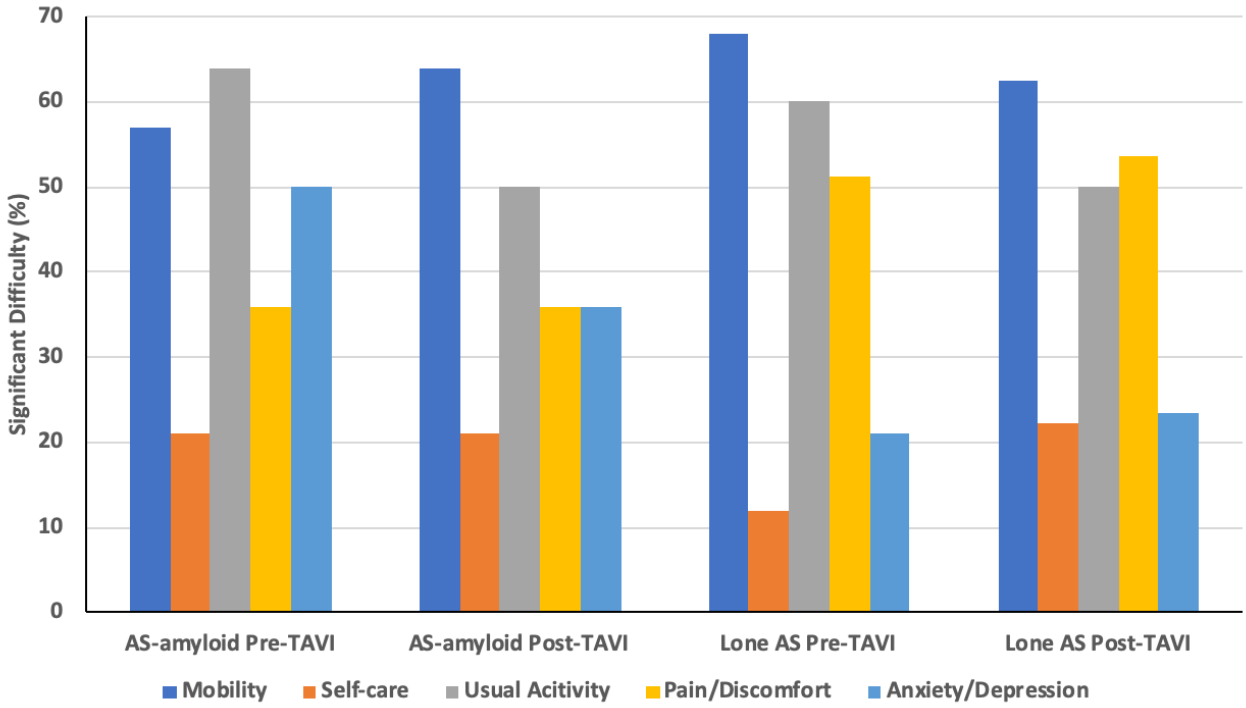

Figure 44: *Baseline and post-TAVI responses to part one of the EQ-5D-5L health questionnaire those patients who completed the questionnaire at both time points (n=99 patients). Responses are further divided by cohort into AS-amyloid or Lone AS, with the colours of the bars representing each domain of the questionnaire and the percentage of patients reporting significant (moderate or more) difficulty with the respective domain on the y-axis.*

Reported Difficulty	Pre-TAVI	Post-TAVI	*p*-value
AS amyloid (n=14)			
Mobility	57%	64%	1.00
Self-care	21%	21%	1.00
Usual Activities	64%	50%	0.63
Pain/Discomfort	36%	36%	1.00
Anxiety/depression	50%	36%	0.63
Lone AS (n=85)			
Mobility	68%	62%	0.38
Self-care	12%	22%	0.06
Usual Activities	60%	50%	0.22
Pain/Discomfort	51%	54%	0.74
Anxiety/depression	21%	24%	0.84

Table 10: *Comparison of EQ-5D-5L responses pre- and post-TAVI in those patients who completed the questionnaire at both time points (n=99, as one lone AS patient who completed follow-up, had not completed the baseline questionnaire).*

3.3 Discussion

AS-amyloid is common – affecting 1 in 8 patients aged 75 and over with severe AS being considered for TAVI. Patients with AS-amyloid are generally older with lower voltages on ECG, lower V/M ratio, a higher incidence of RBBB, greater LVH, poorer longitudinal LV function and higher cardiac biomarkers (NT-proBNP and hsTnT). These patients also report a lower baseline quality of life (EQ-VAS score), with higher levels of anxiety/depression relative to those patients with lone AS.

Periprocedural complications and mortality in patients with AS-amyloid were similar to those with lone AS in the overall cohort. In terms of mortality, numbers were small by 30 months of follow-up, however this the lack of significant mortality difference persisted when follow-up was limited to 1 year and numbers were greater. With over 188 patients, we were powered to detect a doubling of mortality with AS-amyloid compared to lone AS (from 21.4% up to 40% mortality at 1 year), so it is possible that there are smaller mortality differences that we are not appreciating in this cohort of patients. Further, larger, multicentre work is now ongoing to confirm if this signal of no difference in outcome is confirmed. The poorer outcome seen with medical therapy compared to TAVI in patients with lone AS is not surprising, however TAVI also significantly improved outcome in patients with AS-amyloid compared to medical therapy, disproving the preconception that TAVI may be futile in these patients.

Comparison to the Wider Literature

As discussed in chapter one, when this project was starting in 2016 there was only limited evidence for dual AS and cardiac amyloid pathology in the wider literature [172,173]. Our group had also just published work in the SAVR population, showing a prevalence of AS-amyloid of ~6% in those patients aged over 65 with calcific AS [163]. The higher prevalence seen in this TAVI population likely (at least in part) reflects the older age of our cohort (mean age 85-years-old, compared to a mean age of 75-years-old in the SAVR study) – we know that wtATTR is commoner in the elderly and that it's prevalence increases with age [72,163]. The mortality in the SAVR population was much higher in those patients with AS-amyloid compared to those with lone AS (50% vs 6.9% at median 2.3 years follow-up), which does not seem to be the case in the TAVI population [163]. It is possible this is due to these

patients tolerating the minimally invasive nature of the TAVI better than open heart surgery, as we know that wound healing can be impaired in the presence of SAP, which is found in large quantities in amyloid fibrils [101,192].

One important difference from that expected for lone ATTR cardiac amyloidosis, is the gender split seen in our population compared to that of the wider literature. 62% of our AS-amyloid population was male, which is in stark contrast to that seen in the wider literature, which report an overwhelmingly male predominance in wtATTR of up to 94-98% outside of the AS population [73,74]. It is possible that other studies have underestimated female involvement through referral bias associated with the gender dimorphism in the male hypertrophic response seen in AS [35] and Fabry disease [193]) – meaning that for the same degree of infiltration, LVH is more manifest in males. In support of this, another study using DPD screening of 120 patients with HFpEF (with a maximal wall thickness ≥1.2cm), found that only 50% of their 16 patients with cardiac amyloidosis were male [75].

While work was ongoing on this thesis, two other key studies were published in this field. The first of these was a study in 2017 by Cavalcante et al, which was a retrospective study of 113 patients with moderate or severe AS referred clinically for CMR, in which they found a remarkably similar prevalence of AS-amyloid (16%) in those aged over 74 years (n=57) [194]. They also found a higher 1-year mortality in these patients (56% vs 20%, $p<0.001$), which remained significant despite adjusting for AV replacement, Society of Thoracic Surgery predicted risk of mortality and LVEF ($p=0.03$) [194]. There were other important similarities to the data presented here: they too found that none of the AS-amyloid patients met ECG criteria for low voltage and that there was no difference in the prevalence of low flow, flow gradient AS [194]. Their patients with AS-amyloid also had an increased septal wall thickness on echo and increased indexed LV mass on CMR relative to lone AS, however this is perhaps not surprising given their patients were referred clinically, which means their cohort is likely enriched with patients in whom there is a clinical suspicion of an underlying cardiomyopathic process [194].

Their study has important limitations however, the most notable being that it was performed retrospectively, raising the possibility that their recruitment may well have

been biased (as mentioned earlier – clinical referrals for CMR in patients with AS may be being done because there is the suspicion of another underlying cardiac condition) [194]. This may also explain their male predominance (8/9 AS amyloid patients) [194]. Furthermore, the unblinded nature of their CMR results are likely to have impacted outcome in these patients, for example it is possible that a CMR reporting concomitant cardiac amyloidosis may have resulted in patients not undergoing AV replacement (AVR) and we already know that symptomatic severe AS is associated with poor outcomes unless treated with AVR. The diagnosis of AS-amyloid was by CMR predominantly and AL cardiac amyloidosis was not excluded in all patients (due to the retrospective nature of the study), which would have impacted outcome (although AL is less likely than wtATTR cardiac amyloidosis in their demographic) [194]. Looking further at their work, the numbers of patients with AS-amyloid are small (n=9), with even fewer undergoing AVR (n=4), which was in the form of TAVI for all patients (two of these AS-amyloid patients died post-TAVI) [194]. It is likely these numbers are too small to draw robust conclusions from regarding outcome in AS-amyloid (particularly following TAVI) and direct comparison is further confounded by the fact that the predominant intervention in the lone AS cohort was SAVR (42 out of the total 59 AVRs) [194]. Finally, their AS-amyloid patients were significantly older (88±6 vs 70±14, $p<0.001$), which was a predictor of mortality in their univariate analysis ($p=0.001$), but which was not included in their multivariate analysis (although it is possible they ran this model separately, but were limited by the number of variables they could include in the final analysis due to limited events, which they acknowledge) [194].

The second of these was work published the same year by Castaño et al from Columbia University Medical Centre, who found the same AS-amyloid prevalence of 16% in their severe AS population who were undergoing TAVI (24 out of 151 patients) [195]. Here they used PYP scintigraphy (performed within 30 days after TAVI) to screen patients for AS-amyloid. No outcome data was reported in this study. Aside from the prevalence, there were other important similarities to our study – they too found those patients with AS-amyloid were older, with more impaired mitral annular S', lower V/M ratio and higher rates of RBBB [195]. There were also key differences: they had a male predominance (92%), with more low-flow, low-gradient AS in their AS-amyloid cohort [195]. Interestingly, although the median NT-

proBNP and troponin T were higher in the AS-amyloid cohort this did not reach statistical significance (the BNP was however found to be significantly higher) [195]. As in our study, these samples were taken prior to TAVI and the ranges quoted were wide. It is possible this is simply an issue of statistical power, or in fact it may reflect the possibility that the more unwell patients (with potentially higher biomarkers and who may have had AS-amyloid) did not undergo TAVI and therefore were not included in this study.

In this study 68% of patients recruited were male (a greater gender skew than that seen in the Partner 1 and 2 trials, where it was 58% and 54% male respectively [45,48]), which may explain some of the male predominance in the AS-amyloid cohort [195]. Also, the number referred clinically for PYP scintigraphy (i.e. with potential bias) is unclear and PYP scintigraphy was performed pragmatically after TAVI, so periprocedural complications preventing recruitment (e.g. mortality) may be missed in future outcome papers [195]. By comparison, all of the DPD scans performed in our study were performed prior to TAVI, with blinding of the clinicians to the results. Although it is unclear the PYP scanning protocol they used, all patients had a visual score of ≥2, with a H/CL ratio ≥1.5, which was used to diagnose ATTR cardiac amyloidosis in all of their patients in conjunction with the exclusion of a plasma cell dyscrasia in serum and urine. This is not unusual in the US and will be discussed in more detail in chapter five, however does mean that their outcome data may be different from ours, where we have a contingent of patients with grade 1 DPD scans, who may have a milder phenotype and therefore have improved outcomes.

AS-Amyloid vs Lone AS

Despite the lack of difference in mortality or periprocedural complication rates, there are indicators that AS-amyloid is different from lone AS: patients are older, with significantly higher NT-proBNP and hsTnT levels (particularly in those with a grade 2 DPD), lower ECG voltages and V/M ratio, as well as slightly thicker LV walls and an increased LV mass on echo. Of note, these differences in LV wall thickness and blood biomarkers seem to be more pronounced in those with DPD grade 2 AS-amyloid – although numbers in this subgroup analysis are small. NT-proBNP and

hsTnT could potentially play a role in the diagnostic work up and surveillance of these patients, however ranges were wide in this study.

The fact that RBBB on ECG is associated with AS-amyloid is intriguing and may prove relevant in the TAVI population, given that we know RBBB is associated with a higher likelihood of post-TAVI pacemaker implantation [196] and worse outcomes (although neither study investigated for the presence of concomitant cardiac amyloidosis) [196,197]. Castaño et al also found a significantly higher prevalence of RBBB in their AS-amyloid cohort (38% vs 16%, p=0.023) [195]. It is known that cardiac amyloidosis can cause RBBB [198], so it is possible that its presence in this population at baseline may be an indicator of dual pathology that deserves further investigation.

AS-amyloid patients also tended to have a lower baseline quality of life based on their EQ-VAS result (50 vs 65, *p=0.04*). These patients were on average three years older than those with lone AS and it is known that EQ-VAS results tend to decline with increasing age, but not usually to this degree. Based on data from 3395 people aged 18 and over living in the UK, we would only expect a decline of ~8 points in EQ-VAS between those aged 50-59 years and ≥80 years, whereas there was a decline by 15 points in only three years, so this age difference alone is unlikely to explain the whole story [199]. These patients also reported higher levels of anxiety/depression at baseline on EQ-5D-5L compared those with lone AS (46% vs 21% reporting at least moderate anxiety/depression, p=0.005). There is unfortunately little published data on this topic in patients with wtATTR cardiac amyloidosis, however patients with known AL amyloidosis with cardiac symptoms or hereditary TTR amyloidosis (with or without cardiac involvement) are known to suffer the high levels of anxiety and depression [200,201]. By necessity, these are studies of patients who are aware of their amyloid diagnosis – at the time of the baseline questionnaire most of our study patients would not have known their potential diagnosis of concomitant cardiac amyloid (the DPD scan would not yet have happened in many cases), so it is difficult to extrapolate these study findings to this cohort. Without other significant differences in the EQ-5D-5L domains (mobility, self-care, usual activities and pain/discomfort) it is also difficult to hypothesise that these patients felt physically worse relative to their lone AS counterparts (which may have

in turn affected their levels of anxiety/depression). Unfortunately, this may ultimately prove related to factors not quantified by the health questionnaire or the relatively small numbers of patients with AS-amyloid.

There may also be early indicators that patients with AS-amyloid more frequently report no change or a worsening in symptoms at 1-year post-TAVI compared to those with lone AS (57% vs 31%, *p=0.08*), although this did not quite reach statistical significance, nor was it reflected in the EQ-5D-5L results. We touched on earlier that 32.5% of patients in the NOTION trial were still experiencing NYHA II more worse symptoms at 1 year post-TAVI [53] and we see similar results in the PARTNER trial (Cohort A), where a significant proportion of TAVI recipients felt no better or worse at 1-year [57] – the presence of dual pathology may, at least in part, explain this.

In contrast to the wider TAVI literature [42,48,51,53,57], there was no significant improvement in any of the EQ-5D-5L parameters post-TAVI in either cohort. The greatest improvement was seen in the proportion of patients with AS-amyloid reporting at least moderate anxiety/depression, as well as those reporting at least moderate difficulty with their usual activities – both of which reduced by 14%, although these did not reach statistical significance (*p*=0.63 for both). At first glance this may suggest that TAVI offered no significant symptomatic benefit, however care should be taken interpreting these results, given that numbers are small (n=100) and follow-up only took place at a single 1-year timepoint - it is possible that other comorbidities, which may have developed over the 1-year follow-up period, may have attenuated any benefit seen post-TAVI (particularly given that the study population had an average age of 85). The borderline significant rise in the proportion of patients with lone AS struggling with self-care at 1-year post-TAVI may support this hypothesis (from 12% pre-TAVI to 22% 1-year post-TAVI, *p*=0.06). Never-the-less, given the heterogeneous nature of our study patients, who were recruited prospectively from two TAVI centres with very few exclusion criteria, these findings raise interesting questions about the 'real life' symptomatic benefit patients obtain post-TAVI outside the setting of a controlled clinical trial. What should also be considered, but cannot be quantified in this work, is the proportion of patients who have survived to complete their 1-year follow-up, directly as a result of having had their TAVI procedure.

Further work is needed in this area, particularly comparing symptomatic benefit in patients with AS-amyloid and lone AS. To this end, I am involved in ongoing work at our centre – looking at early (six weeks) symptom response post-TAVI, coupled with a more objective 6-minute walk test and biomarker response (NT-proBNP and hsTnT), for which BHF funding has been secured for my successor Dr Kush Patel (FS/19/48/34523).

Limitations

We were powered to detect a doubling of mortality at 1-year (21.4% up to 40%), which we have not demonstrated, but it is possible there are smaller mortality differences that we are missing. Blinding pre-procedure was broken for two reasons: six patients had a plasma cell dyscrasia necessitating unblinding as per protocol (although three of these were performed clinically and were therefore already unblinded) and a proportion of DPD scans were performed clinically (n=16) – it is likely that ~50% of these patients would have been recruited anyway to the study. Not all patients underwent TAVI, particularly in the AS-amyloid group. Follow-up was only mortality and quality of life at 1-year post-TAVI, there was no short-term functional assessment or assessment of readmission rates. The study is underpowered to compare DPD Perugini grade 1 to grade 2.

Conclusions

AS-amyloid is common and affects around 1 in 8 elderly patients with severe AS being considered for TAVI. Dual pathology is not associated with more periprocedural complications and long-term outcome is similar to those patients with lone AS, suggesting that no patient should be denied TAVI based on discovered dual pathology alone.

Chapter 4: ECV Quantification by CT

For this section of work, I was responsible for obtaining the relevant study approvals, for patient recruitment, for coordinating the scans, for the research scan acquisition, for performing the ECV_{CT} analyses and for the subsequent patient follow-up. The echocardiograms were reported clinically, however I quality-controlled analyses and re-analysed these as needed. Dr Kush Patel performed the longitudinal strain analysis on echocardiography and also helped with quality-control of the echocardiogram reports, as well as patient recruitment and ECV_{CT} analysis. Dr Joao Augusto helped with the ECV_{CT} analysis. Dr Bunny Saberwal recruited the control patients as part of a separate study (HEART-QIT: Evaluation of the Heart using Quantitative Imaging Techniques) evaluating the role of CT perfusion (including ECV_{CT}) in patients with suspected coronary artery disease. LV mass analysis on CT was performed by myself, Dr Thomas Treibel and Dr Astrid Putri. I also coordinated the ECG analysis, which was performed by Dr George Thornton and Dr Rebecca Hughes. Ernst Klotz provided physics support and reanalysed scans for interobserver variability assessment. Dr Sucharitha Chadalavada helped with assessing patient mortality.

4.1 Introduction

As we have discussed already, bone scintigraphy now offers a non-invasive means of diagnosing ATTR cardiac amyloidosis [88], however is not available in many UK centres and involves an additional separate test in patients who are often elderly and are already undergoing numerous cardiac (and non-cardiac) investigations.

As part of routine TAVI work-up, patients typically undergo CT to assess annulus dimensions, coronary artery height (and patency, where possible) and vascular access. The extracellular nature of amyloid deposition increases myocardial ECV higher than any other non-ischaemic cardiomyopathy [123] – increases which are detectable using ECV_{CT} [132]. We had just validated ECV_{CT} using a 5-minute post-contrast acquisition [132], making it a simple addition to an already clinically indicated TAVI work-up CT, which could be performed in the same sitting. Importantly, ECV also offers a means of quantifying cardiac amyloid burden in both

ATTR and AL cardiac amyloidosis, which is both prognostic and can track response to therapy [126,127,202].

The aim of this chapter was to assess whether ECV_{CT}, added to the clinical TAVI work-up CT, could be used to reliably detect cardiac amyloidosis as a screening tool. In order to facilitate easier and safer incorporation into clinical work-flow, we also sought to optimise the protocol in terms of radiation dose and assess whether using an earlier 3-minute post-contrast acquisition was feasible.

4.2 Results

109 patients were included in this part of thesis, as the remaining patients had already undergone their TAVI work-up CT prior to recruitment or were recruited at the John Radcliffe site, where we were not performing ECV_{CT}.

Early Technical Development

104 of the 109 patients (aged 86±5 years, 42% male) completed both 3- and 5-minute post-contrast acquisitions. In the five patients who did not complete both scans: one patient missed their 3-minute acquisition due to a technical issue, the remaining four patients did not receive the later acquisition (two for patient comfort and two were performed after validating the 3-minute acquisition, so we had begun to optimise the protocol by removing the 5-minute scan by that point). There was excellent correlation between both time points ($r^2 = 0.95$, $p<0.001$, figure 45). The 3-minute acquisition resulted in an acceptable ECV_{CT} result with very little bias – 0.68±1.2% lower than the 5-minute acquisition (figure 45 and 46). This bias appeared to increase above an ECV_{CT} of 40%, where such increases would not alter diagnostic accuracy.

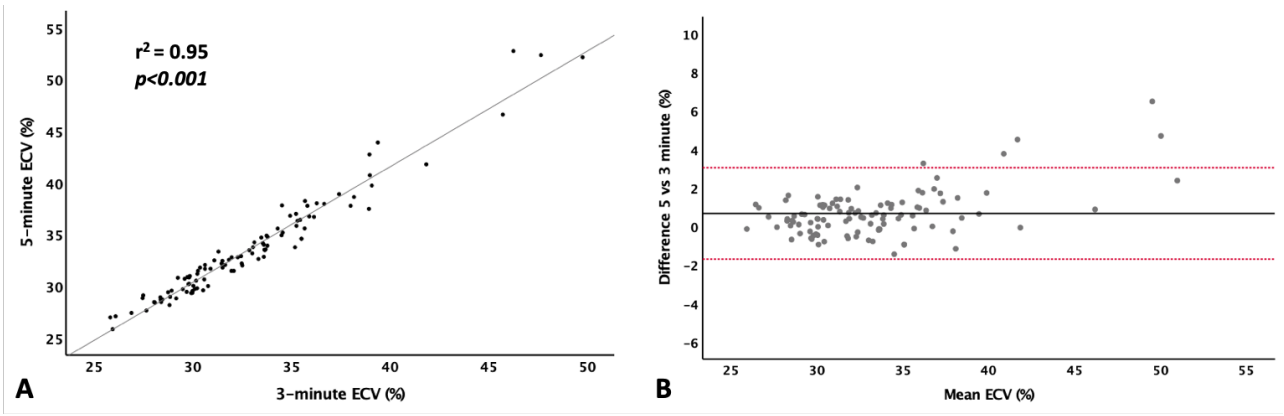

Figure 45: *A scatter plot (**A**) demonstrating an excellent correlation (r^2 = 0.95, p<0.001) between ECV_{CT} calculated using 5- and 3-minute post-contrast acquisitions, which is supported by findings on the Bland Altman plot (**B**). On the Bland Altman plot (**B**) the 95% limits of agreement are shown in red (-1.70% and 3.06%) and the mean difference is shown as the solid black line (0.68±1.2%). Note the slight increase in bias above an ECV of 40%. Differences are calculated as five minus three-minute post-contrast acquisition.*

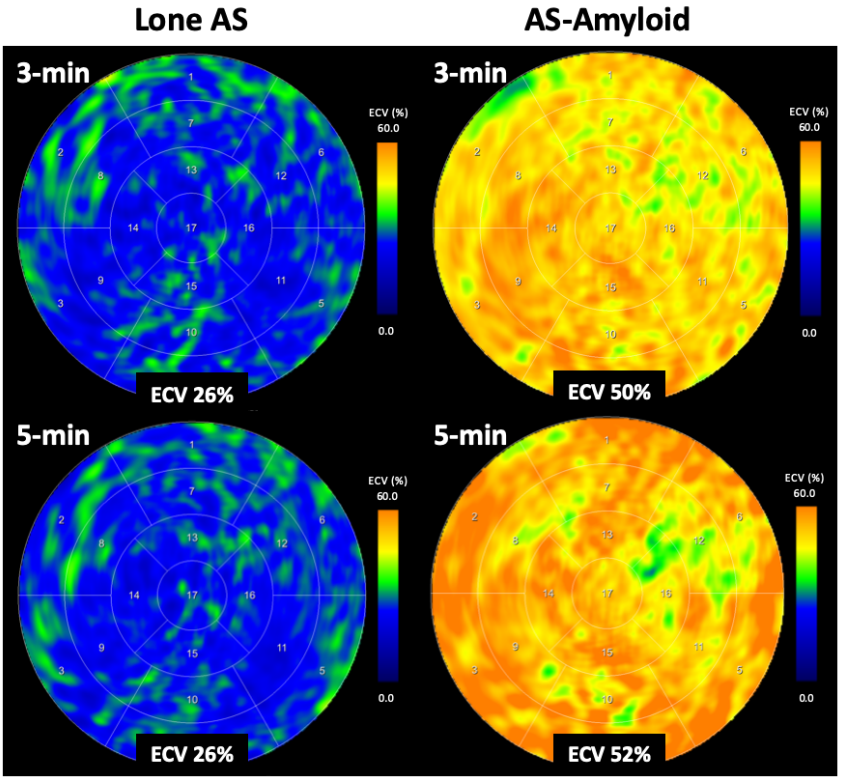

Figure 46: *Polar maps of ECV_{CT} using both 3- and 5-minute post-contrast acquisitions demonstrating almost identical results. On the left, an 89-year-old lady with lone AS and a normal global ECV of 26%. On the right, an 88-year-old lady with AS-amyloid (grade 2 DPD) and a markedly elevated global ECV of 50-52%.*

Detection of Cardiac Amyloidosis

109 patients (43% male, aged 86±5 years) underwent ECV_{CT}, along with 20 controls (65% male, aged 60±11 years). Patient characteristics (demographics, comorbidities, ECG, echocardiographic, CT, blood tests) are described in table 11.

As might be expected, hypertension, hypercholesterolemia, diabetes mellitus and atrial fibrillation were common. Overall LVEF was 54±11%, average peak AV velocity was 4.1±0.6m/s, average mean AV pressure gradient 41±14mmHg and AVA 0.71±0.23. Venous haematocrit was 0.38±0.04, which was usually taken on the same day as the CT scan (median 0 days, IQR 0-22 days).

16 patients (15%) had AS-amyloid by DPD scintigraphy (5 Perugini grade 1, 11 grade 2), 56% male and aged 88±5 years. A plasma cell dyscrasia was detected in 5 patients (31%) – AL cardiac amyloid was considered unlikely in all following a comprehensive clinical work-up (which included fat aspirate and ^{123}I-labelled serum amyloid P scintigraphy in 4/5 patients). As in chapter three, all patients genotyped (n=9) were wild-type.

	AS-amyloid (n=16)	Lone AS (n=93)	*p*-value
Demographics			
Male	9 (56%)	38 (41%)	0.25
Age (years)	88±5	85±5	0.08
Clinical Parameters			
Hypertension	13 (81%)	73 (78%)	1.00
Hypercholesterolemia	7 (44%)	37 (40%)	0.77
Diabetes Mellitus	1 (6%)	24 (26%)	0.11
Atrial Fibrillation	8 (50%)	41 (44%)	0.66
Permanent Pacemaker	2 (13%)	12 (13%)	1.00
ECG Parameters			
Heart rate (bpm)	70±14	73±16	0.46
Low voltage limb leads	0 (0%)	1 (1%)	1.00
S-L Criteria (mV)	1.8±0.5	2.6±1.0	**0.048**
1st Degree AV Block*	1 (7%)	20 (22%)	0.30
QRS duration (ms)	120±20	103±26	**0.01**
LBBB*	2 (13%)	8 (9%)	1.00
RBBB*	6 (38%)	6 (7%)	**0.002**
Echo Parameters			
Left Ventricle			
LVEF (%)	58±10	54±10	0.18
Indexed SV (ml/m^2)	35±9	38±12	0.29
IVSd (cm)	1.4±0.3	1.3±0.2	**0.002**
PWd (cm)	1.3±0.3	1.1±0.2	**<0.001**

Table Continued	AS-amyloid (n=16)	Lone AS (n=93)	*p*-value
Echo Parameters Continued			
Left Ventricle Continued			
RWT (cm)	0.61±0.20	0.48±0.13	**0.002**
Indexed LV mass (g/m^2)	137±31	113±37	**0.01**
MCF (%)	19.4±7.2	24.5±8.4	**0.02**
Mitral annulus S' (m/s)	0.05±0.01	0.06±0.01	0.08
GLS (%)	-16±6	-15±7	0.62
Diastolic Function			
E/A ratio	1.4 (0.9-2.3)	0.8 (0.7-1.1)	0.07
Lateral E/E'	21±15	17±8	0.28
MVDT (ms)	238±80	234±92	0.87
LA diameter (cm)	4.4±0.6	4.0±0.7	0.08
Right Ventricle			
TAPSE (cm)	1.89±0.36	1.92±0.48	0.82
TR peak velocity (m/s)	2.94±0.57	2.80±0.65	0.51
PASP (mmHg)	40±15	37±15	0.62
Aortic Valve			
Peak velocity (m/s)	4.02±0.62	4.12±0.63	0.55
Mean gradient (mmHg)	38±12	42±14	0.36
AVA (cm^2)	0.72±0.21	0.71±0.23	0.92
CT Parameters			
AV Calcium Score (HU)	2170 (1665-3602)	2107 (1491-3109)	0.60
Indexed LV mass (g/m2)	91±24	72±17	**0.01**
ECV_{CT} (%)	41±7	32±3	**<0.001**
Composite Parameters			
V/M ratio (mV/g/m^2)	0.013±0.004	0.026±0.011	**<0.001**
Indexed Matrix Vol (ml/m2)	38±15	23±6	**0.001**
Blood Results			
Haematocrit	0.38±0.05	0.38±0.04	0.92
Creatinine (mmol/L)	115 (96-125)	96 (83-120)	0.07
eGFR (ml/min/1.73m^2)	47±12	54±17	0.12
hsTnT (ng/L)	43 (28-75)	20 (14-34)	**0.001**
NT-proBNP (ng/L)	3668 (1259-5165)	1361 (593-2816)	**0.03**

Table 11: *Basic demographics, clinical, echocardiographic, CT and composite parameters for patients with lone AS and those with dual pathology (AS-amyloid) who underwent ECV_{CT} prior to TAVI. AVA = aortic valve area, eGFR = estimated glomerular filtration rate, hsTnT = high-sensitivity troponin T, HU = Hounsfield units, IVSd = interventricular septum diameter, GLS = global longitudinal strain, LBBB = left bundle branch block, MCF = myocardial contraction fraction, MVDT = mitral valve deceleration time, NT-proBNP = N-terminal pro-brain natriuretic peptide, PWd = posterior wall diameter, RBBB = right bundle branch block, RWT = relative wall thickness, S-L = Sokolow-Lyon, TAPSE = tricuspid annular plane systolic excursion, V/M ratio = voltage/mass ratio. Values represent mean ± standard deviation or median (interquartile range) where appropriate. *Missing ECG data in four lone AS and one AS-amyloid patient – percentages and statistics quoted reflect this.*

There was no difference in the age (88±5 vs 85±5 years, *p=0.08*) or proportion of male patients (56% vs 41%, *p=0.25*). The cardiovascular risk profile (hypertension, hypercholesterolaemia and diabetes mellitus), presence of AF or permanent pacemaker pre-TAVI were similar. Consistent with findings in chapter three, the S-L criteria (1.8±0.5 vs 2.6±1.0mV) and V/M ratio (0.013±0.004 vs 0.026±0.011mV/g/m^2) were both lower in AS-amyloid (*p=0.048* and *<0.001* respectively), with a higher prevalence of RBBB (38% vs 7%, *p=0.002*). The QRS duration was also longer in AS-amyloid (120±20 vs 103±26ms, *p=0.01*). In AS-amyloid, parameters reflecting LV thickness and mass were higher, whereas the MCF was lower (19.4±7.2 vs 24.5±8.4%, *p=0.02*). GLS was impaired in both AS-amyloid and lone AS, but not significantly different (-16±6 vs -15±7%, *p=0.62*). Both hsTnT and NT-proBNP were higher in AS-amyloid, independent of renal function (table 11).

Extracellular Volume

Global ECV$_{CT}$ was 32±3%, 34±4% and 43±6% in Perugini grade 0, 1 and 2 respectively using a 3-minute post-contrast acquisition, *p<0.001* for trend (figures 47 and 48). By comparison, global ECV$_{CT}$ in controls was 28±2% using a 5-minute post-contrast protocol, lower than those patients with lone AS at similar post-contrast timing: (33±4%, *p<0.001*). The ECV$_{CT}$ in the basal septum (average of AHA segments two and three) the ECV$_{CT}$ was 31±3%, 32±4% and 45±7% in DPD Perugini grade 0,1 and 2 respectively, *p<0.001* for trend (figure 41).

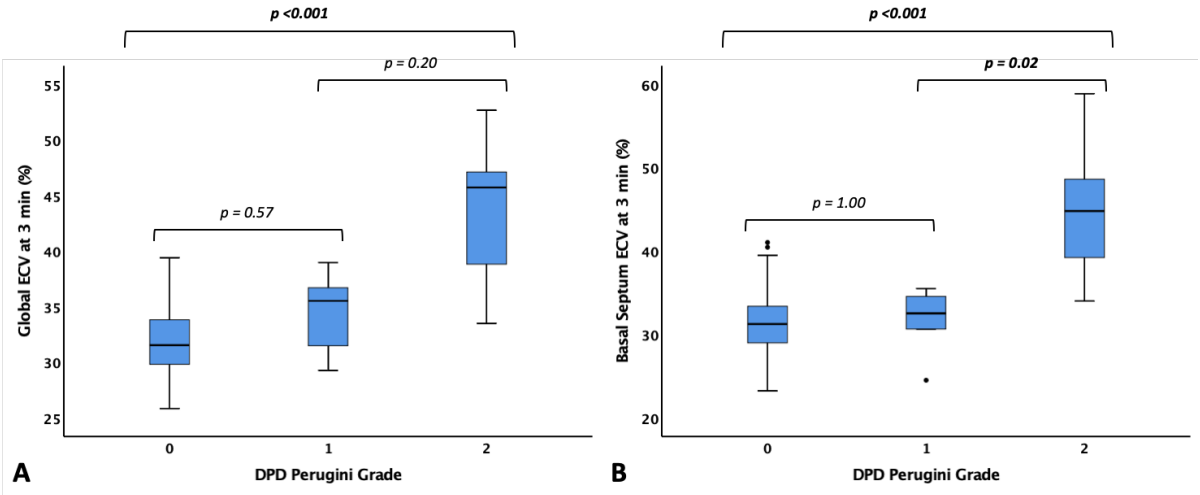

Figure 47: *Box and whisker plot showing the change in the global (**A**) and basal septal (**B**) ECV$_{CT}$ at 3-minutes by DPD Perugini grade: 0 = negative (lone AS), 1-2 = increasingly positive (AS-amyloid). P<0.001 for trend and for the pairwise comparison of grade 0 vs grade 2. DPD = ^{99m}Tc-3,3-diphosphono-1,2-propanodicarboxylic acid scintigraphy, ECV = extracellular volume.*

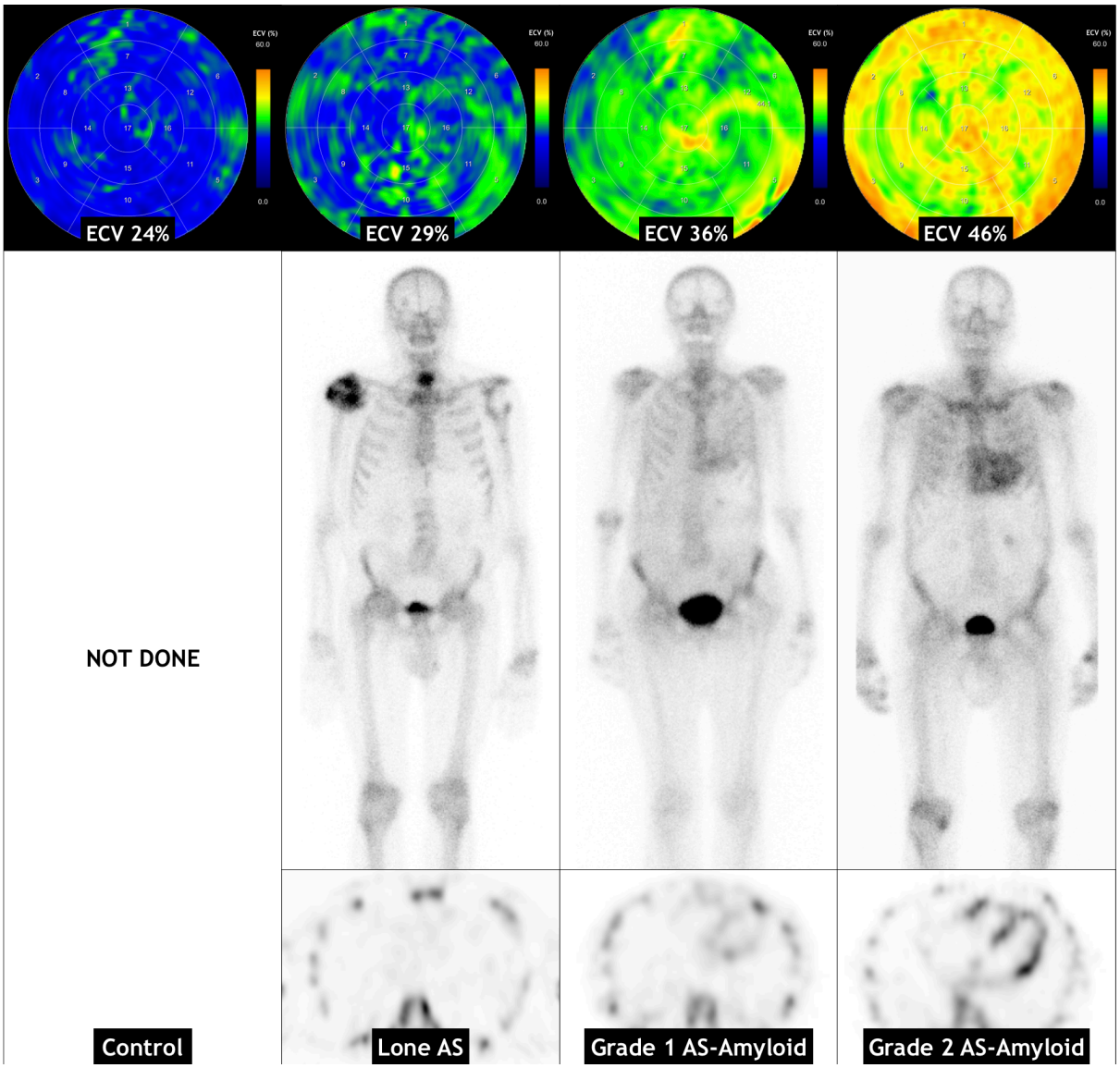

Figure 48: *Example ECV_{CT} polar maps (top), DPD planar (middle) and axial SPECT images (bottom) from the control group (far left) through lone AS, DPD Perugini grade 1 and DPD Perugini grade 2 groups (far right).*

Using global ECV_{CT} for the detection of any cardiac amyloid (DPD Perugini grade 1 or 2) the AUC was 0.87 (95% confidence interval 0.75 - 0.98) using a 3-minute post-contrast acquisition (figure 49). Different ECV thresholds could be set: 29.2% (sensitivity 100% specificity 19%); 31.4% (sensitivity 94%, specificity 48%) or 33.4% (sensitivity 88%, specificity of 66%). If repeated for the detection of only grade 2 AS-amyloid (as there is more uncertainty about the clinical significance of Perugini grade 1 cardiac amyloidosis) the AUC improved to 0.95 (95% confidence interval 0.89-1.00) and an ECV_{CT} of 33.4% offered 100% sensitivity and 64% specificity (figure 50).

Excluding the apical segment (which is often the thinnest area of myocardium and can be challenging to contour), made little difference to the AUC for the detection of *any* cardiac amyloid (0.867 vs 0.870) or the detection of grade 2 cardiac amyloidosis (0.953 vs 0.951). There was also no improvement in sensitivity or specificity compared to global ECV_{CT}.

Using only the septal ECV_{CT}, the diagnostic accuracy for any cardiac amyloid was similar to that for the global ECV_{CT}, with an AUC of 0.85 (95 confidence interval 0.72-0.98) and no particular improvement in sensitivity and specificity (figure 49). If repeated for the detection of established grade 2 AS-amyloid, the AUC improved to 0.98 (95% confidence interval 0.94 to 1.01) (figure 50). An ECV_{CT} of 34% offered 100% sensitivity, but a specificity of 84% (previously 64% using a global ECV_{CT} threshold of 33.4%).

Composite Parameters

The V/M ratio was lower in AS-amyloid and performed similarly well to ECV_{CT} for the detection of *any* cardiac amyloid (AUC 0.87), but not quite as well for the detection of DPD grade 2 cardiac amyloidosis (AUC 0.85). A V/M ratio of <0.021 had a sensitivity of 100%, but a specificity of 62% for the detection of any AS-amyloid. The same threshold had a sensitivity of 100% and specificity of 61% for the detection of only grade 2 AS-amyloid. It outperformed PWd alone (AUC 0.75 and 0.76 for any AS-amyloid and grade 2 AS-amyloid respectively). However, nearly a third of patients (32 in total) had to be excluded from this analysis due the presence of bundle branch block or a ventricular paced rhythm. MCF also performed reasonably well as a screening tool (AUC 0.66 and 0.74 for any AS-amyloid and grade 2 AS-amyloid respectively) in this population (figures 49 and 50).

Similar to ECV_{CT}, the indexed matrix volume increased significantly across DPD grades: 23±6ml/m2 (grade 0) vs 28±4ml/m2 (grade 1) vs 42±16ml/m2 (grade 2), *p<0.001* for trend. Despite the addition of indexed LV mass to the parameter, its diagnostic accuracy remained similar to that of ECV alone for the detection of any cardiac amyloid: AUC 0.86 (95% confidence interval 0.77 - 0.95) (figure 49) and was inferior for the detection of DPD Perugini grade 2 AS-amyloid: AUC 0.88 (95% confidence interval 0.77-1.00) (figure 50).

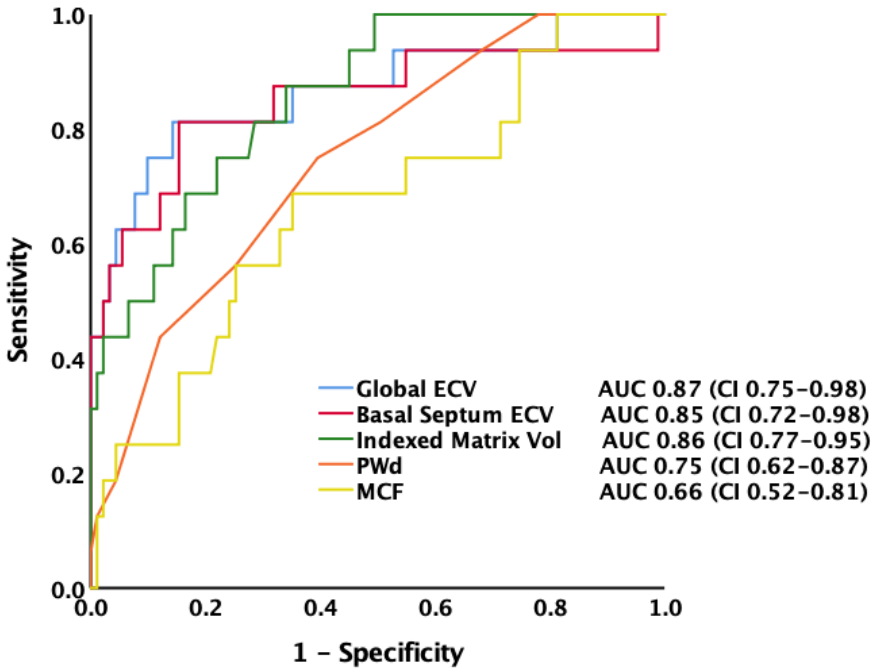

Figure 49: *Receiver operating characteristic (ROC) curves for the detection of <u>any</u> cardiac amyloid (DPD Perugini grade 1 or 2) using ECV_{CT} with a 3-minute post-contrast acquisition, indexed matrix volume (matrix vol), posterior wall diameter (PWd) and myocardial contraction fraction (MCF). Voltage/mass ratio has not been included, as this would exclude a significant proportion of patients for all parameters. AUC = area under the curve, CI = 95% confidence interval, DPD = ^{99m}Tc-3,3-diphosphono-1,2-propanodicarboxylic acid scintigraphy, ECV = extracellular volume.*

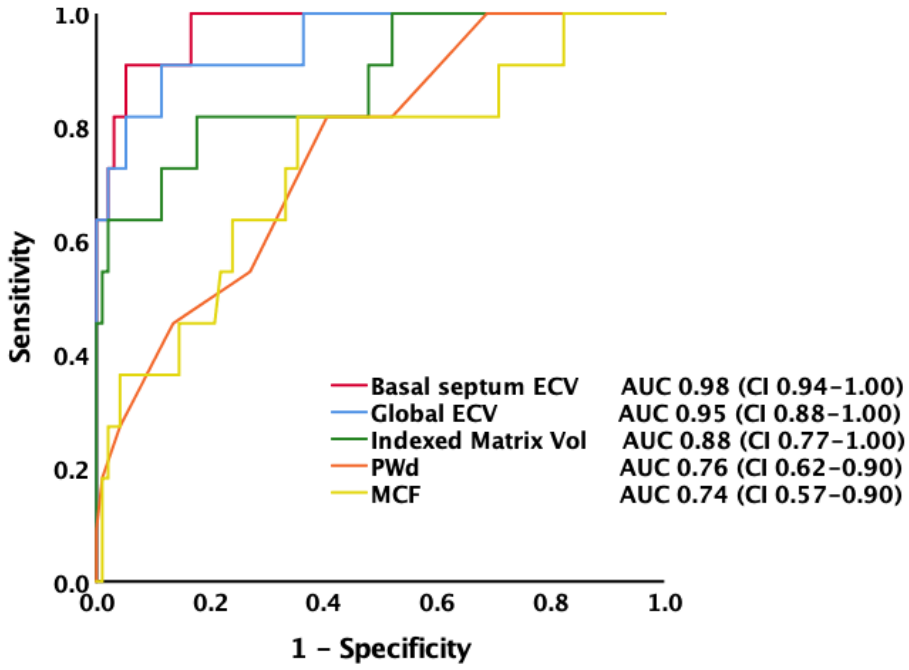

Figure 50: *Receiver operating characteristic (ROC) curve for the detection of <u>DPD Perugini grade 2 AS-amyloid</u> using basal septal and global ECV_{CT} with a 3-minute post-contrast acquisition, indexed matrix volume (matrix vol), posterior wall diameter (PWd) and myocardial contraction fraction (MCF). AUC = area under the curve, CI = 95% confidence interval, DPD = ^{99m}Tc-3,3-diphosphono-1,2-propanodicarboxylic acid scintigraphy, ECV = extracellular volume quantification.*

Predictors of Amyloid Presence

Univariate analysis identified ECV_{CT}, the presence of RBBB and parameters associated with LV wall thickness or mass (IVSd, PWd, indexed LV mass, MCF and V/M ratio) as predictors of AS-amyloid (table 12). Multivariate analysis of age, ECV_{CT}, male gender, PWd and RBBB showed that only ECV_{CT} and the presence of RBBB was associated with AS-amyloid (p = 0.001 and 0.01 respectively, table 12). For every 1% increase in ECV_{CT} there was a 1.6-fold increase in the likelihood of AS-amyloid (95% confidence interval 1.21 – 2.10).

Univariate Analysis			Multivariate Analysis		
Variable	***p*-value**	**Exp (B)**	***p*-value**	**Exp (B)**	**CI for Exp (B)**
Demographics					
Age (per year increase)	0.08	1.10	0.38	1.09	0.90 – 1.30
Gender (male)	0.26	1.86	0.80	0.80	0.14 – 4.54
ECG Parameters					
S-L Criteria (per mV decrease)	0.06	0.26	-		
LBBB	0.60	1.56	-		
RBBB	**0.001**	9.22	**0.01**	16.84	1.89 – 149.94
Echo Parameters					
Left Ventricle					
LVEF (per % increase)	0.18	1.04	-		
Indexed SV (per ml/m^2 decrease)	0.28	0.97	-		
IVSd (per cm increase)	**0.005**	44.66	-		
PWd (per cm increase)	**0.003**	53.83	0.46	4.01	0.10 – 161.09
RWT (per cm increase)	**0.006**	178.47	-		
Indexed LV Mass (per g/m^2 increase)	**0.02**	1.02	-		
MCF (per % decrease)	**0.02**	0.91	-		
Mitral Annulus S' (per m/s decrease)	0.08	0.00	-		
GLS (per % decrease)	0.61	0.98	-		
Diastolic Function					
E/A Ratio (per unit increase)	0.04	1.74	-		
Lateral E/E' (per unit increase)	0.11	1.04	-		
MVDT (per ms increase)	0.87	1.00	-		
LA Diameter (per cm increase)	0.08	2.04	-		
Right Ventricle					
TAPSE (per cm decrease)	0.81	0.87	-		
TR peak velocity (per m/s increase)	0.50	1.46	-		
PASP (per mmHg increase)	0.62	1.01	-		

Univariate Analysis Continued			Multivariate Analysis Continued		
Variable	***p*-value**	**Exp (B)**	***p*-value**	**Exp (B)**	**CI for Exp (B)**
Echo Parameters Continued					
Aortic valve					
Peak velocity (per m/s decrease)	0.55	0.77			
AV Mean PG (per mmHg decrease)	0.36	0.98			
AVA (per cm^2 increase)	0.92	1.12			
CT Parameters					
AV Calcium Score (per HU increase)	0.56	1.00	-		
Indexed LV Mass (per g/m^2 increase)	**0.001**	1.02	-		
ECV_{CT} (per % increase)	**<0.001**	1.49	**0.001**	1.60	1.21 – 2.10
Composite Parameters					
V/M Ratio (per $mV/g/m^2$ decrease)	**0.02**	0.00	-		
Indexed Matrix Vol (per ml/m2 increase)	**<0.001**	1.18	-		
Blood Results					
hsTnT (per ng/L increase)	0.06	1.01	-		
NT-proBNP (per ng/L increase)	0.41	1.00	-		

Table 12: *Univariate and multivariate binary logistic regression analysis, showing that ECV_{CT} and the presence of RBBB was associated with AS-amyloid. For every 1% increase in ECV_{CT} there was a 1.6-fold increased likelihood of AS-amyloid. Only one parameter representing LV wall thickness or mass was included in the multivariate analysis to avoid multicollinearity (in this case PWd, as it had the strongest association on univariate analysis). AV = aortic valve, AVA = aortic valve area, Exp (B) = exponentiation of the B coefficient, GLS = global longitudinal strain, hsTnT = high-sensitivity troponin T, HU = Hounsfield units, IVSd = interventricular septum diameter, LV = left ventricle, LBBB = left bundle branch block, LVEF = left ventricular ejection fraction, MCF = myocardial contraction fraction, MVDT = mitral valve deceleration time, NT-proBNP = N-terminal pro-brain natriuretic peptide, PWd = posterior wall diameter, RBBB = right bundle branch block, RWT = relative wall thickness, S-L = Sokolow-Lyon, TAPSE = tricuspid annular plane systolic excursion.*

Prognosis in Lone AS

Looking at only the lone AS cohort (n=93), of which 41% were male with an average age of 85±5 years and 75 (81%) had undergone TAVI, there were a total of 20 deaths (22%) over a median follow up period of 20 months (IQR 12-27 months).

There were four deaths in the 43 patients with a global ECV_{CT} ≤31% (9%) compared to 16 in the 50 patients with a global ECV_{CT} >31% (32%, *p=0.003*) (figure 51). Dividing the cohort into tertiles based on global ECV_{CT}, there were four deaths in the lowest tertile (ECV_{CT} <30%) out of 28 patients (14%), eight deaths in the 42 patients (19%) in the middle tertile (ECV_{CT} 30-34%) and 8 events in the 23 patients (35%) in the highest tertile (ECV_{CT} >34%, *p=0.10*) (figure 51).

Looking at ECV_{CT} in the septum only, there were 5 deaths in the 44 patients (11%) with a septal ECV_{CT} ≤31%, compared to 15 in the 49 patients (31%) with a septal ECV >31% (*p=0.02*) (figure 51). Dividing the cohort into tertiles based on septal ECV_{CT}, there were 2 deaths in the lowest tertile (ECV_{CT} <29%) out of 24 patients (8%), 8 deaths in the 44 patients (18%) in the middle tertile (ECV_{CT} 29-33%) and 10 events in the 25 patients (40%) in the highest tertile (ECV_{CT} >33%, *p=0.02*) (figure 51).

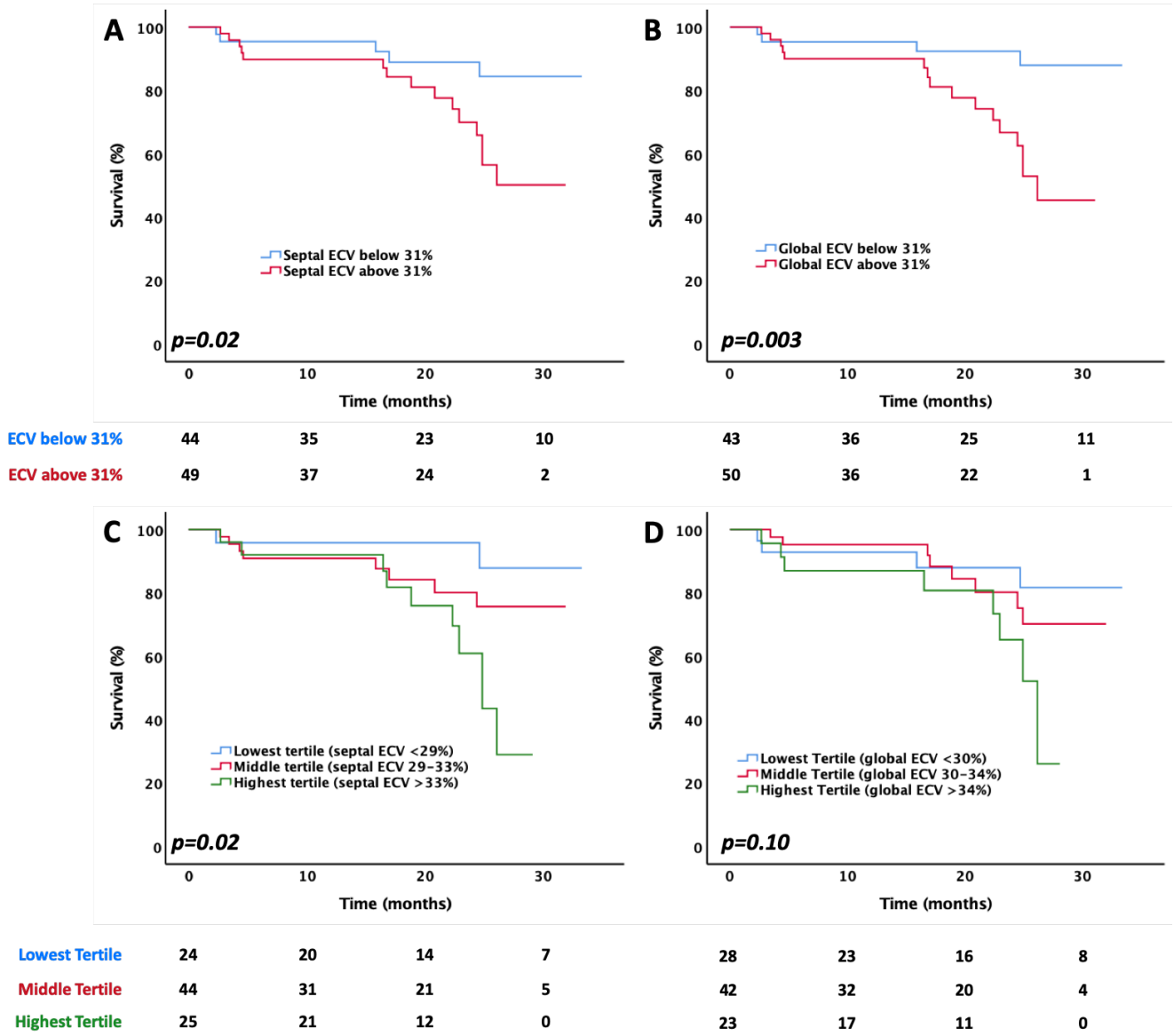

Figure 51: *Kaplan-Meier survival curves in lone AS (n=93) by septal (**A** and **C**) and global ECV_{CT} (**B** and **D**) divided into above or below 31% (**A** and **B**) or into tertiles (**C** and **D**). ECV = extracellular volume.*

Dose Optimisation Results

The dose-length product (DLP) for the full baseline, 3- and 5-minute 'axial shuttle mode' datasets was 182±26mGy.cm, 183±24mGy.cm and 180±24mGy.cm respectively. To investigate dose reduction strategies, we re-analysed ECV_{CT} derived using fewer 'shuttles' (1 or 2 vs 4) for the baseline and 3-minute post-contrast acquisitions in a subset of patients (n=27) to assess for any impact on diagnostic performance. Including 13 patients with lone AS and 14 patients with cardiac amyloid (9 were Perugini grade 2), there was minimal bias for 1 vs 4 shuttles (0.91±2.1%) or 2 vs 4 shuttles (0.28±0.78%) (figure 52). The two outliers with differences beyond the 95% limits of agreement were both patients weighing over 90kg, where dose modulation would likely be used clinically. There was overall excellent correlation between 1 or 2 vs 4 shuttles (r^2 = 0.93 and 0.99 respectively, *p<0.001*, figure 52).

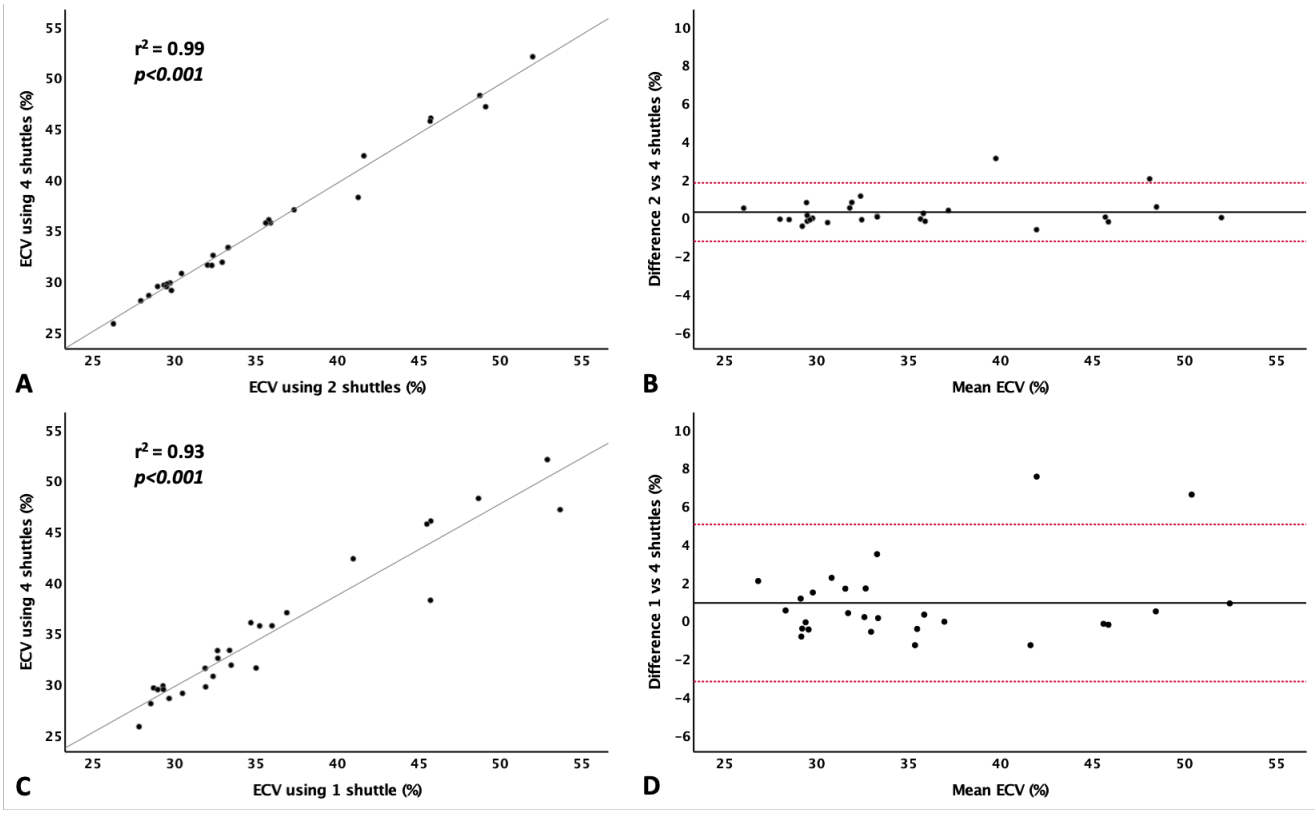

Figure 52: *Correlation between ECV_{CT} acquired using 2 vs 4 shuttles (top row) and 1 vs 4 shuttles (bottom row). Scatter plots (**A** and **C**) show excellent correlation, supported by the corresponding Bland Altman plots (**B** and **D**). The 95% limits of agreement are shown as the red dotted lines (-1.25% and 1.81% for **B**; -3.20% and 5.03% for **D**), with mean difference as the solid black line (0.28% for **B**; 0.91% for **D**). Differences are calculated as one minus four shuttles and two minus four shuttles respectively. Note the two outliers beyond the 95% limits of agreement, both weighing over 90kg.*

Given the current fixed protocol settings, reducing the protocol to a single shuttle pre- and 3-minutes post-contrast would reduce the dose by a factor of four: total DLP would be ~90mGy.cm for both baseline and 3-minute post contrast additional datasets (effective dose 2.3mSv, using the higher cardiac k-factor of 0.026) [203].

Reproducibility and Variability

At the beginning of the ECV_{CT} analysis process in order to quality control analyses the first five patients were dual read by a second, experienced reporter remotely (EK). Inter-observer variability was measured across 75 variables: endocardial, epicardial and mid-myocardial global, basal, mid, apical and septal ECV for each patient. The intraclass correlation coefficient (two-way, mixed-effects model, absolute agreement) was 0.99 (95% confidence interval 0.98-1.00) for single measures.

Intra-observer variability (PS) was also assessed by comparing the global 3-minute ECV_{CT} results for the 27 patients who were re-analysed for dose-reduction assessment (four shuttles), with the initial results for those patients. There was a mean ECV difference between measures (initial minus repeat) of 0.15±0.49% and an intraclass correlation coefficient (two-way, mixed-effects model, absolute agreement) of 0.998 (95% confidence interval 0.995-0.999) for single measures.

4.3 Discussion

Lone AS results in detectable increases in ECV_{CT} compared with control subjects. ECV_{CT} can detect dual AS-amyloid pathology in potential TAVI patients, with only an additional 3-minutes post-contrast acquisition and a small radiation burden (~2.3mSv). It is highly reproducible and measured ECV_{CT} not only detects AS-amyloid, but tracks the degree of infiltration. Furthermore, ECV_{CT} is also associated with outcome in patients with lone AS.

Normal ECV_{CT} is in the region of 27% (adjusted down by 0.68±1.2% for the 3-minute post-contrast equivalent), which is consistent with the wider literature in both CT [204] and CMR [123]. Patients with lone AS had a higher ECV_{CT} (32±3% with 3-minute post-contrast) likely reflecting a degree of myocardial fibrosis [123,205].

ECV_{CT} was even higher in patients with AS-amyloid (41±7%) and seemed to track amyloid burden (as measured by DPD Perugini grade). This is very much in keeping with the extracellular deposition of amyloid fibrils within the myocardium, which are known to result in some of the most profound elevations in ECV_{CMR} (higher than any other non-ischaemic cardiomyopathy) [123]. Given its simplicity, there is likely to be a role for ECV_{CT} as a screening tool to detect cardiac amyloid in patients already undergoing cardiac CT, which will be discussed in more detail in chapter six.

ECV and Outcome

Allowing for the small sample size (n=93) and the fact that 19% of these patients did not undergo TAVI, ECV_{CT} in patients with lone AS seemed to predict prognosis, with those patients with a global ECV_{CT} >31% having a significantly higher mortality than those who do not (32% vs 9%, *p=0.003*), which also held true using a septal ECV_{CT} (31% vs 11%, *p=0.02*). By dividing these patients into tertiles based on their global or septal ECV_{CT} increasing ECV_{CT} seemed to track increasing mortality (*p=0.10* and *0.02* respectively). Septal ECV_{CT} representing more a marker of diffuse fibrosis and global ECV_{CT} a composite of diffuse and focal (infarct) fibrosis in this case. This is the first time that ECV_{CT} has been shown to predict outcome in lone AS and, importantly, it mirrors results seen using LGE to quantify myocardial scar burden in CMR. As discussed earlier in the introduction, a study from the BSCMR Valve Consortium in 674 patients with severe AS who underwent either SAVR (n=399) or TAVI (n=275) showed that scar was present in 51% of patients (18% was infarct and 33% non-infarct pattern) [36]. The presence of any type of scar was associated with double all-cause mortality and three times the cardiovascular mortality over a median follow-up of 3.6 years (independent of whether SAVR or TAVI was performed) [36]. Both infarct and non-infarct scar were associated with similarly adverse outcomes [36].

We know that ECV increases with fibrosis/scar and so it would follow that ECV_{CT} would correlate with mortality in AS in very much the same way that LGE seems to. Given that the BSCMR Valve Consortium found that for every 1% increase in LV myocardial scar there was an 11% higher all-cause mortality [36], it is not surprising that even in smaller numbers of patients (n=93 in our case) there is an excess mortality associated with a higher ECV_{CT}. We know that LV decompensation in AS

is characterised by fibrosis and irreversible myocyte loss, which would both explain these ECV_{CT} elevations and the associated mortality [9,36,206]. Further work is needed to validate this in a larger population, as there may be a role for pre-procedural risk assessment in the TAVI population (and potentially others).

Heterogeneity in ECV in Lone AS

In chapters 1, we briefly discussed the myocardial response to the increased afterload of AS, with varying degrees of appropriate LVH, over time giving way to a more maladaptive response involving myocardial fibrosis and eventual LV impairment [9,31]. Recent work by our own group has shown that this myocardial fibrosis seems to be in the form of three main types: endocardial fibrosis, microscars (mainly subendocardially) and diffuse interstitial fibrosis [205]. This endo- to epicardial gradient in fibrosis in AS was noted in studies as early as the 1970s and 80s and may relate to low endocardial perfusion [205,207,208]. CT, with its superior spatial resolution and isotropic data, offers us a non-invasive means of further exploring these findings. An example of this is that not only can we analyse ECV_{CT} per AHA segment, but we can look at the endo vs mid vs epicardial distribution both for the whole heart or per segment, which did seem to show a similar endo to epi gradient (figure 53), although further work is ongoing.

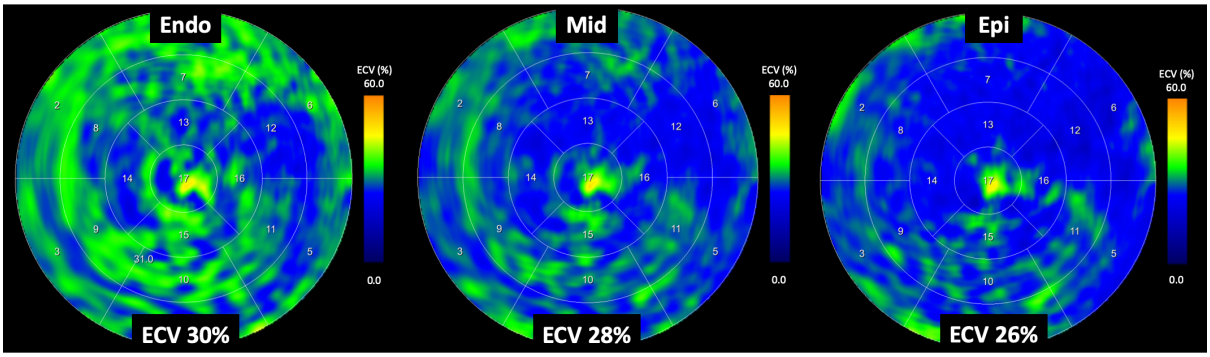

Figure 53: *Subtle endo- (left) to epicardial (right) gradient seen with lone AS, with global ECV_{CT} decreasing from 30% down to 26%. Endocardium was defined as the inner 10-50%, mid-myocardium the middle 25-75% and epicardium the outer 50-90%.*

Further work is ongoing to explore this apparent detectable endo- to epicardial gradient using ECV_{CT}, which is also seen in those patients with AS-amyloid (in keeping with the subendocardial late gadolinium enhancement often seen on CMR in cardiac amyloid [118]).

There was also significant variability in ECV_{CT} within the lone AS cohort – ranging from 26% up to 39%, which (at least in part) likely reflects the heterogeneity of myocardial fibrosis seen in the elderly AS population (figure 54).

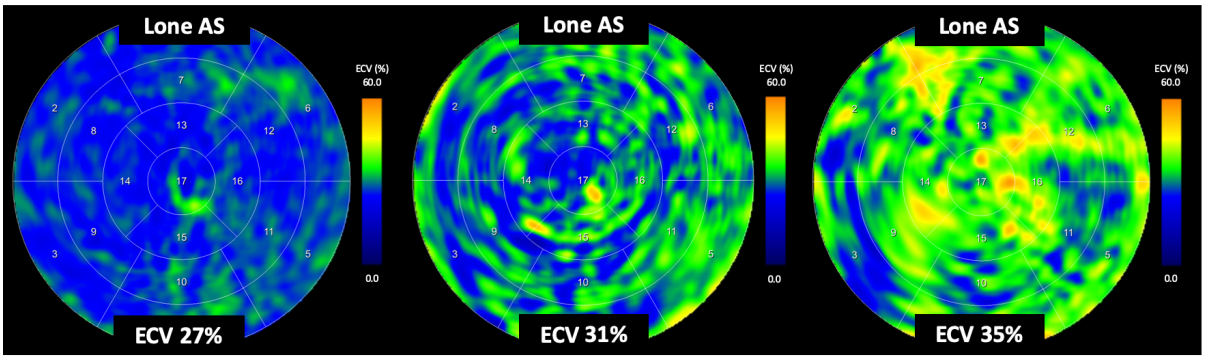

Figure 54: *17-segment polar maps demonstrating the heterogeneity in ECV_{CT} in lone AS. All of these three patients had a negative DPD scan. Note the diffuse elevations in ECV_{CT} in three patients with lone AS (increasing from left to right), which are not in keeping with any single coronary territory.*

We also know that an MI (acute or chronic) significantly increases ECV [123], which introduces another potential reason for the variability, as it is likely that a significant proportion of patients had concomitant ischaemic heart disease (either known or otherwise), which would result in focal areas of ECV elevation corresponding to known coronary territories (figure 55). ~10% of patients in our study had focal elevations of ECV_{CT} with corresponding coronary artery disease on the CTCA or contemporary coronary angiography. We will discuss the impact of this in more detail in the chapter six.

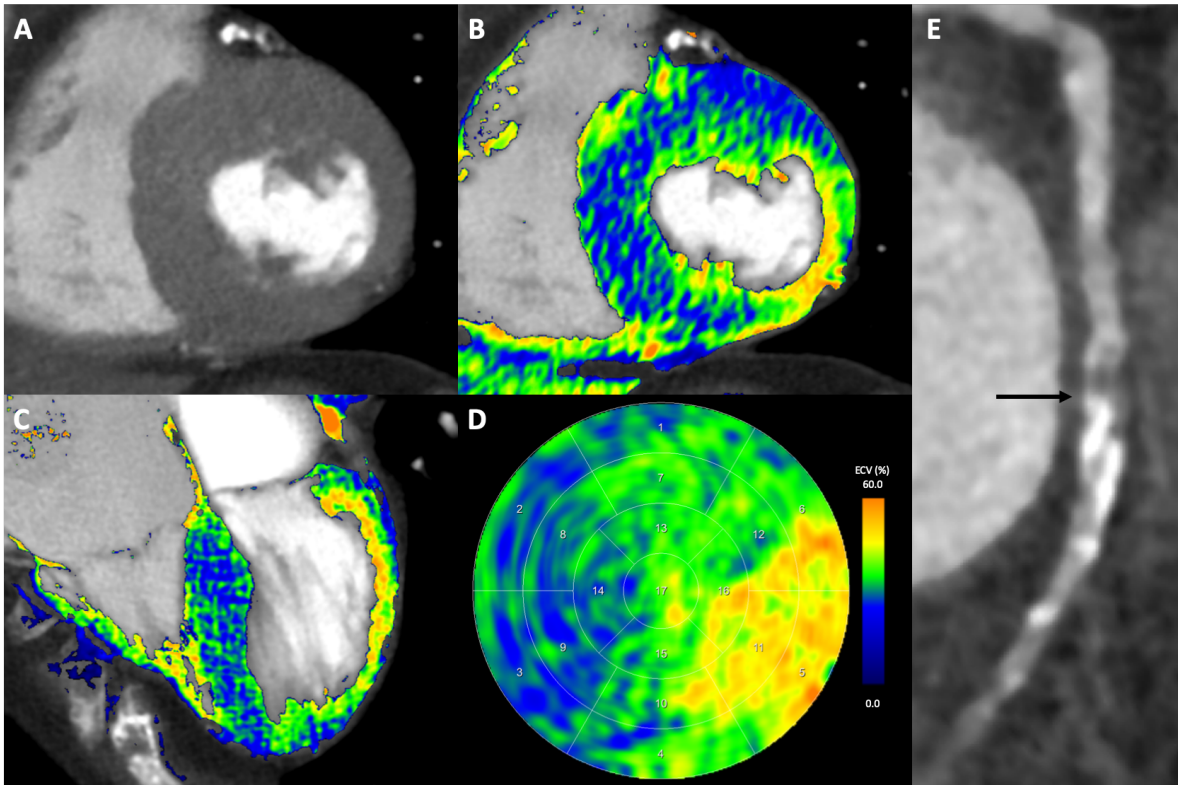

Figure 55: *Contrast enhanced short axis CTCA image (**A**) showing a thinned lateral LV wall with corresponding areas of focal ECV elevation on the fused short-axis (**B**) and four-chamber (**C**) views, as well as the 17-segment polar map (**D**). Assessment of the coronary arteries on the same CTCA was limited due to a high calcium burden, however there is a mixed plaque in the mid left circumflex artery (**E**, arrowed) causing a sub-total occlusion, which is likely the culprit.*

Amyloid Burden

Very much akin to the way in which ECV_{CMR} tracks amyloid burden on DPD [126], ECV_{CT} does the same – increasing from lone AS up to grade 2 AS-amyloid. Therefore, in this current climate of novel amyloid-specific therapies, this could offer an alternative means of monitoring patient response – in the same way that ECV_{CMR} can track primary light-chain (AL) cardiac amyloid regression with therapy [127].

We have already touched on the wealth of data available from these CT datasets, but given the high spatial resolution of the technique, we are also likely to be able to detect and gain insights into particular patterns of amyloid deposition in the myocardium, such as the well-reported apical-sparing pattern seen on longitudinal strain assessment on echocardiography (figure 56) [111].

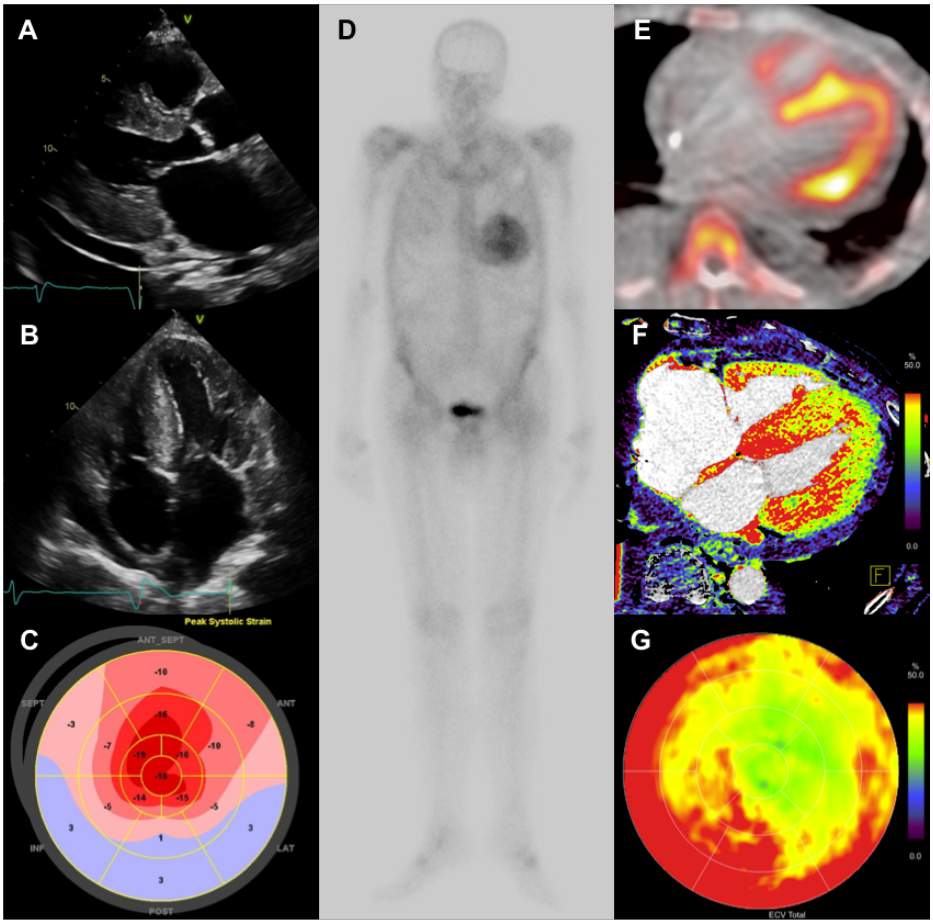

Figure 56: *Multimodality imaging of cardiac amyloidosis.* ***A:*** *echocardiogram parasternal long axis view showing left atrial dilatation, left ventricular hypertrophy, left atrial dilatation and a small pericardial effusion;* ***B:*** *echocardiogram apical four chamber view showing left ventricular hypertrophy with biatrial dilatation;* ***C:*** *polar map of global longitudinal strain on echocardiography showing the characteristic apical sparing strain pattern (areas of red at the apex suggesting normal/near-normal strain);* ***D,E:*** *late (3 hours) whole body planar DPD scintigraphy image (D) and fused SPECT/CT image (E) showing grade 2 Perugini cardiac uptake;* ***F:*** *ECV_{CT} colour map superimposed on the CTCA showing a similar base to apex gradient as shown in the fused SPECT/CT above it;* ***G:*** *ECV_{CT} polar map showing the characteristic apical sparing pattern (areas of green representing lower ECV_{CT} at the apex), remarkably similar to that shown on the echocardiogram strain polar map (C). Note the slightly different ECV_{CT} colour look up table reflecting a previous iteration of this technique.*

Whether there will prove to be differences in myocardial involvement between AL and ATTR cardiac amyloidosis, would prove both interesting from an academic perspective and helpful in differentiating the two conditions, which is of paramount clinical importance. Of course, this would need validation in larger cohorts of patients, across multiple centres and multiple CT vendor platforms.

Other Insights

It is perhaps not surprising ECG and echocardiographic parameters alone struggled to detect AS-amyloid in this population, as they are likely to be confounded by the remodelling seen in lone AS. What was interesting however was that a combination

parameter of both ECG and echocardiography – the V/M ratio performed exceptionally well for cardiac amyloid detection compared to parameters derived from a single technique. Perhaps, on reflection, this should not be wholly surprising as ECV_{CT} and V/M ratio are effectively measuring the same thing: ECV_{CT} measures the proportional size of the space between myocytes and the V/M ratio measures effectively the deficit of electrical depolarisation from what is expected for a measured wall thickness – both fundamentally being measures of 'myocyte dilution' by cardiac amyloid. Unfortunately, this is not valid in patients S-L criteria is not validated in patients with bundle branch block [179], either native or from a ventricular paced rhythm, which effectively excluded 1/3 of our patients. This meant numbers were small in our study to adequately validate this as a screening tool (70 patients in total, including only six patients with AS-amyloid). Furthermore, the need to combine information from two different measurement techniques is a potential barrier to wider uptake as a screening tool in these patients.

Limitations

This was a single centre study. ECV_{CT} performance on other scanners has not been assessed. The suitability of a technique as a screening tool depends in part on the prevalence of the disease you are detecting, it is important to bear in mind that the average patient age in this population was 86±5 years, younger cohorts will have lower rates of discovered AS-amyloid. This represents a subset of the overall study population therefore, although prevalence and other clinical information informs, this is not the primary focus of this chapter. Furthermore, we have not investigated the diagnostic performance of this technique in patients with AL cardiac amyloid. Having excluded the 30% of patients with bundle branch block or ventricular paced rhythm, numbers were small to adequately validate V/M ratio as a screening tool.

Conclusions

Lone AS results in detectable increases in ECV_{CT} compared to controls, which also tracks prognosis in these patients. ECV_{CT} using a low-dose protocol, with a 3-minute post-contrast acquisition can detect AS-amyloid and track its severity in the TAVI population and could be used as a screening tool in those already undergoing a clinically-indicated CT.

Chapter 5: SPECT/CT Quantification of DPD Scintigraphy

The majority of the patients included in this analysis were those recruited to ATTRact-AS (n=61), however in order to provide a better range of results to validate the technique and following discussion with the Joint Research Management Office for Barts Health NHS Trust and Queen Mary University of London, quantification was also performed on clinically acquired DPD scans for the remaining patients (n=39), as part of a registered quality improvement project/audit at BHC (ID 9924).

For this section of work, I was responsible for the recruitment and scanning of all those patients included as part of ATTRact-AS, as well as all of the SPECT/CT and H/CL ratio quantification for all patients. The Medical Physics team at BHC performed the heart and whole-body retention quantification, as well as the heart/whole-body ratio, as part of routine clinical reporting. Elizabeth Morris and Maria Burniston provided physics support for the DPD quantification. Dr Kush Patel performed the re-analysis for interobserver variability assessment.

5.1 Introduction

Bone scintigraphy (DPD, HMDP and PYP) now has a key role to play in the non-invasive diagnosis of cardiac amyloidosis, particularly ATTR cardiac amyloidosis [88].

As discussed in chapters one and two, the current grading system for DPD scintigraphy, devised by Perugini et al in 2005, uses a visual scoring system of the 3-hour (late) planar image – from 0 (negative) to 3 (strongly positive) [86], which unfortunately offers little prognostic significance beyond being positive or negative [92]. It can also be difficult to differentiate subtle cardiac uptake (i.e. a 'mild' Perugini grade 1) from a negative scan with residual blood pool activity – despite the additional use of SPECT imaging. Perugini et al also proposed a semi-quantitative technique that involves using the early and late planar images to calculate heart and whole-body retention, as well as a heart/whole body ratio [86].

PYP is an alternative radiotracer used in the US for the detection of ATTR cardiac amyloidosis, which is generally reported using both a visual grading system and

semi-quantitative heart to contralateral lung (H/CL) ratio from the planar images with ratio ≥1.5 at 1 hour classified as ATTR-positive [98,99]. Furthermore, a H/CL ratio ≥1.6 in patients with ATTR cardiac amyloidosis seems to predict a worse outcome [100].

SPECT allows the 3D visualization of radioactivity within the body, which can be used to display a standardised uptake value (SUV) – a semi-quantitative representation of the concentration of radiopharmaceutical in the respective tissues. Unlike PET SUV quantification, quantitative SPECT imaging has only been used in a limited number of roles within Nuclear Medicine including: dementia imaging [209], tumour dosimetry in radioimmunotherapy [210], lobar function assessment prior to lung resection [211] or lung uptake during shunt studies for liver cancer prior to radio-embolisation [212]. In terms of cardiac applications, published data is even more limited to studies using SPECT with thallium-201 to quantify regional myocardial blood flow in canines [213] or as a method for quantifying absolute ^{99m}Tc-sestamibi uptake in the heart in a porcine model [214].

The aim of this chapter was to assess whether SPECT/CT-derived SUV quantification would improve DPD diagnostic accuracy over and above that offered by planar quantification, as well as offer a means of quantifying amyloid burden and therefore of monitoring response to novel amyloid-specific therapies.

5.2 Results

The DPD scans of 100 patients were analysed (aged 84±9 years, 52% male), of which 40 were grade 0, 12 grade 1, 41 grade 2 and 7 grade 3. Average injected dose was 731±26 MBq. There was a higher proportion of male patients in the DPD-positive cohorts likely reflecting referral bias.

Of the 60 patients with a positive DPD scan (Perugini grade 1,2 or 3): 34 patients (57%) were diagnosed with wild-type ATTR, 16 (27%) with variant ATTR and 3 (5%) with AL-amyloid. The remaining 7 patients (12%) either declined or were awaiting further investigation. Two out of the three patients with AL-amyloid had a grade 1 DPD scan.

Conventional Planar Quantification

Heart, whole-body retention and heart/whole-body ratio increased with increasing DPD grade (*p<0.001* for trend) (table 13). Pairwise comparison revealed a significant difference between only grades 0 and 2 and 0 and 3 for all of these parameters.

	Grade 0 (n=40)	Grade 1 (n=12)	Grade 2 (n=41)	Grade 3 (n=7)	*p*-value
Demographics					
Male	12 (30%)	9 (75%)	27 (66%)	4 (57%)	**0.003**
Age	86±5	83±12	82±10	80±8	0.11
SUV_{peak}					
Cardiac	1.0±0.4	3.7±1.5	11.9±3.8	10.6±1.5	**<0.001**
Paraspinal	0.6±0.1	0.9±0.2	1.0±0.3	1.3±0.3	**<0.001**
Vertebral	8.4±1.5	7.2±1.2	6.2±1.9	4.6±0.17	**<0.001**
Hepatic	0.6±0.2	0.6±0.2	0.6±0.3	0.5±0.2	0.87
SUV Retention Index	0.07±0.03	0.48±0.28	2.04±0.82	3.24±1.04	**<0.001**
Conventional Planar					
Heart Retention	3.6±0.8	4.6±0.9	6.0±1.4	6.7±0.9	**<0.001**
WB Retention	74.5±7.8	81.2±6.6	83.2±7.0	90.3±4.6	**<0.001**
Heart/WB Ratio	4.9±0.9	5.7±0.9	7.2±1.6	7.4±1.1	**<0.001**
Heart/CL Ratio	1.01±0.10	1.35±0.21	2.23±0.55	2.12±0.59	**<0.001**

Table 13: *Summary table of basic patient demographics, with a breakdown of SUV_{peak}, conventional planar quantification and heart/contralateral ratio results by DPD Perugini grade. P-values represent the trend across DPD grades. H/CL = heart/contralateral, SUV_{peak} = peak standardised uptake value, WB = whole-body.*

Heart/Contralateral Lung Ratio

The H/CL ratio increased from grade 0 up to grade 2 and then plateaued between grade 2 and 3 (*p<0.001* for trend) (table 13 and figure 57). Pairwise comparison revealed a significant difference between all grades, except between grades 1 and 3 (*p=0.41*) and 2 and 3 (*p=1.00*).

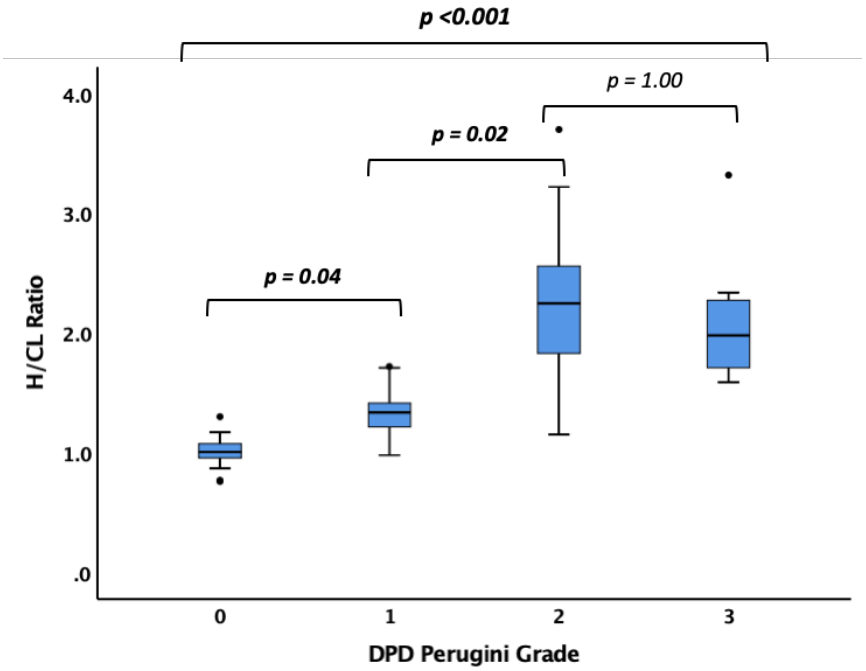

Figure 57: *Box and whisker plot demonstrating the trend in H/CL ratio with increasing DPD Perugini grade – note the plateauing seen between grades 2 and 3.*

There was no significant difference in H/CL ratio between the two patients with cardiac AL and a grade 1 DPD scan and those with ATTR and a grade 1 DPD scan (*p=0.83*).

SPECT Quantification

Cardiac SUV_{peak} increased from DPD Perugini grade 0 up to grade 2, however plateaued between grade 2 and 3 (*p<0.001* for trend) (table 13 and figure 58). Pairwise comparison revealed a significant difference between all grades except 1 and 3 (*p=0.46*) and 2 and 3 (*p=1.00*). Paraspinal muscle SUV_{peak} increased from grade 0 to 3 (*p<0.001* for trend), whereas vertebral SUV_{peak} did the opposite (*p<0.001* for trend) (table 13 and figure 58). There was no difference in hepatic SUV_{peak} between grades (*p=0.87* for trend) (table 13).

The composite parameter of SUV retention index helped overcome the plateauing of the cardiac SUV_{peak} between grades 2 and 3 – increasing across all grades (*p<0.001* for trend) (table 13 and figure 58). Pairwise comparison showed a significant difference between all grades except 2 and 3 (*p=1.00*).

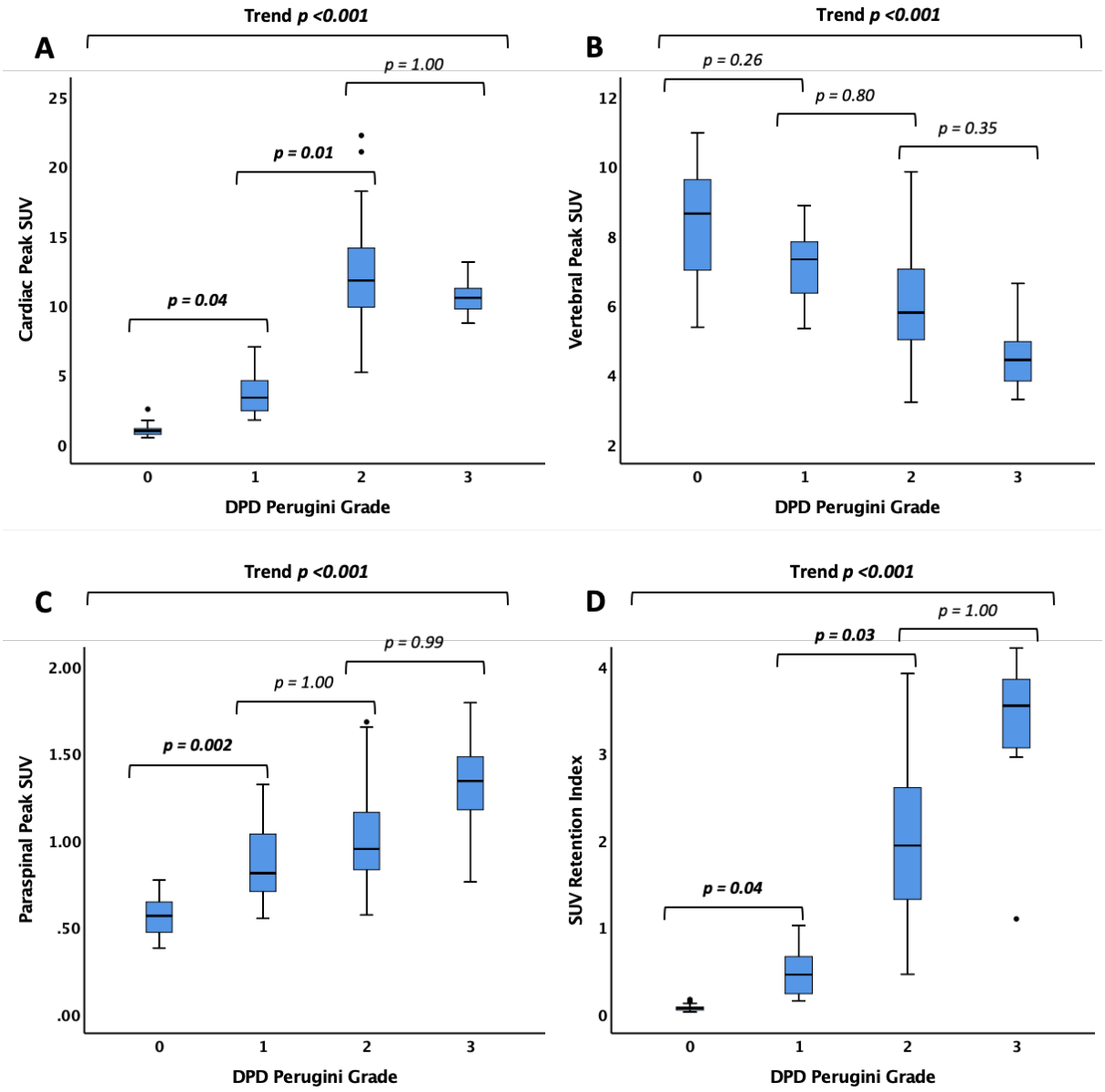

Figure 58: *Box and whisker plots illustrating the trend seen with increasing DPD Perugini grade in SUV_{peak} in the heart (**A**), vertebra (**B**), paraspinal muscle (**C**) and the composite SUV retention index (**D**). SUV = standardised uptake value.*

There was no significant difference between the two patients with cardiac AL and a grade 1 DPD scan and those with ATTR and a grade 1 DPD scan in terms of cardiac SUV_{peak} (*p=0.26*) or SUV retention index (*p=0.97*).

Comparison between planar and SPECT Quantification

The diagnostic accuracy for the detection of any cardiac amyloid was excellent for cardiac SUV_{peak}, with an AUC of 0.999 (95% confidence interval 0.996 – 1.000), with a cut-off of >1.7 giving a sensitivity of 100% and a specificity of 75% (figure 59). The SUV retention index performed similarly well with an AUC of 0.999 (95% confidence

interval 0.998 – 1.000) and a cut off of >0.14 provided the same sensitivity and specificity (figure 59).

In terms of planar quantification techniques, the H/CL ratio performed the best with an AUC of 0.987 (95% confidence interval 0.966 – 1.000), with a ratio of >0.97 giving a sensitivity of 100%, but a specificity of only 38% (figure 59). The conventional heart and whole-body retention, as well as the heart/whole-body ratio did not perform quite so well, with AUCs of 0.916 (95% confidence interval 0.858 – 0.974), 0.803 (95% confidence interval 0.715 – 0.892) and 0.869 (95% confidence interval 0.800 – 0.939) respectively (figure 59).

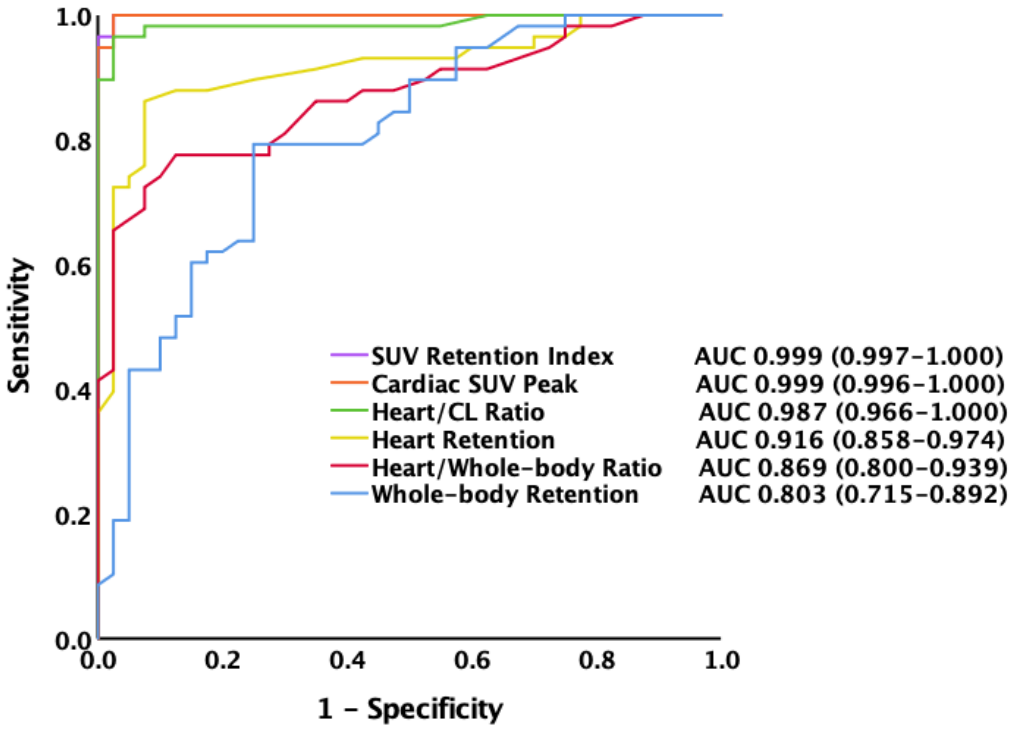

Figure 59: *Receiver operating characteristic (ROC) curves for the detection of cardiac amyloidosis using the different methods of quantification of DPD scintigraphy. Note the overlap in the curves for SUV retention index (purple) and cardiac SUV_{peak} (orange). AUC = area under the curve (values in brackets represent 95% confidence intervals), H/CL = heart/contralateral lung, SUV = standardised uptake value.*

Comparison with ECV by CT

In a subgroup of patients (n=44, aged 87±5 years, 41% male), comparison was made between cardiac SUV_{peak} and ECV_{CT}, as well as H/CL ratio and ECV_{CT}. All patients had severe aortic stenosis: left ventricular ejection fraction 57±8%, peak AV velocity 4.25±0.63m/s, mean gradient 44±14mmHg and AVA 0.67±0.21cm^2. 29

patients were DPD Perugini grade 0, 5 were grade 1 and 10 were grade 2. Cardiac SUV_{peak} and H/CL ratio both increased from grade 0 to 2 as seen in the overall cohort (*p<0.001* for trend for both). Myocardial ECV_{CT} increased from 31±3% (grade 0) to 34±4% (grade 1) to 44±5% (grade 2) (*p<0.001* for trend). There was good correlation between cardiac SUV_{peak} and ECV_{CT} (r^2 = 0.73, *p<0.001*), as well as H/CL ratio and ECV_{CT} (r^2 = 0.74, *p<0.001*) (figure 60).

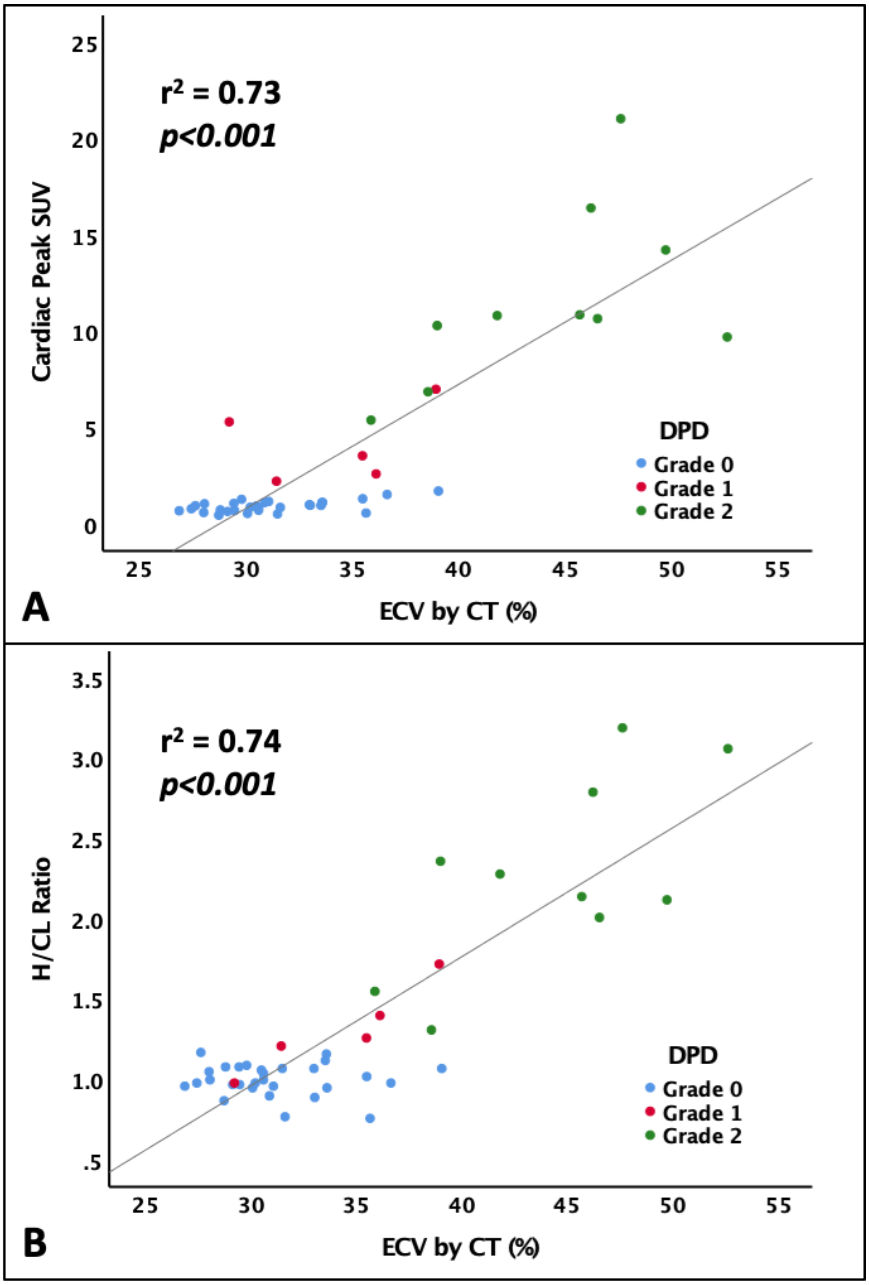

Figure 60: *Scatter plots of cardiac SUV_{peak} against myocardial ECV_{CT} (**A**) and H/CL ratio against myocardial ECV_{CT} (**B**), showing good correlation (r^2 = 0.73 and 0.74 respectively, p<0.001) across DPD Perugini grades 0-2. Note the wide range of ECV results for those patients with a grade 0 DPD (blue dots). DPD = ^{99m}Tc-labelled-3,3-diphosphono-1,2-propanodicarboxylic acid, ECV = extracellular volume, H/CL = heart/contralateral lung ratio, SUV = standardised uptake value.*

Reproducibility and Variability

In order to assess intra-observer variability, SPECT/CT quantification was repeated for 10 patients (3 Perugini grade 3, 2 grade 1, 3 grade 2 and 2 grade 3) by the same reporter (PS) in a separate sitting and blinded to the first set of results. In total 50 parameters were assessed (cardiac, vertebral, hepatic and paraspinal muscle SUV_{peak}, as well as the SUV retention index for each patient). The mean difference in SUV across all measurements (repeat minus initial measurement) was 0.01±0.38. Importantly, looking at just the cardiac SUV_{peak} (n=10 measurements) the mean difference remained small at 0.11±0.37. The intraclass correlation coefficient (two-way, mixed-effects model, absolute agreement) for all 50 parameters was 0.997 (95% confidence interval 0.994-0.998) for single measures.

Comparing the intra-observer variability for H/CL ratio for the same 10 patients, the mean difference between the results was 0.03±0.11. The intraclass correlation coefficient (two-way, mixed-effects model, absolute agreement) was 0.993 (95% confidence interval 0.972-0.998) for single measures.

Inter-observer variability was also assessed for SPECT/CT quantification and H/CL ratio in five patients by a second reporter (KP), who was blinded to the initial results. The mean difference in SUV across all measurements (KP minus PS, n=25 measurements) was -0.17±0.71. For cardiac SUV_{peak} alone (n=5 measurements) this difference was -0.11±0.20. The intraclass correlation coefficient (two-way, mixed-effects model, absolute agreement) for all 25 parameters was 0.989 (95% confidence interval 0.975-0.995) for single measures.

Looking only at the H/CL ratio for the same five patients the mean difference (KP minus PS) was 0.05±0.11. The intraclass correlation coefficient (two-way, mixed-effects model, absolute agreement) was 0.994 (95% confidence interval 0.954-0.999) for single measures.

5.3 Discussion

In terms of diagnostic accuracy, SPECT/CT quantification of DPD scintigraphy using either cardiac SUV_{peak} or the composite SUV retention index is exceptional and outperforms planar quantification techniques. It is a simple, reproducible tool that

can help the reporting clinician to make a diagnosis of cardiac amyloidosis particularly in subtle cases. In centres where SPECT/CT is not available, H/CL ratio is a viable alternative planar quantification technique, which performs well and with a similar diagnostic accuracy to that seen for the diagnosis of ATTR cardiac amyloidosis in the PYP literature (AUC 0.987 vs 0.960-0.992) [99,100]. Although well established in PYP reporting, further work is needed to validate the role of the H/CL ratio in DPD – for example, prognostic thresholds, imaging timepoints (1 hour vs 3 hours) and how results compare between cardiac AL and ATTR [99].

Conventional planar quantification using heart and whole-body retention, as well as heart/whole-body ratio proved inferior in terms of diagnostic accuracy and as a result we have moved away from these in our clinical practice at BHC, obviating the need for the early planar images – improving patient experience and departmental workflow.

Quantifying Cardiac Amyloid Burden

Unfortunately, what is apparent is that quantification of cardiac amyloid burden at higher Perugini grades is confounded by competition for the radiotracer from surrounding soft tissue/muscle, resulting in little detectable difference between grades 2 and 3 using cardiac SUV_{peak} alone or the H/CL ratio. This mirrors findings of two other studies, also looking at quantification techniques in DPD scintigraphy [215,216]. One of which was actually a feasibility study of SPECT/CT quantification using a similar SUV-derived parameter in 13 patients (8 with confirmed ATTR cardiac amyloidosis), which was recently published in September this year and showed a similar plateauing of cardiac SUV_{peak} between DPD grades 2 and 3 [216].

This makes sense given that increased overlying soft tissue or muscle uptake is the likely reason for the 'mild/absent bone uptake,' which forms part of the definition of a Perugini grade 3 DPD, as it is obscuring the underlying bone [86,87,92]. Indeed, work from the NAC in 602 patients showed an increasing soft tissue to femur ratio with increasing Perugini grade on DPD scintigraphy, with little overlap between those with a grade 2 and grade 3 DPD ($p<0.001$) [92].

This is further supported by the increasing paraspinal SUV_{peak} and reducing vertebral SUV_{peak} seen across all grades in our study population. This means that a direct measure of cardiac uptake alone is unlikely to prove sufficient, reflecting the complexity of the condition we are dealing with. This being said, it is reassuring that both cardiac SUV_{peak} and H/CL ratio track amyloid burden up to grade 2 as measured by ECV_{CT}. This would suggest a potentially important role for these quantification techniques in DPD scintigraphy reporting, given that we already know that ECV_{CMR} can detect disease regression with therapy in cardiac AL amyloid [127] and also carries prognostic significance in both ATTR [126] and AL cardiac amyloidosis [125]. This is also supported by the fact, which we touched on in earlier, that a H/CL ratio of ≥1.6 is prognostically significant in PYP scintigraphy in ATTR cardiac amyloidosis [100]. These would all suggest that both cardiac SUV_{peak} (or in turn the derived SUV retention index) and H/CL ratio in DPD scintigraphy may be used to monitor amyloid regression and may also be associated with prognosis. Further validation is warranted, particularly outside of the elderly AS population studied here, where the variation in ECV_{CT} in those patients without cardiac amyloid is likely to be less and therefore the correlation may well prove even better with both cardiac SUV_{peak} and H/CL ratio.

The composite SUV retention index tries to account for the competition for the DPD from both the vertebra and the paraspinal muscle and perhaps offers a means of better quantifying the amyloid burden, which is otherwise apparent on the planar images. Further validation in larger, multi-centre studies is needed, however it would serve as a potential imaging biomarker of response to therapy in upcoming and ongoing clinical trials. Further work is also needed on the role it may offer in differentiating AL from ATTR cardiac amyloidosis, which would prove invaluable from an imaging perspective.

Confounding of Heart to Contralateral Lung Ratio

In terms of planar quantification techniques, H/CL ratio had the highest diagnostic agreement with the visual Perugini scoring system, however was still confounded by the soft tissue uptake seen at higher grades. There is another concern that it may be further confound by concomitant lung uptake, which is not infrequently reported with bone scintigraphy – in fact one study of 62 patients with ATTR cardiac

amyloidosis showed that 58% of patients had some degree of lung uptake using HMDP scintigraphy [217], something that I have also seen from experience reporting DPD scans (although perhaps not as prevalent and not apparent in the patients studied here). In these situations, clearly SPECT/CT, which offers 3D visualisation of the heart is preferable.

Limitations

The range of patients reported here reflect the clinical practice of a large tertiary cardiac centre, however there are relatively small numbers of DPD Perugini grade 1 and grade 3 patients, which is likely to impact our results. We also only have 3 patients with AL-amyloid, meaning any conclusions drawn primarily relate to the ATTR cardiac amyloidosis population. ECV_{CT} was only performed in the subgroup of elderly patients with severe AS, which we know from chapter four, likely explains the significant variation in ECV_{CT} seen in those without cardiac amyloid. This is likely to have had an impact on the correlation seen with cardiac SUV_{peak}, which may well prove even better outside of this population.

Conclusions

SPECT/CT quantification in DPD scintigraphy is possible and outperforms conventional planar quantification techniques in terms of diagnostic accuracy and tracking of DPD Perugini grade. Differentiation of Perugini grade 2 or 3 is confounded by soft tissue uptake, which can be overcome by a composite SUV retention index. This index can help in the diagnosis of cardiac amyloidosis and may offer a means of quantifying cardiac amyloid burden and monitoring response to therapy. In centres where SPECT/CT is not available H/CL ratio is a viable alternative, which performs well.

Chapter 6: Overall Discussion

AS and cardiac amyloidosis are known to be common in the elderly and therefore dual pathology seemed likely, but before starting this work there was only limited evidence to support this in the TAVI population. During this thesis I prospectively recruited 200 patients aged 75 and over, with severe AS, who had been referred for consideration of TAVI prospectively across two centres: the BHC in London and the John Radcliffe Hospital in Oxford. In addition to routine clinical ECG and echocardiography, these patients underwent blinded DPD scintigraphy prior to intervention, along with baseline blood tests and a quality of life questionnaire. A proportion of patients (n=109), also underwent ECV_{CT} at the time of their clinical TAVI work-up CT prior to intervention. Patients were followed up with a health questionnaire at 1-year and for mortality, as well as periprocedural complication. In an effort to develop a means of quantify amyloid burden, beyond the Perugini visual grading system [86], I also explored and validated a novel means of DPD quantification using SPECT/CT in 100 patients.

6.1 Dual AS and Cardiac Amyloid Pathology

We demonstrated that AS-amyloid was common, effecting 13% of elderly patients referred for consideration of TAVI (26/200). Based on our experience with the SAVR population [163], our initial expectations were that this would be associated with a worse outcome compared to patients with lone AS, however that was not the case in our cohort. There was no difference in periprocedural complication or mortality between the two cohorts and patients with AS-amyloid derived a significant mortality benefit from TAVI relative to medical therapy alone, suggesting that these patients should not be turned down for the procedure on the basis of dual pathology alone.

All of our patients who were genotyped had wild-type ATTR, however importantly a nearly a quarter of patients with a positive DPD scan had a significant plasma cell dyscrasia. Although none were felt likely to have primary AL amyloid (following detailed review by the managing team and/or NAC) – it should nevertheless emphasise the importance of ensuring serum free light chains, serum and urine immunofixation are sent on all patients with a positive DPD scan. This is also

emphasised in the recent expert consensus recommendations for multimodality imaging in cardiac amyloidosis [89].

The majority of AS-amyloid detected was DPD Perugini grade 2 (69%), which is quite striking in a study which effectively screened for the presence of an occult bystander disease. To discover a higher burden of more advanced disease (grade 2) does not fit with a conventional model of amyloid accumulation combined with discovery by screening ('early' grade 1 should be more prevalent). There may be an interaction between the 'AS-primed' myocardium and the amyloid fibrils, which predisposes to fibril deposition. This may also in part explain the similar male/female ratio seen in our AS-amyloid population – with the AS 'priming' the myocardium more equally between genders. The absence of patients with DPD Perugini grade 3 AS-amyloid in these patients may suggest censoring by mortality, but this is beyond the scope of this data. We know that there may be a long pre-clinical phase with cardiac amyloid and that prevalence increases with age – becoming the primary cause of death in supercentenarians [218]. The spectrum therefore potentially extends from 'bystander' to the primary cause of symptoms and adverse outcome, depending on the time of diagnosis and the myocardial tolerance. In turn, these are likely to be affected by amyloid burden, rate of amyloid deposition, the ability of the myocardium to adapt, and other myocardial "hits", such as, in this case, the increased afterload from AS. Further work is needed in this area – perhaps one way of addressing this would be to screen the elderly healthy population to ascertain if the prevalence of amyloid in the AS population (13%) is much higher. It is possible that other common cardiac conditions may prime the myocardium in a similar fashion.

The typical echocardiographic findings of cardiac amyloidosis have been discussed in chapter one, but can often be quite marked when the disease is well established. Although present, differences in LV wall thickness and mass were modest between those patients with AS-amyloid and lone AS (1-2mm and ~18g/m^2 respectively), with no difference in disproportionate hypertrophy (8% vs 4%, *p=0.33*), which is a little surprising even allowing for the confounding presence of severe AS and patient comorbidities.

Although patient numbers were small and the study underpowered to assess this, exploratory subgroup analysis revealed that there was a trend to increasing LV wall thickness, E/A ratio and blood biomarkers with increasing DPD Perugini grade, which intrinsically makes sense and fits with the wider literature (albeit outside the AS population) [114]. These results suggest that differentiating between DPD grade 1 cardiac amyloid and the normal myocardial response to AS is likely prove challenging (with less profound echocardiographic and blood biomarker changes) and whether this degree of amyloid deposition in elderly patients with AS can sometimes be considered bystander is unknown and needs larger multi-centre studies to ascertain.

These may suggest that AS-amyloid is not like 'typical' cardiac amyloidosis and therefore we should not assume that the impact of amyloid-specific therapies such as Tafamidis [93], Patisiran [94] and Inotersen [95], will be the same. Given the high prevalence of AS and the increasing rates of TAVI, a study of amyloid-specific therapy in AS-amyloid is urgently needed.

Finally, it is surprising that despite patients with AS-amyloid being older, with a worse baseline quality of life and significantly more elevated blood biomarkers, that they do not do worse than those with lone AS. One consideration for future work is if, given this lack of increased mortality, TAVI and the afterload reduction that comes with it is perhaps helping to stabilise the amyloid fibrils within the myocardium (akin to reverse myocardial remodelling seen following AV replacement) [189]. Further work is needed, however what is clear from this data is that teams should not be withholding TAVI in those patients with severe AS and DPD Perugini grade 1 or 2 wtATTR cardiac amyloidosis.

6.2 Refining a Screening Tool for AS-amyloid

In centres where ECV_{CT} is not readily available, initial screening for AS-amyloid could form part of the basic clinical assessment, with multivariate analysis suggesting that: older patient age, presence of RBBB and elevated hsTnT are associated with its presence. ROC analysis suggests that a hsTnT of ≥24ng/L would have an 81% sensitivity, but only a 57% specificity for the detection of AS-amyloid in the severe AS population. Echocardiography alone unfortunately struggles to

differentiate between the remodelling seen with lone AS and dual AS-amyloid pathology (with only subtle differences in LV mass and wall thickness noted in our cohort), but these may have an additive role in a combined risk score in the future. V/M ratio has potential as a screening tool (using a cut of <0.021 in our cohort offered a sensitivity of 100% and specificity of 63% for the detection of any AS-amyloid). Unfortunately, this is not valid in patients with a bundle branch block or ventricular paced rhythm, which is likely to be a significant proportion of these patients (30% of patients in our study) and we have already shown that the prevalence of RBBB is higher in patients with AS-amyloid. The need to combine information from two different measurement techniques is also a potential barrier to wider uptake. Furthermore, numbers were small in this subgroup in our study (having excluded 30% of the cohort), so further validation is needed in larger populations. I am currently involved with multi-centre work developing a composite scoring system based on basic clinical and echocardiographic parameters to estimate the likelihood of AS-amyloid.

ECV_{CT} is an appealing alternative that we have shown can be used to screen for AS-amyloid, but also importantly for 'lone' cardiac amyloid outside of the AS population. Although bone scintigraphy plays a key role in the non-invasive diagnosis of ATTR cardiac amyloidosis, its availability in the UK remains limited and it involves the need for additional testing for the patient. ECV_{CT} by comparison can be performed as a simple addition to an already clinically-indicated CT. Uptake of this technique could be large – enabling better patient care, better resource utilisation (by guiding onward referral for DPD scintigraphy) and helping to facilitate some of the much-needed research in this area.

As mentioned in chapter four, 10% of our lone AS study population had focal ECV_{CT} elevations, with corresponding significant coronary artery disease on either the CTCA or contemporary invasive angiography, suggestive of an MI. One approach to improve the specificity of ECV_{CT} as a screening test for ATTR cardiac amyloidosis would be to exclude segments affected by focal MI, however without always having diagnostic CTCA images in these patients or contemporary invasive coronary angiography this becomes challenging. It would involve assessment of regional wall motion and thinning on echocardiography, in conjunction with ECG and clinical

history (otherwise one would risk excluding focal elevations potentially due to either AS or cardiac amyloidosis), which would make this a rather unwieldy screening tool for cardiac amyloidosis. On the other hand, it seems unnecessary to exclude these patients altogether, given that this heterogeneity reflects the population we hope to screen in the first place, we cannot exclude 10% of it before we have begun. This was the primary reason for exploring two other aspects of ECV quantification: the first was using the indexed matrix volume, which added little to the diagnostic accuracy of the technique. The second was to look at just the basal septum (more specifically the average of AHA segments two and three), which is less frequently affected by infarct and more reflects what is done in CMR routinely for ECV analysis (where a ROI is drawn in the basal septum). Unfortunately, this made little difference to the diagnostic performance of ECV_{CT} for the detection of any AS-amyloid. There was a small improvement in diagnostic accuracy relative to global ECV_{CT} for the detection of DPD Perugini grade 2 AS-amyloid – for an ECV_{CT} threshold of 34% the sensitivity was 100% and specificity was 84% (having been 64% using a global ECV_{CT} cut off of 33.4%), which would prove helpful if screening patients only for DPD Perugini grade 2 AS-amyloid. A possible screening algorithm is shown below (figure 61).

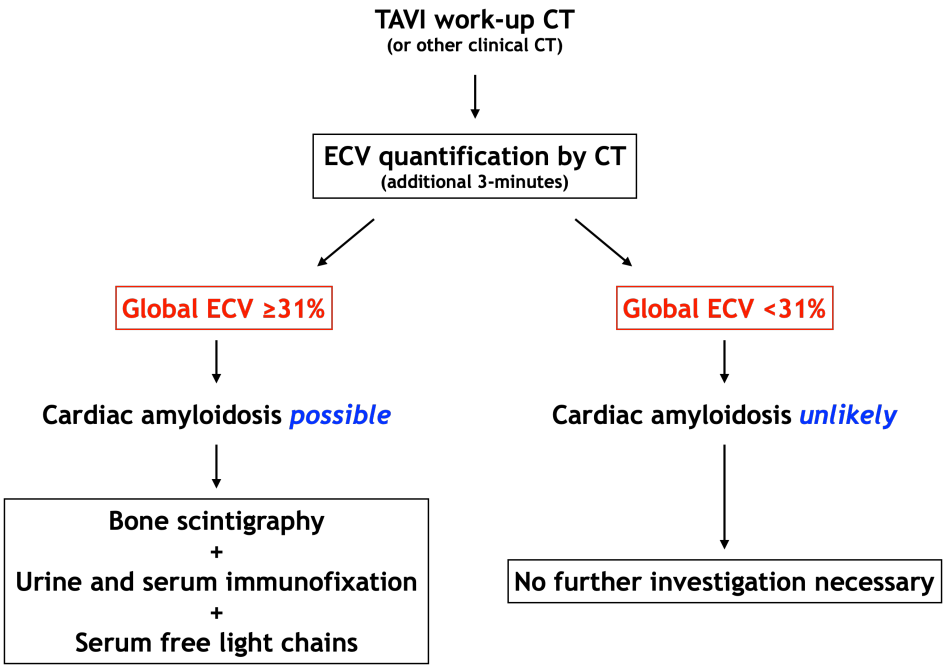

Figure 61: *Proposed ECV_{CT} screening algorithm for incorporation into routine clinical workflow. Note: algorithm can be adjusted to a global ECV_{CT} threshold of ≥29% for the detection of all patients with AS-amyloid (including DPD Perugini grade 1).*

This algorithm still uses bone scintigraphy (with the exclusion of AL amyloid by serum free light chains, serum and urine immunofixation) [88], but increases the test yield by gate-keeping access. Using the ECV_{CT} threshold would provide a sensitivity of 94% and a specificity of 45% and would mean that all DPD Perugini grade 2 AS-amyloid cases would be detected, but a small proportion (1 in 5 in our cohort) of DPD grade 1 cases would be missed. These thresholds can be adjusted (global ECV_{CT} ≥29%) to detect all patients with AS-amyloid (including grade 1), however for a sensitivity of 100%, the specificity drops to below 20%, which would result in probably an unacceptably high referral rate for DPD scintigraphy. If a screening tool to detect only those patients with DPD Perugini grade 2 AS-amyloid was needed, a septal ECV_{CT} threshold of ≥34% would be optimal (sensitivity 100%, specificity 84%), but this would miss a greater proportion of DPD Perugini grade 1 AS-amyloid patients (3/5 in our cohort). The proposed algorithm above (figure 51) perhaps provides the optimum balance at present given the current uncertainty regarding the clinical significance of Perugini grade 1 in ATTR cardiac amyloidosis. This decision may in part be driven by the treatment thresholds for the novel amyloid-specific therapies which are being developed – for example the use of Tafamidis is likely to be restricted (at least in the first instance) to those with DPD Perugini grade 2 or 3.

The ability to detect ATTR cardiac amyloidosis non-invasively using bone scintigraphy has led to the increased realisation that particularly wtATTR cardiac amyloidosis is not rare in the elderly. We now know that it is common in the elderly AS population [163,194,195,219], but even outside of this group of patients it is prevalent – 13% of patients with heart failure with preserved ejection fraction may have underlying cardiac amyloid [75] and 5% of those with LVH may have variant ATTR cardiac amyloidosis (this study used genotyping to screen LVH patients and so will have missed those with wild-type ATTR cardiac amyloidosis [220]. ECV_{CT} has the potential to screen all of these groups of patients, who are likely to be undergoing clinically-indicated CTCA at some stage in their encounters with Cardiology.

Finally, we know that ECV_{CMR} can assess amyloid burden in AL cardiac amyloidosis, as well as ATTR [126,202] – it is likely that ECV_{CT} could do the same (in contrast to bone scintigraphy, which is positive in only ~40% of patients with AL cardiac

amyloidosis and then usually only weakly so) [88]. Being able to use ECV_{CT} to screen for both ATTR and AL cardiac amyloidosis in the same sitting could be extremely helpful clinically, given the poor prognosis associated with particularly the latter. Further work is needed to assess ECV_{CT} in this population.

6.3 ECV Quantification by CT and Prognosis in Lone AS

Importantly, ECV_{CT} tracked mortality in our patients with lone AS. Numbers were small (n=93), with 19% of patients not undergoing TAVI. Despite this, these findings are very much in keeping with the wider CMR literature [36]. Given this excess associated mortality, with further refinement and validation in a larger cohort to identify appropriate ECV_{CT} thresholds, it is conceivable that this could be built into a pre-procedural risk assessment for patients with AS being considered for valve intervention, which would prove an easy addition to an often already clinically-indicated TAVI work-up CT. Whether it could be used to guide earlier intervention in patients with severe AS with little in the way of symptoms needs further investigation, but the EVOLVED-AS trial (Early Valve Replacement Guided by Biomarkers of LV Decompensation in Asymptomatic Patients with Severe AS, NCT03094143) may go some way to answering this question.

6.4 Quantifying Amyloid burden using DPD Scintigraphy

One of the appeals of the current Perugini visual grading system is its simplicity, however this same simplicity is also likely to make it inadequate for accurate disease monitoring [86]. SPECT/CT quantification offers a means of better diagnosing and quantifying amyloid burden, which has good correlation with ECV_{CT} and may also help overcome some of the current discrepancies between centres using different imaging protocols, tracers and reporting techniques. In those centres not performing SPECT/CT routinely as part of their DPD scan protocol, H/CL ratio is an alternative quantification technique that could be used.

In terms of quantifying cardiac amyloid burden, it is apparent that there is a large spectrum of disease that is not captured in the Perugini grading system (perhaps unsurprising, given there are only 3 grades of positivity used to describe a complex, multisystem condition) [86]. An example of this is the variation in cardiac SUV_{peak}

seen between patients with a grade 2 DPD scan, which can range from 5 up to 21 (figure 62).

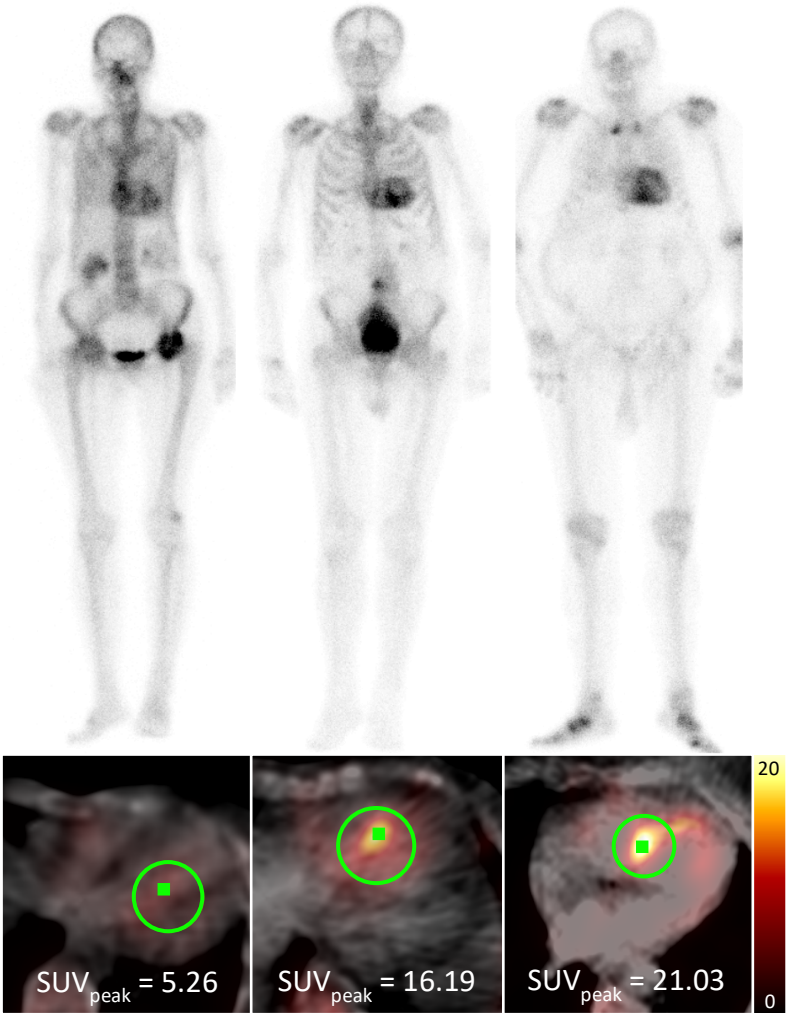

Figure 62: *The unappreciated spectrum of disease. Planar images from three patients all demonstrating Perugini grade 2 cardiac uptake, however the cardiac SUV_{peak} is markedly different between the patients – illustrating the wide range of cardiac involvement that is not apparent on planar imaging alone. SUV_{peak} = peak standardised uptake value.*

The Perugini grading system alone is therefore unlikely to prove sufficiently sensitive to facilitate the monitoring of response (or lack thereof) to amyloid-specific therapies in the future.

One significant barrier to research in this area involving bone scintigraphy is (among other things) the heterogeneity in radiotracers, scanning protocols and reporting techniques used. We have already touched on some of these aspects already, but another example is something as fundamental as the visual scoring system. In the US the visual grading system for PYP scintigraphy (table 14) [89,98], which is similar

to that proposed by Perugini et al [86], never the less has subtle, important differences.

Grade	Myocardial ^{99m}Tc-PYP Uptake
Grade 0	no uptake and normal bone uptake
Grade 1	uptake less than rib uptake
Grade 2	uptake equal to rib uptake
Grade 3	uptake greater than rib uptake with mild/ absent rib uptake

Table 14: *Visual grading system for PYP scintigraphy at 3-hours from the American Society of Nuclear Cardiology and recent expert consensus recommendations [89,98]. Note the subtle differences to the Perugini grading system (described in the introduction) [86].*

This grading system relates visual cardiac uptake to adjacent rib uptake only (akin to the H/CL ratio). The reason for this is that the planar imaging in PYP scintigraphy usually only includes the chest and therefore bone suppression from increased soft tissue uptake outside of this field of view cannot be appreciated. It is feasible that a large proportion of patients who are considered a grade 2 DPD using the Perugini scoring system, may constitute a grade 3 using the US grading system and vice versa (as, from personal experience, there seems to be greater emphasis on absent bone uptake when differentiating a grade 2 from a grade 3 using the Perugini system). It may also be that, given these subtle differences, cardiac SUV_{peak} would not be quite so confounded by competition for radiotracer and therefore would not plateau quite so much between US grades 2 and 3. This may make it suitable alone for disease monitoring, although clearly validation of this hypothesis is needed.

Aside from these differences in reporting between PYP and DPD scintigraphy, there may be fundamental differences in radiotracer distribution further complicating direct comparisons. One US study, published early last year, demonstrated in 57 patients with ATTR cardiac amyloidosis (43 visual grade 2, 14 visual grade 3), that there was no difference in skeletal muscle uptake of PYP (assessed both qualitatively and quantitatively at 3-hours, similar to DPD protocols) between grades 2 or 3 [221]. This is in stark contrast to what we see in DPD scintigraphy [87,92], as we have already discussed. Ultimately this may reflect different radiotracer properties,

combined with subtle differences in grading. It is easy to see how this may hugely complicate future international collaboration efforts – SPECT/CT quantification could help to overcome this, but further validation would be needed using both PYP and HMDP radiotracers and different imaging timepoints.

Chapter 7: Future/Ongoing Work

7.1 Prevalence and Outcome of AS-amyloid in the TAVI Population

This is an exciting area of Cardiology, which is generating a great deal of interest, driven in part by the novel therapies that are becoming available, but also our burgeoning realisation of the true prevalence of cardiac amyloidosis. Further, multi-centre work is urgently needed to begin addressing many of the important outstanding questions in this field:

Are amyloid-specific therapies as effective in the treatment of AS-amyloid and what role do they have in conjunction with TAVI?

- Is there a role for a randomised placebo-controlled trial looking at such amyloid-specific therapies pre- or post-TAVI?

Is AS-amyloid a distinct entity from cardiac amyloidosis?

- I am already involved in ongoing work to compare ECG and echocardiographic parameters, as well as blood biomarkers in age-matched healthy controls, lone AS, AS-amyloid and lone amyloid patients (n~400 overall) to help ascertain this.

Is there an interaction between the amyloid deposition and AS?

- I am involved in work with my successor Dr Kush Patel in which we are recruiting healthy controls to undergo DPD scintigraphy to ascertain the background prevalence of wtATTR cardiac amyloidosis and BHF funding is in place for this (FS/19/48/34523).
- Another way to address this question would be to ascertain whether TAVI has a positive effect on amyloid deposition (be that stabilisation or indeed regression), which could be assessed by interval (pre- and post-TAVI) DPD scintigraphy with SPECT/CT quantification.

Is DPD Perugini grade 1 more than just bystander disease (which will need larger, multicentre studies to ascertain)?

- We have approached another large European centre, which has been carrying out similar work to our own, regarding collaboration. The result

would be a cohort of over 50 patients with AS-amyloid, which we could use to begin trying to answer this question (among others).

Do patients with AS-amyloid derive the same symptomatic response from TAVI in the short-term as those with lone AS? Is this reflected in objective parameters such as change in 6-minute walk test distance and blood biomarkers?

- I am already involved in this ongoing work with my successor Dr Kush Patel at BHC, recruitment is underway and BHF funding has been secured for this (FS/19/48/34523).

7.2 ECV Quantification by CT

We have now optimised our ECV_{CT} protocol for AS-amyloid detection at BHC, by removing the 5-minute post-contrast acquisition, which will improve study patient experience and reduce the radiation dose they receive. Further work is ongoing at BHC in this area under my successor Dr Kush Patel.

Is ECV_{CT} ready for incorporation into a clinical workflow given the low radiation penalty and minimal additional time in CT?

- I am involved with discussions now at BHC with the Cardiomyopathy, TAVI and Cardiac Imaging teams to ascertain whether this is the case. It may be that in the first instance a registry is established to capture all TAVI patients undergoing CT work-up (n~500/year) for a short trial period. My successor is likely to be taking this work forward.

How does ECV_{CT} perform on other CT scanners and analysis platforms?

- Multi-centre studies are now needed in this area and I am involved with discussions with other centres in the UK and US to facilitate this.

Given the spatial resolution of CT, what other insights into both AS and cardiac amyloidosis can be gained?

- I am involved with ongoing work looking now at the endo- to epicardial fibrosis gradient in more detail using ECV_{CT}, as well as patterns of amyloid deposition and fibrosis in lone AS.

How does ECV_{CT} perform in other populations?

- I am involved with ongoing studies both at BHC and elsewhere looking at ECV_{CT} in patients with ischaemic heart disease, dilated cardiomyopathy and renal failure.

Can we refine a screening protocol for AS-amyloid from clinical and echocardiographic parameters for use in centres where ECV_{CT} is not available?

- I am involved with ongoing multi-centre work looking at basic clinical and echocardiographic parameters and whether these can be combined in a scoring system that could be used to calculate the pre-test likelihood of AS-amyloid in the AS population.

7.3 SPECT/CT Quantification of DPD Scintigraphy

As mentioned in chapter five, at BHC we have already optimised our DPD scanning protocol, by removing the early planar image and need for conventional planar quantification, improving patient experience and departmental workflow. Key questions however remain:

Does SPECT/CT quantification track prognosis in patients with cardiac amyloidosis?

- I am now investigating whether SPECT/CT quantification tracks prognosis in our ATTRact-AS patients, however validation will also be needed outside the AS population.

Does SPECT/CT quantification offer a means of monitoring a response to amyloid-specific therapies?

- Now that Tafamidis has been approved for use under the Early Access to Medicines Scheme and with other amyloid-specific therapies becoming available I hope that there will be the opportunity to assess the role SPECT/CT quantification may have in monitoring therapeutic response.

Should SPECT/CT quantification replace the visual grading system?

- To do this would require further validation of SPECT/CT quantification in DPD scintigraphy against another modality – the obvious choice being

CMR (likely ECV_{CMR} particularly). Work is ongoing at our centre in this area and I would hope to be able to investigate this further in due course.

As with early research in a rapidly advancing field, we have generated more questions than there are answer – questions which are both important and pressing, given the implications for patient care and the advances being made in amyloid-specific therapies [93–95]. There is an urgent need now for multi-centre studies, with larger patient numbers to begin addressing many of these questions.

Chapter 8: Overall Conclusions

AS-amyloid is common and affects around 1 in 8 elderly patients with severe AS being considered for TAVI. It appears different from lone AS, but there are also suggestions of a biological interaction between the AS and the amyloid. Dual pathology does not seem to be associated with more periprocedural complications or worse long-term outcome. Patients with AS-amyloid derive significant mortality benefit from TAVI compared to medical therapy, suggesting that no patient should be denied TAVI based on discovered dual pathology alone.

AS-amyloid can be detected using ECV_{CT}, which could act as a gatekeeper to further investigation for cardiac amyloidosis in those already undergoing clinically-indicated CT. ECV_{CT} could be easily performed in routine clinical practice with only a small additional radiation burden and time delay. Furthermore, ECV_{CT} is an important marker of prognosis in patients with lone AS.

Finally, SPECT/CT quantification of DPD scintigraphy is possible, with H/CL ratio being a viable potential alternative in centres not routinely performing SPECT/CT. They may offer a means of quantifying amyloid deposition and provide us with a potential imaging biomarker for monitoring response to therapy.

Chapter 9: References

[1] Thaden JJ, Nkomo VT, Enriquez-Sarano M. The Global Burden of Aortic Stenosis. Prog Cardiovasc Dis 2014;56:565–71. https://doi.org/10.1016/j.pcad.2014.02.006.

[2] Baumgartner H, Hung J, Bermejo J, Chambers JB, Evangelista A, Griffin BP, et al. Echocardiographic assessment of valve stenosis: EAE/ASE recommendations for clinical practice. Eur J Echocardiogr 2009;10:1–25. https://doi.org/10.1093/ejechocard/jen303.

[3] Ward C. Clinical significance of the bicuspid aortic valve. Heart 2000;83:81–5. https://doi.org/10.1136/heart.83.1.81.

[4] Tzemos N. Outcomes in Adults With Bicuspid Aortic Valves. JAMA 2008;300:1317. https://doi.org/10.1001/jama.300.11.1317.

[5] Roberts WC. Frequency by Decades of Unicuspid, Bicuspid, and Tricuspid Aortic Valves in Adults Having Isolated Aortic Valve Replacement for Aortic Stenosis, With or Without Associated Aortic Regurgitation. Circulation 2005;111:920–5. https://doi.org/10.1161/01.CIR.0000155623.48408.C5.

[6] Zühlke L, Engel ME, Karthikeyan G, Rangarajan S, Mackie P, Cupido B, et al. Characteristics, complications, and gaps in evidence-based interventions in rheumatic heart disease: the Global Rheumatic Heart Disease Registry (the REMEDY study). Eur Heart J 2015;36:1115–22. https://doi.org/10.1093/eurheartj/ehu449.

[7] Iung B. A prospective survey of patients with valvular heart disease in Europe: The Euro Heart Survey on Valvular Heart Disease. Eur Heart J 2003;24:1231–43. https://doi.org/10.1016/S0195-668X(03)00201-X.

[8] Marijon E, Mirabel M, Celermajer DS, Jouven X. Rheumatic heart disease. The Lancet 2012;379:953–64. https://doi.org/10.1016/S0140-6736(11)61171-9.

[9] Dweck MR, Boon NA, Newby DE. Calcific Aortic Stenosis. J Am Coll Cardiol 2012;60:1854–63. https://doi.org/10.1016/j.jacc.2012.02.093.

[10] Otto CM. Calcific Aortic Stenosis — Time to Look More Closely at the Valve. N Engl J Med 2008;359:1395–8. https://doi.org/10.1056/NEJMe0807001.

[11] Baumgartner H, Hung J, Bermejo J, Chambers JB, Edvardsen T, Goldstein S, et al. Recommendations on the Echocardiographic Assessment of Aortic Valve Stenosis: A Focused Update from the European Association of Cardiovascular Imaging and the American Society of Echocardiography. J Am Soc Echocardiogr 2017;30:372–92. https://doi.org/10.1016/j.echo.2017.02.009.

[12] Nishimura RA, Otto CM, Bonow RO, Carabello BA, Erwin JP, Guyton RA, et al. 2014 AHA/ACC Guideline for the Management of Patients With Valvular Heart Disease: A

Report of the American College of Cardiology/American Heart Association Task Force on Practice Guidelines. Circulation 2014;129:e521–643. https://doi.org/10.1161/CIR.0000000000000031.

[13] Baumgartner H, Falk V, Bax JJ, De Bonis M, Hamm C, Holm PJ, et al. 2017 ESC/EACTS Guidelines for the management of valvular heart disease. Eur Heart J 2017. https://doi.org/10.1093/eurheartj/ehx391.

[14] Nishimura RA, Grantham JA, Connolly HM, Schaff HV, Higano ST, Holmes DR. Low-Output, Low-Gradient Aortic Stenosis in Patients With Depressed Left Ventricular Systolic Function: The Clinical Utility of the Dobutamine Challenge in the Catheterization Laboratory. Circulation 2002;106:809–13. https://doi.org/10.1161/01.CIR.0000025611.21140.34.

[15] Monin J-L, Quéré J-P, Monchi M, Petit H, Baleynaud S, Chauvel C, et al. Low-Gradient Aortic Stenosis: Operative Risk Stratification and Predictors for Long-Term Outcome: A Multicenter Study Using Dobutamine Stress Hemodynamics. Circulation 2003;108:319–24. https://doi.org/10.1161/01.CIR.0000079171.43055.46.

[16] Levy F, Laurent M, Monin JL, Maillet JM, Pasquet A, Le Tourneau T, et al. Aortic Valve Replacement for Low-Flow/Low-Gradient Aortic Stenosis. J Am Coll Cardiol 2008;51:1466–72. https://doi.org/10.1016/j.jacc.2007.10.067.

[17] Clavel M-A, Ennezat PV, Maréchaux S, Dumesnil JG, Capoulade R, Hachicha Z, et al. Stress Echocardiography to Assess Stenosis Severity and Predict Outcome in Patients With Paradoxical Low-Flow, Low-Gradient Aortic Stenosis and Preserved LVEF. JACC Cardiovasc Imaging 2013;6:175–83. https://doi.org/10.1016/j.jcmg.2012.10.015.

[18] Cueff C, Serfaty J-M, Cimadevilla C, Laissy J-P, Himbert D, Tubach F, et al. Measurement of aortic valve calcification using multislice computed tomography: correlation with haemodynamic severity of aortic stenosis and clinical implication for patients with low ejection fraction. Heart 2011;97:721–6. https://doi.org/10.1136/hrt.2010.198853.

[19] Aggarwal SR, Clavel M-A, Messika-Zeitoun D, Cueff C, Malouf J, Araoz PA, et al. Sex Differences in Aortic Valve Calcification Measured by Multidetector Computed Tomography in Aortic Stenosis. Circ Cardiovasc Imaging 2013;6:40–7. https://doi.org/10.1161/CIRCIMAGING.112.980052.

[20] Clavel M-A, Messika-Zeitoun D, Pibarot P, Aggarwal SR, Malouf J, Araoz PA, et al. The Complex Nature of Discordant Severe Calcified Aortic Valve Disease Grading. J Am Coll Cardiol 2013;62:2329–38. https://doi.org/10.1016/j.jacc.2013.08.1621.

[21] Messika-Zeitoun D, Bielak LF, Peyser PA, Sheedy PF, Turner ST, Nkomo VT, et al. Aortic valve calcification: determinants and progression in the population. Arterioscler Thromb Vasc Biol 2007;27:642–8. https://doi.org/10.1161/01.ATV.0000255952.47980.c2.

[22] Clavel M-A, Pibarot P, Messika-Zeitoun D, Capoulade R, Malouf J, Aggarval S, et al. Impact of aortic valve calcification, as measured by MDCT, on survival in patients with aortic stenosis: results of an international registry study. J Am Coll Cardiol 2014;64:1202–13. https://doi.org/10.1016/j.jacc.2014.05.066.

[23] Pawade T, Clavel M-A, Tribouilloy C, Dreyfus J, Mathieu T, Tastet L, et al. Computed Tomography Aortic Valve Calcium Scoring in Patients With Aortic Stenosis. Circ Cardiovasc Imaging 2018;11:e007146. https://doi.org/10.1161/CIRCIMAGING.117.007146.

[24] Messika-Zeitoun D, Lloyd G. Aortic valve stenosis: evaluation and management of patients with discordant grading. E-J Cardiol Pract 2018;15.

[25] Stewart BF, Siscovick D, Lind BK, Gardin JM, Gottdiener JS, Smith VE, et al. Clinical factors associated with calcific aortic valve disease. Cardiovascular Health Study. J Am Coll Cardiol 1997;29:630–4. https://doi.org/10.1016/s0735-1097(96)00563-3.

[26] Otto CM, Lind BK, Kitzman DW, Gersh BJ, Siscovick DS. Association of aortic-valve sclerosis with cardiovascular mortality and morbidity in the elderly. N Engl J Med 1999;341:142–7. https://doi.org/10.1056/NEJM199907153410302.

[27] Olsen MH, Wachtell K, Bella JN, Gerdts E, Palmieri V, Nieminen MS, et al. Aortic valve sclerosis relates to cardiovascular events in patients with hypertension (a LIFE substudy). Am J Cardiol 2005;95:132–6. https://doi.org/10.1016/j.amjcard.2004.08.080.

[28] Taylor HA, Clark BL, Garrison RJ, Andrew ME, Han H, Fox ER, et al. Relation of aortic valve sclerosis to risk of coronary heart disease in African-Americans. Am J Cardiol 2005;95:401–4. https://doi.org/10.1016/j.amjcard.2004.09.043.

[29] Nkomo VT, Gardin JM, Skelton TN, Gottdiener JS, Scott CG, Enriquez-Sarano M. Burden of valvular heart diseases: a population-based study. The Lancet 2006;368:1005–11. https://doi.org/10.1016/S0140-6736(06)69208-8.

[30] Lindroos M, Kupari M, Heikkilä J, Tilvis R. Prevalence of aortic valve abnormalities in the elderly: an echocardiographic study of a random population sample. J Am Coll Cardiol 1993;21:1220–5.

[31] Barone-Rochette G, Piérard S, De Meester de Ravenstein C, Seldrum S, Melchior J, Maes F, et al. Prognostic Significance of LGE by CMR in Aortic Stenosis Patients Undergoing Valve Replacement. J Am Coll Cardiol 2014;64:144–54. https://doi.org/10.1016/j.jacc.2014.02.612.

[32] Salcedo EE, Korzick DH, Currie PJ, Stewart WJ, Lever HM, Goormastic M. Determinants of left ventricular hypertrophy in patients with aortic stenosis. Cleve Clin J Med 1989;56:590–6.

[33] Dweck MR, Joshi S, Murigu T, Gulati A, Alpendurada F, Jabbour A, et al. Left ventricular remodeling and hypertrophy in patients with aortic stenosis: insights from cardiovascular magnetic resonance. J Cardiovasc Magn Reson 2012;14:50. https://doi.org/10.1186/1532-429X-14-50.

[34] Orlowska-Baranowska E, Placha G, Gaciong Z, Baranowski R, Zakrzewski D, Michalek P, et al. Influence of ACE I/D genotypes on left ventricular hypertrophy in aortic stenosis: gender-related differences. J Heart Valve Dis 2004;13:574–81.

[35] Treibel TA, Kozor R, Fontana M, Torlasco C, Reant P, Badiani S, et al. Sex Dimorphism in the Myocardial Response to Aortic Stenosis. JACC Cardiovasc Imaging 2018;11:962–73. https://doi.org/10.1016/j.jcmg.2017.08.025.

[36] Musa TA, Treibel TA, Vassiliou VS, Captur G, Singh A, Chin C, et al. Myocardial Scar and Mortality in Severe Aortic Stenosis: Data From the BSCMR Valve Consortium. Circulation 2018;138:1935–47. https://doi.org/10.1161/CIRCULATIONAHA.117.032839.

[37] Pellikka PA. Outcome of 622 Adults With Asymptomatic, Hemodynamically Significant Aortic Stenosis During Prolonged Follow-Up. Circulation 2005;111:3290–5. https://doi.org/10.1161/CIRCULATIONAHA.104.495903.

[38] Ross J, Braunwald E. Aortic stenosis. Circulation 1968;38:61–7.

[39] Schwarz F, Baumann P, Manthey J, Hoffmann M, Schuler G, Mehmel HC, et al. The effect of aortic valve replacement on survival. Circulation 1982;66:1105–10.

[40] Turina J, Hess O, Sepulcri F, Krayenbuehl HP. Spontaneous course of aortic valve disease. Eur Heart J 1987;8:471–83.

[41] Bonow RO, Carabello BA, Chatterjee K, de Leon AC, Faxon DP, Freed MD, et al. ACC/AHA 2006 Guidelines for the Management of Patients With Valvular Heart Disease: A Report of the American College of Cardiology/American Heart Association Task Force on Practice Guidelines (Writing Committee to Revise the 1998 Guidelines for the Management of Patients With Valvular Heart Disease): Developed in Collaboration With the Society of Cardiovascular Anesthesiologists: Endorsed by the Society for Cardiovascular Angiography and Interventions and the Society of Thoracic Surgeons. Circulation 2006;114:e84–231. https://doi.org/10.1161/CIRCULATIONAHA.106.176857.

[42] Leon MB, Smith CR, Mack M, Miller DC, Moses JW, Svensson LG, et al. Transcatheter Aortic-Valve Implantation for Aortic Stenosis in Patients Who Cannot Undergo Surgery. N Engl J Med 2010;363:1597–607. https://doi.org/10.1056/NEJMoa1008232.

[43] Hoffmann R, Almutairi B, Herpertz R, Lotfipour S, Stöhr R, Aktug O, et al. Two-year mortality after transcatheter aortic valve implantation versus medical therapy for

high-surgical risk or inoperable aortic stenosis patients. J Heart Valve Dis 2013;22:71–8.

[44] Deeb GM, Reardon MJ, Chetcuti S, Patel HJ, Grossman PM, Yakubov SJ, et al. 3-Year Outcomes in High-Risk Patients Who Underwent Surgical or Transcatheter Aortic Valve Replacement. J Am Coll Cardiol 2016;67:2565–74. https://doi.org/10.1016/j.jacc.2016.03.506.

[45] Smith CR, Leon MB, Mack MJ, Miller DC, Moses JW, Svensson LG, et al. Transcatheter versus Surgical Aortic-Valve Replacement in High-Risk Patients. N Engl J Med 2011;364:2187–98. https://doi.org/10.1056/NEJMoa1103510.

[46] Mack MJ, Leon MB, Smith CR, Miller DC, Moses JW, Tuzcu EM, et al. 5-year outcomes of transcatheter aortic valve replacement or surgical aortic valve replacement for high surgical risk patients with aortic stenosis (PARTNER 1): a randomised controlled trial. Lancet Lond Engl 2015;385:2477–84. https://doi.org/10.1016/S0140-6736(15)60308-7.

[47] National Institute for Health and Care Excellence. Transcatheter aortic valve implantation for aortic stenosis. Interventional procedures guidance 586. 2017.

[48] Leon MB, Smith CR, Mack MJ, Makkar RR, Svensson LG, Kodali SK, et al. Transcatheter or Surgical Aortic-Valve Replacement in Intermediate-Risk Patients. N Engl J Med 2016;374:1609–20. https://doi.org/10.1056/NEJMoa1514616.

[49] Kodali S, Thourani VH, White J, Malaisrie SC, Lim S, Greason KL, et al. Early clinical and echocardiographic outcomes after SAPIEN 3 transcatheter aortic valve replacement in inoperable, high-risk and intermediate-risk patients with aortic stenosis. Eur Heart J 2016;37:2252–62. https://doi.org/10.1093/eurheartj/ehw112.

[50] Reardon MJ, Van Mieghem NM, Popma JJ, Kleiman NS, Søndergaard L, Mumtaz M, et al. Surgical or Transcatheter Aortic-Valve Replacement in Intermediate-Risk Patients. N Engl J Med 2017;376:1321–31. https://doi.org/10.1056/NEJMoa1700456.

[51] Mack MJ, Leon MB, Thourani VH, Makkar R, Kodali SK, Russo M, et al. Transcatheter Aortic-Valve Replacement with a Balloon-Expandable Valve in Low-Risk Patients. N Engl J Med 2019;380:1695–705. https://doi.org/10.1056/NEJMoa1814052.

[52] Popma JJ, Deeb GM, Yakubov SJ, Mumtaz M, Gada H, O'Hair D, et al. Transcatheter Aortic-Valve Replacement with a Self-Expanding Valve in Low-Risk Patients. N Engl J Med 2019;380:1706–15. https://doi.org/10.1056/NEJMoa1816885.

[53] Thyregod HGH, Steinbrüchel DA, Ihlemann N, Nissen H, Kjeldsen BJ, Petursson P, et al. Transcatheter Versus Surgical Aortic Valve Replacement in Patients With Severe Aortic Valve Stenosis. J Am Coll Cardiol 2015;65:2184–94. https://doi.org/10.1016/j.jacc.2015.03.014.

[54] Thyregod HGH, Ihlemann N, Jørgensen TH, Nissen H, Kjeldsen BJ, Petursson P, et al. Five-Year Clinical and Echocardiographic Outcomes From the NOTION Randomized Clinical Trial in Patients at Lower Surgical Risk. Circulation 2019;139:2714–23. https://doi.org/10.1161/CIRCULATIONAHA.118.036606.

[55] Cribier A. Percutaneous Transcatheter Implantation of an Aortic Valve Prosthesis for Calcific Aortic Stenosis: First Human Case Description. Circulation 2002;106:3006–8. https://doi.org/10.1161/01.CIR.0000047200.36165.B8.

[56] Puri R, Iung B, Cohen DJ, Rodés-Cabau J. TAVI or No TAVI: identifying patients unlikely to benefit from transcatheter aortic valve implantation. Eur Heart J 2016;37:2217–25. https://doi.org/10.1093/eurheartj/ehv756.

[57] Reynolds MR, Magnuson EA, Wang K, Thourani VH, Williams M, Zajarias A, et al. Health-Related Quality of Life After Transcatheter or Surgical Aortic Valve Replacement in High-Risk Patients With Severe Aortic Stenosis. J Am Coll Cardiol 2012;60:548–58. https://doi.org/10.1016/j.jacc.2012.03.075.

[58] Ludman PF, Moat N, de Belder MA, Blackman DJ, Duncan A, Banya W, et al. Transcatheter aortic valve implantation in the United Kingdom: temporal trends, predictors of outcome, and 6-year follow-up: a report from the UK Transcatheter Aortic Valve Implantation (TAVI) Registry, 2007 to 2012. Circulation 2015;131:1181–90. https://doi.org/10.1161/CIRCULATIONAHA.114.013947.

[59] Green P, Arnold SV, Cohen DJ, Kirtane AJ, Kodali SK, Brown DL, et al. Relation of frailty to outcomes after transcatheter aortic valve replacement (from the PARTNER trial). Am J Cardiol 2015;116:264–9. https://doi.org/10.1016/j.amjcard.2015.03.061.

[60] Herrmann HC, Pibarot P, Hueter I, Gertz ZM, Stewart WJ, Kapadia S, et al. Predictors of mortality and outcomes of therapy in low-flow severe aortic stenosis: a Placement of Aortic Transcatheter Valves (PARTNER) trial analysis. Circulation 2013;127:2316–26. https://doi.org/10.1161/CIRCULATIONAHA.112.001290.

[61] Nombela-Franco L, Eltchaninoff H, Zahn R, Testa L, Leon MB, Trillo-Nouche R, et al. Clinical impact and evolution of mitral regurgitation following transcatheter aortic valve replacement: a meta-analysis. Heart Br Card Soc 2015;101:1395–405. https://doi.org/10.1136/heartjnl-2014-307120.

[62] Banypersad SM, Moon JC, Whelan C, Hawkins PN, Wechalekar AD. Updates in Cardiac Amyloidosis: A Review. J Am Heart Assoc 2012;1:e000364–e000364. https://doi.org/10.1161/JAHA.111.000364.

[63] Westermark P, Benson MD, Buxbaum JN, Cohen AS, Frangione B, Ikeda S-I, et al. A primer of amyloid nomenclature. Amyloid 2007;14:179–83. https://doi.org/10.1080/13506120701460923.

[64] Selvanayagam JB, Hawkins PN, Paul B, Myerson SG, Neubauer S. Evaluation and Management of the Cardiac Amyloidosis. J Am Coll Cardiol 2007;50:2101–10. https://doi.org/10.1016/j.jacc.2007.08.028.

[65] Rahman JE, Helou EF, Gelzer-Bell R, Thompson RE, Kuo C, Rodriguez ER, et al. Noninvasive diagnosis of biopsy-proven cardiac amyloidosis. J Am Coll Cardiol 2004;43:410–5. https://doi.org/10.1016/j.jacc.2003.08.043.

[66] Feng D, Edwards WD, Oh JK, Chandrasekaran K, Grogan M, Martinez MW, et al. Intracardiac Thrombosis and Embolism in Patients With Cardiac Amyloidosis. Circulation 2007;116:2420–6. https://doi.org/10.1161/CIRCULATIONAHA.107.697763.

[67] Al Suwaidi J, Velianou JL, Gertz MA, Cannon RO, Higano ST, Holmes DR, et al. Systemic amyloidosis presenting with angina pectoris. Ann Intern Med 1999;131:838–41.

[68] Sperry BW, Tang WHW. Amyloid heart disease: genetics translated into disease-modifying therapy. Heart 2017;103:812–7. https://doi.org/10.1136/heartjnl-2016-309914.

[69] Kyle RA, Gertz MA. Primary systemic amyloidosis: clinical and laboratory features in 474 cases. Semin Hematol 1995;32:45–59.

[70] Kyle RA, Gertz MA, Greipp PR, Witzig TE, Lust JA, Lacy MQ, et al. Long-term survival (10 years or more) in 30 patients with primary amyloidosis. Blood 1999;93:1062–6.

[71] Gillmore JD, Wechalekar A, Bird J, Cavenagh J, Hawkins S, Kazmi M, et al. Guidelines on the diagnosis and investigation of AL amyloidosis. Br J Haematol 2015;168:207–18. https://doi.org/10.1111/bjh.13156.

[72] Tanskanen M, Peuralinna T, Polvikoski T, Notkola I, Sulkava R, Hardy J, et al. Senile systemic amyloidosis affects 25% of the very aged and associates with genetic variation in *alpha2-macroglobulin* and *tau* : A population-based autopsy study. Ann Med 2008;40:232–9. https://doi.org/10.1080/07853890701842988.

[73] Connors LH, Sam F, Skinner M, Salinaro F, Sun F, Ruberg FL, et al. Heart Failure Resulting From Age-Related Cardiac Amyloid Disease Associated With Wild-Type Transthyretin: A Prospective, Observational Cohort Study. Circulation 2016;133:282–90. https://doi.org/10.1161/CIRCULATIONAHA.115.018852.

[74] Gillmore JD, Damy T, Fontana M, Hutchinson M, Lachmann HJ, Martinez-Naharro A, et al. A new staging system for cardiac transthyretin amyloidosis. Eur Heart J 2017. https://doi.org/10.1093/eurheartj/ehx589.

[75] González-López E, Gallego-Delgado M, Guzzo-Merello G, de Haro-del Moral FJ, Cobo-Marcos M, Robles C, et al. Wild-type transthyretin amyloidosis as a cause of heart

failure with preserved ejection fraction. Eur Heart J 2015;36:2585–94. https://doi.org/10.1093/eurheartj/ehv338.

[76] Maurer MS, Hanna M, Grogan M, Dispenzieri A, Witteles R, Drachman B, et al. Genotype and Phenotype of Transthyretin Cardiac Amyloidosis: THAOS (Transthyretin Amyloid Outcome Survey). J Am Coll Cardiol 2016;68:161–72. https://doi.org/10.1016/j.jacc.2016.03.596.

[77] Dungu JN, Papadopoulou SA, Wykes K, Mahmood I, Marshall J, Valencia O, et al. Afro-Caribbean Heart Failure in the United KingdomCLINICAL PERSPECTIVE: Cause, Outcomes, and ATTR V122I Cardiac Amyloidosis. Circ Heart Fail 2016;9:e003352. https://doi.org/10.1161/CIRCHEARTFAILURE.116.003352.

[78] Givens RC, Russo C, Green P, Maurer MS. Comparison of cardiac amyloidosis due to wild-type and V122I transthyretin in older adults referred to an academic medical center. Aging Health 2013;9:229–35. https://doi.org/10.2217/ahe.13.10.

[79] Planté-Bordeneuve V, Said G. Familial amyloid polyneuropathy. Lancet Neurol 2011;10:1086–97. https://doi.org/10.1016/S1474-4422(11)70246-0.

[80] Suhr OB, Lindqvist P, Olofsson B-O, Waldenström A, Backman C. Myocardial hypertrophy and function are related to age at onset in familial amyloidotic polyneuropathy. Amyloid Int J Exp Clin Investig Off J Int Soc Amyloidosis 2006;13:154–9. https://doi.org/10.1080/13506120600876849.

[81] Drugge U, Andersson R, Chizari F, Danielsson M, Holmgren G, Sandgren O, et al. Familial amyloidotic polyneuropathy in Sweden: a pedigree analysis. J Med Genet 1993;30:388–92.

[82] Koike H, Tanaka F, Hashimoto R, Tomita M, Kawagashira Y, Iijima M, et al. Natural history of transthyretin Val30Met familial amyloid polyneuropathy: analysis of late-onset cases from non-endemic areas. J Neurol Neurosurg Psychiatry 2012;83:152–8. https://doi.org/10.1136/jnnp-2011-301299.

[83] Ikeda S. Cardiac Amyloidosis: Heterogenous Pathogenic Backgrounds. Intern Med 2004;43:1107–14. https://doi.org/10.2169/internalmedicine.43.1107.

[84] Sattianayagam PT, Hahn AF, Whelan CJ, Gibbs SDJ, Pinney JH, Stangou AJ, et al. Cardiac phenotype and clinical outcome of familial amyloid polyneuropathy associated with transthyretin alanine 60 variant. Eur Heart J 2012;33:1120–7. https://doi.org/10.1093/eurheartj/ehr383.

[85] Kula RW, Engel WK, Line BR. Scanning for soft-tissue amyloid. Lancet Lond Engl 1977;1:92–3.

[86] Perugini E, Guidalotti PL, Salvi F, Cooke RMT, Pettinato C, Riva L, et al. Noninvasive Etiologic Diagnosis of Cardiac Amyloidosis Using 99mTc-3,3-Diphosphono-1,2-

Propanodicarboxylic Acid Scintigraphy. J Am Coll Cardiol 2005;46:1076–84. https://doi.org/10.1016/j.jacc.2005.05.073.

[87] Hutt DF, Quigley A-M, Page J, Hall ML, Burniston M, Gopaul D, et al. Utility and limitations of 3,3-diphosphono-1,2-propanodicarboxylic acid scintigraphy in systemic amyloidosis. Eur Heart J - Cardiovasc Imaging 2014;15:1289–98. https://doi.org/10.1093/ehjci/jeu107.

[88] Gillmore JD, Maurer MS, Falk RH, Merlini G, Damy T, Dispenzieri A, et al. Nonbiopsy Diagnosis of Cardiac Transthyretin Amyloidosis. Circulation 2016;133:2404–12. https://doi.org/10.1161/CIRCULATIONAHA.116.021612.

[89] Dorbala S, Ando Y, Bokhari S, Dispenzieri A, Falk RH, Ferrari VA, et al. ASNC/AHA/ASE/EANM/HFSA/ISA/SCMR/SNMMI expert consensus recommendations for multimodality imaging in cardiac amyloidosis: Part 1 of 2—evidence base and standardized methods of imaging. J Nucl Cardiol 2019. https://doi.org/10.1007/s12350-019-01760-6.

[90] Dorbala S, Ando Y, Bokhari S, Dispenzieri A, Falk RH, Ferrari VA, et al. ASNC/AHA/ASE/EANM/HFSA/ISA/SCMR/SNMMI expert consensus recommendations for multimodality imaging in cardiac amyloidosis: Part 2 of 2—Diagnostic criteria and appropriate utilization. J Nucl Cardiol 2019:s12350-019-01761–5. https://doi.org/10.1007/s12350-019-01761-5.

[91] Stats MA, Stone JR. Varying levels of small microcalcifications and macrophages in ATTR and AL cardiac amyloidosis: implications for utilizing nuclear medicine studies to subtype amyloidosis. Cardiovasc Pathol Off J Soc Cardiovasc Pathol 2016;25:413–7. https://doi.org/10.1016/j.carpath.2016.07.001.

[92] Hutt DF, Fontana M, Burniston M, Quigley A-M, Petrie A, Ross JC, et al. Prognostic utility of the Perugini grading of 99mTc-DPD scintigraphy in transthyretin (ATTR) amyloidosis and its relationship with skeletal muscle and soft tissue amyloid. Eur Heart J - Cardiovasc Imaging 2017;18:1344–50. https://doi.org/10.1093/ehjci/jew325.

[93] Maurer MS, Schwartz JH, Gundapaneni B, Elliott PM, Merlini G, Waddington-Cruz M, et al. Tafamidis Treatment for Patients with Transthyretin Amyloid Cardiomyopathy. N Engl J Med 2018;379:1007–16. https://doi.org/10.1056/NEJMoa1805689.

[94] Solomon SD, Adams D, Kristen A, Grogan M, González-Duarte A, Maurer MS, et al. Effects of Patisiran, an RNA Interference Therapeutic, on Cardiac Parameters in Patients With Hereditary Transthyretin-Mediated Amyloidosis: Analysis of the APOLLO Study. Circulation 2019;139:431–43. https://doi.org/10.1161/CIRCULATIONAHA.118.035831.

[95] Dasgupta NR, Benson M. IMPROVED SURVIVAL OF PATIENTS WITH TRANSTHYRETIN AMYLOID CARDIOMYOPATHY WITH INOTERSEN (TTR SPECIFIC ANTISENSE

OLIGONUCLEOTIDE). J Am Coll Cardiol 2019;73:811. https://doi.org/10.1016/S0735-1097(19)31418-4.

[96] Rapezzi C, Quarta CC, Guidalotti PL, Pettinato C, Fanti S, Leone O, et al. Role of 99mTc-DPD Scintigraphy in Diagnosis and Prognosis of Hereditary Transthyretin-Related Cardiac Amyloidosis. JACC Cardiovasc Imaging 2011;4:659–70. https://doi.org/10.1016/j.jcmg.2011.03.016.

[97] Galat A, Rosso J, Guellich A, Van Der Gucht A, Rappeneau S, Bodez D, et al. Usefulness of ^{99m} Tc-HMDP scintigraphy for the etiologic diagnosis and prognosis of cardiac amyloidosis. Amyloid 2015;22:210–20. https://doi.org/10.3109/13506129.2015.1072089.

[98] Dorbala S, Bokhari S, Miller, Edward, Bullock-Palmer, Renee, Soman P, Thompson, Randall. 99mTechnetium-Pyrophosphate Imaging for Transthyretin Cardiac Amyloidosis 2019.

[99] Bokhari S, Castaño A, Pozniakoff T, Deslisle S, Latif F, Maurer MS. ^{99m} Tc-Pyrophosphate Scintigraphy for Differentiating Light-Chain Cardiac Amyloidosis From the Transthyretin-Related Familial and Senile Cardiac Amyloidoses. Circ Cardiovasc Imaging 2013;6:195–201. https://doi.org/10.1161/CIRCIMAGING.112.000132.

[100] Castano A, Haq M, Narotsky DL, Goldsmith J, Weinberg RL, Morgenstern R, et al. Multicenter Study of Planar Technetium 99m Pyrophosphate Cardiac Imaging: Predicting Survival for Patients With ATTR Cardiac Amyloidosis. JAMA Cardiol 2016;1:880–9. https://doi.org/10.1001/jamacardio.2016.2839.

[101] Hawkins PN, Lavender JP, Myers MJ, Pepys MB. DIAGNOSTIC RADIONUCLIDE IMAGING OF AMYLOID: BIOLOGICAL TARGETING BY CIRCULATING HUMAN SERUM AMYLOID P COMPONENT. The Lancet 1988;331:1413–8. https://doi.org/10.1016/S0140-6736(88)92235-0.

[102] Hawkins PN, Lavender JP, Pepys MB. Evaluation of Systemic Amyloidosis by Scintigraphy with ^{123} I-Labeled Serum Amyloid P Component. N Engl J Med 1990;323:508–13. https://doi.org/10.1056/NEJM199008233230803.

[103] Hazenberg BPC, van Rijswijk MH, Piers DA, Lub-de Hooge MN, Vellenga E, Haagsma EB, et al. Diagnostic Performance of 123I-Labeled Serum Amyloid P Component Scintigraphy in Patients with Amyloidosis. Am J Med 2006;119:355.e15-355.e24. https://doi.org/10.1016/j.amjmed.2005.08.043.

[104] Pepys MB, Dyck RF, de Beer FC, Skinner M, Cohen AS. Binding of serum amyloid P-component (SAP) by amyloid fibrils. Clin Exp Immunol 1979;38:284–93.

[105] Sachchithanantham S, Wechalekar AD. Imaging in systemic amyloidosis. Br Med Bull 2013;107:41–56. https://doi.org/10.1093/bmb/ldt021.

[106] Lovat LB, Persey MR, Madhoo S, Pepys MB, Hawkins PN. The liver in systemic amyloidosis: insights from 123I serum amyloid P component scintigraphy in 484 patients. Gut 1998;42:727–34. https://doi.org/10.1136/gut.42.5.727.

[107] Cueto-Garcia L, Tajik AJ, Kyle RA, Edwards WD, Greipp PR, Callahan JA, et al. Serial echocardiographic observations in patients with primary systemic amyloidosis: an introduction to the concept of early (asymptomatic) amyloid infiltration of the heart. Mayo Clin Proc 1984;59:589–97.

[108] Rapezzi C, Merlini G, Quarta CC, Riva L, Longhi S, Leone O, et al. Systemic Cardiac Amyloidoses: Disease Profiles and Clinical Courses of the 3 Main Types. Circulation 2009;120:1203–12. https://doi.org/10.1161/CIRCULATIONAHA.108.843334.

[109] Siqueira-Filho AG, Cunha CL, Tajik AJ, Seward JB, Schattenberg TT, Giuliani ER. M-mode and two-dimensional echocardiographic features in cardiac amyloidosis. Circulation 1981;63:188–96. https://doi.org/10.1161/01.CIR.63.1.188.

[110] Kramer CM, Narula J. CMR of Amyloidosis: Looking Between the Sheets. JACC Cardiovasc Imaging 2014;7:210–1. https://doi.org/10.1016/j.jcmg.2013.12.005.

[111] Quarta CC, Solomon SD, Uraizee I, Kruger J, Longhi S, Ferlito M, et al. Left Ventricular Structure and Function in Transthyretin-Related Versus Light-Chain Cardiac Amyloidosis. Circulation 2014;129:1840–9. https://doi.org/10.1161/CIRCULATIONAHA.113.006242.

[112] Bravo PE, Fujikura K, Kijewski MF, Jerosch-Herold M, Jacob S, El-Sady MS, et al. Relative Apical Sparing of Myocardial Longitudinal Strain Is Explained by Regional Differences in Total Amyloid Mass Rather Than the Proportion of Amyloid Deposits. JACC Cardiovasc Imaging 2019;12:1165–73. https://doi.org/10.1016/j.jcmg.2018.06.016.

[113] Rapezzi C, Fontana M. Relative Left Ventricular Apical Sparing of Longitudinal Strain in Cardiac Amyloidosis. JACC Cardiovasc Imaging 2019;12:1174–6. https://doi.org/10.1016/j.jcmg.2018.07.007.

[114] Martinez-Naharro A, Treibel TA, Abdel-Gadir A, Bulluck H, Zumbo G, Knight DS, et al. Magnetic Resonance in Transthyretin Cardiac Amyloidosis. J Am Coll Cardiol 2017;70:466–77. https://doi.org/10.1016/j.jacc.2017.05.053.

[115] Fontana M, Chung R, Hawkins PN, Moon JC. Cardiovascular magnetic resonance for amyloidosis. Heart Fail Rev 2015;20:133–44. https://doi.org/10.1007/s10741-014-9470-7.

[116] Scully PR, Bastarrika G, Moon JC, Treibel TA. Myocardial Extracellular Volume Quantification by Cardiovascular Magnetic Resonance and Computed Tomography. Curr Cardiol Rep 2018;20. https://doi.org/10.1007/s11886-018-0961-3.

[117] Kim RJ, Albert TSE, Wible JH, Elliott MD, Allen JC, Lee JC, et al. Performance of Delayed-Enhancement Magnetic Resonance Imaging With Gadoversetamide Contrast for the Detection and Assessment of Myocardial Infarction: An International, Multicenter, Double-Blinded, Randomized Trial. Circulation 2008;117:629–37. https://doi.org/10.1161/CIRCULATIONAHA.107.723262.

[118] Syed IS, Glockner JF, Feng D, Araoz PA, Martinez MW, Edwards WD, et al. Role of cardiac magnetic resonance imaging in the detection of cardiac amyloidosis. JACC Cardiovasc Imaging 2010;3:155–64. https://doi.org/10.1016/j.jcmg.2009.09.023.

[119] Dungu JN, Valencia O, Pinney JH, Gibbs SDJ, Rowczenio D, Gilbertson JA, et al. CMR-Based Differentiation of AL and ATTR Cardiac Amyloidosis. JACC Cardiovasc Imaging 2014;7:133–42. https://doi.org/10.1016/j.jcmg.2013.08.015.

[120] Messroghli DR, Moon JC, Ferreira VM, Grosse-Wortmann L, He T, Kellman P, et al. Clinical recommendations for cardiovascular magnetic resonance mapping of T1, T2, T2* and extracellular volume: A consensus statement by the Society for Cardiovascular Magnetic Resonance (SCMR) endorsed by the European Association for Cardiovascular Imaging (EACVI). J Cardiovasc Magn Reson 2017;19. https://doi.org/10.1186/s12968-017-0389-8.

[121] Flett AS, Hayward MP, Ashworth MT, Hansen MS, Taylor AM, Elliott PM, et al. Equilibrium Contrast Cardiovascular Magnetic Resonance for the Measurement of Diffuse Myocardial Fibrosis: Preliminary Validation in Humans. Circulation 2010;122:138–44. https://doi.org/10.1161/CIRCULATIONAHA.109.930636.

[122] Wong TC, Piehler KM, Kang IA, Kadakkal A, Kellman P, Schwartzman DS, et al. Myocardial extracellular volume fraction quantified by cardiovascular magnetic resonance is increased in diabetes and associated with mortality and incident heart failure admission. Eur Heart J 2014;35:657–64. https://doi.org/10.1093/eurheartj/eht193.

[123] Sado DM, Flett AS, Banypersad SM, White SK, Maestrini V, Quarta G, et al. Cardiovascular magnetic resonance measurement of myocardial extracellular volume in health and disease. Heart 2012;98:1436–41. https://doi.org/10.1136/heartjnl-2012-302346.

[124] Haaf P, Garg P, Messroghli DR, Broadbent DA, Greenwood JP, Plein S. Cardiac T1 Mapping and Extracellular Volume (ECV) in clinical practice: a comprehensive review. J Cardiovasc Magn Reson 2017;18. https://doi.org/10.1186/s12968-016-0308-4.

[125] Banypersad SM, Fontana M, Maestrini V, Sado DM, Captur G, Petrie A, et al. T1 mapping and survival in systemic light-chain amyloidosis. Eur Heart J 2015;36:244–51. https://doi.org/10.1093/eurheartj/ehu444.

[126] Martinez-Naharro A, Kotecha T, Norrington K, Boldrini M, Rezk T, Quarta C, et al. Native T1 and Extracellular Volume in Transthyretin Amyloidosis. JACC Cardiovasc Imaging 2019;12:810–9. https://doi.org/10.1016/j.jcmg.2018.02.006.

[127] Martinez-Naharro A, Abdel-Gadir A, Treibel TA, Zumbo G, Knight DS, Rosmini S, et al. CMR-Verified Regression of Cardiac AL Amyloid After Chemotherapy. JACC Cardiovasc Imaging 2018;11:152–4. https://doi.org/10.1016/j.jcmg.2017.02.012.

[128] Moon JC, Messroghli DR, Kellman P, Piechnik SK, Robson MD, Ugander M, et al. Myocardial T1 mapping and extracellular volume quantification: a Society for Cardiovascular Magnetic Resonance (SCMR) and CMR Working Group of the European Society of Cardiology consensus statement. J Cardiovasc Magn Reson 2013;15:92. https://doi.org/10.1186/1532-429X-15-92.

[129] National Institute for Health and Care Excellence (NICE). Chest pain of recent onset: assessment and diagnosis: clinical guideline [CG95] 2016.

[130] Nacif MS, Kawel N, Lee JJ, Chen X, Yao J, Zavodni A, et al. Interstitial Myocardial Fibrosis Assessed as Extracellular Volume Fraction with Low-Radiation-Dose Cardiac CT. Radiology 2012;264:876–83. https://doi.org/10.1148/radiol.12112458.

[131] Bandula S, White SK, Flett AS, Lawrence D, Pugliese F, Ashworth MT, et al. Measurement of Myocardial Extracellular Volume Fraction by Using Equilibrium Contrast-enhanced CT: Validation against Histologic Findings. Radiology 2013;269:396–403. https://doi.org/10.1148/radiol.13130130.

[132] Treibel TA, Bandula S, Fontana M, White SK, Gilbertson JA, Herrey AS, et al. Extracellular volume quantification by dynamic equilibrium cardiac computed tomography in cardiac amyloidosis. J Cardiovasc Comput Tomogr 2015;9:585–92. https://doi.org/10.1016/j.jcct.2015.07.001.

[133] Antoni G, Lubberink M, Estrada S, Axelsson J, Carlson K, Lindsjo L, et al. In Vivo Visualization of Amyloid Deposits in the Heart with 11C-PIB and PET. J Nucl Med 2013;54:213–20. https://doi.org/10.2967/jnumed.111.102053.

[134] Lee S-P, Lee ES, Choi H, Im H-J, Koh Y, Lee M-H, et al. 11C-Pittsburgh B PET Imaging in Cardiac Amyloidosis. JACC Cardiovasc Imaging 2015;8:50–9. https://doi.org/10.1016/j.jcmg.2014.09.018.

[135] Dorbala S, Vangala D, Semer J, Strader C, Bruyere JR, Di Carli MF, et al. Imaging cardiac amyloidosis: a pilot study using 18F-florbetapir positron emission tomography. Eur J Nucl Med Mol Imaging 2014;41:1652–62. https://doi.org/10.1007/s00259-014-2787-6.

[136] Osborne DR, Acuff SN, Stuckey A, Wall JS. A Routine PET/CT Protocol with Streamlined Calculations for Assessing Cardiac Amyloidosis Using 18F-Florbetapir. Front Cardiovasc Med 2015;2. https://doi.org/10.3389/fcvm.2015.00023.

[137] Law WP, Wang WYS, Moore PT, Mollee PN, Ng ACT. Cardiac Amyloid Imaging with 18F-Florbetaben PET: A Pilot Study. J Nucl Med 2016;57:1733–9. https://doi.org/10.2967/jnumed.115.169870.

[138] Kircher M, Ihne S, Brumberg J, Morbach C, Knop S, Kortüm KM, et al. Detection of cardiac amyloidosis with 18F-Florbetaben-PET/CT in comparison to echocardiography, cardiac MRI and DPD-scintigraphy. Eur J Nucl Med Mol Imaging 2019;46:1407–16. https://doi.org/10.1007/s00259-019-04290-y.

[139] Dietemann S, Nkoulou R. Amyloid PET imaging in cardiac amyloidosis: a pilot study using 18F-flutemetamol positron emission tomography. Ann Nucl Med 2019;33:624–8. https://doi.org/10.1007/s12149-019-01372-7.

[140] Dispenzieri A, Gertz MA, Kyle RA, Lacy MQ, Burritt MF, Therneau TM, et al. Serum Cardiac Troponins and N-Terminal Pro-Brain Natriuretic Peptide: A Staging System for Primary Systemic Amyloidosis. J Clin Oncol 2004;22:3751–7. https://doi.org/10.1200/JCO.2004.03.029.

[141] Kumar S, Dispenzieri A, Lacy MQ, Hayman SR, Buadi FK, Colby C, et al. Revised Prognostic Staging System for Light Chain Amyloidosis Incorporating Cardiac Biomarkers and Serum Free Light Chain Measurements. J Clin Oncol 2012;30:989–95. https://doi.org/10.1200/JCO.2011.38.5724.

[142] Castaño A, Drachman BM, Judge D, Maurer MS. Natural history and therapy of TTR-cardiac amyloidosis: emerging disease-modifying therapies from organ transplantation to stabilizer and silencer drugs. Heart Fail Rev 2015;20:163–78. https://doi.org/10.1007/s10741-014-9462-7.

[143] Rubinow A, Skinner M, Cohen AS. Digoxin sensitivity in amyloid cardiomyopathy. Circulation 1981;63:1285–8.

[144] Jonsén E, Suhr OB, Tashima K, Athlin E. Early liver transplantation is essential for familial amyloidotic polyneuropathy patients' quality of life. Amyloid Int J Exp Clin Investig Off J Int Soc Amyloidosis 2001;8:52–7.

[145] Stangou AJ, Hawkins PN, Heaton ND, Rela M, Monaghan M, Nihoyannopoulos P, et al. Progressive cardiac amyloidosis following liver transplantation for familial amyloid polyneuropathy: implications for amyloid fibrillogenesis. Transplantation 1998;66:229–33.

[146] Dubrey SW, Davidoff R, Skinner M, Bergethon P, Lewis D, Falk RH. Progression of ventricular wall thickening after liver transplantation for familial amyloidosis. Transplantation 1997;64:74–80.

[147] Okamoto S, Hörnsten R, Obayashi K, Wijayatunga P, Suhr OB. Continuous development of arrhythmia is observed in Swedish transplant patients with familial amyloidotic polyneuropathy (amyloidogenic transthyretin Val30Met variant). Liver Transplant Off Publ Am Assoc Study Liver Dis Int Liver Transplant Soc 2011;17:122–8. https://doi.org/10.1002/lt.22184.

[148] Kpodonu J, Massad MG, Caines A, Geha AS. Outcome of Heart Transplantation in Patients With Amyloid Cardiomyopathy. J Heart Lung Transplant 2005;24:1763–5. https://doi.org/10.1016/j.healun.2004.08.025.

[149] Barrett CD, Alexander KM, Zhao H, Haddad F, Cheng P, Liao R, et al. Outcomes in Patients With Cardiac Amyloidosis Undergoing Heart Transplantation. JACC Heart Fail 2020;8:461–8. https://doi.org/10.1016/j.jchf.2019.12.013.

[150] Lacy MQ, Dispenzieri A, Hayman SR, Kumar S, Kyle RA, Rajkumar SV, et al. Autologous Stem Cell Transplant after Heart Transplant for Light Chain (AL) Amyloid Cardiomyopathy. J Heart Lung Transplant 2008;27:823–9. https://doi.org/10.1016/j.healun.2008.05.016.

[151] Judge DP, Heitner SB, Falk RH, Maurer MS, Shah SJ, Witteles RM, et al. Transthyretin Stabilization by AG10 in Symptomatic Transthyretin Amyloid Cardiomyopathy. J Am Coll Cardiol 2019;74:285–95. https://doi.org/10.1016/j.jacc.2019.03.012.

[152] Hammarstrom P, Jiang X, Hurshman AR, Powers ET, Kelly JW. Sequence-dependent denaturation energetics: A major determinant in amyloid disease diversity. Proc Natl Acad Sci 2002;99:16427–32. https://doi.org/10.1073/pnas.202495199.

[153] Berk JL, Suhr OB, Obici L, Sekijima Y, Zeldenrust SR, Yamashita T, et al. Repurposing Diflunisal for Familial Amyloid Polyneuropathy: A Randomized Clinical Trial. JAMA 2013;310:2658. https://doi.org/10.1001/jama.2013.283815.

[154] Cardoso I, Martins D, Ribeiro T, Merlini G, Saraiva M. Synergy of combined Doxycycline/TUDCA treatment in lowering Transthyretin deposition and associated biomarkers: studies in FAP mouse models. J Transl Med 2010;8:74. https://doi.org/10.1186/1479-5876-8-74.

[155] Richards DB, Cookson LM, Berges AC, Barton SV, Lane T, Ritter JM, et al. Therapeutic Clearance of Amyloid by Antibodies to Serum Amyloid P Component. N Engl J Med 2015;373:1106–14. https://doi.org/10.1056/NEJMoa1504942.

[156] Richards DB, Cookson LM, Barton SV, Liefaard L, Lane T, Hutt DF, et al. Repeat doses of antibody to serum amyloid P component clear amyloid deposits in patients with systemic amyloidosis. Sci Transl Med 2018;10:eaan3128. https://doi.org/10.1126/scitranslmed.aan3128.

[157] Coelho T, Adams D, Silva A, Lozeron P, Hawkins PN, Mant T, et al. Safety and Efficacy of RNAi Therapy for Transthyretin Amyloidosis. N Engl J Med 2013;369:819–29. https://doi.org/10.1056/NEJMoa1208760.

[158] Adams D, Gonzalez-Duarte A, O'Riordan WD, Yang C-C, Ueda M, Kristen AV, et al. Patisiran, an RNAi Therapeutic, for Hereditary Transthyretin Amyloidosis. N Engl J Med 2018;379:11–21. https://doi.org/10.1056/NEJMoa1716153.

[159] Ackermann EJ, Guo S, Booten S, Alvarado L, Benson M, Hughes S, et al. Clinical development of an antisense therapy for the treatment of transthyretin-associated polyneuropathy. Amyloid 2012;19:43–4. https://doi.org/10.3109/13506129.2012.673140.

[160] Benson MD, Waddington-Cruz M, Berk JL, Polydefkis M, Dyck PJ, Wang AK, et al. Inotersen Treatment for Patients with Hereditary Transthyretin Amyloidosis. N Engl J Med 2018;379:22–31. https://doi.org/10.1056/NEJMoa1716793.

[161] Maurer MS, Heitner S, Drachman B, Whelan C, Guthrie S, Tai L, et al. INOTERSEN IMPROVES QUALITY OF LIFE IN PATIENTS WITH HEREDITARY TRANSTHYRETIN AMYLOIDOSIS WITH POLYNEUROPATHY AND CARDIOMYOPATHY: RESULTS OF THE PHASE 3 STUDY NEURO-TTR. J Am Coll Cardiol 2018;71:A658. https://doi.org/10.1016/S0735-1097(18)31199-9.

[162] Vrana JA, Gamez JD, Madden BJ, Theis JD, Bergen HR, Dogan A. Classification of amyloidosis by laser microdissection and mass spectrometry-based proteomic analysis in clinical biopsy specimens. Blood 2009;114:4957–9. https://doi.org/10.1182/blood-2009-07-230722.

[163] Treibel TA, Fontana M, Gilbertson JA, Castelletti S, White SK, Scully PR, et al. Occult Transthyretin Cardiac Amyloid in Severe Calcific Aortic StenosisCLINICAL PERSPECTIVE: Prevalence and Prognosis in Patients Undergoing Surgical Aortic Valve Replacement. Circ Cardiovasc Imaging 2016;9:e005066. https://doi.org/10.1161/CIRCIMAGING.116.005066.

[164] Quarta CC, Gonzalez-Lopez E, Gilbertson JA, Botcher N, Rowczenio D, Petrie A, et al. Diagnostic sensitivity of abdominal fat aspiration in cardiac amyloidosis. Eur Heart J 2017;38:1905–8. https://doi.org/10.1093/eurheartj/ehx047.

[165] Mercan R, Bıtık B, Tezcan ME, Kaya A, Tufan A, Ozturk MA, et al. Minimally invasive minor salivary gland biopsy for the diagnosis of amyloidosis in a rheumatology clinic. ISRN Rheumatol 2014;2014:354648. https://doi.org/10.1155/2014/354648.

[166] Foli A, Palladini G, Caporali R, Verga L, Morbini P, Obici L, et al. The role of minor salivary gland biopsy in the diagnosis of systemic amyloidosis: results of a prospective study in 62 patients. Amyloid 2011;18:80–2. https://doi.org/10.3109/13506129.2011.574354029.

[167] Fine NM, Arruda-Olson AM, Dispenzieri A, Zeldenrust SR, Gertz MA, Kyle RA, et al. Yield of Noncardiac Biopsy for the Diagnosis of Transthyretin Cardiac Amyloidosis. Am J Cardiol 2014;113:1723–7. https://doi.org/10.1016/j.amjcard.2014.02.030.

[168] Kyle RA, Therneau TM, Rajkumar SV, Larson DR, Plevak MF, Offord JR, et al. Prevalence of Monoclonal Gammopathy of Undetermined Significance. N Engl J Med 2006;354:1362–9. https://doi.org/10.1056/NEJMoa054494.

[169] Deckers JW, Hare JM, Baughman KL. Complications of transvenous right ventricular endomyocardial biopsy in adult patients with cardiomyopathy: A seven-year survey of 546 consecutive diagnostic procedures in a tertiary referral center. J Am Coll Cardiol 1992;19:43–7. https://doi.org/10.1016/0735-1097(92)90049-S.

[170] Chimenti C, Frustaci A. Contribution and Risks of Left Ventricular Endomyocardial Biopsy in Patients With Cardiomyopathies: A Retrospective Study Over a 28-Year Period. Circulation 2013;128:1531–41. https://doi.org/10.1161/CIRCULATIONAHA.13.001414.

[171] Bennett MK, Gilotra NA, Harrington C, Rao S, Dunn JM, Freitag TB, et al. Evaluation of the Role of Endomyocardial Biopsy in 851 Patients With Unexplained Heart Failure From 2000–2009. Circ Heart Fail 2013;6:676–84. https://doi.org/10.1161/CIRCHEARTFAILURE.112.000087.

[172] Nietlispach F, Webb JG, Ye J, Cheung A, Lichtenstein SV, Carere RG, et al. Pathology of Transcatheter Valve Therapy. JACC Cardiovasc Interv 2012;5:582–90. https://doi.org/10.1016/j.jcin.2012.03.012.

[173] Narotsky DL, Kodali SK, Maurer MS, Bokhari S, Hamid N, Pozniakoff T, et al. Screening for Transthyretin Cardiac Amyloidosis Using 99mTc-Pyrophosphate Scintigraphy in Patients Undergoing Transcatheter Aortic Valve Replacement. Circulation 2015;132.

[174] Duncan A, Ludman P, Banya W, Cunningham D, Marlee D, Davies S, et al. Long-Term Outcomes After Transcatheter Aortic Valve Replacement in High-Risk Patients With Severe Aortic Stenosis. JACC Cardiovasc Interv 2015;8:645–53. https://doi.org/10.1016/j.jcin.2015.01.009.

[175] Fairbairn TA, Meads DM, Mather AN, Motwani M, Pavitt S, Plein S, et al. Serial change in health-related quality of life over 1 year after transcatheter aortic valve implantation: predictors of health outcomes. J Am Coll Cardiol 2012;59:1672–80. https://doi.org/10.1016/j.jacc.2012.01.035.

[176] Willenheimer R, Erhardt LR. Value of 6-min-walk test for assessment of severity and prognosis of heart failure. The Lancet 2000;355:515–6. https://doi.org/10.1016/S0140-6736(99)00445-6.

[177] Sokolow M, Lyon TP. The ventricular complex in left ventricular hypertrophy as obtained by unipolar precordial and limb leads. Am Heart J 1949;37:161–86. https://doi.org/10.1016/0002-8703(49)90562-1.

[178] Carroll JD, Gaasch WH, McAdam KP. Amyloid cardiomyopathy: characterization by a distinctive voltage/mass relation. Am J Cardiol 1982;49:9–13.

[179] Hancock EW, Deal BJ, Mirvis DM, Okin P, Kligfield P, Gettes LS. AHA/ACCF/HRS Recommendations for the Standardization and Interpretation of the Electrocardiogram: Part V: Electrocardiogram Changes Associated With Cardiac Chamber Hypertrophy: A Scientific Statement From the American Heart Association

Electrocardiography and Arrhythmias Committee, Council on Clinical Cardiology; the American College of Cardiology Foundation; and the Heart Rhythm Society: *Endorsed by the International Society for Computerized Electrocardiology*. Circulation 2009;119. https://doi.org/10.1161/CIRCULATIONAHA.108.191097.

[180] Wharton G, Steeds R, Allen J, Phillips H, Jones R, Kanagala P, et al. A minimum dataset for a standard adult transthoracic echocardiogram: a guideline protocol from the British Society of Echocardiography. Echo Res Pract 2015;2:G9–24. https://doi.org/10.1530/ERP-14-0079.

[181] Nagueh SF, Smiseth OA, Appleton CP, Byrd BF, Dokainish H, Edvardsen T, et al. Recommendations for the Evaluation of Left Ventricular Diastolic Function by Echocardiography: An Update from the American Society of Echocardiography and the European Association of Cardiovascular Imaging. J Am Soc Echocardiogr 2016;29:277–314. https://doi.org/10.1016/j.echo.2016.01.011.

[182] Lang RM, Badano LP, Mor-Avi V, Afilalo J, Armstrong A, Ernande L, et al. Recommendations for Cardiac Chamber Quantification by Echocardiography in Adults: An Update from the American Society of Echocardiography and the European Association of Cardiovascular Imaging. Eur Heart J – Cardiovasc Imaging 2015;16:233–71. https://doi.org/10.1093/ehjci/jev014.

[183] Devereux RB, Alonso DR, Lutas EM, Gottlieb GJ, Campo E, Sachs I, et al. Echocardiographic assessment of left ventricular hypertrophy: comparison to necropsy findings. Am J Cardiol 1986;57:450–8. https://doi.org/10.1016/0002-9149(86)90771-x.

[184] Rubin J, Steidley DE, Carlsson M, Ong M-L, Maurer MS. Myocardial Contraction Fraction by M-Mode Echocardiography Is Superior to Ejection Fraction in Predicting Mortality in Transthyretin Amyloidosis. J Card Fail 2018;24:504–11. https://doi.org/10.1016/j.cardfail.2018.07.001.

[185] Quantitative Nuclear Medicine Imaging: Concepts, Requirements and Methods. Vienna: INTERNATIONAL ATOMIC ENERGY AGENCY; 2014.

[186] Kurobe Y, Kitagawa K, Ito T, Kurita Y, Shiraishi Y, Nakamori S, et al. Myocardial delayed enhancement with dual-source CT: Advantages of targeted spatial frequency filtration and image averaging over half-scan reconstruction. J Cardiovasc Comput Tomogr 2014;8:289–98. https://doi.org/10.1016/j.jcct.2014.06.004.

[187] Ramirez-Giraldo JC, Yu L, Kantor B, Ritman EL, McCollough CH. A strategy to decrease partial scan reconstruction artifacts in myocardial perfusion CT: Phantom and *in vivo* evaluation: Strategy to decrease artifacts in myocardial perfusion CT. Med Phys 2011;39:214–23. https://doi.org/10.1118/1.3665767.

[188] Nacif MS, Liu Y, Yao J, Liu S, Sibley CT, Summers RM, et al. 3D left ventricular extracellular volume fraction by low-radiation dose cardiac CT: Assessment of

interstitial myocardial fibrosis. J Cardiovasc Comput Tomogr 2013;7:51–7. https://doi.org/10.1016/j.jcct.2012.10.010.

[189] Treibel TA, Kozor R, Schofield R, Benedetti G, Fontana M, Bhuva AN, et al. Reverse Myocardial Remodeling Following Valve Replacement in Patients With Aortic Stenosis. J Am Coll Cardiol 2018;71:860–71. https://doi.org/10.1016/j.jacc.2017.12.035.

[190] Kappetein AP, Head SJ, Généreux P, Piazza N, van Mieghem NM, Blackstone EH, et al. Updated standardized endpoint definitions for transcatheter aortic valve implantation: the Valve Academic Research Consortium-2 consensus document. Eur Heart J 2012;33:2403–18. https://doi.org/10.1093/eurheartj/ehs255.

[191] Horstkotte D, Loogen F. The natural history of aortic valve stenosis. Eur Heart J 1988;9 Suppl E:57–64. https://doi.org/10.1093/eurheartj/9.suppl_e.57.

[192] Naik-Mathuria B, Pilling D, Crawford JR, Gay AN, Smith CW, Gomer RH, et al. Serum amyloid P inhibits dermal wound healing. Wound Repair Regen Off Publ Wound Heal Soc Eur Tissue Repair Soc 2008;16:266–73. https://doi.org/10.1111/j.1524-475X.2008.00366.x.

[193] Nordin S, Kozor R, Medina-Menacho K, Abdel-Gadir A, Baig S, Sado DM, et al. Proposed Stages of Myocardial Phenotype Development in Fabry Disease. JACC Cardiovasc Imaging 2019;12:1673–83. https://doi.org/10.1016/j.jcmg.2018.03.020.

[194] Cavalcante JL, Rijal S, Abdelkarim I, Althouse AD, Sharbaugh MS, Fridman Y, et al. Cardiac amyloidosis is prevalent in older patients with aortic stenosis and carries worse prognosis. J Cardiovasc Magn Reson 2017;19. https://doi.org/10.1186/s12968-017-0415-x.

[195] Castaño A, Narotsky DL, Hamid N, Khalique OK, Morgenstern R, DeLuca A, et al. Unveiling transthyretin cardiac amyloidosis and its predictors among elderly patients with severe aortic stenosis undergoing transcatheter aortic valve replacement. Eur Heart J 2017;38:2879–87. https://doi.org/10.1093/eurheartj/ehx350.

[196] Auffret V, Webb JG, Eltchaninoff H, Muñoz-García AJ, Himbert D, Tamburino C, et al. Clinical Impact of Baseline Right Bundle Branch Block in Patients Undergoing Transcatheter Aortic Valve Replacement. JACC Cardiovasc Interv 2017;10:1564–74. https://doi.org/10.1016/j.jcin.2017.05.030.

[197] Watanabe Y, Kozuma K, Hioki H, Kawashima H, Nara Y, Kataoka A, et al. Pre-Existing Right Bundle Branch Block Increases Risk for Death After Transcatheter Aortic Valve Replacement With a Balloon-Expandable Valve. JACC Cardiovasc Interv 2016;9:2210–6. https://doi.org/10.1016/j.jcin.2016.08.035.

[198] Dubrey SW, Cha K, Anderson J, Chamarthi B, Reisinger J, Skinner M, et al. The clinical features of immunoglobulin light-chain (AL) amyloidosis with heart involvement.

QJM Mon J Assoc Physicians 1998;91:141–57. https://doi.org/10.1093/qjmed/91.2.141.

[199] Kind P, Dolan P, Gudex C, Williams A. Variations in population health status: results from a United Kingdom national questionnaire survey. BMJ 1998;316:736–41. https://doi.org/10.1136/bmj.316.7133.736.

[200] Smorti M, Cappelli F, Bergesio F, Perfetto F. Anxiety and depression among AL amyloidosis patients: the role of cardiac symptoms. Amyloid Int J Exp Clin Investig Off J Int Soc Amyloidosis 2012;19:123–8. https://doi.org/10.3109/13506129.2012.687420.

[201] Amyloidosis Foundation. Understanding the patient voice in hereditary transthyretin-mediated amyloidosis (ATTR amyloidosis) 2017.

[202] Banypersad SM, Sado DM, Flett AS, Gibbs SDJ, Pinney JH, Maestrini V, et al. Quantification of Myocardial Extracellular Volume Fraction in Systemic AL Amyloidosis: An Equilibrium Contrast Cardiovascular Magnetic Resonance Study. Circ Cardiovasc Imaging 2013;6:34–9. https://doi.org/10.1161/CIRCIMAGING.112.978627.

[203] Trattner S, Halliburton S, Thompson CM, Xu Y, Chelliah A, Jambawalikar SR, et al. Cardiac-Specific Conversion Factors to Estimate Radiation Effective Dose From Dose-Length Product in Computed Tomography. JACC Cardiovasc Imaging 2018;11:64–74. https://doi.org/10.1016/j.jcmg.2017.06.006.

[204] Kurita Y, Kitagawa K, Kurobe Y, Nakamori S, Nakajima H, Dohi K, et al. Estimation of myocardial extracellular volume fraction with cardiac CT in subjects without clinical coronary artery disease: A feasibility study. J Cardiovasc Comput Tomogr 2016;10:237–41. https://doi.org/10.1016/j.jcct.2016.02.001.

[205] Treibel TA, López B, González A, Menacho K, Schofield RS, Ravassa S, et al. Reappraising myocardial fibrosis in severe aortic stenosis: an invasive and non-invasive study in 133 patients. Eur Heart J 2018;39:699–709. https://doi.org/10.1093/eurheartj/ehx353.

[206] Hein S, Arnon E, Kostin S, Schönburg M, Elsässer A, Polyakova V, et al. Progression from compensated hypertrophy to failure in the pressure-overloaded human heart: structural deterioration and compensatory mechanisms. Circulation 2003;107:984–91. https://doi.org/10.1161/01.cir.0000051865.66123.b7.

[207] Schwarz F, Flameng W, Schaper J, Langebartels F, Sesto M, Hehrlein F, et al. Myocardial structure and function in patients with aortic valve disease and their relation to postoperative results. Am J Cardiol 1978;41:661–9. https://doi.org/10.1016/0002-9149(78)90814-7.

[208] Cheitlin MD, Robinowitz M, McAllister H, Hoffman JI, Bharati S, Lev M. The distribution of fibrosis in the left ventricle in congenital aortic stenosis and

coarctation of the aorta. Circulation 1980;62:823–30. https://doi.org/10.1161/01.cir.62.4.823.

[209] Soderlund TA, Dickson JC, Prvulovich E, Ben-Haim S, Kemp P, Booij J, et al. Value of Semiquantitative Analysis for Clinical Reporting of 123I-2- -Carbomethoxy-3 -(4-Iodophenyl)-N-(3-Fluoropropyl)Nortropane SPECT Studies. J Nucl Med 2013;54:714–22. https://doi.org/10.2967/jnumed.112.110106.

[210] Dewaraja YK, Schipper MJ, Roberson PL, Wilderman SJ, Amro H, Regan DD, et al. 131I-Tositumomab Radioimmunotherapy: Initial Tumor Dose-Response Results Using 3-Dimensional Dosimetry Including Radiobiologic Modeling. J Nucl Med 2010;51:1155–62. https://doi.org/10.2967/jnumed.110.075176.

[211] Ohno Y, Koyama H, Nogami M, Takenaka D, Matsumoto S, Yoshimura M, et al. Postoperative Lung Function in Lung Cancer Patients: Comparative Analysis of Predictive Capability of MRI, CT, and SPECT. Am J Roentgenol 2007;189:400–8. https://doi.org/10.2214/AJR.07.2084.

[212] Willowson K, Bailey DL, Baldock C. Quantifying lung shunting during planning for radio-embolization. Phys Med Biol 2011;56:N145–52. https://doi.org/10.1088/0031-9155/56/13/N01.

[213] Iida H, Eberl S, Kim K-M, Tamura Y, Ono Y, Nakazawa M, et al. Absolute quantitation of myocardial blood flow with 201Tl and dynamic SPECT in canine: optimisation and validation of kinetic modelling. Eur J Nucl Med Mol Imaging 2008;35:896–905. https://doi.org/10.1007/s00259-007-0654-4.

[214] Da Silva AJ, Tang HR, Wong KH, Wu MC, Dae MW, Hasegawa BH. Absolute quantification of regional myocardial uptake of 99mTc-sestamibi with SPECT: experimental validation in a porcine model. J Nucl Med Off Publ Soc Nucl Med 2001;42:772–9.

[215] Ross JC, Hutt DF, Burniston M, Page J, Steeden JA, Gillmore JD, et al. Quantitation of ^{99m} Tc-DPD uptake in patients with transthyretin-related cardiac amyloidosis. Amyloid 2018;25:203–10. https://doi.org/10.1080/13506129.2018.1520087.

[216] Caobelli F, Braun M, Haaf P, Wild D, Zellweger MJ. Quantitative 99mTc-DPD SPECT/CT in patients with suspected ATTR cardiac amyloidosis: Feasibility and correlation with visual scores. J Nucl Cardiol 2019. https://doi.org/10.1007/s12350-019-01893-8.

[217] Cappelli F, Gallini C, Costanzo EN, Tutino F, Ciaccio A, Vaggelli L, et al. Lung uptake during 99mTc- hydroxymethylene diphosphonate scintigraphy in patient with TTR cardiac amyloidosis: An underestimated phenomenon. Int J Cardiol 2018;254:346–50. https://doi.org/10.1016/j.ijcard.2017.10.027.

[218] Coles LS, Young RD. Supercentenarians and transthyretin amyloidosis: The next frontier of human life extension. Prev Med 2012;54:S9–11. https://doi.org/10.1016/j.ypmed.2012.03.003.

[219] Scully PR, Treibel TA, Fontana M, Lloyd G, Mullen M, Pugliese F, et al. Prevalence of Cardiac Amyloidosis in Patients Referred for Transcatheter Aortic Valve Replacement. J Am Coll Cardiol 2018;71:463–4. https://doi.org/10.1016/j.jacc.2017.11.037.

[220] Damy T, Costes B, Hagège AA, Donal E, Eicher J-C, Slama M, et al. Prevalence and clinical phenotype of hereditary transthyretin amyloid cardiomyopathy in patients with increased left ventricular wall thickness. Eur Heart J 2016;37:1826–34. https://doi.org/10.1093/eurheartj/ehv583.

[221] Sperry BW, Gonzalez MH, Brunken R, Cerqueira MD, Hanna M, Jaber WA. Non-cardiac uptake of technetium-99m pyrophosphate in transthyretin cardiac amyloidosis. J Nucl Cardiol 2018. https://doi.org/10.1007/s12350-017-1166-7.

Chapter 10: Appendix

10.1 Location of Research

This work for this thesis took place at two sites: BHC in London and the John Radcliffe Hospital in Oxford. Sample analysis took place at BHC. University College London was also involved in sample storage.

10.2 Supervisor Details

Primary Supervisor: **Prof James Moon**
Secondary Supervisor: **Prof Philip Hawkins**

10.3 Personal Contributions

Relevant personal contributions are described at the beginning of chapters 3,4 and 5 of the thesis.

10.4 Funding Details

This work was funded by a British Heart Foundation Clinical Research Training Fellowship (FS/16/31/32185).

10.5 Collaborators

The National Amyloidosis Centre

Prof Philip Hawkins, **Prof Julian Gillmore, Dr Marianna Fontana** and all the team.

The John Radcliffe Hospital

Dr Andrew Kelion, **Dr Nikant Sabharwal**, **Dr Jim Newton, Sergei Pavlitchouk, Simon Overy, Ellie Corps, Stephanie Lloyd** and all the team.

Siemens Healthineers

Ernst Klotz and **Ulrike Haberland**.

University College London

Prof Christopher G McGregor.

10.6 Prizes/Awards related to Research

I have been short listed for the Young Investigator Award at the European Association of Cardiovascular Imaging – Best of Imaging 2020 conference in December 2020.

I was a finalist for the Young Investigator Award at the International Conference on Nuclear Cardiology and Cardiac CT in Lisbon in May 2019 for my work on AS-amyloid and outcome.

I won the British Nuclear Cardiology Society Young Investigator Award at the British Cardiovascular Imaging Meeting in Edinburgh in May 2018 for my early work on AS-amyloid.

I was a finalist for the British Society of Cardiovascular Imaging/British Society of Cardiovascular Computed Tomography Young Investigator Award at the same meeting in May 2018 for my work on ECV_{CT} in AS-amyloid.

Finally, I won first prize for my presentation regarding AS-amyloid at British Nuclear Cardiology Society Annual General Meeting in May 2016.

10.7 Publications related to or during Research

1. Papers/Research Letters:

Scully PR, Patel KP, Saberwal B, Klotz E, Augusto JB, Thornton GD, Hughes RK, Manisty C, Lloyd G, Newton JD, Sabharwal N, Kelion A, Kennon S, Ozkor M, Mullen M, Hartman N, Cavalcante J, Menezes LJ, Hawkins PN, Treibel TA, Moon JC, Pugliese F. Identifying Cardiac Amyloid in Aortic Stenosis: ECV Quantification by CT in TAVR Patients. *JACC Cardiovasc Imaging* 2020;13(10):2177-2189. DOI: 10.1016/j.jcmg.2020.05.029 (see attached for copy).

Scully PR, Morris E, Patel KP, Treibel TA, Burniston M, Klotz E, Newton JD, Sabharwal N, Kelion A, Manisty C, Kennon S, Ozkor M, Mullen M, Hartman N, Elliott PM, Pugliese F, Hawkins PN, Moon JC, Menezes LJ. DPD Quantification in Cardiac Amyloidosis: a Novel Imaging Biomarker. *JACC Cardiovasc Imaging* 2020; **13**(6):1353-1363. DOI: 10.1016/j.jcmg.2020.03.020 (see attached for copy).

Scully PR, Patel KP, Treibel TA, Thornton GD, Hughes RK, Chadalavada S, Katsoulis M, Hartman N, Fontana M, Pugliese F, Sabharwal N, Newton JD, Kelion A, Ozkor M, Kennon S, Mullen M, Lloyd G, Menezes LJ, Hawkins PN, Moon JC. Prevalence and outcome of dual aortic stenosis and cardiac amyloid pathology in patients referred for transcatheter aortic valve implantation. *Eur Heart J* 2020;**41**(29):2759-2767. DOI: 10.1093/eurheartj/ehaa170 (see attached for copy).

Torlasco C, D'Silva A, Bhuva AN, Faini A, Augusto JB, Knott KD, Benedetti G, Jones S, Van Zalen J, Scully P, Lobascio I, Parati G, Lloyd G, Hughes AD, Manisty CH, Sharma S and Moon JC. Age Matters: differences in exercise-induced cardiovascular remodelling in young and middle aged healthy sedentary individuals. *Eur J Prev Cardiol* 2020; online ahead of print. DOI: 10.1177/2047487320926305.

D'Silva A, Bhuva AN, Van Zalen J, Bastiaenen R, Adbel-Gadir A, Jones S, Nadarajan N, Menacho Medina KD, Ye Y, Augusto J, Treibel TA, Rosmini S, Ramlall M, Scully PR, Torlasco C, Willis J, Finocchiaro G, Papatheodorou E, Dhutia H, Cole D, Chis Ster I, Hughes AD, Sharma R, Manisty C, Lloyd G, Moon JC, Sharma S. Cardiovascular Remodelling Experienced by Real-World, Unsupervised, Young, Novice Marathon Runners. *Front Physiol* 2020;11:232. DOI: 10.3389/fphys.2020.00232.

Bhuva AN, D'Silva A, Torlasco C, Nadarajan N, Jones S, Boubertakh R, Van Zalen J, Scully P, Knott K, Benedetti G, Augusto JB, Bastiaenen R, Lloyd G, Sharma S, Moon JC, Parker KH, Manisty CH, Hughes AD. Non-invasive assessment of ventriculo-arterial coupling using aortic wave intensity analysis combining central blood pressure and phase-contrast cardiovascular magnetic resonance. *Eur Heart J Cardiovasc Imaging* 2020;**21**(7):805-813. DOI: 10.1093/ehjci/jez227.

Bollache E, Knott KD, Jarvis K, Boubertakh R, Dolan RS, Camaioni C, Collins L, Scully P, Rabin S, Treibel T, Carr JC, van Ooij P, Collins JD, Geiger J, Moon JC, Barker AJ, Petersen SE, Markl M. Two-Minute k-Space and Time-accelerated Aortic Four-dimensional Flow MRI: Dual-centre Study of Feasibility and Impact on

Velocity and Wall Shear Stress Quantification. *Radiol Cardiothorac Imaging* 2019;**1**(2):e180008. DOI: 10.1148/ryct.2019180008.

Scully PR, Treibel TA, Fontana M, Lloyd G, Mullen M, Pugliese F, Hartman N, Hawkins PN, Menezes LJ, Moon JC. Prevalence of Cardiac Amyloidosis in Patients Referred for Transcatheter Aortic Valve Replacement. *J Am Coll Cardiol* 2018;**71**(4):463-464. DOI: 10.1016/j.jacc.2017.11.037 (see attached for copy).

Treibel TA, Fontana M, Gilbertson JA, Castelletti S, White SK, Scully PR, Roberts N, Hutt DF, Rowczenio DM, Whelan C, Ashworth MA, Gillmore JD, Hawkins PN, Moon JC. Occult Transthyretin Cardiac Amyloid in Severe Calcific Aortic Stenosis: Prevalence and Prognosis. *Circ Cardiovasc Imaging* 2016;**9**(8):e005066. DOI: 10.1161/CIRCIMAGING.116.005066.

2. Editorials:

Treibel TA, Scully PR, Moon JC. Myocardial Hypertrophy, Matrix Expansion and Focal Scar – progression and regression in Aortic Stenosis. *Circ Cardiovasc Imaging* 2018;**11**:e007975. DOI: 10.1161/CIRCIMAGING.118.007975.

3. Letters to the Editor:

Scully PR, Moon JC, Treibel TA. Cardiac Amyloidosis in Aortic Stenosis: the Tip of the Iceberg. *J Thorac Cardiovasc Surg* 2018; **156**(3):965-966. DOI: 10.1016/j.jtcvs.2018.03.142.

4. Reviews:

Fontana M, Corovic A, Scully PR, Moon JC. Myocardial Amyloidosis – the Exemplar Interstitial Disease. *JACC Cardiovasc Imaging* 2019, [Epub ahead of print]. DOI: 10.1016/j.jcmg.2019.06.023.

Scully PR, Bastarrika G, Moon JC, Treibel TA. Myocardial Extracellular Volume Quantification by Cardiovascular Magnetic Resonance and Computed Tomography. *Curr Cardiol Rep* 2018;**20**(3):15. DOI: 10.1007/s11886-018-0961-3.

5. Case Reports:

Scully PR, Klotz E, Mullen M, Lloyd G, Menezes L, Hawkins PN, Pugliese F, Moon JC. Dual Aortic Stenosis and Amyloid Pathology. *J Heart Valve Dis* (accepted for publication).

6. Abstracts:

Scully PR, Patel K, Treibel TA, Pavlitchouk S, Lloyd G, Pugliese F, Newton J, Sabharwal N, Kelion A, Kennon S, Ozkor M, Mullen M, Menezes LJ, Hawkins PN, Moon JC. Cardiac amyloid in TAVI patients – bystander or disease modifier? *Eur Heart J Cardiovasc Imaging* 2019;**20**(Suppl 3). DOI: 10.1093/ehjci/jez151.002.

Scully PR, Treibel TA, Klotz E, Augusto J, Herrey AS, Newton J, Sabharwal N, Kelion A, Kennon S, Ozkor M, Mullen M, Menezes LJ, Hawkins PN, Moon JC, Pugliese F. Amyloid-AS: detecting occult Cardiac Amyloid during TAVI work-up Computed Tomography. *Eur Heart J Cardiovasc Imaging* 2019;**20**(Suppl 3). DOI: 10.1093/ehjci/jez142.

Scully PR, Morris E, Patel K, Saberwal B, Chadalavada S, Testanera G, Subhani S, Ferreira S, Hartman N, Mullen M, Elliott P, Fontana M, Hawkins PN, Moon JC, Menezes LJ. SUV Quantification in DPD Scintigraphy. *Eur Heart J Cardiovasc Imaging* 2019;**20**(Suppl 3). DOI: 10.1093/ehjci/jez145.001.

Patel K, Scully PR, Treibel T, Kennon S, Ozkor M, Mullen MJ, Herrey A, Menezes L, Moon JC, Pugliese F. Clinical Utility of CT angiography over and above TAVI procedural planning. *Eur Heart J Cardiovasc Imaging* 2019;**20**(Suppl 3). DOI:10.1093/ehjci/jez144.001.

Primus CP, Clay T, Al-Khayfawee A, Scully PR, Wong K, Uppal R, Das S, Serafino-Wani R, Bhattacharyya, Davies LC, Woldman S, Menezes L. ^{18}F-FDG PET/CT improves diagnostic certainty in native and prosthetic valve infective endocarditis over the modified Duke's criteria. *Eur Heart J Cardiovasc Imaging* 2019;**20**(Suppl 3). DOI: 10.1093/ehjci/jez144.008.

Menacho Medina KD, Culotta V, Bhuva A, Scully PR, Westwood M, Gosh A,

Moon JC, Menezes L, Manisty C. Variability of left ventricular ejection fraction measurement by imaging modality for cardiotoxicity screening: comparison between Radionuclide Ventriculography, 2D and 3D Echocardiography and CMR. *Eur Heart J Cardiovasc Imaging* 2019;**20**(Suppl 3). DOI: 10.1093/ehjci/jez146.004

Scully PR, Treibel TA, Klotz E, Castle E, Yap-Sanderson J, Saberwal B, Ahmadvazir S, Gangil N, Davies C, Mullen M, Kennon S, Ozkor M, Menezes LJ, Hawkins PN, Moon JC, Pugliese F. The Detection of Cardiac Amyloidosis using Extracellular Volume Quantification by Computed Tomography. *Heart* 2018;**104**(Suppl 5):A2. DOI: 10.1136/heartjnl-2018-BCVI.3.

Scully PR, Treibel TA, Fontana M, Hartman N, Lloyd G, Pugliese F, Sabharwal N, Newton J, Kelion A, Mullen M, Ozkor M, Kennon S, Menezes LJ, Hawkins PN, Moon JC. A Multi-centre Study of Cardiac Amyloidosis in TAVI Patients. *Heart* 2018;**104**(Suppl 5):A15. DOI: 10.1136/heartjnl-2018-BCVI.42.

Scully PR, Morris E, Burniston M, Treibel TA, Jerrum M, Bedford K, Queenan H, Hartman N, Mullen M, Ozkor M, Kennon S, Newton J, Sabharwal N, Kelion A, Elliott PM, Moon JC, Hawkins PN, Menezes LJ. SPECT/CT Quantification of DPD Scintigraphy in Cardiac Amyloid. *Heart* 2018;**104**(Suppl 5):A16. DOI: 10.1136/heartjnl-2018-BCVI.44.

Scully PR, Schofield R, Treibel TA, Fontana M, Hawkins PN, Moon JC, Elliott PM, Menezes LJ. Bone Scintigraphy in Left Ventricular Hypertrophy. Preliminary results of a new service in a Tertiary Hospital. *EHJ CVI* 2017;**18**(Suppl 1): P177. DOI: 10.1093/ehjci/jex077.

10.8 Presentations and Posters related to or during Research

I have included here only oral presentations or posters that I have presented myself.

11/2020 Myocardial fibrosis quantification by cardiac CT predicts outcome in severe aortic stenosis. Young investigator award virtual presentation recorded in advance of the European Association of Cardiovascular Imaging – Best of Imaging 2020 Conference due in December 2020.

05/2019 Cardiac Amyloid in TAVI Patients – bystander or disease modifier? Young investigator award podium presentation at the International Conference on Nuclear Cardiology and Cardiac CT on 12/5/19 in Lisbon.

05/2019 Amyloid-AS: detecting occult Cardiac Amyloid during TAVI work-up CT. Moderated poster presentation at the International Conference on Nuclear Cardiology and Cardiac CT on 12/5/19 in Lisbon.

05/2019 SUV Quantification in DPD Scintigraphy. Moderated poster presentation at the International Conference on Nuclear Cardiology and Cardiac CT on 13/5/19 in Lisbon.

05/2018 A Multi-Centre Study of Cardiac Amyloidosis in TAVI Patients. BNCS young investigator award podium presentation at the British Cardiovascular Imaging Meeting 2018 in Edinburgh on 3/11/18 (winner).

05/2018 The Detection of Cardiac Amyloidosis using Extracellular Volume Quantification by Computed Tomography. Podium presentation at the British Cardiovascular Imaging Meeting 2018 in Edinburgh on 2nd May 2018 (finalist YIA).

05/2018 SPECT/CT Quantification of DPD Scintigraphy in Cardiac Amyloid. Moderated poster presentation at the British Cardiovascular Imaging Meeting 2018 in Edinburgh from 2nd – 4th May 2018.

01/2018 Extracellular Volume Quantification by Computed Tomography. Poster presentation at the Society of Cardiovascular Computed Tomography Winter Meeting at the RSM in London from 30th – 31st January 2018.

05/2017 Bone Scintigraphy in Left Ventricular Hypertrophy. Preliminary results of a new service in a Tertiary Hospital. Poster presentation at the International Conference on Nuclear Cardiology and Cardiac CT on 7th May 2017.

02/2017 Off-resonance error following aortic valve replacement: the effect on myocardial T1. Poster presentation at SCMR 20th Annual Scientific Sessions, Washington DC from 1st – 4th February 2017.

02/2017 Ockham's Razor put to the test (case report). Poster presentation at SCMR 20th Annual Scientific Sessions, Washington DC from 1st – 4th February 2017.

05/2016 Left Ventricular Hypertrophy in Aortic Stenosis. Podium presentation at British Nuclear Cardiology Society Annual General Meeting on 4th May 2016 (awarded first prize).

10.9 Invited Lectures

06/2019 Cardiac amyloid in AS: presentation to 80 visiting delegates from Spain at Barts Heart Centre.

05/2019 RSM General Day 7: patients with valvular heart disease and the prevention and management of endocarditis (cardiac amyloid in AS).

05/2019 Peruvian Congress of Cardiology (four lectures on topics involving both cardiac CT and Nuclear Cardiology).

04/2019 British Nuclear Medicine Society Annual Spring Meeting in Oxford (DPD scintigraphy).

12/2018 RSM Cardiac Imaging Training Day on Multimodality Imaging in AS (multimodality imaging).

01/2018 UK Radiopharmacy Group Workshop 2018 in Bournville (DPD scintigraphy).

09/2016 North Thames Regional Nuclear Medicine Day (DPD scintigraphy).

10.10 Attached Relevant Publications